INFORMATION TO USERS

This manuscript has been reproduced from the microfilm master. UMI films the text directly from the original or copy submitted. Thus, some thesis and dissertation copies are in typewriter face, while others may be from any type of computer printer.

The quality of this reproduction is dependent upon the quality of the copy submitted. Broken or indistinct print, colored or poor quality illustrations and photographs, print bleedthrough, substandard margins, and improper alignment can adversely affect reproduction.

In the unlikely event that the author did not send UMI a complete manuscript and there are missing pages, these will be noted. Also, if unauthorized copyright material had to be removed, a note will indicate the deletion.

Oversize materials (e.g., maps, drawings, charts) are reproduced by sectioning the original, beginning at the upper left-hand corner and continuing from left to right in equal sections with small overlaps. Each original is also photographed in one exposure and is included in reduced form at the back of the book.

Photographs included in the original manuscript have been reproduced xerographically in this copy. Higher quality 6" x 9" black and white photographic prints are available for any photographs or illustrations appearing in this copy for an additional charge. Contact UMI directly to order.

UMI

A Bell & Howell Information Company
300 North Zeeb Road, Ann Arbor, MI 48106-1346 USA
313/761-4700 800/521-0600

ASYMMETRY IN THE CEREBRAL CORTEX OF *MACACA FASCICULARIS*: A BASAL SUBSTRATE FOR THE EVOLUTION OF BRAIN MECHANISMS UNDERLYING LANGUAGE

By

Patrick John Gannon

A dissertation submitted to the Graduate Faculty in Anthropology in partial fulfillment of the requirements for the degree of Doctor of Philosophy, The City University of New York.

1995

UMI Number: 9521270

Copyright 1995 by
Gannon, Patrick John
All rights reserved.

UMI Microform Edition 9521270
Copyright 1995, by UMI Company. All rights reserved.

This microform edition is protected against unauthorized
copying under Title 17, United States Code.

UMI

300 North Zeeb Road
Ann Arbor, MI 48103

Copyright © 1995

PATRICK JOHN GANNON

All Rights Reserved

APPROVAL PAGE

This manuscript has been read and accepted for the Graduate Faculty in Anthropology in satisfaction of the dissertation requirement for the degree of Doctor of Philosophy.

January 20, 1995

Date

Dr Jeffrey T. Laitman
The City University of New York
Chair of Examining Committee

January 23, 1995

Date

Dr Shirley Lindenbaum
Executive Officer
PhD Program in Anthropology
The City University of New York

Supervisory Committee:

Dr Eric Delson
The City University of New York
Co-Chair of Examining Committee

Dr Frederick S. Szalay
The City University of New York

Dr Efrain C. Azmitia
New York University

THE CITY UNIVERSITY OF NEW YORK

ABSTRACT

Asymmetry in the Cerebral Cortex of *Macaca fascicularis*: A Basal Substrate for the Evolution of Brain Mechanisms Underlying Language

by

Patrick John Gannon

Advisor: Professor Jeffrey T. Laitman

A central question in anthropology involves the evolution of brain substrates underlying human language. This study tests the hypothesis that these substrates have a long evolutionary history within primates and were present in basal form in the common ancestor of cercopithecoids and hominoids, if not earlier. In humans, left hemisphere cortical areas which subserve language functions are asymmetric, being larger than their contralateral homotypes. These human language areas have homologs in the cerebral cortex of macaques. This dissertation investigates whether human-like patterns of asymmetry are present in macaques.

Unlike previous studies, all brain specimens of *Macaca fascicularis* (n = 44) were fixed *in situ* by trans-cardiac perfusion to control for fixation-induced artifact. Further, the application of new techniques and incorporation of a series of new measures allowed for more precise delineation of subtle patterns of brain asymmetry. Measures of cortical structures associated with language region homologs were made both directly from brains (n = 18) and from brain photographs (n=34). New measures used included the dimensions of sulci deep to the surface of the brain. Included were the arcuate, central

and superior temporal sulci, sylvian fissure, surface features of adjacent cortical gyri, frontal and occipital petelias and frontal and parietal hemispheric widths.

Results showed that dimensions of frontal lobe structures *deep* to the brain's surface were significantly larger in the left hemisphere while brain *surface* structures tended to be larger in the right. Petelial patterns and co-occurrence were similar to humans, while hemispheric widths were symmetric. Some measures showed marked sex differences; for example, *left* central sulcus depth was significantly larger only in females ($P = 0.05$), and the height of the vertical limb of the *right* arcuate sulcus was significantly larger only in males ($P = 0.04$).

The patterns of asymmetry seen in the cerebral cortex of macaques indicates a mosaic of neural substrates organized somewhat different to humans. Although the vocal-auditory channel has become the primary modality in humans, this may not be the case for non-human primates. Accordingly, these neural mechanisms probably reflect a species-specific pattern of incorporation into a functional substrate which subserves primarily visual-gestural communication.

DEDICATION

I would like to dedicate this dissertation to my parents, Johnny and Joan Gannon, who always went out of their way to make sure that I had the educational opportunities that were not made available to them. Thank you from my heart mum and dad for making many sacrifices and working hard to ensure my advancement in life; I couldn't have done it without you.

ACKNOWLEDGMENTS

First and foremost I would like to thank my advisor and friend Jeffrey Todd Laitman for providing me with much initial encouragement and the critical measure of self confidence boosting needed to embark on an arduous graduate school career. Further, there is no question, I would probably never have realized that physical anthropology was the ultimate key to understanding and fulfillment without his influence. Thanks Jeff for all your help and support, physical, emotional and political, over the years and especially during my recent sprint to the finish line.

After being in graduate school for almost eight years, I am convinced, however, that attainment of the Doctor of Philosophy is the last remaining vocational calling. Not that I am complaining, don't get me wrong, I cannot imagine doing anything else with what's left with my life. On the contrary, I feel privileged to have accumulated a depth of understanding and knowledge that has been gleaned both from Jeff and the many other knowledgeable and gifted individuals that I have been exposed to and interacted with. In this vein, I would like to thank Professors Frederick Szalay of Hunter College and Eric Delson of Lehman College, first for all of the immeasurable help and guidance they have given me in their role as members of my dissertation committee over the last three years, and second for the knowledge they willingly bestowed upon me as I matured in my professional career under their expert guidance. Another such special individual is Professor Efrain Charles Azmitia of the Department of Biology, New York University, who was a great help to me in his role as my outside reader. Thank you Efrain

for all your help and guidance. I hope that my future contributions to evolutionary neuroscience will be worthy of the faith you placed in me.

A number of special individuals that have both inspired me and taught me a great deal along the way include: Professor Frank Spencer, who showed me the importance of understanding the history of anthropological thinking; Professor Ralph Holloway, who has been a great help and stimulus to me over the years; Professor Todd Olsen, who taught me much, including how *not* to organize a lecture like an Agatha Christie novel; Professor Dean Falk, with whom I have had many fruitful and fascinating interactions; Professor John Oates, who provided me with much insight into primate communicative behavior and cognition; Professor Ian Tattersall, who has helped and supported me over the last eight years; Professor Warren Kinzey; Professor Philip Lieberman; Professor Terrence Deacon; Professor Bernard Cohen; Professor Misia Landau; Professor Alexander Marshack; Professors Allen and Beatrice Gardner; Professor Brunetto Chiarelli; and Professor Harry Jerison.

I would especially like to thank Avrim Eden MD, with whom I have been involved for many years conducting research into the function of the middle ear and eustachian tube. Thank you Avrim for providing me with the opportunity to both earn a living and advance myself in graduate school. You have taught me a great deal, both about the complexities and uncertainties of a career in research and about my strengths and limitations. I also thank my Chairman, Hugh Biller MD and the Department of Otolaryngology at Mount Sinai Hospital, New York City, for their long term support and faith in my ability to succeed. All of the funding for the many aspects of my graduate school career were provided by them for which I am extremely grateful. Thanks also to Ira Sanders MD for his friendship, help

and support when I needed it most. More recently, Mark Urken MD has also provided me with much help and continued support for which I am grateful.

Many people were responsible for pushing me into the big decision to get my PhD and convinced me, against many doubts on my part, that I could succeed. These individuals, who had great faith in my abilities include my close friends and colleagues David Muir PhD, Leila Laitman MD, Joy Reidenberg PhD, David Solomon MD PhD, Alan Braun MD, Ed Gresik PhD and Marcus Valdez MS. Thanks especially to my good friend Karen Chandross PhD, who provided me with much encouragement and support during the difficult, examination ridden, early years of graduate school. I thank you all very much and I am happy to report that your faith in me finally came to bear fruit.

The majority of the large sample of perfusion-fixed primate brains used in this study were generously provided by William Doyle PhD of the Children's Hospital of Pittsburgh. Due to the critical nature of the specific requirements for my tissue preparation methods there is simply no way I could have done this study without this resource. Thank you for all the macaque brains Bill, and for your hospitality, warmth and the many hours of enjoyable and productive conversation during my several specimen collection trips to your laboratory in Pittsburgh. I look forward to many years of collaborating with you. Thanks also to the NIH for funding Bill's exciting middle ear research out of which I obtained the brains. Special thanks also to Gay Holstein PhD, of Mount Sinai School of Medicine for her many years of friendship, encouragement and support and for also providing me with a number of the macaque brains used in this study.

In recognition of the many levels of support afforded to me by my anthropology friends and colleagues, especially during the times when the

hurdles and chasms of my graduate school experience simply got the better of me, I really do appreciate your efforts. Thank you to all the faculty I have interacted with, and to the support staff, especially Terry Vulcano. To my graduate student contemporaries, peers and personal friends such as: Rebecca Araya, Sylvia Atsalis, Doug Broadfield, Ana Bueno, David Dean, David Friedland, Valerie Galishon, Haviva Goldman, Tess Green, Gillian Harper, Eugene Harris, Berrian Hobby, Reiko Matsuda, Colleen McAnn, Kelly MacFarland, James McMahon, Eric Sargis, Brain Stafford, Elizabeth Strasser, and last but not least Suzanne Walker; good luck to you all in your respective endeavors, and I look forward to continued interactions with you good people down the line. In this regard I would like to thank especially my close personal friends and student colleagues Robert Costello, Wendy Dirks, Samuel Marquez, and Lodewyk Werre who have been there for me and provided me with their support, not to mention a grueling game of darts, or a collegial discussion on subjects ranging from marine aquariums to tropical rain forest ecology, over a gaelic pint of Liberty Ale at Kinsales Pub, during many a tough period. I look forward to the many future years of knowing you special people as friends and colleagues.

Last but not least, I would like to thank the lovely lady in my life, my mate Nancy Kheck, who has always been there for me when I needed help and emotional support. I also thank my beatuiful daughter Colleen Patricia Gannon for providing me with lots of love and much fun and laughter during her eight years in my life. You two have been my main source of hope and inspiration and I thank you for all you have freely given. I love you both very much and I look forward to a happy and productive future for us all.

TABLE OF CONTENTS

TITLE PAGE i

COPYRIGHT PAGE ii

APPROVAL PAGE iii

ABSTRACT iv

DEDICATION v

ACKNOWLEDGMENTS vi

TABLE OF CONTENTS xi

LIST OF TABLES xx

LIST OF FIGURES xxi

LIST OF APPENDIX xxvii

CHAPTER 1 - INTRODUCTION AND OVERVIEW

1.1 INTRODUCTION 1

1.2 OVERVIEW OF CHAPTERS 3 - 7

1.2.1. Chapter 2 - Background 4

1.2.2 Chapter 3 - Materials and methods and anatomy and variation of cerebral cortex in *Macaca fascicularis* 6

1.2.3. Chapter 4 - Three dimensional (3-D) morphometry of brain surface structures 6

1.2.4. Chapter 5 - Two dimensional (2-D) morphometry of brain surface structures 7

1.2.5. Chapter 6 - Three dimensional morphometry of structures deep to the surface of the brain 8

1.2.6. Chapter 7 - Discussion and conclusions 9

CHAPTER 2 - BACKGROUND

2.1. INTRODUCTION 10

2.2. HISTORY OF LANGUAGE LOCALIZATION IN THE HUMAN BRAIN

2.2.1. Phrenology and the pre-aphasiology period 14

2.2.2. The discovery of cerebral asymmetry for human language functions 15

2.2.3. Contributions of aphasiology to language localization in human brains 18

2.3. PHYSIOLOGICAL STUDIES OF LANGUAGE LOCALIZATION IN THE HUMAN BRAIN

2.3.1. Introduction 20

2.3.2. Electrical stimulation mapping 21

2.3.3. The dichotic listening test 25

2.3.4. The Wada test 28

2.3.5. Computerized imaging of language functions 30

2.3.5.1. Anatomical imaging of inter-hemispheric asymmetry in brain language substrates 31

2.3.5.2. Functional imaging of inter-hemispheric asymmetry in brain language substrates 39

2.3.6. Role of the right hemisphere in human language functions 48

2.3.7. Handedness and language in humans 55

2.4. GROSS ANATOMICAL CORRELATES OF HEMISPHERIC LOCALIZATION OF LANGUAGE IN HUMANS

2.4.1. Introduction 62

2.4.2. The temporal lobe and Wernicke's area 62

2.4.3. The frontal lobe and Broca's area 66

2.4.4. Development of brain language areas and asymmetries 67

2.4.5. Cerebrocortical architectonic asymmetries 69

2.4.5.1. Architectonics of Wernicke's Area I: "Area Tpt" of the superior temporal gyrus 70

2.4.5.2. Architectonics of Wernicke's Area II: "Area PG" of the inferior parietal lobule 72

2.4.5.3 Architectonics of Broca's Area of the inferior frontal lobe 73

2.4.5.4. The arcuate fasciculus 73

2.5. STUDIES IN NON-HUMAN PRIMATES

2.5.1. Anatomical asymmetries in non-human primate brains 74

2.5.1.1. Asymmetries of the sylvian fissure 74
2.5.1.2. Other sulcal asymmetries 78
2.5.1.3. Petelial and hemispheric width asymmetries 80

2.5.2. Cortico-motoneuronal projections in primates 83

2.5.3. Physiology of non-human primate communication 84

2.5.3.1. Electrical stimulation techniques 85
2.5.3.2. Brain lesion techniques 87
2.5.3.3. Dichotic listening and right ear advantage 90

2.5.4. Handedness in non-human primates

2.5.4.1. Relevance of handedness to language and brain asymmetries 92
2.5.4.2. Handedness for simple reaching tasks 94
2.5.4.3. Handedness for complex tasks 97
2.5.4.4. Current theories of non-human primate handedness 100

2.5.5. Non-vocal aspects of human and non-human primate communication

2.5.5.1. Studies in humans 102
2.5.5.2 Studies in non-human primates 103

2.6. HOMOLOGY IN THE NERVOUS SYSTEM

2.6.1 Introduction 105

2.6.2. Historical foundation for the concept of homology 106

2.6.3. Homology in the nervous system 111

2.6.4. Evidence for homology of human brain language areas in the cerebral cortex of *Macaca* 116

2.6.4.1. Evidence for homology of Broca's Area in human and macaque brains 118
2.6.4.2. Evidence for homology of Wernicke's Area in human and macaque brains 121
2.6.4.3. Neural connectivity evidence for homology of Broca's and Wernicke's Area in human and macaque brains 123

2.6.5. Conclusions 127

CHAPTER 3 - MATERIALS AND METHODS AND ANATOMY AND VARIATION OF CEREBRAL CORTEX IN *MACACA FASCICULARIS*

3.1. CHAPTER OVERVIEW 129

3.2. ANATOMICAL METHODS

3.2.1. Choice of species 130

3.2.2. Procurement of animals 133

3.2.3. Brain tissue preparation 134

3.2.4. Preparation of fixative 135

3.2.5. Trans-cardiac perfusion method

3.2.5.1. Anesthesia 135
3.2.5.2. Insertion of perfusion cannula 136
3.2.5.3. Perfusion regime 137

3.2.6. Removal of brain from skull 137

3.2.7. Post-fixation of brain 138

3.2.8. Potential for fixation induced artifact 139

3.2.9. Brain volume measurement 140

3.2.10. Archival photography of brains

3.2.10.1. Equipment and materials 141
3.2.10.2 Standardized views of the brain 141

3.3. CEREBRAL ANATOMY AND VARIATION 154

3.3.1. Frontal lobe structures 154

3.3.1.1. Arcuate sulcus, Pattern I 156
3.3.1.2. Arcuate sulcus, Pattern II 162
3.3.1.3. Arcuate sulcus, Pattern III 163
3.3.1.4. Sub-central dimple, Patterns I, II, and III 164

3.3.2. Temporal lobe structures

3.3.2.1. Sylvian fissure and sylvian point 165
3.3.2.2. Sylvian point, Pattern I 166
3.3.2.3. Sylvian point, Pattern II 167
3.3.2.4. Sylvian point, Pattern III 171
3.3.2.5. The posterior temporal gyrus, inferior parietal gyrus and the supra-sylvian dimple and gyrus 177

CHAPTER 4 - THREE DIMENSIONAL MORPHOMETRY OF BRAIN SURFACE STRUCTURES

4.1. CHAPTER OVERVIEW 181

4.2. 3-D MEASUREMENT METHOD 183

4.3. 3-D LINEAR MEASURES OF FRONTAL LOBE STRUCTURES

4.3.1. Method for measuring 3-D length of arcuate sulcus 184

4.3.2. Results and analysis of 3-D arcuate sulcus measures

4.3.2.1. Left hemisphere arcuate sulcus, 3-D length 185
4.3.2.2. Right hemisphere arcuate sulcus, 3-D length 185
4.3.2.3. Hemispheric differences in 3-D arcuate sulcus length 188
4.3.2.4. Statistical analysis 193

4.3.3. Method for measuring 3-D length of central sulcus 193

4.3.4. Results and analysis of 3-D central sulcus measures

4.3.4.1. Left hemisphere central sulcus, 3-D length 194
4.3.4.2. Right hemisphere central sulcus, 3-D length 195
4.3.4.3. Hemispheric differences in 3-D central sulcus length 195
4.3.4.4. Statistical analysis 195

4.4. 3-D LINEAR MEASURES OF TEMPORAL LOBE STRUCTURES

4.4.1. Method for measuring 3-D length of sylvian fissure 202

4.4.2. Results and analysis of 3-D sylvian fissure measures

4.4.2.1. Left hemisphere sylvian fissure, 3-D length 204
4.4.2.2. Right hemisphere sylvian fissure, 3-D length 204
4.4.2.3. Hemispheric differences in 3-D sylvian fissure length 207
4.4.2.4. Statistical analysis 207

4.4.3. Method for measuring the 3-D length of superior temporal sulcus 212

4.4.4. Results and analysis of 3-D superior temporal sulcus measures

4.4.4.1. Left hemisphere superior temporal sulcus, 3-D length 213
4.4.4.2. Right hemisphere superior temporal sulcus, 3-D length 213
4.4.4.3. Hemispheric differences in 3-D superior temporal sulcus length 214
4.4.4.4. Statistical analysis 215

CHAPTER 5
TWO DIMENSIONAL MORPHOMETRY OF BRAIN SURFACE STRUCTURES

5.1. CHAPTER OVERVIEW 223

5.2. 2-D MEASUREMENT METHOD 227

5.3. FRONTAL LOBE STRUCTURES

5.3.1. 2-D linear measures of frontal lobe structures 228

5.3.1.1. Linear distance A-Cv 228
5.3.1.2. Linear distance A-Ci 228
5.3.1.3. Linear distances A-Cii, A-CIII and A-Civ 229
5.3.1.4. Linear distance A-SCD 229
5.3.1.5. Linear distance C-SCD 229
5.3.1.6. Linear distance AS-v 229

5.3.2. 2-D area measures of frontal lobe structures 230

5.3.2.1. Area A-Ci² 230
5.3.2.2. Area A-Cii² 230

5.3.3. Results of 2-D measures of frontal lobe structures 234

5.3.3.1 Vertical limb of arcuate sulcus 234
5.3.3.2 Series of five linear distance measures from arcuate sulcus to central sulcus 241
5.3.3.3. Linear distance from sub-central dimple to arcuate and central sulci 266
5.3.3.4 Area measures I & II of cortex between the arcuate sulcus and central sulcus 274

5.4. TEMPORAL LOBE STRUCTURES

5.4.1. 2-D linear measures of temporal lobe structures 281

5.4.1.1. Linear length SF-ap 281
5.4.1.2. Linear length STS-ap 282
5.4.1.3. Linear distances STG-v 283
5.4.1.4. Linear distance STG-i, STG-ii, STG-iii and STG-iv 284

5.4.2. 2-D area measures of temporal lobe structures 284

5.4.2.1. Area STG-Tpt² 284
5.4.2.2. Area STG-tot² 285

5.4.3. Results and analysis of 2-D measures of temporal lobe structures 290

5.4.3.1 Length of the sylvian fissure 290
5.4.3.2 Length of the superior temporal sulcus 293

5.4.3.3. Linear measure of superior temporal gyrus width, STG-i, STG-ii, STG-iii, STG-iv and STG-v 297
5.4.3.4. Area measures of the total superior temporal gyrus 317
5.4.3.5. Area measures of the posterior region of the superior temporal gyrus 321

5.5. FRONTAL AND OCCIPITAL PETELIAS AND HEMISPHERIC WIDTH

5.5.1. 2-D linear measures of hemispheric petelial projections 325
5.5.1.1. Linear distance FR-pet 326
5.5.1.2. Linear distance OC-pet 327
5.5.2. 2-D linear measures of hemispheric widths
5.5.2.1. Linear distance FRw-a 327
5.5.2.2. Linear distance FRw-p 328
5.5.2.3. Linear distance PAw-a 328
5.5.2.4. Linear distance PAw-p 329
5.5.3. Results and analysis of 2-D measures of frontal and occipital lobe petelias
5.5.3.1 Frontal lobe petelias 332
5.5.3.2 Occipital lobe petelias 335
5.5.3.3. Co-occurrence of frontal and occipital lobe petelias 338
5.5.4. Results and analysis of 2-D measures of hemispheric width 343
5.5.4.1 Anterior frontal lobe width 343
5.5.4.2 Posterior frontal lobe width 346
5.5.4.3. Anterior parietal lobe width 350
5.5.4.4 Posterior parietal lobe width 353

CHAPTER 6 - MORPHOMETRY OF STRUCTURES DEEP TO THE SURFACE OF THE BRAIN

6.1. CHAPTER OVERVIEW 357

6.2. SULCAL DEPTH MEASUREMENT METHOD 359

6.3. MEASURES OF SULCAL AND FISSURAL DEPTHS IN THE FRONTAL AND TEMPORAL LOBES

6.3.1. Depth of the arcuate sulcus 361

6.3.2. Depth of the central sulcus 361

6.3.3. Depth of the posterior sylvian fissure 361

6.4. RESULTS AND ANALYSIS OF SULCAL AND FISSURAL DEPTH MEASURES

6.4.1. Depth of arcuate sulcus

6.4.1.1. Interhemispheric dimensions of arcuate sulcus depth 365
6.4.1.2. Statistical analysis of interhemispheric distribution of arcuate sulcus depth 368

6.4.2. Depth of central sulcus

6.4.2.1. Interhemispheric dimensions of central sulcus depth 371
6.4.2.2. Statistical analysis of interhemispheric distribution of central sulcus depth 374

6.4.3. Depth of posterior sylvian fissure

6.4.3.1. Interhemispheric dimensions of sylvian fissure depth 377
6.4.3.2. Statistical analysis of interhemispheric distribution of sylvian fissure depth 383

6.4.4. Co-occurrence of depth measures of the arcuate sulcus, central sulcus and posterior sylvian fissure on the left and right hemispheres 384

CHAPTER 7 - DISCUSSION AND CONCLUSIONS

7.1. INTRODUCTION 387

7.2 ADVANCES IN METHODS AND SAMPLING IN THIS STUDY OF THE EVOLUTION OF PRIMATE BRAIN ASYMMETRY

7.2.1. Advances in tissue preparation and animal sample 387

7.2.2. Advances in measurement of brain structures 389

7.3 DISCUSSION OF THE RESULTS OF THIS STUDY

7.3.1. Anatomy and variation of structures examined in this study

7.3.1.1. Arcuate sulcus 392
7.3.1.2. Sub-central dimple 394
7.3.1.3. Sylvian point 394
7.3.1.4. Suprasylvian gyrus and supra-sylvian dimple 396

7.3.2. Morphometry of frontal lobe structures

7.3.2.1 3-D Measures of arcuate sulcus length 398
7.3.2.2. Two dimensional measures of arcuate sulcus and post arcuate cortex 402
7.3.2.3. Depth of the arcuate sulcus 404
7.3.2.4 Summary 406

7.3.3. Measures of the central sulcus
7.3.3.1. Central sulcus length 406
7.3.3.2. Central sulcus depth 407
7.3.4. Morphometry of temporal lobe structures
7.3.4.1. Sylvian fissure length 407
7.3.4.2. Sylvian fissure depth 408
7.3.4.3. Contrasting findings on sylvian fissure dimensions 409
7.3.4.4. Measures of the superior temporal gyrus and sulcus 410
7.3.4.5. Comparison of these finding with other studies of the superior temporal sulcus and superior temporal gyrus 412
7.3.5. Measures of frontal and occipital lobe petelias
7.3.5.1. Frontal lobe petelias 414
7.3.5.2. Occipital lobe petelias 415
7.3.5.3. Co-occurrence of frontal and occipital petelias 415
7.3.6. Measures of frontal and parietal lobe widths 416
7.3.7. Conclusions regarding petelial and hemispheric width asymmetries 417

7.4. EVOLUTIONARY IMPLICATIONS 418

APPENDIX FOR CHAPTER 5 427

BIBLIOGRAPHY 486

LIST OF TABLES

CHAPTER 3

Table 3-1 Semi quantitative analysis of anatomy and variation of the arcuate sulcus, subcentral dimple and sylvian point 172

CHAPTER 4

Table 4-1 Three dimensional linear measures of total arcuate sulcus length and paired t-Tests of hemispheric differences 186

Table 4-2 Three dimensional linear measures of total central sulcus length and paired t-Tests of hemispheric differences 196

Table 4-3 Three dimensional linear measures of total sylvian fissure length and paired t-Tests of hemispheric differences 205

Table 4-4 Three dimensional linear measures of total superior temporal sulcus length and paired t-Tests of hemispheric differences 216

CHAPTER 5

Table 5-1 Two dimensional linear measures of the length of the vertical portion of the arcuate sulcus, and paired t-Tests of hemispheric differences 235

CHAPTER 7

Table 7-1 Summary table of results, showing *P* values and hemispheric predominance, for all of the measures used in this study to assess cerebrocortical asymmetries 235

LIST OF FIGURES

CHAPTER 3

Figure 3-1 Low magnification photographs of superior and inferior aspects of *Macaca fascicularis* brain 144

Figure 3-2 Low magnification photographs of lateral aspects of left and right hemispheres in *Macaca fascicularis* brain 146

Figure 3-3 High magnification photographs of left and right frontal lobe in *Macaca fascicularis* brain 148

Figure 3-4 High magnification photographs of left and right posterior temporal and inferior parietal lobes in *Macaca fascicularis* brain 150

Figure 3-5 High magnification photographs of left and right anterior temporal lobe in *Macaca fascicularis* brain 152

Figure 3-6 Photographs of Patterns I and II of the arcuate sulcus 158

Figure 3-7 Photographs of Patterns II and III of the arcuate sulcus 160

Figure 3-8 Photographs of Patterns I, II and III of the sylvian point 169

Figure 3-9 Graph of anatomy and variation of the arcuate sulcus, subcentral dimple and sylvian point 175

Figure 3-10 Photographs of the posterior temporal and inferior parietal lobes with suprasylvian dimple and suprasylvian gyrus 178

CHAPTER 4

Figure 4-1 Scatter plots of 3-D linear measures of the length of the arcuate sulcus in total sample, females only and males only 189

Figure 4-2 Plots of hemispheric differences in the 3-D length of the arcuate sulcus in total sample, females only and males only 191

Figure 4-3 Scatter plots of 3-D linear measures of the length of the central sulcus in: total sample, females only and males only 198

Figure 4-4 Plots of hemispheric differences in the 3-D length of the central sulcus in total sample, females only and males only..... 200

Figure 4-5 Scatter plots of 3-D linear measures of the length of the sylvian fissure in: total sample, females only and males only 208

Figure 4-6 Plots of hemispheric differences in the 3-D length of the sylvian fissure in: total sample, females only and males only 210

Figure 4-7 Scatter plots of 3-D linear measures of the length of the superior temporal sulcus in: total sample, females only and males only..... 218

Figure 4-8 Plots of hemispheric differences in the 3-D length of the superior temporal sulcus in: total sample, females only and males only..... 220

CHAPTER 5

Figure 5-1 Diagram of frontal lobe illustrating the 2-D linear and area digital measures *A-Ci* - *A-Cv*, *A-Ci*^{2} and *A-Cii*^{2} made from lateral photographs..... 232

Figure 5-2 Plots of hemispheric differences in the 2-D length of the vertical portion of the arcuate sulcus in: total sample, females only and males only 238

Figure 5-3 Histograms of means and standard deviations for each of the five 2-D linear measures of the distance between the arcuate and central sulci in: total sample, females only and males only..... 242

Figure 5-4 Plots of hemispheric differences in lengths of measure *A-Ci*; the 2-D linear distance between the arcuate and central sulci in: total sample, females only and males only 246

Figure 5-5 Plots of hemispheric differences in lengths of measure *A-Cii*; the 2-D linear distance between the arcuate and central sulci in: total sample, females only and males only 249

Figure 5-6 Plots of hemispheric differences in lengths of measure *A-Ciii*; the 2-D linear distance between the arcuate and central sulci in: total sample, females only and males only 253

Figure 5-7 Plots of hemispheric differences in lengths of measure *A-Civ*; the 2-D linear distance between the arcuate and central sulci in: the total sample, females only and males only 256

Figure 5-8 Plots of hemispheric differences in lengths of measure *A-Cv*; the 2-D linear distance between the arcuate and central sulci in: the total sample, females only and males only 260

Figure 5-9 Plots of hemispheric differences in lengths for the five combined 2-D linear measures *A-Ci - A-Cv*; the distance between the arcuate and central sulci in: the total sample, females only and males only 264

Figure 5-10 Plots of hemispheric differences in lengths of the measure *A-SCD*; the 2-D linear distance between the arcuate sulcus and sub-central dimple in: the total sample, females only and males only 268

Figure 5-11 Plots of hemispheric differences in lengths of the measure *C-SCD*; the 2-D linear distance between the central sulcus and sub-central dimple in: the total sample, females only and males only 271

Figure 5-12 Plots of hemispheric differences in the area measure $A\text{-}Ci^2$; a global 2-D measure of the area of cortex between the arcuate and central sulci in: the total sample, females only and males only 275

Figure 5-13 Plots of hemispheric differences in the area measure $A\text{-}Cii^2$; a more restricted 2-D measure of the area of cortex between the arcuate and central sulci in: the total sample, females only and males only 279

Figure 5-14 Diagram of lateral aspect of the brain illustrating the 2-D linear and area digital measures, *SF-ap*, *STS-ap* and *STG-tot*, made from lateral photographs 286

Figure 5-15 Diagram of temporal lobe of the brain illustrating the 2-D linear and area digital measures, *STGi - STGv and STG-Tpt*^{2} made from lateral photographs 288

Figure 5-16 Plots of hemispheric differences in lengths of the measure *SF-ap*; the 2-D length of the sylvian fissure in: the total sample, females only and males only 291

Figure 5-17 Plots of hemispheric differences in lengths of the measure *STS-ap*; the 2-D length of the superior temporal sulcus in: the total sample, females only and males only 295

Figure 5-18 Plots of hemispheric differences in lengths of measure *STG-i*; the 2-D linear distance of the width of the superior temporal gyrus in: the total sample, females only and males only 299

Figure 5-19 Plots of hemispheric differences in lengths of measure *STG-ii*; the 2-D linear distance of the width of the superior temporal gyrus in: the total sample, females only and males only 302

Figure 5-20 Plots of hemispheric differences in lengths of measure *STG-iii*; the 2-D linear distance of the width of the superior temporal gyrus in: the total sample, females only and males only 305

Figure 5-21 Plots of hemispheric differences in lengths of measure *STG-iv*; the 2-D linear distance of the width of the superior temporal gyrus in: the total sample, females only and males only 308

Figure 5-22 Plots of hemispheric differences in lengths of measure *STG-v*; the 2-D linear distance of the width of the superior temporal gyrus in: the total sample, females only and males only 311

Figure 5-23 Plots of hemispheric differences in lengths for the five combined 2-D linear distance measures *STG-i - STG-v*; the width of the superior temporal gyrus in: the total sample, females only and males only 315

Figure 5-24 Plots of hemispheric differences in area of measure *STG-tot*^{2}; the 2-D area of the superior temporal gyrus in: the total sample, females only and males only 319

Figure 5-25 Plots of hemispheric differences in area of measure *STG-tot*^{2}; the 2-D area of the posterior region of the superior temporal gyrus in: the total sample, females only and males only..... 322

Figure 5-26 Diagram of superior aspect of the brain illustrating the 2-D linear digital measures, *FRw-a, FRw-p, PAw-a, PAw-p, FR-pet* of hemispheric width, and *FR-pet & OC-pet* of petelial projections, made from macrophotographs 330

Figure 5-27 Plots of hemispheric differences in the linear measure *FR-pet;* the petelial projections of the frontal lobe in: the total sample, females only and males only..... 333

Figure 5-28 Plots of hemispheric differences in the linear measure *OC-pet;* the petelial projections of the occipital lobe in: the total sample, females only and males only..... 336

Figure 5-29 Plots of left vs right hemispheric differences and co-occurrence of petelial projections of the frontal lobe and occipital lobe, in the total sample..... 340

Figure 5-30 Plots of hemispheric differences in the linear measure *FRw-a;* the width of the anterior portion of the frontal lobe, in: the total sample, females only and males only 344

Figure 5-31 Plots of hemispheric differences in the linear measure *FRw-p;* the width of the posterior portion of the frontal lobe, in: the total sample, females only and males only..... 348

Figure 5-32 Plots of hemispheric differences in the linear measure *OCw-a;* the width of the anterior portion of the occipital lobe, in: the total sample, females only and males only..... 351

Figure 5-33 Plots of hemispheric differences in the linear measure *OCw-p;* the width of the posterior portion of the occipital lobe, in: the total sample, females only and males only 354

CHAPTER 6

Figure 6-1 Diagram of the lateral aspect of the brain of *Macaca fascicularis* illustrating the sites along the arcuate and central sulci and posterior sylvian fissure of the measures of sulcal/fissural depth AS-d, CS-d and SF-d, and measurement constraints 363

Figure 6-2 Measures of arcuate sulcus depth on the left and right hemispheres; histograms of means and standard deviations; and paired t-Tests of hemispheric differences in: the total sample, females only and males only 366

Figure 6-3 Plots of hemispheric differences in the measure *AS-d;* the depth of the arcuate sulcus of the frontal lobe, in: the total sample, females only and males only 369

Figure 6-4 Measures of central sulcus depth on the left and right hemispheres; histograms of means and standard deviations; and paired t-Tests of hemispheric differences in: the total sample, females only and males only 372

Figure 6-5 Plots of hemispheric differences in the measure *CS-d;* the depth of the central sulcus of the frontal and parietal lobes, in: the total sample, females only and males only 375

Figure 6-6 Measures of sylvian fissure depth on the left and right hemispheres; histograms of means and standard deviations; and paired t-Tests of hemispheric differences in: the total sample, females only and males only 379

Figure 6-7 Plots of hemispheric differences in the measure *SF-d;* the depth of the sylvian fissure of the temporal lobe, in: the total sample, females only and males only 381

Figure 6-8 Plots of co-occurrence of the inter-hemispheric distribution of depth predominance in the arcuate sulcus, central sulcus and sylvian fissure in the total sample 385

LIST OF APPENDIX

CHAPTER 5 2-DIMENSIONAL MORPHOMETRY OF BRAIN SURFACE STRUCTURES

Appx 5-1 Table of values for the 2-D linear measures *A-Ci - A-Cv* of the distance between the arcuate sulcus and central sulcus on the left and right hemispheres 428

Appx 5-2 Paired sample t-Tests of values for the 2-D linear measures *A-Ci, A-Cii, and A-Ciii* of the distance between the arcuate sulcus and central sulcus on the left and right hemispheres in: the total sample, females only and males only 430

Appx 5-3 Paired sample t-Tests of values for the 2-D linear measures *A-Civ and A-Cv* of the distance between the arcuate sulcus and central sulcus on the left and right hemispheres in: the total sample, females only and males only 432

Appx 5-4 Histograms with standard deviations, and paired sample t-Tests of pooled values for the 2-D linear measures *A-Ci - A-Cv* of the distance between the arcuate sulcus and central sulcus on the left and right hemispheres in: the total sample, females only and males only 434

Appx 5-5 Table of values for the 2-D linear measure *A-SCD* of the distance between the arcuate sulcus and the sub-central dimple on the left and right hemispheres 436

Appx 5-6 Histograms with standard deviations, and paired sample t-Tests of values for the 2-D linear measure *A-SCD* of the distance between the arcuate sulcus and sub-central dimple on the left and right hemispheres in: the total sample, females only and males only 438

Appx 5-7 Table of values for the 2-D linear measure *C-SCD* of the distance between the central sulcus and the sub-central dimple on the left and right hemispheres 440

Appx 5-8 Histograms with standard deviations, and paired sample t-Tests of values for the 2-D linear measure *C-SCD* of the distance between the central sulcus and sub-central dimple on the left and right hemispheres in: the total sample, females only and males only 442

Appx 5-9 Table of values for the two 2-D area measures *A-Ci²* and *A-Cii²* of the area of cortex between the arcuate and central sulci on the left and right hemispheres 444

Appx 5-10 Paired sample t-Tests of values for the two 2-D area measures *A-Ci²* and *A-Cii²* of the area of cortex between the arcuate and central sulci on the left and right hemispheres in: the total sample, females only and males only 446

Appx 5-11 Table of values for the 2-D linear measure *SF-ap* of the length of the sylvian fissure on the left and right hemispheres 448

Appx 5-12 Paired sample t-Tests of values for the 2-D linear measures *SF-ap* and *STS-ap* of the lengths of the sylvian fissure and superior temporal sulcus on the left and right hemispheres in: the total sample, females only and males only 450

Appx 5-13 Table of values for the 2-D linear measure *STS-ap* of the length of the superior temporal sulcus on the left and right hemispheres in the total sample 452

Appx 5-14 Table of values for the five independent 2-D linear measures *STG-i* - *STG-v* of the width of the superior temporal gyrus on the left and right hemispheres in the total sample 454

Appx 5-15 Paired sample t-Tests of values for the 2-D linear measures *STG-i, STG-ii, and STG-iii* of the width of the superior temporal gyrus on the left and right hemispheres in: the total sample, females only and males only 456

Appx 5-16 Paired sample t-Tests of values for the 2-D linear measures *STG-iv and STG-v* of the width of the superior temporal gyrus on the left and right hemispheres in: the total sample, females only and males only; and histograms of means and standard deviations of the five measures *STG-i* - *STG-v* 468

Appx 5-17 Table of values for the 2-D area measure *STG-tot²* of the total area of the superior temporal gyrus on the left and right hemispheres in the total sample 460

Appx 5-18 Histograms with standard deviations, and paired sample t-Tests of values for the 2-D area measure *STG-tot²* of the total area of the superior temporal gyrus on the left and right hemispheres in: the total sample, females only and males only 462

Appx 5-19 Table of values for the 2-D area measure *STG-Tpt²* of the area of the posterior portion of the superior temporal gyrus on the left and right hemispheres in the total sample 464

Appx 5-20 Histograms with standard deviations, and paired sample t-Tests of values for the 2-D area measure *STG-Tpt²* of the area of the posterior portion of the superior temporal gyrus on the left and right hemispheres in: the total sample, females only and males only 466

Appx 5-21 Table of values for the 2-D linear measures *FR-pet* and *OC-pet* of the hemispheric distribution of petelial projections of the frontal and occipital poles in the total sample 468

Appx 5-22 Histograms with standard deviations, and two sample, assuming equal variance t-Tests, of values for petelial projections of the frontal lobes in: the total sample, females only and males only 470

Appx 5-23 Histograms with standard deviations, and two sample (assuming unequal variance) t-Tests, of values for petelial projections of the occipital lobes in: the total sample, females only and males only 472

Appx 5-24 Table of values for the two independent 2-D linear measures *FRw-a* and *FRw-p* of the width of the anterior and posterior portions of the frontal lobe in the left and right hemispheres of the total sample 474

Appx 5-25 Histograms with standard deviations, and two sample (assuming unequal variance) t-Tests, of values for the width of the anterior portion of the frontal lobe in the left and right hemispheres in: the total sample, females only and males only 476

Appx 5-26 Histograms with standard deviations, and two sample (assuming unequal variance) t-Tests, of values for the width of the posterior portion of the frontal lobe in the left and right hemispheres in: the total sample, females only and males only 478

Appx 5-27 Table of values for the two independent 2-D linear measures *PAw-a* and *PAw-p* of the width of the anterior and posterior portions of the parietal lobe in the left and right hemispheres of the total sample 480

Appx 5-28 Histograms with standard deviations, and two sample (assuming unequal variance) t-Tests, of values for the width of the anterior portion of the parietal lobe in the left and right hemispheres in: the total sample, females only and males only 482

Appx 5-29 Histograms with standard deviations, and two sample (assuming unequal variance) t-Tests, of values for the width of the posterior portion of the parietal lobe in the left and right hemispheres in: the total sample, females only and males only 484

CHAPTER 1

INTRODUCTION AND OVERVIEW

1.1 INTRODUCTION

This chapter provides a brief overview of the organization and direction of this dissertation. Full discussion of each of the issues mentioned here, with full literature citations, will be found in subsequent chapters.

A central question in anthropology concerns when and how language arose during hominid evolution. The role played by the brain in the evolutionary processes underlying language acquisition in hominids is not well understood. This dissertation contributes to testing the hypothesis that: *the neural substrate for human language has a long evolutionary history within primates and was present in basal form in the common ancestor of cercopithecoids and hominoids.* For the purposes of this study I have constrained my approach to this evolutionary level within primates. However, it is quite likely that there may have been an even earlier primate common ancestor that expressed this neural character.

In this evolutionary hypothesis, which proposes a long evolutionary history within primates for these brain mechanisms, the following succession of events probably took place. Subsequent to the divergence of hominoids and cercopithecoids, during the early period of hominoid evolutionary differentiation, this neural substrate was incorporated and modified to subserve the increasingly more complex communicative milieu. Later, during early hominid evolution, these neural refinements progressed even

further in order to complement the major cognitive advances occurring at this time.

In contrast, it has also been proposed that the brain mechanisms underlying human language evolved quite recently in a punctuated manner, are unique to *Homo sapiens*, and have no neural precursor. This alternate view is based upon two different lines of evidence: 1) the assumption that the universality and unique nature of human linguistic structure reflects an equally unique neural substrate; and 2) that the relatively recent appearance of art in the archeological record indicates the advent of language in modern humans.

This dissertation focuses on the first hypothesis in which it is proposed that brain mechanisms for language in humans have evolutionary precursors in the brains of cercopithecoid primates. In humans, there are a number of regions in the cerebral cortex that have been shown to be involved primarily with language functions. These regions, which are located in the left hemisphere, are known as Broca's and Wernicke's expressive and receptive language areas respectively. Structures on the surface of the human brain that are associated with these cortical language regions show anatomic asymmetry in their hemispheric expression. As discussed in detail in Chapter 2, a brain region that is primarily involved with a specific function is generally larger than the contralateral non-functional side, hence: functional asymmetry (with side predominance) equals anatomical asymmetry (with same side predominance). With regard to human brain language substrates, asymmetries underlie the co-occurrence of functional localization and primary gross anatomical expansion of *left hemisphere* cortical regions in both the frontal and temporal lobes. This basic tenet of anatomical and functional asymmetry has been in place for more than a century and, indeed,

has more recently been brought to the forefront in the 1960's by the seminal work of Norman Geschwind (see Chapter 2).

In macaques some cerebrocortical structures considered homologous to these human language regions have been identified. Whether these homologous cortical regions in macaques also subserve communicative functions is currently unknown. If these homologous regions in macaques also show a similar pattern of hemispheric asymmetry to that seen in humans it would support the hypothesis that a similar pattern of functional localization is also present. Obviously, macaques do not use an identical communicative modality as that used by humans. However, within the constraints of species-specific communicative requirements, it could be argued that a similar role might be played by these neural substrates.

This dissertation involved quantitation and analysis of hemispheric asymmetry of these homologous cortical regions in macaques. Results are compared to patterns of asymmetry known for humans. Further, the observations made in this study of brain asymmetry are incorporated into the existing theoretical framework regarding hemispheric asymmetry and functional localization of communicative functions in both human and non-human primates. Finally, these theoretical underpinnings in combination with the results obtained from this study are used to develop a model of the probable sequence of events that took place during hominoid evolution that gave rise to the evolutionary advent of language during early hominid evolution.

1.2. OVERVIEW OF CHAPTERS 2 - 7

This section provides overviews of the material covered in chapters two through seven. This dissertation is divided into four main sections. The first section (Chapter 2) presents the background material upon which this dissertation was based. The second section (Chapter 3) details methodological advances and constraints, as well as issues pertaining to inter-individual variation within the sample. The third section (Chapters 4-6) presents results of the multiple approaches to quantitation of inter-hemispheric asymmetry in the cerebral cortex. Finally, the fourth section (Chapter 7) provides an overview of the results of this dissertation compared to previous work and places these results in an evolutionary perspective.

1.2.1. Chapter 2 - Background

This chapter provides an overview of the theoretical framework upon which this dissertation was based. First, a historical overview of the localization of language functions in the cerebral cortex of humans is presented. The underlying scientific thinking in the early nineteenth century that gave rise to the advent of aphasiology, the study of functional localization of language by observation of deficits after brain lesions, is discussed within the context of phrenology, the period paradigm of the early nineteenth century.

Subsequent sections focus on the results obtained from more recently developed techniques for assessing the physiological mechanisms underlying brain language substrates. These techniques include electrical stimulation mapping, dichotic listening, the Wada test and both anatomic and functional imaging as they have been used to assess the anatomic and physiologic basis of language in the brain. The controversial issue of a right hemisphere

involvement in conjunction with the left hemisphere is presented in light of new evidence that the role of these right hemisphere homotypic regions, operating within the functional mosaic underlying language, is more important than was previously thought. The relationship between patterns of cerebral localization for language and for handedness in humans is also considered since this may be directly relevant to the origins of language in hominids.

In order to provide a comparative framework, both for my results and those reported in previous studies of non-human primates, the history of studies on patterns of gross anatomic inter-hemispheric asymmetry present in human brain language related areas is reviewed. This is followed by a review of both anatomic and physiologic studies conducted in non-human primates. These non-human primate studies include investigations using experimental techniques, similar to those used in humans, such as electrical stimulation mapping and post lesion functional deficits as well as studies of cerebrocortical inter-hemispheric asymmetry. Finally, results from studies of handedness and non-vocal, visual-gestural, communication in non-human primates are discussed with regard to their similarities to the human condition.

This overview is followed by a section on the nature of homology in the nervous system. Specifically, the nature of, and evidence for, the homologous relationship between established language regions in human brains and in the brains of non-human primates is discussed. The body of evidence supporting these homology hypotheses is detailed since this dissertation is based upon the evolutionary hypothesis that regions in *Macaca fascicularis* brains that are homologous to human language regions also express a similar pattern of gross anatomic hemispheric asymmetry.

1.2.2. Chapter 3 - Materials and methods and anatomy and variation of cerebral cortex in *Macaca fascicularis*

The first section outlines the rationale for the Old World monkey species used in this study. Methods used for the collection and preparation of brains are discussed and compared to those of other studies. In addition, the technical advances incorporated into this study are detailed. Finally, the procedure used to produce a series of photographs of brains in standard positions for use in two dimensional digital measures is described along with color plate illustrations of the brain regions under study.

Subsequent sections describe the anatomy and variation present within the cerebrocortical structures chosen for digital quantification. An analysis of the pattern of anatomical expression and sample distribution of brain surface structures in *Macaca fascicularis* such as the arcuate sulcus, sub-central dimple, sylvian fissure and sylvian point is presented. This analysis of sample variation provided a detailed anatomical framework upon which the multiple two and three dimensional measures presented in chapters four, five and six were founded and upon which results were analyzed and interpreted.

1.2.3. Chapter 4 - Three dimensional (3-D) morphometry of brain surface structures

This chapter presents methods and results of a specific series of measures that were taken directly from cerebrocortical structures located on the surface of perfusion-fixed macaque brains. Initially, the specific methods used for data collection and the precise technical definitions for each of the measures used are described.

Although structures such as gyri and fissures were measured as they coursed across the three dimensional surface of the brain, values are not

represented by a three dimensional (3-D) coordinate data matrix (i.e., x, y, and z coordinates). Instead, *curvilinear* measures, which were made directly from the surface of brains, were transposed into two-dimensional (2-D) linear values for subsequent quantitation and statistical analysis. However, since these transposed values reflect directly the length of the complex 3-D contour (and thus contain potentially critical information beyond a 2-D assessment) they will be referred to in this dissertation as "three-dimensional" measures. This also serves to distinguish these measures from my true "two dimensional" linear measures that were taken solely from brain photographs.

Structures measured in this portion of my study include the arcuate sulcus and central sulcus of the frontal lobe and the sylvian fissure and superior temporal sulcus of the temporal lobe. These measures were made on both the left and right cerebral hemispheres. Results for the total sample were subjected to statistical analysis using paired t-tests, then males and females analyzed and compared separately. Further, the distribution of hemispheric differences in side predominance for each of the measures are presented graphically for both the total sample and for sex specific sub-samples.

1.2.4. Chapter 5 - Two dimensional (2-D) morphometry of brain surface structures

Chapter five presents methods and results of a large series of two dimensional measures of cerebrocortical structures located on the lateral surface of perfusion-fixed macaque brains. These measures were made from both high and low magnification photographs of both cerebral hemispheres. A second series of measures were made from photographs of the dorsal surface of the brain. These latter measures involved quantitation of frontal

and occipital pole petelias and left and right hemispheric widths of the frontal and parietal lobes. All measures were made directly from photographs of macaque brains using a digitizing stylus and pad or in the case of petelias, directly from a calibrated microscope. The specific definitions for measures of frontal lobe and temporal lobe structures are presented separately at the beginning of each subsection. In each subsection, paired sample t-Tests were used to compare the size of structures on the left and right hemispheres and ascertain the presence of hemispheric predominance. Further, for each series of measures the absolute difference in size of individual structures on the left and right hemispheres is plotted to show the sample distribution pattern. For measures of frontal and occipital petelial projections the sample distribution of patterns of co-occurrence is analyzed for comparison to that of humans. Since the data from chapter five is extensive, the majority of tables and statistical analyses are located in the appendix. Graphs of the sample distribution of inter-hemispheric differences in various measures are included in text.

1.2.5. Chapter 6 - Three dimensional (3-D) morphometry of structures deep to the surface of the brain

Chapter 6 presents the methods used and results obtained from a series of measures of the depth of structures that are adjacent to cortical regions homologous to human brain language centers. Structures measured include the arcuate sulcus and central sulcus (adjacent to the region homologous to Broca's Area) of the frontal lobe, and the posterior portion of the sylvian fissure between the temporal and parietal lobes (adjacent to the region homologous to Wernicke's Area). Results of sulcal depth measures on the left and right hemispheres were analyzed using paired t-Tests to ascertain

patterns of cerebral asymmetry and hemispheric predominance. Further, the sample distribution and magnitude of hemispheric differences in each of the three depth measures are plotted for all individuals within the sample and separately for males and females. Finally, the patterns of hemispheric co-occurrence of the three depth measures are analyzed.

1.2.6. Chapter 7 - Discussion and conclusions

Chapter 7 is divided into three main sections. The first section presents issues concerning the methodological advances made in this study. This includes tissue preparation methods and the accuracy of measurement techniques detailed in Chapter 3. The second part is divided into sub-sections which discuss results from each of the different studies and measures presented in Chapters 3 - 6 and compares them to data and conclusions made in previous studies. Finally, the third part of Chapter 7 presents a discussion of the evolutionary implications resulting from both this and other studies as they relate to the origins of language during human evolution.

CHAPTER 2

BACKGROUND

2.1. INTRODUCTION

The evolutionary origins of vocal-auditory language, that uniquely human trait, is an issue that has long fascinated biological scientists. For example, Charles Darwin addressed this in: *Descent of Man, and Selection in Relation to Sex*, "As the voice was used more and more, the vocal organs would have been strengthened and perfected through the principle of the inherited effects of use; and this would have reacted on the power of speech. But the relation between the continued use of language and the development of the brain has no doubt been far more important. The mental powers in some early progenitor of man must have been more highly developed than in any existing ape, before even the most perfect form of speech could have come into use; but we may confidently believe that the continued use and advancement of this power would have reacted on the mind itself, by enabling and encouraging it to carry on long trains of thought." (Darwin, 1887: 87-88). More than a century later, similar concepts of interactions between cognitive and communicative traits have been presented in light of evidence from current neurobiological and cognitive sciences (e.g., Deacon,

1992a). In a similar manner, the central hypothesis of this dissertation is grounded within this global concept of continuity between the neural substrate for communication in humans and their catarrhine ancestors.

Darwin also spoke of the many differences in "mental faculties" between humans and "higher" primates, which, although great in some cases, were considered simply a matter of degree, with one exception (Darwin, 1887). This one exception was human language. Again, more than a century later, the linguist Noam Chomsky proposed a similar hypothesis to that of Darwin's; that since the underlying linguistic structure of human language is unique, it could not have a precursor in non-human primates (Chomsky, 1980). Chomsky concluded that human language arose de novo in a punctuated evolutionary event giving rise to the "language organ" of the human brain. In contrast, the underlying hypothesis of continuity in brain mechanisms for communication within primates, central to this dissertation, does not view human language as a unique entity. Instead, it is viewed as the product of a series of evolutionary changes, and one that reflects the major cognitive advances that were shaped during human evolution.

The neural substrate for vocal-auditory communication in humans is one of the most complex processing networks in the brain involving multiple interacting elements (Bachman and Albert, 1991; Ojemann, 1991). Due perhaps to this complexity, simplistic models describing the localization of language/speech functions in human cerebral cortex changed little for almost

a hundred years since their conception during the nineteenth century of Marc Dax and Paul Broca (Broca, 1861; Dax, 1865a, b). In turn, these individuals were influenced by antecedent phrenologic principles.

Since the middle of the twentieth century, more sophisticated data on brain language substrates has been obtained using a variety of innovative techniques. These techniques include functional 3-D imaging of regional cerebral bloodflow (Flowers et al., 1991), recording of neural electrical activity (Wallesch et al., 1985; Flowers et al., 1991), cortical stimulation (Ojemann, 1990,91), cerebral localization of signed and second languages (Bellugi, et al., 1983, 1988), and the study of functional deficits after brain lesions. The synthesis of data acquired from such recent technology is beginning to revolutionize our understanding of the cortical organization of language.

This chapter presents an overview of our current understanding of the anatomical and functional bases of human language processing in the brain. Also reviewed are studies of non-human primate brain anatomy and physiology as it applies to the study of brain language mechanisms. This includes studies of functional and anatomic brain asymmetry and functional localization, and the homology of brain areas related to speech and language in humans and communication in non-human primates (for a review of homology in the brain see Section 2.6) . The question of whether the brain mechanisms underlying our species-specific form of vocal-auditory

communication are unique among primates has been open to much debate. Although the existence of a unique "speech organ" in the human brain has been proposed (Chomsky, 1980) there is no other example of such a radical departure from pre-existing architecture in the mammalian nervous system. Neuroscientists have recently shown that there is good evidence in Old World monkeys for the presence of a neural framework homologous to that used for speech and language in humans, e.g. see (Pandya and Sanides, 1973; Galaburda and Pandya, 1982; Deacon, 1988, 1992a). The functions of such putative homologous circuitry in monkeys and apes in their communicative capacity, however, are not well understood. However, studies of the neural mechanisms underlying non-human primate vocalizations have been unable to establish a relationship between these and the brain mechanisms human language (McLean and Newman, 1988). Studies of primate communicative behavior have incorporated an appreciation of subtle, and not necessarily vocalization-based, communicative repertoires. Such communicative modalities may well form cognitive precursors to the language abilities of humans and be subserved by similar brain mechanisms (Ristau and Robbins, 1982).

2.2. HISTORY OF LANGUAGE LOCALIZATION IN THE HUMAN BRAIN

2.2.1. Phrenology and the pre-aphasiology period

The early nineteenth century was a period when radical advances were being made with regard to our understanding of the localization of general functions within the brain. It was within this intellectual ferment that the pseudo-scientific discipline of phrenology was being actively practiced by many researchers using both humans and animals as their subjects.

For example, the work of the phrenologist Franz Joseph Gall (1758-1828), in particular, contributed much to the discipline. His work inspired many others to study the localization of brain organization thought to underlie human behaviors and thought processes. In his work on the brain, Gall concluded that the cerebral cortex comprised twenty seven "organs", each of which subserved a discrete psychological function (Gall, 1819). Although Gall placed the cerebral localization of functions, such as verbal memory and speech, in the "anterior lobe" (= the frontal lobe) he did not make any distinction between the two hemispheres. In fact, he concluded that functions in the brain, like all other organs in the body, were bilaterally represented (Gall, 1810). This concept of anatomical and functional cerebral symmetry versus Broca's later reports on hemispheric specialization and functional asymmetry, represented the period paradigm of the early

nineteenth century. This followed largely from the influence of the prominent French physician and physiologist Marie François Xavier Bichat who professed that "Harmony is to the functions of the organs what symmetry is to their conformation; it supposes a perfect equality of force and action, as symmetry indicates an exact analogy in the external forms and internal structure. It is a consequence of symmetry; for two parts essentially alike in their structure, cannot be different in their mode of acting." (cited in Harris, 1991, p.5). It is important to note, however, that the work of Bichat, Gall and their contemporaries such as Pierre Flourens and Jean-Baptiste Boillaud, set the stage, and provided a fertile intellectual climate for later, more scientifically based discoveries regarding the asymmetric localization of functions in the cerebral cortex of humans.

2.2.2. The discovery of cerebral asymmetry for human language functions

The discovery that aspects of human language functions were specifically localized to the third convolution in the left frontal lobe of the brain was first published by the French physician Paul Broca in 1861 (see also Broca, 1865a, b). His observations were at this point preliminary, being based on a limited series of patients, including the well known "Tan" (who was so named as this was the only syllable he could speak). Broca presented only limited aspects of the linguistic deficit and pathology of the lesion. His observations were

based on neurological-functional testing of deficits resulting from lesions of the cerebral cortex in the region of the inferior frontal lobe.

Some years later, Gustav Dax, the son of Marc Dax, presented evidence (Dax,G, 1865a, b) that his father had previously reported that language functions were localized to the left frontal lobe twenty five years earlier in 1836. As such, he claimed that the intellectual priority of such a major discovery should rightly belong to his father and not Broca. However, since the original communication by Dax was in the form of an unpublished memo made in Montpellier in 1836, the case was decided against by the scientific community of the time. The memo was finally published, however, in 1865 (Dax,M, 1865).

Broca made his definitive statement on brain language localization in a presentation to meeting of the Société Anthropologique (Broca, 1865a). He made the first observations on the relationship between the brain localization of handedness and speech. Right handed individuals were described as being predominantly left hemisphere dominant for both language and handedness, while left handed individuals were suggested to be right hemisphere dominant for speech functions. This view regarding left-hemisphere dominance for language in right handers soon became dogma. However, in 1899 Bramwell reported exceptions, demonstrating for the first time a case of "crossed aphasia" (Bramwell, 1899). Crossed aphasia involved aphasic symptoms that resulted from lesions in the right cerebral hemisphere in both

left and right handers. It was discovered later that this was the case mostly in left handers being relatively rare in right handers. Further, it is now well documented that only a small proportion of left-handed individuals are right hemisphere dominant for speech functions (Joanette, 1989).

Although Broca had not specifically reported that *all* left-handed individuals were right hemisphere dominant for speech, he did allude to the possibility. The notion was rapidly adopted by many individuals and propagated throughout the scientific community, becoming known as the "conjunction principle". This principle reached the status of a neurophysiological law within a short period, being supported by many prestigious physicians and scientists of the time, e.g. (Jackson, 1880; Paget, 1887) and even being incorporated in a standard neurology text (Gowers, 1885). Although there were many dissenters who presented contradictory evidence, the conjunction principle was upheld as an accepted law for a century (Joanette, 1989). Over eighty years later, in 1949, the first studies to challenge seriously the conjunction principle were made by the German neurologist Klaus Conrad (1949). A series of supporting studies followed in the next two decades, and the conjunction principle was finally put to rest.

This presently well characterized relationship between cerebral localization for handedness and speech functions has significance for our understanding of the evolution of language in hominids. The question of how

such a relationship may have arisen inspired many studies of handedness in non-human primates.

2.2.3. Contributions of aphasiology to language localization in human brains

Less than a decade after the 1865 report by Broca, the German physician Carl Wernicke reported that another region of the cerebral cortex, when damaged, gave rise to aphasia-like symptoms (Wernicke, 1874). This region was located in the posterior region of the superior temporal gyrus and portions of the adjacent parietal lobe. These two cerebrocortical regions, defined by observation of lesion-induced functional deficits over more than a century, are still known to this day as Broca's and Wernicke's language areas.

Until quite recently the classical method used to study cerebral localization of language functions was aphasiology. Aphasiology involved the study of the speech and language abilities of individuals with specific brain lesions (caused by cerebral hemorrhage or the like). Although these studies contributed much to our understanding of language function localization in the brain, they were prone to many problems, giving rise to interpretative inaccuracies. For example, in some individuals, even though extremely large lesions were localized to these lesion-defined language areas, speech functions were essentially intact. In contrast, other individuals with lesions outside the borders of the "classic" speech areas showed substantial speech or

comprehension deficits (Caplan, 1981). Anomalies such as these were noted as early as 1914 in a comprehensive review correlating diagnoses made by testing functional deficits with findings of lesion placement made upon post-mortem examination (von Monakow, 1914). In his report, von Monakow categorized the various types of lesions that fit with specific, defined symptoms of aphasia as well as those that did not. A later text by Goldstein (1927) also pointed out the problems of correlating lesions with deficits without a good understanding of the underlying and complicating variables. These variables include such things as lesions that do not involve the specific cortical language area but may be located along the route of a fiber pathway that does. This could potentially prevent a major influence coming to a language area from a distal site (Seldon, 1985).

A recent report exemplifies the confusion and interpretative ambiguity inherent to the functional evaluation of aphasic symptoms (Daffner et al., 1991). They described a patient who showed the classic language deficit profile symptomatic of Broca's aphasia. They then subjected the individual to various tests of cerebral localization such as magnetic resonance imaging and cortical stimulation, and discovered that the lesion was in fact localized to Wernicke's posterior speech reception area. They concluded that the brain-behavior correlations in this patient cannot be understood in terms of the formulations of traditional aphasiology.

The use of aphasiology as a tool for understanding the localization of language functions in the human brain has been in use for more than a century. Although it has provided us with a good basal framework, the recent development of a myriad of more precise physiological techniques has expanded our knowledge considerably. Some of the more recent techniques that have been used to study language localization in the human brain will now be reviewed.

2.3. PHYSIOLOGICAL STUDIES OF LANGUAGE LOCALIZATION IN THE HUMAN BRAIN

2.3.1. Introduction

Since the middle of the twentieth century a number of alternatives to the use of aphasiology to study functional localization of language in the cerebral cortex of humans have been discovered. These more refined techniques have provided the means to understand better the complex relationships that are present between some language-related areas of the cerebral cortex. For example, instead of the often gross poorly defined lesions that were used in aphasiology studies, temporary lesions, only a few millimeters in diameter could be induced by the use of local electrical stimulation. Such refinements are still being introduced; for example, the use of non-invasive functional imaging of the language-activated cortex in awake humans, is but one of

these new techniques that allows precise localization of specific sub-sets of language functions.

2.3.2 Electrical stimulation mapping

Electrical stimulation mapping was developed in the 1940's by neurosurgeons at the Montreal Neurological Institute as a powerful new method of cortical language localization in humans (Penfield and Rasmussen, 1950; Penfield and Welch, 1951; Penfield and Roberts, 1959). Unlike aphasiology it allowed for a specific localization of discrete cortical sub-areas (to a resolution of ~5mm) involved with language functions.

These workers developed a technique which allowed them to perform surgical excision of, e.g. brain tumors or epileptic foci, that were located adjacent to areas of the speech/language cortex in the left hemisphere (e.g. Broca's or Wernicke's areas) while maximally retaining post-operative language functions. The method involves use of local anesthesia to remove a window of bone from the skull and expose the surface of the cerebral cortex in fully awake and alert patients. Electrical stimulation electrodes are then applied to the surface of the cortex and an weak alternating current administered. This stimulation gives rise to multiple effects on brain function such as blockade of nerve fiber impulse conduction, primary or secondary neuronal excitation or inhibition (both proximally or distally) (Ranck, 1975).

It has been shown that electrical stimulation can reliably and predictably disrupt ongoing language tasks. As such, it appears to act as a "temporary lesion" with no post-stimulation after-effects (Ojemann, 1983). Tests administered during the stimulation period involve several aspects of language related functions, including e.g., object naming, reading, short-term verbal memory, orofacial mimicry, and phoneme identification (Ojemann, 1983). Unfortunately, since the duration of stimulation is usually fifteen seconds or less only short-term, thus more limited, language tasks, can be used (Ojemann, 1983).

Using electrical stimulation mapping, neurosurgeons were able to spare areas of cortex involved with language functions as much as possible and thus improve the quality of life of the patient post-operatively. Furthermore, in a large samples of patients it was possible to map systematically the distribution and variation of cortical sites involved with language functions (Penfield and Roberts, 1959). For the firsts time these early studies determined that there were no magic "pigeon holes" in the cerebral cortex where individual words were sorted out as had been previously thought (Penfield and Roberts, 1959).

Later, more detailed studies, which also used a similar electrical stimulation mapping approach to cortical localization of language functions, were conducted largely by George Ojemann and co-workers (Ojemann, 1978, 1983, 1991, 1992; Creutzfeldt et al., 1989; Haglund et al., 1993). These

studies demonstrated that language representation in the human brain was more widely distributed than previously thought and was compartmentalized into multiple separate systems, each subserving different tasks (Ojemann, 1991). In support of results from aphasiology studies, it was shown that also present were certain "essential areas" which corresponded to the classic speech-language areas of Broca and Wernicke. It was shown, however, that there was a great deal of inter-individual variation in the cortical location of many of these functional sites. For example, electrical stimulation of multiple sites *within* the margins of the classic Broca's area elicited no discernible language changes in 21% of subjects (Ojemann, 1991). Likewise, stimulation within the margins of the traditional Wernicke's area showed no functional change in 36% of individuals. Similar phenomena have been described in aphasiologic studies where lesions involving these classic cortical speech/language sites do not give rise to any language deficit, see e.g. (Bogen and Bogen, 1975).

Although Broca's and Wernicke's areas have been well studied by electrical stimulation techniques, secondary language areas such as the supplementary motor cortex and basal temporal region, are not as well studied and their role is less well known. However, a recent study using subdural electrical stimulation electrodes implanted into the left hemisphere "basal temporal language area" demonstrated that stimulation of this region gave rise to global receptive and expressive aphasia with speech arrest

(Lüders et al., 1991). It was suggested that the basal temporal language area may correspond to what Wernicke originally called the "Wortschatz" (word-vocabulary), an area involved with establishment of a link between symbolic verbal material and corresponding non-verbal expressions. Wernicke originally thought this functional site was located around the posterior language area. Since the behavioral outcome of these stimulation studies of sub-cortical sites was similar to that seen after lesion of the two classic cortical language areas, it was suggested that interference at many points within the interconnected language regions could give rise to identical deficits (Lüders et al., 1991).

Using the same electrical stimulation methods, the cortical sites of multiple language representation have been studied. For example, in polyglots, the localization of cortical sites associated with naming objects can show a considerable degree of dissociation (Ojemann and Whitaker, 1978). Cortical sites, which when stimulated, gave rise to naming deficits, were consistently larger for the second (thus presumably less proficient) languages. It was thought that this reflected a less efficient (thus larger) cortical functional organization which would be reduced as second language competency increased. Further, that "exact cortical sites related to a language process may not be stable over time even in adult life, expanding or shrinking in relation to facility with a particular function (Ojemann, 1983).

One of the most significant advances made by electrical stimulation mapping studies for our understanding of language localization in human brains is that Broca's and Wernicke's areas are not singular modalities (i.e., self-sufficient functional units). Instead, they appear to serve as convergence zones operating within a much larger, more distributed network of language sub-areas. For example it has been shown that electrical stimulation of cortical sites well outside the classic language areas in the frontal, temporal and parietal lobes gave rise to specific language deficits (Ojemann, 1991). Ojemann has concluded that in order to elucidate the organization language functions in the brain, future studies should incorporate a model based on the concept of multiple modular cortical systems (Ojemann, 1991). In this model, each of the language sub-systems is involved with specific aspects of language and comprises both multiple "essential areas" or foci (e.g., Broca's and Wernicke's areas), as well as more dispersed "sub-areas". All elements, or sub-populations of the multiple distinct units, are activated in parallel (Ojemann, 1991). Ojemann's concept of language localization in the human brain has been supported by evidence from many other approaches and techniques.

2.3.3. The dichotic listening test

The dichotic listening test was developed to determine non-invasively the cerebral lateralization of (vocal auditory) language reception and processing

functions in the temporal lobe of humans (Broadbent, 1954; Kimura, 1961; Bryden, 1967). This method involves presentation of either spoken human speech components, such as individual digits and consonant-vowel syllables, or non-verbal stimuli like a metronome or non-speech, delivered separately via headphones, (e.g., see Shankweiler and Studdert-Kennedy, 1967; Studdert-Kennedy and Shankweiler, 1970; Jäncke, 1992). Individuals are presented simultaneously with a series of different combinations of auditory stimuli to the left and right ears. Subjects are then required to indicate (e.g., by pushing a button) when they perceive a particular pre-defined target stimulus, or to repeat it vocally (Bryden, 1988).

In right-handed individuals, a strong right-ear (= left hemisphere) advantage was most clearly apparent by use of the consonant-vowel test (Bryden, 1988; Jäncke, 1992). This means that although different auditory stimuli are presented contemporaneously, the one presented to the right ear is preferentially perceived. Auditory information from the right ear cochlea is transmitted along neural pathways which pass primarily to structures in the contralateral left hemisphere. As such, this right ear advantage is thought to represent an enhanced ability of the left hemisphere cortex for temporal discrimination of auditory information. In addition, there is an eight millisecond advantage in the latency of neural impulses to the cortex of the dominant hemisphere (Romani et al., 1982)

One of the problems with the dichotic listening method is that there is a great deal of variation in outcomes between the different test types (e.g. verbal/non verbal/stimulus type) and both within and between individuals tested at different times (Blumstein,JL et al., 1975; Jäncke et al., 1992). The presence of such variation has raised questions as to whether results from dichotic listening tests truly represent preferential activation of language/speech mechanisms in the "dominant" hemisphere. Alternatively, did the results represent a mosaic of distinct neural processing mechanisms.

In order to address this problem, a recent study compared left- and right-handed individuals using different verbal and non-verbal auditory presentation stimuli including digit list recall, consonant/vowel recall vs monitoring, and Morse code recall, (Jäncke et al., 1992). Results showed either low or no correlation between results from different tests in the same individuals. As such, it was not clear whether the different measures of auditory lateralization represented a single "linguistic device" in either hemisphere, and as such, whether "receptive language dominance" in the dominant hemisphere could be reliably predicted (Jäncke et al., 1992). Likewise, it has been suggested that dichotic listening tests and more invasive and global tests of language lateralization (such as the Wada test, see below) do not measure the same neural substrate (Strauss et al., 1987).

The localization of language versus non-language functions such as music appreciation has also been studied using dichotic listening. For

example, the majority of individuals showed a left ear advantage for musical stimuli whereas musicians showed a distinct right ear advantage (Bever and Chiarello, 1974). Similarly, most subjects show a left ear advantage to non-verbal voice stimuli suggesting right hemisphere processing (Bryden, 1988). These studies have demonstrated that the hemispheric localization of language and other functions are not necessarily subserved by simple discrete mechanisms, but more likely by ones that are present in both cerebral hemispheres. As such. whether dichotic listening methods represent a specific measure of the hemispheric substrate for language perception or "an array of separate processing mechanisms" remains to be determined (Jäncke et al., 1992).

In sum, the different dichotic listening methods used for determination of cerebral lateralization of language functions give rise to variable outcomes. However, when such variables are controlled for, and if the results are interpreted within the framework of potential limitations, dichotic listening methods provide a powerful tool for the study of language localization in the brain.

2.3.4. The Wada test

A powerful new method for language localization in the brain was first developed at the Montreal Neurological Institute (Wada, 1949). It was shown that a unilateral injection of "amobarbital" (sodium amylobarbitone),

via a percutaneous puncture into the internal carotid artery, temporarily halted or paralyzed cognitive functions of the ipsilateral cerbral hemisphere, but had no effect on life sustaining functions. Due to the inherent trauma of direct cannulation of the internal carotid arteries, more refined techniques have recently been developed. These recent techniques involve the introduction of a cannula into the right femoral artery which is then advanced superiorly, under fluoroscopic control, into either the left or right internal carotid artery (Rausch and Risinger, 1990).

The intra-carotid sodium amylobarbitone test (Wada test) is an invasive method used to determine the cerebral dominance for speech and language functions in humans, especially in individuals with either left or mosaic handedness profiles (Wada, 1949; Wada and Rasmussen, 1960; Serafetinides et al., 1965). This test has been proposed as *the* definitive method for determination of the dominant language-related cerebral hemisphere (Rausch and Risinger, 1990). This is because the contribution of each hemisphere to a wide array of language tasks can be evaluated independently, although they have to be conducted over a short period.

Prior to the Wada test procedure, a baseline series of language and cognitive tests are performed. These results are used subsequently as comparators for those attained during test conditions. Immediately after injection of amobarbital the subject is asked to perform a series of language related tasks such as counting, word repetition, word definition, reading,

picture object naming, sequential language and word fluency, as well as simple motor tasks (Rausch and Risinger, 1990). Before the effects of injection wear off about twelve minutes are available to assess the subject with an array of language tasks. Usually, the language dominant hemisphere is ascertained by demonstration of the presence of symptoms of global aphasia after ipsilateral amobarbital injection or no effects upon injection of the opposite hemisphere (Rausch and Risinger, 1990). Furthermore, if language deficits result from injections of both hemispheres it is usually assumed that both hemispheres subserve language functions.

Although this test is reliable for gross determination of hemispheric role in primary aspects of language functions, it does include assessment of the role of right hemisphere homotypic areas (in left hemisphere dominant, right-handed individuals) in critical language functions such as intonation and prosody (Joanette et al., 1990; Bradvik et al., 1991; Ferreira, 1993; Moen, 1993). Unlike the dichotic listening test described above, the Wada test of hemispheric dominance has not been used experimentally to assess the cerebral localization of putative homologous communicative functions in non-human primates.

2.3.5. Computerized imaging of language functions.

More recently, powerful new imaging techniques have enabled researchers to probe into the depths of brain function and provide new

insight into the brain mechanisms underlying language. These methods have provided new knowledge regarding both the anatomy and functional localization of brain language mechanisms.

2.3.5.1. Anatomical imaging of inter-hemispheric asymmetry in brain language substrates

Prior to functional imaging (see section 2.3.4.2.), anatomical brain imaging techniques such as *anatomic* magnetic resonance imaging (*a*MRI) and X-ray computerized tomography (CT) allowed for 3-D visualization of deep brain structures in a series of 1-5mm slices, (see e.g., Naeser and Hayward, 1978; Damasio et al., 1979; and for recent reviews Damasio, 1989; Jernigan, 1990). Images obtained from CT can provide a series of detailed sections of deep brain structures in which one can clearly distinguish cortical structures (grey matter) versus fiber pathways (white matter). Images produced by *a*MRI provide sections of the brain that more clearly delineate between gray and white matter, approximate the degree of resolution available at autopsy and do not use ionizing radiation for imaging (Doyle et al., 1981). Using these methods, homotypic structures on the left and right hemispheres of the cerbral cortex can be compared with regard to size, shape and volume. "Homotypic" structures of the brain have a similar relationship as other ":serially" homologous structures such as, for example, left and right index fingers. In the brain however, although these structures may at least

be superficially similar morphologically and positionally etc., they may perform totally different functions.

Importantly, it has been demonstrated that the anatomical results obtained from brain imaging methods can be used within the established framework of knowledge regarding regional functional neural systems. This framework involves the cortical localization of functional areas as defined, e.g., by fissural boundaries, cytoarchitectonic zones and connectivity (Rademacher et al., 1992, 1993). Within this methodological framework, *a*MRI and CT methods have allowed for visualization of the extent of brain lesions giving rise to aphasic symptoms as well as the distribution of inter-hemispheric asymmetries in language-related regions of the brain.

CT studies of brain asymmetry

Studies using CT in awake individuals have clearly shown a wide range of cerebral asymmetries that may be related to language and handedness functions. These include frontal and parietal lobe widths, frontal and occipital "petelias" (projection of one lobe beyond the other), direction of straight sinus deviation, and various volumetric asymmetries in a range of subjects including both right and left handed males and females, (e.g., see LeMay and Kido, 1978; Chui and Damasio, 1980; Pieniadz and Naeser, 1984; Bear et al., 1986). For example, it has been shown that irrespective of left or right handedness, left occipital petelia were significantly more common than

on the right (Chui and Damasio, 1980). Further, it was demonstrated that straight sinus deviation was more common on the right (Chui and Damasio, 1980). However, *no* frontal petelia was the most common condition. Results for hemispheric width were less marked, with the frontal lobe being wider on the left in 22% and on the right in 36% while the occipital lobe was wider on the left in 36% and wider on the right in 20% of individuals. Interestingly, in all but three cases, petelias were associated with ipsilateral or absent hemispheric predominance for widths of the frontal or occipital hemispheres (Chui and Damasio, 1980). It is concluded that 1) handedness and cerbral asymmetry were independent variables since there were no significant differences between right-handed and non-right handed individuals, and 2) at least in right-handed individuals, cerebral asymmetries were independent of sex.

An extensive study which used CT imaging methods was designed to align the left and right hemispheres in the same axis (computerized trans-axial tomography, CTT). Results showed significant differences in right handers in which there was an increased occurrence of left occipital petelias in 66% of individuals versus 14% on the right. Likewise, occipital hemispheric width was larger in the left hemisphere in 66% of individuals versus 10% on the right (LeMay, 1977). There was also an increased frequency of right frontal petelias in 66% vs 14% larger on the left. In turn, frontal width was larger on the right in 61% of individuals versus 19% that

were larger on the left. Left handers were reported to either be more symmetric (with no significant differences) in these measures, or showed a trend towards the reverse pattern. Data showed frequencies of left frontal width predominance in 35% versus that for the right in 36%. Likewise, left occipital petelias were present in 36% of individuals versus 35% on the right (LeMay, 1977). No significant differences between males and females for any of these measures were reported.

Contradictory results regarding sex differences were shown in a later study (males n=30, females n=36). This study reported a reduction and more common reversal of inter-hemispheric structural asymmetries such as petelias and hemispheric widths in females (Bear et al., 1986). These results supported a previous study which reported sex differences in brain asymmetry (Wada et al., 1975) and organization, (for a review see McGlone, 1980). A significant linear correlation was demonstrated relating anterior and posterior difference measures. Likewise, those individuals, usually males, with a marked right frontal predominance also tended to show a prominent occipital petelia. Interestingly, the greatest difference in all measures between the handedness groups was left occipital width, with non-right-handers being significantly reduced in this measure (Bear et al., 1986)

The method of CT imaging has also been used to understand better the localization of lesions giving rise to "conduction aphasia". Conduction aphasia is the condition in which there is largely fluent, grammatic and

meaningful but paraphasic (= partial aphasia; employs wrong words or words in incorrect combinations) speech, and no major comprehension deficits, but with severely impaired naming and repetition (Bachman and Albert, 1991). Originally, Wernicke suggested that these symptoms were due to disconnection of anterior and posterior language areas (Bachman and Albert, 1991). More recently, it has been suggested that disruption of the arcuate fasciculus is responsible for this speech/language deficit (Geschwind et al., 1968).

Studies have demonstrated that there are at least two lesion localization patterns that give rise to symptoms of conduction aphasia (Damasio and Damasio, 1980, 1983). The first involves the supratemporal plane of the temporal lobe in the left hemisphere, and includes both the auditory cortex and insula. This lesion type, however, does not involve the main part of Wernicke's area in the posterior aspect of the superior temporal gyrus and the temporoparietal region. The second involves the angular gyrus and adjacent associated nerve fiber tracts, but again, other Wernicke's area structures are not involved. However, other CT-based clinical correlation studies have suggested that lesions in parts of Wernicke's area may be responsible for conduction aphasia (Mazzocchi and Vignolo, 1979)

aMRI studies of brain asymmetry in normal individuals

In addition to CT, *a*MRI has been used for in-depth quantitative studies of aspects of language asymmetries in the brains of awake individuals (for review see Jernigan, 1990). For example, a recent *a*MRI study addressed the critical issue of the influence on cerebral asymmetries of handedness and sex in a large sample of left-handed and right handed males and females (Kertesz et al., 1990). The right hemisphere was reported to be significantly larger (width and cross-sectional area) across both sex and handedness groups when considered as a total sample. However, in left-handed individuals, left frontal width was greater, and in right-handed individuals, right frontal, left parietal and left occipital widths were greater. Significant sex versus handedness differences were shown in which there was a larger parietal area ratio in both left-handed males and females (Kertesz et al., 1990).

In order to provide more detailed anatomical information for comparison with previous post-mortem studies Kulynych et al. (1993) employed a new approach in which a series of *a*MRI section images were used to produce 3-D surface renderings of the planum temporale region. The use of derived surface renderings of the planum temporale provided a major advantage over previous studies using sections only (e.g., Larsen et al., 1989; Steinmetz et al., 1989), since critical landmarks defining regional functional boundaries can be more clearly seen. This new method allowed for good 3-D

visualization of the planum temporale region that was comparable to its post-mortem appearance. Results from studies using this new *a*MRI 3-D surface reconstruction method showed a statistically significant predominance of the left hemisphere planum temporale in males (Kulynych et al., 1993).

A study by Falk and co-workers (1991) also used *a*MRI sections to create 3-D reconstructions of the entire external surface of human brains in an effort to quantify sulcal lengths bilaterally. It was found that: *1)* the anterior limb of pars triangularis (Part of Broca's area in the left hemisphere) was significantly longer, and showed an almost significant tendency (P = 0.09), to increased surface area on the right hemisphere; *2)* the ascending limb of the sylvian fissure was longer on the left hemisphere; *3)* although 75% (6/8) individuals showed right frontal with left occipital petelias, frontal petelia patterns did not show significant asymmetry; and *4)* in 75% of individuals the right medial central sulcus was situated rostral to that on the left, and the ascending sylvian sulcus was lower on the left (Falk et al., 1991).

aMRI studies of brain asymmetry in dyslexic individuals

In addition to the study of sex and handedness differences in the expression of hemispheric asymmetries a number of studies have used *a*MRI to study asymmetries in pathologic cases such as dyslexia (e.g., see Hynd and Semrud-Clikeman, 1989; Sjöberg and Kanje, 1990; Tison et al., 1990). Results from studies of these language disorders, similar to aphasiology, can

give added insight into the localization and morphological substrate of language in human brains. Dyslexia is a developmental problem in which human children of normal or above average intelligence are unable to learn to read spell and write at the normal rate (Hynd, 1989). These problems can manifest themselves even in later life with persistent deficits in language tasks such as phonological awareness (Leonard et al., 1993).

A study of morphological differences in hemispheric asymmetry in both dyslexic and normal controls showed several differences in the patterns of hemispheric asymmetry between the groups (Duara et al., 1991). At the level of the angular gyrus (part of Wernicke's area in the inferior parietal lobe), the area of the right hemisphere slice in dyslexics was significantly larger compared to the asymmetry seen in normals. Likewise, dyslexics showed a larger splenium of the corpus callosum than non dyslexics, with female dyslexics being proportionally larger than male dyslexics (Duara et al., 1991). Since the splenial region of the corpus callosum connects the region of the angular gyrus in the two hemispheres, it was suggested that dyslexia was related to a defect of the angular gyrus.

In a similar manner, Leonard et al. (1993) used αMRI to measure inter-hemispheric asymmetries in lengths of the temporal lobe and parietal lobe portions of the planum temporale in normals, dyslexics, and relatives of the dyslexic subjects. Results showed that in all three groups, the temporal lobe portions of the planum temporale were larger on the left hemisphere, while

parietal lobe portions were larger on the right hemisphere. However, the dyslexic group showed more pronounced left hemisphere asymmetries than did normals. More dyslexics also showed anomalies such as missing or duplicated gyri in the planum temporale or surrounding region (Leonard et al., 1993).

These studies of brain pathologies related to language deficits may offer new insight into the functional lateralization of speech and language. Similar studies in non-human primates with communication deficits may also serve to advance our understanding of their neural communication substrates.

2.3.5.2. Functional imaging of inter-hemispheric asymmetry in brain language substrates

Recently developed functional imaging methods have allowed for direct assessment of localization of cerebral activity during performance of various cognitive tasks. These methods, unlike their anatomical counterparts discussed above, have been applied to the mapping of specific neural activity during the performance of language tasks in humans. The several methods in current use include "functional magnetic resonance imaging" (*f*MRI) and "positron emission tomography" (PET). These functional localization methods have also been used in combination with the anatomical imaging methods in order to localize neural .activity more specifically.

Although these techniques provide a powerful means of mapping the physiological and anatomical characteristics of brain regions involved with language they have three main limitations, sensitivity, temporal resolution and spatial resolution (Frackowiak, 1994). These limitations create problems for interpreting results from mapping of transient neural events taking place during language processing. The temporal resolution of αMRI (for anatomy) with PET (for function) combined is 45-90 seconds, a language task has to be maintained over this prolonged period. Such a long period may not accurately represent the more temporally limited neural processes of interest. Likewise, the physical constraint of measuring responsive increases of local cerebral bloodflow corresponding to a particular language task presents an array of intrinsic physiological limitations. These constraints reflect what is being measured as increases or decreases in synaptic activity of corresponding neural elements with concomitant changes in local blood perfusion and glucose consumption (Raichle, 1987). However, the resolution available with PET, for example, is approximately 6 x 6 x 6mm (with two sections in different planes at right angles to each other) which when opposed to an adjoining section can resolve distinct neural metabolic compartments as small as 2mm (Frackowiak and Friston, 1994). Using these new functional imaging methods a number of advances have been made over the last several years in our understanding of speech-language related mechanisms. Application of these methods to communication tasks in living

non-human primates may further advance our knowledge with regard to the potential similarity of the neural mechanisms involved.

Cerebral localization of auditory perception functions in humans

Since the introduction of functional imaging technology, many studies have utilized it to map the activity underlying aspects of language perception in humans (e.g., Raichle, 1987; Petersen et al., 1988; Posner et al., 1989; Wise et al., 1991a, b; Price et al., 1992; Petersen and Fiez, 1993). For example, in a recent auditory perception study, Zatorre and co-workers (1992) used PET to measure changes in regional cerebral bloodflow in the auditory cortex in response to meaningless noise bursts vs acoustically matched speech syllables. Results showed that primary auditory cortex alone was activated by noise bursts, but for speech syllables, secondary auditory cortex was activated bilaterally. Further, lateralized cortical systems were activated for tasks involving judgments of speech attributes. Changes in pitch gave rise to increased activation of the *right* prefrontal cortex, a cortical region subserving pitch perception. Furthermore, speech tasks involving discrimination of phonetic structure gave rise to activation of Broca's area in the *left* hemisphere frontal lobe, supposedly the speech output substrate. These findings were thought to indicate a role for articulatory recoding in phonetic perception (Zatorre et al., 1992). Similar to conclusions made by Ojemann (1991) who used cortical stimulation techniques, these

workers concluded that their results supported a model whereby "auditory information undergoes discrete processing stages, each of which depends on separate neural subsystems" (Zatorre et al., 1992: 848). This study was able to define subtle aspects of auditory processing by the brain that could not have been approached by any other method.

Grasby and co-workers (1993) also used PET to measure increased regional cerebral bloodflow and thus identify regions involved in auditory-verbal long-term memory functions. They used two types of tasks: a "subspan" task - where individuals had to remember and recall immediately, one after the other, nine different five-item word lists that were read out loud by the investigator during the two minute period of the PET scan; and a "supraspan" task - in which subjects were required to remember and immediately recall three presentations of the same 1-item word list. During the supraspan task increased activity was seen, for example, bilaterally, both in the prefrontal cortex across the middle and superior frontal gyri (Brodmann's areas 9, 10 and 46). Relative decreases were evident during the supraspan task in the middle and superior temporal gyri (STG) compared to the subspan task, with maximal decreases being located in the posterior portions of STG and the insula bilaterally. (Grasby et al., 1993). These investigators, also similar to Ojemann (1991), concluded that their data indicated a series of individual components within a distributed system for signal processing and storage of information and governing aspects of

auditory-verbal memory functions (Grasby et al., 1993). Likewise, an earlier PET study looking at cerebral activation patterns after stimulation with both auditory and visually presented words, concluded that their data supported a concept whereby there were multiple, parallel routes between localized sensory-specific, phonological, articulatory and semantic-coding areas (Petersen et al., 1988), again supporting Ojemann's (1991) theory of a language substrate mosaic.

Cerebral localization of speech functions in humans

Numerous studies have recently used PET or *f*MRI to study regional bloodflow changes associated with cerebral activity underlying various aspects of speech and language in humans. These include studies of: general language production (Wallesch et al., 1985), speech from memory tasks (Tamas et al., 1993), generation of single words (McCarthy et al., 1993; Petersen and Fiez, 1993), the production of "internal speech" (Hinke et al., 1993), and during *kana* (one of two Japanese writing systems) word reading (Sakurai et al., 1993).

In a PET study, patterns of functional activation were compared between subjects at rest versus others undergoing a speech from memory task (Tamas et al., 1993). This speech task involved recalling verbally from memory all events of the previous day starting prior to, and continuing during, the eight minute period of the PET scan. There was pronounced local activity within

Broca's area and the medial temporal lobe of the left hemisphere. These results corresponded to the well established input and output areas for language processing (Tamas et al., 1993). Other areas were also activated such as the cerebellar hemispheres and pre-motor areas bilaterally, the right frontal operculum (the contralateral homotypic site to Broca's area), the supplementary motor area and the right parietal lobe (Tamas et al., 1993). Most of these activated areas correspond to regions known to be involved with expressive speech functions, while the temporal lobe was thought to represent the global and verbal memory component. Likewise, activation of frontal lobe structures of the right hemisphere was thought to represent processes underlying affective and contextual (e.g., prosody and intonation) aspects of speech (Heilman et al., 1986). The reason for activation of cerebellar cortex was less well understood, however, although it had been demonstrated previously in a study of single word processing of the cerebellum (Petersen et al., 1990). Although the cerebellum (and basal ganglia) had long been thought to be primarily involved in fine-tuning or "smoothing" of motor output, recent studies have suggested that they may also play a more direct role in higher cognitive functions such as processing of speech and language functions (e.g., Leiner et al., 1991; Schmahmann, 1991; Akshoomoff and Courchesne, 1992). Currently, concepts regarding the significance of the roles being played by the cerebellum and right hemisphere

homotypic areas in language functions, are discussed below are becoming incorporated into the literature.

Echo-planar *f*MRI is another new technique that indicates local activation of brain elements by measurement of increased levels of deoxygenated hemoglobin which act as an endogenous para-magnetic contrast agent (Blamire et al., 1992). Unlike PET, *f*MRI does not require the use of ionizing radioactive probes. Further, the spatial resolution of *f*MRI matches that of *a*MRI and is better than either cortical stimulation or PET. A recent study using the *f*MRI technique was recently conducted in order to measure the patterns of cerebral activation resulting from "internal speech" (Hinke et al., 1993). In this study, during *f*MRI image acquisition, subjects were required to perform a language task involving silent word generation from the alphabet (A-apple, B-ball, C-cat etc.) but with no physical articulation or vocalization. A second *f*MRI scan was acquired during the subsequent rest period during which the subjects were required to focus their attention on the hum of the machine and not think about words. Results showed that cerebral activity was localized *deep* to the cortical surface representation of Broca's area within the depths of anterior and posterior portions of the adjacent ascending limb of the sylvian fissure (Hinke et al., 1993). In addition, significant increases in activity were seen in the right hemisphere homologue of Broca's area in six of the nine subjects. These results are interesting since they indicate that Broca's area may be involved

in more complex functions than sequencing of motor output underlying the motor aspects of language. Similar imaging studies of schizophrenic individuals experiencing "inner voices" e.g. (McGuire et al., 1993), discussed below, also implicate a role for Broca's area in the generation of silent, non-articulated "inner" speech.

One of the limitations of *fMRI* has been its sensitivity to motion induced by head movements during physical speech. This is the reason why the "inner speech" methods were devised. However, a recent study, modeled upon the classic PET studies of Petersen's group (1988, 1990) used *f*MRI to examine activation of frontal cortex during a wide variety of language tasks, including spoken word generation (McCarthy et al., 1993). This study used subjects held in a fixed position by a foam rubber head holder and wearing ear plugs. Subjects were required to perform several language tasks of varied complexity, including: generation of tongue, lip and jaw movements without any speech or sub-vocalization; immediate repetition of common nouns; and immediate generation of a complementary verb for a given noun (e.g. response for "car" would be "drive"). Control tasks included quiet resting, passive listening to read common nouns or letters of the alphabet, and generation of "inner speech" involving generating complementary verbs to presented nouns. Results showed activation of inferior frontal regions, such as Brodmann's area 47 extending to area 10, during the verb generation and repetition tasks (McCarthy et al., 1993). Interestingly, similar to the

results of Hinke (Hinke et al., 1993), described above, significant activation was also seen in homologous regions of the right hemisphere inferior frontal cortex. Little or no activation of this region was noted for the tasks involving passive listening, inner speech, or mouth movement tasks. Results from this study, showing no activation of Broca's area after volitional mouth movements without speech are particularly interesting since prior to this study it was assumed that activation of Broca's area during "inner speech" reflected non-volitional/covert motor movements of the vocal tract musculature.

The use of anatomical and functional 3-D imaging methods have recently provided us with a wealth of new information regarding the involvement and localization of neural substrates underlying vocal-auditory communication in humans. Anatomical and functional imaging methods, similar to other techniques, such as electrical stimulation mapping, demonstrate the presence of a diverse and widely distributed system of substrates which may underlie speech and language functions. These data extend our concept of brain language areas well beyond those in use for over a century. In turn, application of these imaging methods to auditory-vocal or visual-gestural communicative processing in non-human primates may provide us with information regarding the species specific functions of those brain areas that are homologous to language areas in humans.

2.3.6. Role of the right hemisphere in human language functions

In order to have any meaningful understanding of the functional substrates underlying the gross inter-hemispheric asymmetries measured in this dissertation, it is important to include an appreciation of the potential differential role played by right hemisphere brain regions. The classic view of language localization in the human brain held that it was essentially controlled by cerebrocortical structures located in the left hemisphere, at least in left-lateralized (usually right-handed) individuals. This view has been pervasive, even though the right hemisphere was proposed to be the seat of expressive language only a decade after Broca's first observations of the role of the left hemisphere (Jackson, 1874). Even as recently as 1976, Julian Jaynes, in an influential psychological literary thesis, spoke of the "apparent" lack of function of large portions of the right hemisphere of the brain including what corresponds to (i.e., was homotypic to) Wernicke's area. However, it is becoming evident that these conclusions were based on an incomplete understanding of the complexity of inter-hemispheric processes in language functions of (for a recent review, see Baynes, 1990).

It has been concluded that the contribution of the right hemisphere involves, at the very least, lexico-semantic processes, comprehension and/or the expression of prosody (pitch/tone, intonation, and stress/intensity) and the apprehension and processing of contextual information necessary for efficient verbal communication (Joanette et al., 1990). Further, functional

studies have demonstrated a key role for the right hemisphere in: *1)* perception and expression of "intonation contours" (Blumstein,S and Cooper, 1974), *2)* an ability to distinguish prosodic features providing "phonemic" (i.e. lexical) or "emphatic" (word stress or weighting) information (Weintraub et al., 1981), *3)* "prosodic encoding", as distinct from sentence syntax (Ferreira, 1993), *4)* skilled reading (Hutner and Liederman, 1991), and *5)* critical, evaluation of the emotional content of sentences depicting facial and gestural expressions (Ahern et al., 1991; Blonder et al., 1991; Mandal et al., 1991) or the perception and expression of "lexically-based" emotional communication (Bloom et al., 1990; Borod et al., 1992). The importance, and presumably the adaptive advantage, of these aspects of our communicative repertoire, as noted by Joanette et al., is that other than having a good understanding of rules governing the use of contextual language, it is necessary that "...to understand the intention of a speaker, one must also be able to take into consideration both the literal meaning of the message and its intonation, or prosody, while also noting the context in which the message is spoken" (Joanette et al., 1990: xii). As such, the integrity of these right hemisphere communicative substrates is thought to be critical for maintaining the contextual appropriateness of communication behavior.

It has been proposed that prosodic aspects of speech such as intonation, accent, temporal structure, emotional gesturing, and voice qualities are subserved by separate and functionally distinct regions in the right

cerebrocortical hemisphere. These areas are presumably serially homologous, or homotypic, to speech-language areas in the left hemisphere (Ross,ED and Mesulam, 1979; Yamadori, 1992). Furthermore, it was suggested that the functional and anatomical organization of these regions in the right hemisphere mirror that of propositional speech in the left hemisphere. This concept has been supported by data from a number of studies (e.g., Heilman et al., 1975; Ross,ED and Mesulam, 1979; Kent and Rosenbeck, 1982; Gorelick and Ross, 1987). In a study by Ross (Ross EE, 1981) of individuals with various right hemisphere lesions, established tests that had been used for assessment of propositional speech deficits were modified to examine disorders of affective language (Ross,EE, 1981). These tests for the nature of prosodic deficits involved: evaluation of spontaneous prosody and gesturing, auditory comprehension of the affective component of prosody, and visual comprehension of emotional gesturing. Results showed that the organization of affective functions in the right hemisphere was, in fact, similar to that known for proposition language in the left hemisphere. Furthermore, Ross (EE, 1981) concluded that these affective disorders could be classified in the same manner as the aphasia and proposed that the various (analogous) disorders modify the term "aprosodia", like those used for the term "aphasia", with the various classificatory terms such as motor, global, sensory, conduction, or trans-cortical (e.g., conduction aprosodia) (Ross & Mesulam, 1979). A similar study by Darby (1993) in individuals

with lesions of the inferior division of the right middle cerebral artery, giving rise to "sensory aprosodia" supports the concept of compartmentalization of prosodic functions. In Darby's study, sensory aprosodia was represented by an impaired prosodic affective comprehension and repetition (but with spared expression), and impaired comprehension of emotional gesturing. Likewise, specific damage of regions in the right hemisphere can give rise to output of monotonous speech that is devoid of affective modulation, defined as "motor aprosodia", as well as distorted supra-segmental linguistic features (Ackermann et al., 1993).

In order to assess disturbances of speech prosody a recent study used various lesions in the *right* cerebral hemisphere with a combination of CT imaging, electroencephalography (EEG), regional cerebral bloodflow measures (using cerbral angiography or cervical doppler), and tests of various prosodic qualities of speech (Bradvik et al., 1991). Evidence was presented for disturbance of several "linguistically-related" qualities of speech, such as impaired identification of emotional messages and impaired identification (cognition) and/or production of prosodic aspects of speech, none of which were related to a more generalized affective disorder. However, their data did not support the concept of an organization of prosody in the right hemisphere that would present as a mirror of propositional speech in the left hemisphere, as proposed and described by Ross (Ross,EE, 1981).

The potential for a task-specific role of the left hemisphere in linguistic functions was investigated in individuals with various right hemisphere lesions (Yamadori, 1992). In one series of right-handed patients with lesions in the right hemisphere peri-sylvian area, the individuals showed excessive production of linguistic output in the form of writing. Although the output was extensive it was not well organized. This neurological phenomenon has been referred to previously as "hypergraphia" (Waxman and Geschwind, 1974). In another series of right-handed patients with lesions in the right hemisphere parieto-temporal area, individuals also manifested excessive linguistic output expressed as loquaciousness within an almost endless low and monotonous conversation. This condition was previously referred to by Yamadori et al. as "hyperlalia" (Yamadori et al., 1990). Since the syndromes were the outcome of similarly placed lesion in the right hemisphere, Yamadori speculated that the condition of "rivalry" or "coordination" (Denny-Brown, 1958) between left and right hemisphere language-related regions had been disrupted. Normally a dynamic equilibrium would be maintained In the event that the left hemisphere is responsible for the mechanical or instrumental aspects of language whereas the right hemisphere subserves a role in situational and behaviorally meaningful aspects, "dynamic coordination between the two hemispheres each contributing in its own way may be a necessary prerequisite for a total linguistic behavior" (Yamadori, 1992: 76). Disruption of this dynamic equilibrium after right hemisphere

lesion, therefore, may give rise to left hemisphere autonomy which is expressed as an uninhibited linguistic output at the mechanical level (Yamadori, 1992).

One approach to ascertaining the role and plasticity of the right hemisphere in language has been to observe the capacity of callostomy patients, i.e. individuals with disruption of their corpus callosum, the major fiber tract connecting the two hemispheres. For example, patients who have had their corpus callosum sectioned in order to control debilitative epilepsy, provided a unique opportunity to observe the capacities of each hemisphere in isolation from the other (Baynes, 1990). Results demonstrated that the right hemisphere was unable to give a verbal response to visual stimuli presented laterally(e.g. numbers, words, letters, or pictures) (Gazzaniga and Sperry, 1967). However, when a non-verbal response was initiated, the right hemisphere readily performed tasks such as multiple choice pointing responses to identification of numbers, letters or words and matching of printed and spoken words. In contrast, the right hemisphere had limited cognitive skills, and if presented with images of a *match* and a pile of *firewood*, it could not infer "*fire*" even though it could identify pictures of these three elements (Gazzaniga and Smylie, 1984). Although the right hemisphere has a lexicon that allows for simple referential naming tasks, it does not possess the conceptual substrate for making serial inferences from this information (Baynes and Gazzaniga, 1988).

Some right-handed epileptic individuals have been shown to manifest rapid development of complex language skills in the right hemisphere post commisurectomy. These cases were attributed to an early adaptive response, with functional reorganization of the right hemisphere for language functions, due to the left hemisphere location of the epileptic focus (Gazzaniga et al., 1979; Baynes, 1990). An interesting observation in these commisurectomized individuals with right hemisphere language abilities was a dissociation between the ability to comprehend syntactically constrained sentences and to judge their grammaticality (Baynes and Gazzaniga, 1988). Since the right hemisphere has been previously shown to be highly skilled at assessing proper grammar, judgments by this intellectually compromised hemisphere may be "data driven" and thus be independent of the complex cognitive systems that may underlie comprehension (Baynes and Gazzaniga, 1988). Interestingly, it has been suggested that reduction of this inter-hemispheric dissociation, with a concomitant ability to coordinate more effectively left and right hemisphere processing during early human development, may be linked to the neural substrate for intellectual giftedness (O'Boyle et al., 1991).

The concept of a vital role for right hemisphere structures in human communicative functions is becoming increasingly incorporated into our knowledge of the functional localization of language in the brain. In keeping with other investigations into the neural substrates for speech and language

in humans, the role of these right hemisphere regions fits with functional models depicting a highly complex dispersed network of independent, but highly interconnected, neural components. A better understanding of the role of right hemisphere neural structures in non-human primate communication may provide insight into the evolutionary origins of these hemisphere-specific communicative components in humans.

2.3.7. Handedness and language in humans

The relationship between hemispheric dominance for speech and handedness in humans is still not well understood, even though it is more than a century since it was first noted by Paul Broca (Broca, 1865a). Approximately 90% of humans are right-handed, a lateral preference that is present as early as the end of the first trimester as indicated by *in utero* studies of thumb sucking preferences (Hepper et al., 1990, 1991). Such a left hemisphere predisposition appears to be highly stable, both within (Gilbert and Wysocki, 1992), and between cultures (Connolly and Bishop, 1992). It has also been shown that predominance of right handedness in modern human populations, has been in place for at least five thousand years, as evidenced by archaeological data from early Egypt (Coren and Porac, 1977). Likewise, there is evidence based on features of some Cro-Magnon cave paintings that right handedness likely predominated (Babcock, 1993). Indeed, the antecedents of handedness in human history may extend to 1.4

million years ago, if not earlier based on evidence from methods of stone tool making (Toth, 1990; Babcock, 1993). As such, the distribution of human handedness profiles may represent a long term stable polymorphism.

In apparent contradiction of this stability of population level handedness patterns, studies have shown different distribution patterns. For example, a study of native Amazonians (Tucano), reported that all 65 were right-handed, as determined by a 26 item handedness questionnaire (Bryden et al., 1993). The unusual distribution of handedness in the Tucano sample was explained by the fact that in this culture the use of the right hand for skilled tasks such as tool use was positively reinforced (Bryden et al., 1993). It was noted that in some other groups, such as Muslim and Japanese societies, the use of the right hand is required for eating or writing and that use of the left hand may even be actively punished (Bryden et al., 1993). For example, the large degree of variation in reports of left handedness for writing, which can vary from as little as 1% in an Asian culture to as much as 13% in a Western culture (Spiegler and Yeni-Komshian, 1983), may also represent cultural pressure for task-specific hand use. It is interesting to note that even in Western cultures there is a great deal of discrimination against left handed individuals.

There is a well established link between the neurobiological substrates for language and handedness. Left hemisphere dominance for language in right-handed individuals is the general rule, with very few exceptions

(Alekoumbides, 1978). Contrary to prevailing thought since Broca, the majority of left-handed individuals are also left hemisphere dominant for speech-language functions (Harris, 1991). Interestingly, left-handed individuals are more likely to have right hemisphere dominance, or co-dominance, for speech-language functions, than are right-handed individuals (Alekoumbides, 1978; Segalowitz and Bryden, 1983). Approximately 5% of right-handed, compared to 30% of left-handed, individuals have language functions localized in the right hemisphere (McManus, 1991). In addition, in left-handed individuals, a significant relationship has been demonstrated between familial sinistrality and bilateral distribution, or hemispheric equipotentiality, for the representation of language (Hécaen et al., 1981). It was noted, however, that in these "ambilateral" individuals, the inter-hemispheric distribution of language functions may be represented as a matrix of functionally specific regions, with little bilateral representation of similar functions (Hécaen et al., 1981).

There appears to be increased inter-hemispheric representation in left-handed individuals. A study by Witelson (1985) looked at post-mortem corpus callosum size in both right handed and mixed handed individuals. Handedness was established prior to death using a standard series of tests of unimanual skills (Annett, 1992). Witelson noted that *consistent* left handedness was quite rare, and that no examples were present in her sample. Results demonstrated that in ambidextrous and (essentially) left-

handed individuals, the area of the corpus callosum was, on average, 11% larger than that of right-handed individuals (Witelson, 1985). It was proposed that this difference may reflect the increased bilateral representation of cognitive functions in non-right-handers, and as such, a greater degree of interactivity and connectivity - via the corpus callosum (Witelson, 1985). A subsequent study used intracarotid sodium amytal tests followed by *a*MRI to study corpus callosum size differences between individuals that were left or right hemisphere dominant for language functions (O'Kusky et al., 1988). Results from this study demonstrated that the area of the corpus callosum was 19-28% (109-159mm^2) larger in individuals with right hemisphere dominance for speech-language functions compared to those with left hemisphere or bilateral speech-language representation. It was concluded that such a size difference could represent an additional 37-54 million axons in the corpus callosum in these individuals (O'Kusky et al., 1988). More recently, another *a*MRI study measured multiple dimensions of the corpus callosum (Cowell et al., 1993). In this study, data were analyzed with respect to both the direction and consistency (= degree) of preferred handedness. Results showed that there were significant handedness vs consistency effects with regard to regional organization of the corpus callosum. A consistent right hand preference across handedness tasks was highly correlated with size of the isthmus of the corpus callosum. Furthermore, it was shown that anterior regions of the

corpus callosum varied as a function of sex and right vs left handedness (Cowell et al., 1993). It was concluded that although the *direction* of asymmetry is an important functionally relevant variable, the *degree* of asymmetry is also an important substrate underlying both neuroanatomic and behavioral organization in the brain (Cowell et al., 1993).

Functional imaging technology has been used to define the localization and extent of hemispheric involvement in different tasks involving preferred versus non-preferred hands. Previously, it had been shown that the effects of left hemisphere motor cortex lesions (subserving right hand motor control), were more pronounced than lesions in the corresponding region on the right side. For example, left side lesions impaired function in both hands whereas right side lesions did not affect right hand function. In order to study functional aspects of this differential cortical involvement, *f*MRI was used to look at activation of neural tissue in the hand region of the pre-central motor cortex bilaterally during a motor task, e.g., involving repetitive apposition of the thumb and four fingers (Kim et al., 1993). Results showed that, in both left and right-handed subjects, the right motor cortex was activated largely by left hand movements. In contrast, left motor cortex was activated both during right and left hand movements, especially in right-handed individuals (Kim et al., 1993). No sex differences were reported. It was concluded that hemispheric asymmetry for handedness was more pronounced in right-

handed individuals, even at the level of the pre-central gyrus (i.e., the effective end station of cortical motor processing).

A behavioral method of assessing handedness involves use of the "dual task paradigm". A study using this method supported the later results from Kim's *f*MRI analysis described above, although at the time the underlying reasons were not known (Simon and Sussman, 1987). The dual task paradigm is particularly relevant to language-handedness relations in the cerebral cortex since it is a potential indicator of the neural processing overlap between speech and handedness substrates in the left hemisphere. As such, it has been used to infer the hemispheric lateralization of language, (e.g., Hicks, 1975). In this test, subjects with known handedness profiles are required to tap the key of a counter as fast as possible, using their left or right index fingers, while either verbally silent (control state) or during language tasks such as describing a picture, reading aloud and speaking extemporaneously. As may be expected right handed individuals generally showed more right than left hand tapping disruption during language tasks while left handers showed the opposite effect (Orsini et al., 1985). Results from an extensive study using 260 individuals showed that the dominant hand underwent more tapping interference than the opposite hand, regardless of handedness (Simon and Sussman, 1987). This result was thought to reflect a degree of control of the left hand by the ipsilateral hemisphere; an idea that later proved to be the case using current technology

(Kim et al., 1993). Unlike the later *f*MRI study by Kim (1993), however, this dual task paradigm study reported a major sex effect in which females experienced a significantly greater overall disruption of finger tapping during concurrent verbalization (Simon and Sussman, 1987). The small sample size and possible limits of resolving power of the *f*MRI study may not have allowed for this sex effect to be recognized.

The results of handedness studies such as those described above are particularly important for understanding the differences and variation in neural connectivity and processing substrates that may also underlie speech and language functions in humans. Although patterns of handedness in non-human primates differ from that of humans, an understanding of these patterns and how they may relate to brain communication circuitry is critical to understanding functional aspects of the mechanisms involved. Further, the gross hemispheric asymmetries present in the frontal lobes of some non-human primates may reflect, at least in part, the presence of functional asymmetries underlying handedness.

2.4. GROSS ANATOMICAL CORRELATES OF LANGUAGE LOCALIZATION IN HUMAN BRAINS

2.4.1. Introduction

In addition to the large number of physiological studies, described above, that have investigated the functional localization of language mechanisms in human brains, other studies have investigated their underlying anatomical bases. These studies have been based on the tenet that a particular sub-area of the cerebral cortex, that is more functionally active than its homotypic counterpart, will reflect this involvement by local differentiation with gross anatomic expansion. Such an area would show ipsilateral hemispheric predominance resulting in a measurable gross anatomic inter-hemispheric asymmetry compared with its contralateral counterpart. However, it should be noted that functional asymmetry may well precede gross anatomic changes. For example, at the early stages of functional localization, cellular, sub-cellular or molecular changes may reflect this functional asymmetry whereas more gross changes have not yet occurred.

2.4.2. The temporal lobe and Wernicke's area

The temporal lobe is one of the most asymmetric regions of the human brain with regard to the neural substrates of language functions. Early studies by Eberstaller (1884) and Cunningham (1892) reported hemispheric asymmetry in the shape and posterior termination of the sylvian fissures. It

was reported that the posterior part of the right sylvian fissure tended to curl superiorly whereas that on the left side did not curl up and continued more posteriorly. Later, in 1936, Pfeifer demonstrated for the first time that the 'temporal operculum" (that part of the temporal lobe cortex located deep to the covering[= opercula]) was larger in the left hemisphere. This region contained the "planum temporale" described below. However, these and other papers were not readily accepted into the scientific paradigm of cerebral localization. In fact, the generally accepted view, that there was no gross anatomical basis for the well described functional left cerebral hemisphere dominance for language functions in humans, persisted until the 1960's (e.g. (von Bonin J, 1962)).

A landmark study by Geschwind and Levitsky (1968) reported on a large number of post-mortem specimens and brought the issue of gross asymmetries underlying brain language regions into the current scientific paradigm. They demonstrated that a known speech-related region of the posterior temporal lobe, the planum temporale, was asymmetric. The planum temporale contains association cortex which gives rise to Wernicke's aphasia when injured (Galaburda, 1984). Geschwind and Levitsky (1968) showed that this region was significantly larger on the left side in 65% of individuals, larger on the right in 12%, with no difference in 23%. They looked at the anatomy of structures related to speech function deep to the surface of the brain, not just on the surface. They used coronal sections of the

whole brain cut in the plane of the posterior part of the superior temporal gyrus.

Carotid arteriography was later used in living humans and showed the same type of deep asymmetry (LeMay and Culebras, 1972). In this method, a radio-opaque substance is injected into the incoming cerebral vasculature followed by lateral radiographs. The different route of cerbral arteries in the region of sylvian fissure and superior temporal gyrus indicated asymmetry of the planum temporale in living individuals.

The length and course of the sylvian fissure, the inferior wall of which comprises the planum temporale, is asymmetric (e.g., Wada et al., 1975; Yeni-Komshian and Benson, 1976). The difference in size of the left versus the right planum temporale can be marked, with the left sometimes being ten times larger than the right, and in other cases the right being virtually absent (Galaburda, 1984). Asymmetry of the shape of the sylvian fissure in adults has been demonstrated by Le May and Culebras (1972) using arteriograms of the middle cerebral artery to demonstrate its different course on the left side. Using this method, the posterior end of the sylvian fissure (sylvian point) was later shown by to be higher on the left in 67% of cases, of equal height in 25%, and higher on the left in 8% . Interestingly, in 28 left-handed individuals, the sylvian point was higher on the left in 21% and on the right in only 8% (Hochberg and LeMay, 1975).

A study of post mortem sylvian fissure morphology assessed asymmetries in both males and females as well as left and right handed individuals (Witelson and Kigar, 1992). The sylvian fissure was divided into three regions: anterior, horizontal and vertical. Results showed that the anterior segment showed no asymmetry, the horizontal segment was significantly larger on the left hemisphere, and the vertical segment was significantly larger on the right hemisphere. These results demonstrated that the precise location of the main asymmetry was at its posterior point where the fissure turned upwards. This posterior morphology was also indicated by the different extents of the inferior parietal and superior temporal gyri (Witelson and Kigar, 1992). Although males showed a good correlation between handedness groups and sylvian fissure morphology, no association was found in females, thus supporting similar results from a previous sex differences study of the corpus callosum (Witelson, 1989). These results indicate that the anatomy of the sylvian fissure was related to functional asymmetries, only in males. It seems that in humans there is a greater dissociation between motoric and perceptual asymmetries in females than in males (Witelson and Kigar, 1992).

The brains that were originally used for the classic study of the planum temporale by Geschwind and Levitsky (1968) were later re- evaluated (Galaburda et al., 1987). Interestingly, they reported a negative correlation between total left and right area of the planum temporale versus the degree

of asymmetry, and that the smaller planum strongly predicted asymmetry whereas the larger did not. They suggest that this indicates asymmetry results from variation in one side only. This supports the their hypothesis that the present condition of hemispheric asymmetry of the planum temporale resulted from reduction of cortex on the non-functional (right) side as opposed to hypertrophy of the functional (left) side, away from the original (ancestral) symmetric situation.

2.4.3. The frontal lobe and Broca's area

Shortly after Broca made his description of the components of the left frontal opercular region, Eberstaller (1884) noted that the ascending limb of the sylvian fissure gave rise to branches more often on the left than on the right side. This indicated that there was more cerebral cortex present, but it was situated deep to the surface, within the depths of the frontal operculum (= covering or lid) complex. The presence of gross anatomic size asymmetry of this region on the surface of the brain, however, was not reported. Falzi and co-workers (1982) resolved this issue of deep versus surface asymmetry in Broca's area. In their study, the total area of cortex (= Broca's area; comprising pars opercularis and pars triangularis of the third frontal convolution) visible on the surface of the brain was compared on the left and right sides. It was found that there was no significant difference in size between the brain surface manifestation of the region in the two

hemispheres. However, in the second part of the study the same regions were cut into sections so that the sulci and gyri deep to the surface were included. The comparison of deep structures showed a marked hemispheric asymmetry with the left side being significantly larger than the right. Falzi et al. (1982) concluded that the asymmetry of the anterior speech region in the expected direction (left larger than right) appears only when the entire region, including the cortex buried in the sulci, is considered. This represents a significant finding for the study of speech-related brain asymmetries in fossil hominid endocasts. Since endocasts represent surface morphology only, the deep to surface asymmetries associated with the presence of left hemisphere localization of language functions cannot be directly observed.

2.4.4. Development of brain language areas and asymmetries

Sylvian fissure asymmetry is present both pre and post-natally before language develops in human children (Wittleson and Pallie, 1973; Wada et al., 1975; Chi et al., 1977). It should be noted, however, that studies of the fetus *in utero* have suggested that it is receptive to speech sounds (Zimmer et al., 1993). This could be due to the fact that the human child has been exposed continuously to its mother's voice, via a liquid transmission route, ever since maturation of the cochlea by the end of the first trimester. Whether environmental auditory stimuli give rise to asymmetric

development of the temporal lobe auditory reception cortex (i.e. planum temporale / Wernicke's area) is currently unknown. It has also been suggested that since the newborn child can vocalize in a gaseous environment as soon as it is born, it may even practice vocalization in the liquid, in-utero, environment (Ishii et al., 1991).

The presence of anatomical asymmetries at birth are well documented, however, it is not clear whether there are underlying functional asymmetries. Two main views are currently operational (see Hahn, 1987; Majnemer and Rosenblatt, 1992). Hahn (1987), for example proposed that around birth, homotypic regions in both hemispheres are equipotential substrates for specialized functions. As the infant matures, functional lateralization occurs, until around puberty when the full adult pattern is in place. Another view, supported by physiological studies, is Kinsbourne's "invariant lateralization model" (Majnemer and Rosenblatt, 1992). This model proposes that functional asymmetries are already present at birth but may not be detectable by testing methods for several years. Somatosensory evoked potentials were used to determine whether functional inter-hemispheric asymmetry (for handedness) was present at birth, two and six months, in three left-handed and six right-handed children (Majnemer and Rosenblatt, 1992. It was concluded that functional hemispheric asymmetries occurs early in development and that lateralization of function is intrinsically preprogrammed. Another study used strength of the grasp reflex in human

newborns as a measure of lateralization for handedness (Tan et al., 1992). It was reported that lateralization of the grasp reflex was already present at birth with a significant right-hand preference in the majority of individuals. Interestingly, females infants were more strongly lateralized than males.

A study of human children with developmental dyslexia by Hynd and co-workers (Hynd et al., 1990) used αMRI to evaluate the pattern of planum temporale asymmetry. This disorder occurs in ~5% of children and is a rare but definable and diagnosable form of reading retardation with some form of central nervous system dysfunction. The diagnosis requires normal intelligence and a significant discrepancy between measured reading ability and reading achievement (Hynd et al., 1990). Only 10% of dyslexic children had the normal pattern of left > right planum temporale asymmetry compared to 70% in normal children. Some individuals showed a reversed pattern of planum temporale asymmetry (R > L) in addition to equal sized plana (L = R). Interestingly, it was also noted that significantly more dyslexic children were left-handed than were normal children.

2.4.5. Cerebrocortical architectonic asymmetries

An underlying assumption regarding gross anatomic asymmetries of the human brain is that they form the substrate for functional hemispheric specialization. It is usually assumed that the largest homotypic cortical area in the two hemispheres is the seat of function. The use of "architectonic"

methods provides an approach to understand better the neural substrate of functional localization (LeBrun-Kemper and Galaburda, 1984). Architectonic analysis uses histological methods to study regional differences in the cortical mantle of variables such as cell type, packing density, fiber distribution pattern, chemical profile, laminar organization, and cortical thickness (Galaburda et al., 1978b; Galaburda, 1980; Galaburda and Pandya, 1982). Some of the various architectonic approaches include: 1) "cytoarchitectonics", the arrangement of (Nissl-stained) neurons in cortex; 2) "angioarchitectonics", the distribution of blood vessels; 3) "myeloarchitectonics", the distribution pattern of myelinated axon fibers; and more recently, 4) "chemoarchitectonics" the study of the neurochemical profile in different areas of the cerebral cortex (Le Brun Kemper and Galaburda, 1984). For example, the cerebral cortex shows distinct differences in cell types and cellular layering or distribution patterns between major regions and within sub-regions (Sanides, 1972). Studies have shown that distinct differences in cytoarchitectural patterns have different connectivity with other brain regions, providing supporting evidence for proposed functional differences (Sanides, 1970).

2.4.5.1. Architectonics of Wernicke's area: "Area Tpt" of superior temporal gyrus

Cytoarchitectonic studies of language related regions of the posterior temporal lobe, in the region of planum temporale, have shown there are

consistent asymmetries present in the specific sub-region "Area Tpt" (Galaburda et al., 1978b; Galaburda and Sanides, 1980). Area Tpt occupies most of the planum temporale region and the adjacent posterior superior temporal gyrus. Due to this, it has been concluded that the previously described planum asymmetries probably reflect asymmetries in an auditory cytoarchitectonic area and therefore may represent, at least in part, the anatomic substrate for language lateralization (Galaburda et al., 1978b). These are the classic areas that give rise to Wernicke's aphasia when damaged.

In humans, Area Tpt occupies a significantly larger area within the left hemisphere cortex in individuals that show a larger planum temporale (Galaburda et al., 1978b; Galaburda and Sanides, 1980). Significant differences of cytoarchitectonically defined volumes of area Tpt in three individuals were shown to be 2540 mm^3, 1080 mm^3, and 1510mm^3 for the left hemisphere and 350 mm^3, 950 mm^3, and 690mm^3 on the right, respectively (Galaburda and Sanides, 1980). In humans, Area Tpt also extends caudally and superiorly into the domain of the suprasylvian region (Galaburda and Sanides, 1980). Area Tpt is thought to be a transitional zone between the highly specialized primary auditory cortex of the temporal lobe and the more generalized association cortex of the inferior parietal lobe (Galaburda and Sanides, 1980) and has been shown to be homologous to a similarly placed

region in rhesus macaques (Pandya and Sanides, 1973; Galaburda and Pandya, 1982).

2.4.5.2. Architectonics of Wernicke's area, II: "Area PG" of inferior parietal lobule

Although Area Tpt, corresponding to the planum temporale in humans, accounts for much of the gross asymmetry shown by the sylvian fissure, recent evidence has shown that adjacent cortical areas may also contribute. For example, *Area PG* an architectonically defined cortical area of the parietal lobe, located inferior to the interparietal sulcus, , has been shown to be significantly larger on the left hemisphere in those individuals with a larger left planum temporale (Eidelberg and Galaburda, 1984). In individuals where the planum temporale was symmetric or larger on the right side, area PG showed a corresponding size relationship, suggesting linkage of asymmetry in these language areas (Eidelberg and Galaburda, 1984). Area PG corresponds to Brodmann's Area 39 (of) in the angular gyrus.

Homology of area PG in the inferior parietal lobe of humans with cytoarchitectonic areas of the parietal lobe of macaques has been demonstrated. In addition to having a similar gross asymmetry profile as area Tpt in humans, area PG in macaques has also been shown to have extensive nerve fiber connections with area Tpt (Pandya and Seltzer, 1982). This connection is currently unknown for humans but it is assumed to exist (Eidelberg and Galaburda, 1984).

2.4.5.3. Architectonics of Broca's area in humans

The pars opercularis of the inferior frontal operculum is the central portion of the larger cortical area included within the designation Broca's area. Using cytoarchitectonic criteria it has been referred to, in humans, as Area 44 by Brodmann (1909). It shows a different cytoarchitectonic profile than the adjacent Area 45 which is also included within the paradigm of Broca's speech area. The anterior border of Brodmann's Area 44 in humans is the ascending limb of the sylvian fissure, posteriorly it is the precentral sulcus, superiorly the inferior frontal sulcus, and inferiorly it extends into the superior wall within the depth of the most anterior sylvian fissure (Galaburda and Pandya, 1982). The cytoarchitectonic profile of this region is described in Section 2.7.4.1. and compared to the homologous region in non-human primates.

2.4.5.4. The arcuate fasciculus

The arcuate fasciculus is an intrinsic fiber tract of the cerebral cortex which provides a major connection between Broca's and Wernicke's areas of the inferior frontal and posterior temporal lobes. It was first described in 1865, around the time that Broca ascribed language functions to the third frontal convolution, but before the role of the temporo-parietal area in speech reception was known (Meynert, 1865; Eidelberg and Galaburda, 1984).

2.5. STUDIES IN NON-HUMAN PRIMATES

2.5.1. Anatomical asymmetries in non-human primate brains

The brains and skulls of a number of non-human primates have been studied in order to determine whether patterns of anatomical asymmetry, as found in humans, are also present in brains of non-human primates. Studies have been performed in a wide range of primates including apes and New World and Old World monkeys (e.g., Groves and Humphrey, 1973; LeMay and Geschwind, 1975; LeMay, 1976; Yeni-Komshian and Benson, 1976; Falk, 1978a, b; Cain and Wada, 1979; LeMay et al., 1982; Sherman et al., 1982; Heilbroner and Holloway, 1989). These studies have been conducted in order to compare patterns of asymmetry in different non-human primates and compare them to those known for humans. It should be remembered, however, that lateral asymmetries are not unique to primates, and have been demonstrated in many species including birds and mammals (e.g., Bradshaw, 1988; Chueca et al., 1992; Tan, 1992)

2.5.1.1. Asymmetries of the sylvian fissure

In humans, the left sylvian fissure is longer than that on the right hemisphere in the majority of individuals that are left hemisphere dominant for speech and language functions, (e.g., Geschwind and Levitsky, 1968; LeMay and Culebras, 1972). This is due to the fact that the posterior region of the sylvian fissure on the left hemisphere is extended posteriorly due to

asymmetric expansion of the left hemisphere planum temporale (part of Wernicke's speech reception area). In the right hemisphere, the sylvian fissure terminates more anteriorly and courses in a more anterior direction as compared to the left.

Studies have measured the inter-hemispheric dimensions of the sylvian fissure, an important indicator of language function related inter-hemispheric asymmetry in humans, in a series of non-human primates. Results of these non-human primate studies suggest that the neural substrate for sylvian fissure asymmetry may have already been present early in primate evolution. However, it should be remembered that asymmetries of the sylvian fissure may not be unique to primates as many studies in non-primates such as rats, cats, birds, and even reptiles have demonstrated (Sherman et al., 1982). For example, in a study of sylvian fissure length in adult domestic cats *Felis domesticus* no asymmetry of the sylvian fissure was evident in the total sample (Tan, 1992). However, when the sample was considered with regard to sex, the left sylvian fissure was relatively longer than the right in females (L>R) whereas the opposite was the case for males (R>L).

One of the earliest comparative studies of sylvian fissure morphology was made by Cunningham who measured its length in a series of primates including *Pan, Pongo, Macaca, Papio, Cercocebus* and *Cebus* (Cunningham, 1892). No consistent pattern of sylvian fissure asymmetry was shown. For

example, the right sylvian fissure was longer in *Pongo*, whereas the left was longer in *Pan*. However, the sample sizes were so small that no conclusive statements could be made from his analysis. In a study of New and Old World monkey species, and both lesser and great apes, it was shown that only in great apes was there was a significant asymmetry in the position of the sylvian point (= the posterior end of the Sylvian fissure), similar to that shown for humans (LeMay and Geschwind, 1975). Surprisingly, sylvian fissure asymmetry was most marked in *Pongo*, and least marked in *Gorilla*. In the sample of 28 great ape brains, 16 showed a higher position of the sylvian point in the right hemisphere, while only one was larger in the left. In *Macaca fascicularis* and *M. mulatta* there was no difference in the dorso-ventral position of the sylvian point on the left and right hemispheres as in humans and great apes (LeMay and Geschwind, 1975; LeMay et al., 1982).

Using latex endocasts of eight genera of Old World monkeys, including both colobines and cercopithecines, Falk (1978) reported that both the sylvian fissure and superior temporal sulcus were significantly longer in the right hemisphere. Later, however, in a study using a 3-D digitizer she showed that the left sylvian fissure was significantly longer than the right as in humans (Falk et al., 1986). This indicated the presence of the homolog of Wernicke's area. In an extensive comparative study of sylvian fissure length in humans, chimpanzees and *Macaca mulatta*, it was shown that 84% of humans, 80% of chimpanzees, but only 44% of macaques, showed a sylvian

fissure that was longer in the left hemisphere (Yeni-Komshian and Benson, 1976). Also, equal lengths of the sylvian fissure were not found in humans, but were present in 12% of chimpanzees and 36% of macaques. In agreement with Falk's earlier conclusions (1986), a study which used immersion fixed brains reported that the sylvian fissure was significantly longer in the left hemisphere in all the Old and New World monkeys studied except *Saimiri sciureus* (Heilbroner and Holloway, 1988). Interestingly, results of length measures of the anterior portion of the sylvian fissure (that part located anterior to the central sulcus) also showed a trend towards left hemisphere predominance, even in *Saimiri sciureus*. This result is somewhat surprising since one would have predicted that the posterior portion of the sylvian fissure would be more asymmetric, due to the posterior position of Area Tpt (which is expanded in the left hemisphere of macaques), the cortical region homologous to Wernicke's area in humans. The posterior portion of the sylvian fissure (posterior to the central sulcus), however, was reported as being symmetric (Heilbroner and Holloway, 1988), unlike the marked asymmetry shown for humans. However, the position of the inferior part of the central sulcus has been shown to be placed more posteriorly on the left hemisphere in of 9 of 12 *Pongo* brains and 5 of 7 *Papio* brains (LeMay et al., 1982). As such, use of this highly asymmetric frontal-parietal lobe landmark for the demarcation of temporal lobe structure measures may not be informative.

In the recent extensive metric study discussed above (Heilbroner and Holloway, 1988), the use of formalin-fixed brains allowed for more accurate measurement of brain surface landmarks such as the sylvian fissure than did earlier measures taken on latex endocasts (Falk, 1978a, b). However, since the brains used were immersion fixed at some unspecified time after death, they may have manifested considerable and/or differential shrinkage problems related to post-mortem and immersion fixation

2.5.1.2. Other sulcal asymmetries

A range of other surface features, located adjacent to regions shown to be homologous to human speech-language areas, have been quantified in order to compare the distribution of inter-hemispheric asymmetries. These include the arcuate, principal and central sulci of the frontal lobe. It should be noted, as discussed above, that the region of cortex on the posterior-inferior margin of the vertical limb of the arcuate sulcus is homologous to Broca's area of humans. As such, one would predict that this region would be more extensive in the left hemisphere of non-human primates if a similar pattern of functional localization is already present. .

Falk's study of inter-hemispheric arcuate sulcus length, using latex endocasts, showed it to be significantly longer in the left hemisphere of *Colobus*, and a tendency to be longer in *Nasalis, Presbytis, Rhinopithecus, Macaca* and *Papio* (Falk, 1978a,b). To the contrary, the right arcuate sulcus

was shown to be longer in other taxa, for example *Pygathrix, Cercocebus, Cercopithecus* and *Theropithecus* (Falk, 1978b). A second measure used by Falk involved the distance between the posterior termination of the principal (rectus) sulcus and the adjacent part of the vertical limb of the arcuate sulcus, which she named the "rectus-arcuate gap". She showed that the rectus-arcuate gap was larger in the right hemisphere of cercopithecoids (Falk, 1978b). In addition, in 21 cases where the principal sulcus actually extended to the arcuate sulcus, 20 were on the left side, again showing a right hemisphere size predominance of prefrontal cortex anterior to the arcuate sulcus in these species. Falk commented that this represented differentiation of the adjacent cortical region (Brodmann's Area 46 - possibly homologous to part of Broca's area in humans) with concomitant elongation of the left principal sulcus (Falk, 1978a).

Another study of *Macaca mulatta* and *Macaca fascicularis* using immersion-fixed brains, measured the length of the horizontal limb of the arcuate sulcus in order to determine whether the macaque homologue of Broca's area was larger in the left hemisphere (Heilbroner and Holloway, 1989). Based on measures of this brain surface feature they reported symmetry of this measure. Similarly, data from humans have shown that the external parts of Broca's area are symmetric while those dimensions deep to the surface show significant, left hemisphere dominant, asymmetries (Falzi et al., 1982)

2.5.1.3. Petelial and hemispheric width asymmetries

In humans, a number of brain asymmetries are present that are thought to correspond to the primary left hemisphere localization of speech and handedness (LeMay, 1984; Kertesz et al., 1992). These asymmetries, for example, include larger right anterior frontal width corresponding to larger left occipital and parietal widths in individuals that are left hemisphere dominant for handedness (Kertesz et al., 1992). CT studies have also shown that right-handed individuals have more protuberant right frontal poles combined with more protuberant left occipital poles - generally referred to as "petelias" . In contrast, left-handed individuals show either symmetry or the reverse pattern, in either case, non significantly (LeMay and Kido, 1978; LeMay, 1984), however see Chui and Damasio (1980) in which significant asymmetries were not identified. Such human-like petelial patterns have even been reported to be present in fossil hominids (Holloway, 1980, 1981; Holloway and De La Coste-Lareymondie, 1982; LeMay et al., 1982). An alternate view to the hypothesis of functional neural substrates underlying petelial asymmetries in cercopithecoids and hominoids has suggested that they arose in relation to that of a shift in the pattern of drainage by the dural sinuses (Hennenberg and Symons, 1992). In this pattern, the superior sagittal sinus drains primarily to the transverse sinus on the right side while the much smaller straight sinus drains primarily to the smaller, and more inferiorly placed, left transverse sinus (LeMay and Geschwind, 1981). It has

been suggested that in humans this larger right-side sinus, simply by its physical presence, causes the right occipital lobe to be shorter than the left (Hennenberg and Symons, 1992). It is equally possible that this posterior physical displacement gives rise in turn to a more prominent right frontal pole. However, this view is controversial at present, and the assumption for this dissertation is that such petelial asymmetries are due to asymmetric functional localization of cognitive behaviors in the cerebral cortex.

A number of studies have looked for similar petelial or hemispheric width asymmetries in non-human primates in an effort to correlate these with those known to relate to human patterns of functional localization. For these petelial and width measures it is easier to obtain accuracy and reproducibility since measures do not involve demarcation of ambiguous landmarks such as the exact origin and termination points of sulci. This ease and reliability lends itself to use of these relatively unambiguous measures on fossil endocasts in which many of the important sulci are not well preserved (e.g., Holloway and De La Coste-Lareymondie, 1982). The only critical element involved is to ensure that the exact position of the brain, and thus the relative optical "viewpoint" used for measures in different individuals, is identical.

The pattern of frontal petelias was studied in a range of Old World monkeys by Falk (1978b) using latex endocasts. She concluded that only in *Presbytis* and *Cercopithecus* did the right frontal pole extend significantly

beyond that on the left hemisphere, with no species showing left frontal pole predominance. A later study by Falk and co-workers (1990) used a large sample of endocasts of *Macaca mulatta* from animals with known genealogies, age and sex, to ascertain, non-metrically, the pattern of frontal and occipital petelias. Again, it was demonstrated that the right frontal pole projected significantly beyond the left (R>L in 191, L>R in 102, L=R n=93) but that there was no predicted co-occurrence or sample predominance of a left occipital petelia (R>L n=143, L>R n=138, L=R n=91) as in humans. Similarly, in a study of perfusion-fixed *Papio papio* (n=6) and *Papio anubis* (n=1) brains, it was shown that in six of seven brains the right frontal pole extended beyond that of the left by up to 2mm (mean = 1.2mm), including that of *P. anubis* (Cain and Wada, 1979). In the seventh brain, both sides were equal. In a study of asymmetry in skulls of the mountain gorilla, *Gorilla gorilla beringei* it was shown the left side was longer in 17 while there was no difference in 21 animals (Groves and Humphrey, 1973). Interestingly, there was no such asymmetry present in skulls of the coastal gorilla, *G. g. gorilla*. Whether these data on antero-posterior skull dimensions in gorillas reflect cerebral asymmetry or are related to asymmetry of the masticatory apparatus, which are more developed in the mountain gorilla, is unknown.

2.5.2. Cortico - motoneuronal projections in primates

An important aspect of the ability of the cerebral cortex to exercise fine volitional control of peripheral structures such as the facial and laryngeal muscles, is the directness of axonal projections from cortical output (efferent) neurons onto motor neurons in the brainstem. The motor neuron nuclei in the brainstem, which include 1) *trigeminal motor nucleus* of the masticatory muscles, 2) *facial motor nucleus* of the facial musculature including orbit and mouth, 3) *nucleus ambiguus* of the larynx and pharynx, and 4) *hypoglossal nucleus* of the tongue, directly innervate the peripheral musculature, all four groups of which are involved in human vocal-auditory communication. The time (in milliseconds) taken to perform a motor act is reduced several fold if the cortico-motoneuron projection is direct rather than via one or more interneurons. Likewise, the speed of sensory information coming back in allows for rapid adjustment of the initial motor outcome, thus enhancing fineness of motor control. This refined neuro-motor capacity appears to have occurred during later primate evolution (Sokoloff and Deacon, 1990).

Data supporting the idea of an enhanced and primary role of the face in volitional communication in Old World monkeys is provided by Alan Sokoloff and terry Deacon (1990) who demonstrated that direct projections from motor cortex to motoneurons in the facial motor nucleus were present in macaques, but not in any of the non primates studied. This direct projection could allow for much finer cortical control of facial movements in an animal who probably

requires considerable subtlety and diversity of facial expressive capacity for effective communication. Direct projections from motor cortex to laryngeal motoneurons (nucleus ambiguus) are known to exist in humans (Kuypers, 1958a) and to a lesser degree in chimpanzees (Kuypers, 1958b). However, direct cortical projections to nucleus ambiguus do not appear to be present in either *Saimiri sciureus* (Jürgens, 1976), or *Macaca mulatta* (Kuypers, 1958b; Zealear, 1991). However, these methods were derived from methods involving response latency times after electrical stimulation of cortex e.g., (Zealear, 1991), which may be subject to interpretative errors. Insensitive outdated methods (cortical ablation/brainstem terminal degeneration) were also used for many of these latter studies(Kuypers, 1958b). The use of modern, sensitive neural tract-tracing methods to map projections from cerebral cortex to brainstem laryngeal motoneurons, such as those done for cortico-facial (Sokoloff and Deacon, 1990), and cortico-hypoglossal (Sokoloff, 1989) projections still have to be done.

2.5.3. Physiology of non-human primate communication

A wealth of literature has dealt with the abilities of non-human primates and other mammals with regard to the underlying physiological substrates of their central and peripheral vocal communication capacity (e.g., Robinson, 1967; Lieberman et al., 1969; Jurgens and Ploog, 1970; Steklis and Raleigh, 1979; Ploog, 1981; , Laitman, 1983; Laitman and Reidenberg, 1988, 1993;

Lieberman, 1984; de Lanerolle and Lang, 1988; McLean and Newman, 1988; Newman, 1988; Sutton and Jürgens, 1988; Crelin, 1989; Newman et al., 1991, Laitman et al, 1992; Lieberman et al., 1992). Studies to date have focused on the vocal-auditory channel as being the primary communicative modality in non-human primates. Studies have not focused on, or even considered, the neurobiological aspects of visual communication abilities in non-human primates, other than simple facial recognition (non-communicative) in monkeys and signing in the great apes. The neural mechanisms underlying the various modes of primate vocalization are still poorly understood. Studies on the neural localization of vocalization substrates range from laboratory characterizations of specific vocalizations such as the isolation call of cats and monkeys, the howls of timber wolves (Tooze et al., 1990), and even the croaks of frogs (Bauer, 1993) to field projects examining responses to calls played over a loudspeaker (see review by Cheney and Seyfarth, 1990).

2.5.3.1. Electrical stimulation techniques

As discussed above, in humans electrical stimulation of area 44 of the inferior frontal lobe (Broca's area) can interrupt speech-language related functions while stimulation of the supplementary speech area can induce repetitive vocalization. Stimulation of the inferior precentral motor cortex (face, lips, tongue and larynx motor output region) can give rise to production

of movements of either the vocal folds or other vocal tract and face associated muscles (Brickner, 1940; Erickson and Woolsey, 1951; Penfield and Welch, 1951; Penfield and Roberts, 1959; Ojemann, 1992). Studies in non-human primates have shown that stimulation of these homologous cortical regions in both *Macaca mulatta* and *Saimiri* (Sugar et al., 1948; Hast and Milojevic, 1966; O'Brien et al., 1971) do not elicit vocalizations. Although phonation did not result, these studies supported a direct connection between monkey cerebrocortical homologs of human speech areas and certain aspects of lower level phonatory neural control mechanisms. Whether these cortico-motoneuronal connections are directly related to communicative mechanisms, however, is currently unknown.

Vocalizations were elicited in lightly anesthetized chimpanzees upon electrical stimulation of the inferior premotor cortex anterior to the motor face area (Leyton and Sherrington, 1917; Dusser de Barenne et al., 1941). These results suggest that great apes, such as chimpanzees, may represent the intermediate condition of this neural control circuitry between monkeys and humans. The use of great apes in this kind of invasive research is no longer possible, but perhaps with the refinement of non-invasive 3-D functional imaging techniques, differences between the neural substrates for communication in apes and monkeys may be further explored.

Most studies have conclude that monkeys have no cortical involvement in vocalization and that subcortical regions and mechanisms solely subserve

this process e.g., see (Sutton and Jürgens, 1988). For example, electrical stimulation of the anterior cingulate or other structures in *Hylobates lar,* (Apfelbach, 1972), and *Macaca mulatta* (Robinson, 1967), and *Saimiri* (Jurgens and Ploog, 1970) gave rise to the full array of species-specific vocalizations. It was shown by these studies that the neural substrates for the different types of species-specific vocalizations were not randomly distributed but occurred in specific loci (Robinson, 1967). In humans, bilateral lesions of the anterior cingulate cortex gives rise to a deficits of emotional expression, and as such may be responsible for the volitional verbalization of emotions (von Cramon and Jürgens, 1983).

It has been demonstrated that at least in *Macaca mulatta*, the glottal sounds arising from subcortical vocalization mechanisms can be subject to further modification by use of the supralaryngeal vocal tract in a form of call "articulation" (Hauser et al., 1993). It was commented that these articulatory maneuvers contribute to the animal's potential acoustic space, thereby potentially increasing the array of meaningful vocalizations within the repertoire (Hauser et al., 1993).

2.5.3.2. Brain lesion techniques

An alternative approach to electrical stimulation of the cerebral cortex involving the use of localized brain lesions has been used by some researchers. This approach involves making controlled lesions in various

cortical sites with subsequent observation of the effects on specific calls. One such study involved removal of portions of cerebral cortex in *Macaca mulatta* homologous to human speech areas, such as Broca's area, transitional parieto-association cortex, and temporal association cortex (Sutton et al., 1974). Results of this study showed that the neural control, of at least learned discriminative phonation in monkeys, was not mediated by cortical regions homologous to human speech areas. Ablation of anterior cingulate gyrus (subcortical-limbic associated) however, did affect call performance considerably, supporting the view of a singular role for subcortical mediation systems.

Ablation of the anterior cingulate cortex in *Macaca mulatta* disrupted both spontaneous and conditioned vocalizations but had no discernible effect on non-vocal social behavior (Aitken, 1981). However, lesions of Broca's and Wernicke's area homologs had no effect on either vocalization or non-vocal social behaviors. This outcome is in marked contrast to the studies by Myers and co-workers who showed major deficits in social behavior in individuals that had lesions of the inferior frontal lobe (Myers and Swett, 1970, 1973; Myers, 1972). For example, after lesions of Broca's area in macaques there was a major disruption of facial signaling patterns. This resulted in an inability of the lesioned animal to re-establish itself within the social group to which it had belonged from birth, when it was released back into the social group (Myers, 1972). This outcome may have been due to an inability of the

lesioned animal to process and deliver appropriate visual communicative signals and be unrelated to vocalization deficits. The contrast between the outcome from lesions of Broca's area by Aitken's and Myers' groups, with regard to retention and loss, respectively, of non-vocal communicative social behaviors, may be due to the fact that in Myers case the lesioned animals were released back into a free-ranging situation within a long established social group, as opposed to Aitken's more restricted caged experimental setting.

Studies in the New World monkey *Saimiri sciureus* showed that ablation of lower sensorimotor face cortex (including the Broca's area homologue) did not give rise to any differences in call types (Kirzinger and Jürgens, 1982). Further, it was shown that extensive ablation of the lower sensorimotor face representation, which prevented the animals even from chewing, licking or swallowing, did not affect their vocalizations. Unlike the studies in macaques mentioned above, however, these studies did not assess deficits of non-vocal communicative behavior. Lesion studies have also been conducted with subcortical sites in squirrel monkeys. For example, one study ablated different aspect of the rostral midline limbic cortex, a subcortical site that has been shown to elicit "isolation call" vocalizations upon electrical stimulation (McLean and Newman, 1988). It was concluded that an array of limbic cortical loci were involved in the call but that there was no contribution by the adjacent midline frontal neocortex. This is not surprising

since the isolation call or "distress call" may be an extremely basal mechanism which is distributed widely amongst mammals (McLean, 1985), and as such would not be expected to be a higher cortical function.

It appears from results of most studies that the homolog of Broca's area in both Old World and New World monkeys is essentially dispensable for the production of vocalizations (Jürgens, 1976). This has been attributed to the fact that unlike humans, monkeys do not have direct projections from cortex to brainstem laryngeal motoneurons (i.e., nucleus ambiguus). As such, human cerebral cortex exerts a more refined control on phonation than that in monkeys. There are direct projections from macaque cerebral cortex to tongue, jaw and face brainstem motoneurons (Sokoloff, 1989; Sokoloff and Deacon, 1990). However, the data for cortico-motoneuronal projections to laryngeal/vocal tract motoneurons is far from definitive in monkeys, and is known to be present already in apes as discussed above.

2.5.3.3. Dichotic listening and right ear advantage

Studies of dichotic listening in humans, described above in section 2.3.3., demonstrate a right ear / left hemisphere advantage for various speech tasks. These studies have suggested that the left hemisphere of humans is functionally specialized for language perception. Similar studies have also been conducted in some non human primates (e.g., Beecher, 1979; Kuhl, 1979; Snowdon, 1979; Zoloth and Green, 1979; May, 1989; Moody et al.,

1989). For example, studies by Moody and co-workers have used the "categorical perception" model of auditory perception in which Japanese macaques (*Macaca fuscata*) were required to discriminate species-specific vocalizations using a variant of the dichotic listening paradigm (Beecher, 1979; Moody et al., 1989). This contrasts with the "temporal decoding" model used by Tallal and co-workers, outlined below, which describes a purely mechanistic aspect of the auditory perception decoding mechanism (Tallal, et al., 1993). Results of these categorical perception studies in Japanese macaques demonstrated that, at least in this species, there are specialized brain processing mechanisms present for such things as "perceptual constancy" and "categorical perception" which are similar to those shown to be involved in human speech perception (Moody et al., 1989). These specialized mechanisms are also, like in humans, functionally lateralized to the left hemisphere as indicated by the right ear advantage for conspecific vocalizations (Beecher et al., 1979; May et al., 1989).

A right ear / left hemisphere advantage for auditory processing, interestingly, is not limited to primates or even to species-specific communicative sounds. Instead, the left hemisphere may be more fundamentally specialized for the decoding of temporally spaced tonal sequences. For example, work in rats has shown a distinct right ear advantage for tone sequence discrimination particularly in males (Fitch et al., 1993). It has been suggested that this left hemisphere specialization for

the decoding of temporally spaced tones may have provided the evolutionary precursor for left hemisphere language mechanisms. This result is also similar to that reported for humans which also show temporal decoding mechanisms, leading some to suggest that this may actually represent the most basal brain language mechanism allowing us, for example, to distinguish between the two consonant vowel pairs /ba/ and /da/ (Tallal, 1993).

2.5.4. Handedness in non-human primates

2.5.4.1. Relevance of handedness to language and brain asymmetries

Many studies of the cerebral localization of speech-language and handedness functions in humans have indicated that there is some kind of a relationship between the neural substrates that subserve these otherwise distinct traits. Similar, though less extensive, behavioral and experimental studies have also been conducted in a range of non-human primates in an attempt to compare patterns of handedness preferences and their underlying neural substrates to that already known for humans. If patterns of handedness are absent in non-human primates, the situation in humans, in which ~90% of individuals are both strongly right-handed and left hemisphere dominant for speech-language functions, would represent a *de novo* acquisition. As the studies reviewed below suggest, however, handedness is in fact present in many of the non-human primates studied,

but it is represented at a different level of neural processing and only becomes apparent during task-specific behavioral sequences. Further, it is clear that non-human primates show patterns of hand preferences that are quite different to those that characterize humans (MacNeilage et al., 1987). In addition, many studies have described the use of tools both by great apes as well as by Old World and New World monkeys.

The relationship of skilled tool use to handedness preferences has been a focus of a many anthropological studies. This has been particularly important in light of suggestions that tool use in early hominids such as *Paranthropus robustus* (Susman, 1988), or *Homo habilis* (Tobias, 1965), is considered to be the underlying adaptive force which gave rise to the marked prevalence of right handedness, and possibly hemispheric dominance for language, in modern humans (e.g., Steklis and Harnad, 1976; Corballis, 1983)

Population-level asymmetries for handedness in non-human primates are unlike those known for humans (for reviews see e.g., Warren and Nonneman, 1976; Walker, 1980; Bryden et al., 1983; Corballis, 1983). Recently however, extensive reviews of the non-human primate handedness literature by McNeilage and co-workers (1987) and Fagot and Vauclair (1991) concluded that there was good evidence for significant, complex task specific, behavioral asymmetry, present at the population level.

2.5.4.2. Handedness for "simple reaching" tasks

A large series of studies have looked at "simple food reaching" in a range of primates from prosimians (including seven species of the genus *Lemur*, as well as *Varecia variegata* and *Galago senegalensis*), New World monkeys (including *Cebus* and *Callithrix*), Old World monkeys (including *Erythrocebus, Rhinopithecus, Presbytis*, 5 species of *Macaca*, and three species of *Papio*) and apes (including *Hylobates lar, Pongo, Gorilla gorilla*, and *Pan troglodytes*); for a list of these studies see Table 1 in the review by Fagot & Vauclair (1991). Studies were conducted in various conditions ranging from free-ranging in a wild setting to the more restricted environment of laboratory cages. Various criteria for reaching preference were used. For example, in the study by Tokuda (1969), eight out of a total of ten reaches by the same hand in one individual, determined hand preference. Among the 41 statistically viable reports across primates, 38 studies were unable to demonstrate a significant difference ($P<0.05$) between the left and right hands for a simple food reaching task.

Among prosimians, significant ($p<0.05$) hand preferences for reaching tasks were shown in only two of 14 studies reviewed by Fagot and Vauclair (1991), including: 19 of 29 (including 3 with no preference) free-ranging *Lemur macaco*, and 15 of 24 (including 4 with no preference) *Lemur fulvus* in which distinct left-hand dominance was apparent (Ward et al., 1990). In sum, there is some limited evidence that a left hand preference for simple

food reaching is present in certain groups of prosimian primates but it is not clear whether this is manifested at the population level

Few studies of simple reaching tasks have been conducted in New World monkeys. However, one study reported a significant left hand preference for food reaching in six of eight *Callithrix jacchus* (Box, 1977). A later study of *Cebus apella* showed no significant asymmetry of hand preference (Fragaszy and Mitchell, 1990). In this latter study, however, three individuals did show a left-hand preference versus one right-hand and three with none, suggesting a trend towards left handedness. These more limited results appear consistent with the trend for left handedness reported for prosimians. However, again these results represent a small locally biased sample, and as such, are probably not representative at the population level.

Three studies in Old World monkeys showed a tendency ($P=<0.1$) towards a preference of the left-hand for reaching: in 12 of 19 (2 with no preference) caged *Macaca mulatta* (Brookshire and Warren, 1962), 149 of 394 (127 with no preference) (Itani et al., 1963), and in 17 of 41 (16 with no preference) (Tokuda, 1969), free ranging *Macaca fuscata*. In contrast, one study showed a tendency ($p<0.1$) towards a right hand preference for food reaching in 10 of 16 (including 3 with no preference) *Presbytis* (Yuanye et al., 1986). An earlier study by Mitani of reaching in *Macaca fuscata,* however, showed a significant ($p<0.05$) left hand preference in 30 of 69 (including 23 with no preference) (Itani, 1957).

Of the six studies on ape simple-reaching reviewed by Fagot and Vauclair (1991) none demonstrated a significant hand preference, although sample sizes in some cases were quite small (range of n = 5 to 26). Results from an reaching task study (n=26) conducted in *Pan troglodytes* showed equal representation of hand preference as well as five cases of ambidextrality (Steklis and Marchant, 1987).

In sum, the results for simple reaching tasks throughout primates do not support unequivocally the condition in which there is a consistent asymmetric hand preference. Although some studies have shown a trend towards left handedness, these results may simply reflect local group sampling biases or experimental design variables and not represent the population level. In addition, the limited nature of the evidence suggests that there in no lateralized hemispheric specialization for simple reaching tasks and that both hands and both hemispheres are equally capable of effectuating this low-skill motor task. In recognition of this low level of motor skill, Fagot and Vauclair refer to simple food reaching, along with several other gross motor actions such as holding, pulling, and picking up of various objects, as "low-level tasks" (Fagot and Vauclair, 1991). These authors consider that one should not consider lateralization for low-level tasks as a common characteristic of a group or population and that it more likely represents an idiosyncratic feature relating to the situational context.

2.5.4.3. Handedness for complex tasks

In order to describe the differential complexity of various manual tasks in non-human primates, MacNeilage et al. (MacNeilage et al., 1987) offered a descriptive classification. This involved the "simple-reach tasks" described above, as well as other tasks of varied complexity such as "complex reach", "expose and reach", stabilize and reach", "retrieve and reach", and "manipulate and reach" tasks (MacNeilage et al., 1987)(p.248). In all cases a series of more complex tasks, such as stabilizing an object in which the food is placed or opening a loose hasp, precede the final "food reaching" task. A similar approach was also later used to classify the complexity, and as such, the inferred "precision level" of different manipulative tasks, but the concept was taken a step further by stipulating the extent of complexity in terms of the movement precision, relative to the spatio-temporal dimension of the task (Fagot and Vauclair, 1991).

Within this model, failure to demonstrate handedness for a particular behavioral task may simply represent the inadequacy (inherent simplicity) of the task, and as such the lack of requirement for a highly skilled, and more likely lateralized (asymmetric) neural substrate. These tasks, which required a more skilled and complex motor sequence compared to simple reaching, were referred to as "high-level tasks" and included tasks such as *1)* reaching with erect posture - which introduces many spatio-temporal constraints; *2)* extreme reaching; *3)* simple reaching with visuo-spatial

adjustment task; *4)* somatosensory haptic discrimination tasks; *5)* tactile discrimination tasks; *6)* manipulation of a joystick: and finally, *7)* catching or grasping a moving object, involving complex spatial and temporal elements.

In many cases groups of primates that did not show any tendency for asymmetric hand preference with a low-level task, showed a strong handedness for high-level tasks. For example, in a study using 12 gorillas, a significant right-hand preference (10 of 12) was shown in a task which involved obtaining a raisin from a wire suspended above their standing height (Olson et al., 1990). In contrast, for these same animals, no significant difference in handedness was shown for a simple reaching task. Another study used gorillas to contrast a simple (direct access) food-reward reaching task with a more spatially complex food reward access task involving alignment of holes in two sliding plates (Fagot and Vauclair, 1988). Results showed no significant hand preference for gorillas in the simple reaching task but there was a highly significant left-hand preference (7 of 8) for the more spatially complex access task. A study using chimpanzees and rhesus monkeys required use of a joystick to produce a collision of the cursor and a target on the monitor (Hopkins et al., 1989). Again, a significant right-hand preference was shown, both for hand chosen for use of the joystick and in terms of "velocity of target hitting". In the same animals, no asymmetry was shown for a simple reaching task (Hopkins et al., 1989).

In contrast to these high-level motor tasks which elicit a right-hand preference within the group, other high-level tasks have shown an opposite, left-hand preference. For example, several studies have shown a distinct left-hand preference for tasks such as catching live fish by squirrel monkeys (King,JE et al., 1987), catching objects in midair by Japanese macaques (Kawai, 1967), and tactually and visually regulated discrimination tasks in rhesus macaques (Fagot et al., 1991). Results from these studies indicate there may be a right-hemisphere specialization for the neural processing of spatial, temporal, tactile, and visual tasks .

Similar task-specific handedness differences have been shown using other tasks. A joystick study similar to that used by Hopkins and co-workers (1989) which showed a right-hand preference, was later conducted in *Papio papio* by Vauclair and Fagot (1993). However, results from this study showed more skilled use of the left-hand in terms of the measure involving shortest path length to the target. Apparently this parameter provided a better picture of the strategy used by the subject and these spatial components may be more sensitive to laterality than response times. A better understanding of these and other variables would allow for the nature of hemispheric specialization underlying "hand preference" and "hand performance" to be distinguished (Vauclair and Fagot, 1993).

2.5.4.4. Current theories of non-human primate handedness

Based both on the examples described above and many other studies, it is clear that the nature of handedness in non-human primates is different from that present in humans. In addition, it is evident that there are substantial differences in both cognitive status and skilled use of the hand between Old World and New World monkeys and apes, especially with regard to more cognitively advanced manual activities such as tool production and use. Recently, there have been a number of synthetic theories proposed concerning the nature of, and the evolutionary sequence of adaptive events which may underlie the asymmetric cerebral lateralization of handedness in non-human primates.

In a review, McNeilage and co-workers (1987) proposed an evolutionary scenario for the distribution of asymmetries in the hemispheric localization of handedness preferences in living primates (MacNeilage et al., 1987). They proposed that there was good evidence for a consistent, population level, left-hand preference for simple reaching and a right-hand preference for manipulation and practiced performance tasks. These patterns of handedness in non-human primates were considered to be precursors to those present in humans and probably evolved initially as: *1)* a left-hand/right-hemisphere specialization for visually guided reaching, as represented by the prehensile hand of prosimians, which was complemented by the right hand being used for postural support; and *2)* a right-hand/left-

hemisphere specialization for more complex manipulative tasks upon development of an opposable thumb with a concomitant decrease of right-hand use as a vertical postural support, e.g., in monkeys (MacNeilage et al., 1987). Unlike previous views which have proposed more "metafunctional" models of manual specialization (e.g., Calvin, 1982), the critical role of functional adaptation in manual specialization during primate evolution was stressed. However, as discussed above, the behavioral evidence upon which this theory is based is quite weak, and as such, does not unambiguously support their evolutionary hypothesis.

Another view of the evolution of handedness in non-human primates considered various patterns of manual specialization within the framework of task-specific demands (Fagot and Vauclair, 1991) as discussed above. In this model, a specific manual activity is classified as being either "high-level" or "low level". Only high-level tasks showed evidence of an asymmetrical distribution of hand preferences at the population level. A distinction is made between "handedness" which corresponds to the low -level tasks, and "manual specialization" which corresponds to the high-level tasks. This high-level manual specialization in non-human primates is considered homologous to patterns of cerebral lateralization underlying handedness in humans In this case, homology is not affected by the direction or degree of asymmetry since essentially, the critical element is the presence of hemispheric specialization for a particular task.

2.5.5. Non-vocal aspects of human and non-human primate communication

2.5.5.1. Studies in humans

The human communicative repertoire comprises a mosaic of interacting modalities spanning the spectrum from gestural-visual to vocal-auditory. Cortical regions in the right cerebral hemisphere play a role in the processing and interpretation of facial expressions, facial movements during speech, and emotional expression, all of which are important aspects of human face to face communication (Ross,EE, 1981; Ahern et al., 1991), see however (Cancelliere and Kertesz, 1990). For example, it has been shown recently that complementary visual communicative input can modify the processing of speech sounds in auditory cortex (Sams et al., 1991), suggesting an interaction between visual and auditory communicative information that may be more important than is presently appreciated. In fact, the delivery and perception of such socially acceptable facial and gestural expressions may be a key part of the normal human communication repertoire that may have been selected for during human evolution. For example, Grüsser and co-workers (1990) in their work with schizophrenics (who seem to have a disturbance in cognition of these social skills), considered communicative impairment as a possible core symptom of the disorder. Further, it was considered that the paranoiac responses of these individuals may be the result of an impairment in perception and cognition of highly relevant, social,

averbal, communicative signals, and their misinterpretation (Grüsser et al., 1990). If these results are incorporated into an evolutionary framework, it could be hypothesized that the correct use and cognition of such non-verbal communicative repertoires would be under strong selective forces at the population level. In most modern human cultures such socially and communicatively inappropriate individuals are severely alienated.

The work of Tallal's group at Rutgers University has provided some further insight into the mosaic and polymodal nature of the human communicative repertoire. For example, in a study of both normal and language impaired children subjects were given tests of comprehension and expression of "affective intent" using both spoken language as well as facial expressions (Fitch, et al., 1993). As expected, language impaired children performed poorly with regard to comprehension and expression of vocal effect compared to normals. However, the language impaired individuals performed much better than normals with regard to non-vocal aspects of facial affect. It was concluded that language impaired children are limited to deficits of vocal affect and that they may employ compensatory mechanisms which involved enhancement of the gestural-visual modality.

2.5.5.2. Studies in non-human primates

Studies in macaques demonstrated a right hemisphere preference for discrimination of faces of conspecifics in a test situation (Hamilton and

Vermiere, 1985). An interesting hypothesis, which may be relevant to our understanding of the evolutionary progression from monkey communication abilities to those of humans, was recently proposed (Desimone, 1991). This hypothesis is based on data from neurophysiological recordings made from cortical neurons, located in the temporal cortex of macaques, that were specifically responsive to visual images of faces. It was concluded that strong selective pressures led to the evolution of neural mechanisms for the primary use of facial expressions in nonhuman primate communication. This shift is also mirrored in the significant differentiation of the facial musculature in anthropoid primates compared to lower primates and mammals.

Face-responsive cells are more prevalent in the left hemisphere than the right (Perrett et al., 1988, 1992). This region in macaque temporal cortex is the same as that considered to be polymodal language cortex in humans which is homologous to Wernicke's area. This brain region has been considers as a potentially fertile zone for the development of supramodal mechanisms for communication (Desimone, 1991). Interestingly the left vs right hemisphere dominance data are explained as being due to differential processing of facial information, in which left hemisphere "face cells" are involved more in communicative aspects of the face while cells in the right hemisphere are more involved in pattern recognition of faces for recognition of other individuals. This concept of visually mediated communication in the left hemisphere is strikingly similar to that described for the cerebral

localization of human signed languages which is essentially identical to those of speaking humans (Bellugi et al., 1983). Unfortunately, it seems that the non-vocal communication repertoires present in non-human primates have yet to be seriously considered as behavioral precursors to vocal-auditory communication in early hominids. This view is exemplified by comments made by King regarding Snowdon's work on visual signaling in apes (Snowdon, 1990) and Zeller's work on facial expressions in *Macaca sylvanus* (Zeller, 1986), in which she stated "when information is sent and received visually, can communication ever be termed symbolic?" (King,BJ, 1991:102). As discussed above, since brain mechanisms underlying communication in humans are not changed by the communicative modality, it seems that visual communication can be symbolic.

2.6. HOMOLOGY IN THE NERVOUS SYSTEM

2.6.1. Introduction

The theoretical framework of this dissertation, in accord with other current investigations exploring the evolution of neural substrates for human linguistic abilities, is based upon studies showing that regions of the human brain involved with speech and language have (phylogenetic) homologs in the brains of Old World monkeys. The widespread acceptance of this conclusion regarding evolutionary relationships is grounded in evidence from studies of

cortical function conducted in humans over the last one hundred years. This has incorporated evidence obtained, for example, from studies of functional deficits after lesions, from electrical stimulation of the cerebral cortex in awake patients during neurosurgery, and from studies of patterns of cerebral asymmetry and functional localization. More recently, neuroanatomical data from cercopithecoid primates has clearly demonstrated, using a variety of operational criteria, the validity of the homologous relationship between these specific brain regions in humans and catarrhines. Since these studies form the fundamental substrate upon which my evolutionary hypotheses and tests are based, they are detailed below.

2.6.2. Historical foundation for the concept of homology

The meaning and use of the concept of "homology" has been subject to a great deal of variable interpretations since its inception in 1555 by the French anatomist Belon du Mans, whose works on the skeletal system of birds and humans suggested an "equivalence of parts". This notion of morphologic (but not phylogenetic) equivalence in different species, largely founded within the period paradigm of the "Bauplan" or basic plan, was maintained for the next three centuries.

In the nineteenth century, the comparative anatomist Richard Owen was one of the first to advance a more objective definition of homology, stating that homologous structures were "the same organ in different animals under

every variety of form and function" (Owen, 1843: 379). He further defined three types of homology: 1) "Special" homology - "correspondency of part or organ, determined by its relative position and connections, with a part or organ in a different animal; the determination of which homology indicates that animals are constructed on a common type"; 2) "General" homology - "that in which a part or series of parts stands to the fundamental or general type"; and 3) "Serial" homology - "serial repetition or representative relation in the segments of the same skeleton". Owen's early theoretical foundation provided an initial framework for a concept that has become a fundamental, yet much debated, issue in evolutionary biology.

Sixteen years after Owen's definition of homology versus analogy (= a term used to define the non-evolutionary relationship between two structures with regard to their similarity of function; e.g. bat and bird wings are homologous as mammalian forelimbs but analogous as wings). Charles Darwin published his landmark book *The Origin of Species* (Darwin, 1859). The ideas put forward in this book gave rise to a paradigm shift with regard to our understanding of the processes underlying evolutionary change. However, although Darwin made clear his ideas on inheritance of adaptive traits and natural selection, he did not address directly the complexities of the concept of homology in *The Origin of Species.* More than a century later Ernst Mayr commented on the historic significance of Darwin's book to the concept of homologous relationships, stating that: "After 1859 there has only

been one definition of homologous that makes biological sense: A feature (character, structure, and so on) is homologous in two or more taxa if it can be traced back to (derived from) the same (a corresponding) feature in the presumptive common ancestor of these taxa" (Mayr, 1982: 45).

Many independent definitions of homology have been proposed. For example, Eldredge and Cracraft (1980: 37) defined homology as, "Homologous similarities are inferred inherited similarities that define subsets of organisms at some hierarchical level within a universal set of organisms". However, this taxic view is grounded within the methodological framework of cladistic analysis, and as such, implies that it is the ultimate arbiter of homology and homoplasy. Further, it suggests that homology can be known only after the phylogeny of a group is already known. A concise concept was proposed by Van Valen (1982:305), where he considered that "Homology is resemblance caused by a continuity of information". No specific information was offered regarding the nature of this continuity although the specific coding in the genome was explicitly stated and discussed. Van Valen's definition dealt with both historical and iterative (serial) homologies. Likewise, Wiley (1981) has noted that: "A character of two or more taxa is homologous if this character is found in the common ancestor of these taxa, or, two characters (or a linear sequence of characters) are homologues if one is directly (or sequentially) derived from the other(s)." Wiley's definition embodies the traditional Darwinian perspective on historical homology.

The paleoneurologists Striedter and Northcutt (1991: 179), considered Wiley's view to be more definitive compared to other definitions, since it distinguished between static and transformational homologies. These authors defined "*Static homology*" as being the case when, "an ancestral character is retained in two or more descendant taxa without any transformation" and "*transformational homology*" when " the ancestral character is retained in only one of the descendant taxa and is transformed into a different character (or series of characters) by a single transformation (or linear sequence of transformations) in the other taxon (or taxa)" - see above.

Unlike most previous definitions of homology, Wiley's concept excluded cases of non-homologous, homoplaseous characters. Homoplaseous characters include both parallel and convergent traits which evolved independently, and were not present in their earliest common ancestor. These homoplaseous characters are characterized as having been transformed from their common or different morphologic anlage by independent processes.

Operational definitions and the definitive working methods that could be used to distinguish between structures that are true homologues and those that are the result of homoplasy have been proposed. They are dependent on a strict separation of the theoretical and operational definitions of homology. In fact, neither homology or phylogenetic hypotheses can be defined in terms

of similarities. Bock (Bock, 1977: 890) proposed that one way to test homology hypotheses was to ascertain whether the characters involved were those that subserved "...a wide range of biological roles rather than having a single biological role because the probability of a feature serving a wide range of roles evolving independently two or more times is less than one that has only a single biological role and tight correlation with a single or narrowly delimited environmental factor". Bock's view of the use of functional criteria in the testing of homology hypotheses was based on the concept that if the "... evolutionary change is adaptive, then functional and adaptive analyses form an integral part of the analysis (Bock, 1981: 5). Other investigators have cautioned against an over-reliance on the use of these functional and adaptive criteria since it was considered that "...proponents of a functional approach to phylogenetic reconstruction rely too often on subjective authoritarian argumentation" (Cracraft, 1981: 21) and that functional data did not play any role in phylogenetic analysis. However, in the case of testing homology hypotheses in the nervous system, functional-adaptive criteria may well play an important role in character analysis, as discussed below.

Although the theoretical frameworks underlying the global concept of homology in evolutionary biology remain controversial, (e.g. see Van Valen, 1982), the theoretical definition of (phylogenetic) homology at least is clear (Bock, 1981). A wide array of theoretical and working definitions of

homology have been advanced, each with its own advantages, problems and applicability. There are, however, certain problems for testing homology hypotheses which are unique to the nervous system. As such, those theoretical and operational frameworks put forward by evolutionary neurobiologists, that were specifically designed to test homology hypotheses in the nervous system, are utilized for this study of primate brain evolution, (e.g., Campbell and Hodos, 1970; Striedter and Northcutt, 1991).

2.6.3. Homology in the nervous system

The brain differs from most other structures of the body, such as bones and teeth, in that the majority of the morphologic components used for character analysis and testing of homology hypotheses are located deep to the surface of a soft and perishable organ. As such, the fossil record cannot provide us with as precise a record of the evolutionary changes taking place in the brain as can fossils of hard skeletal tissues such as teeth and bones. The fossil record of brain evolution, i.e. endocasts, can however, provide data on the gross morphology of surface structures such as cerebral sulci and gyri. Aspects of cellular cytoarchitecture, chemical identity, regional connectivity and inter-hemispheric asymmetry, however, must be studied by use of a comparative anatomical approach. These data may, in turn, be related to the more limited evidence provided by the fossil record in an attempt to understand the larger picture.

The use of comparative methodology, however, must be approached with a proper understanding of inherent problems. Studies of hypothetically homologous regions involve comparison of the distinct morphological end products of individual species since they shared a common ancestor. This morphological divergence could give rise to end products that are distinct from one another in many ways, making character comparison more difficult. However, the brain has been consistently shown to be a conservative structure which evolves largely by incorporation and modification of pre-existing neural substrates, see, e.g. (Sarnat and Netsky, 1981; Kaas, 1989; Arbas et al., 1991). An example of such incorporation and modification in nervous system evolution is the shift in anthropoid primates to the (more derived) cortical projection system in which there are direct projections from cells in the pre-central motor cortex onto brainstem motoneurons (which in turn innervate muscles of the head and neck). In comparison, the homologous motor circuitry, present in all other mammals, involves intermediary reticular inter-neurons (Sokoloff, 1989; Sokoloff and Deacon, 1990). This evidence for character transformation clearly involved direct incorporation and modification of the basal mammalian circuitry and did not represent a novel projection system. In sum, this widespread and predominant pattern of evolutionary mechanisms provides a robust predictive framework upon which homology hypotheses within the nervous system can be founded.

Indeed, to date, there have never been any reports documenting a brain region arising *de novo* to subserve a new functional outcome or "biological role". In apparent disregard of the contradictory neural evidence, the linguist Noam Chomsky used linguistic evidence alone to propose a new theory for the evolution of human brain speech and language substrates. He argued that as the linguistic structure of human spoken language was unique, it could not possibly have a behavioral precursor. Hence, the neural mechanisms underlying human speech and language, Chomsky's "speech organ", must also be unique. This mechanism, by extension, thus arose *de-novo* presumably during recent human evolution and had no apparent neural precursor or pre-adapted elements (Chomsky, 1980)

Proper theoretical definitions of historical homology do not, and should not, include the criteria by which tests of homology hypotheses are conducted. Since this involves tests of *specific* types of anatomical relationship between potentially homologous structures, these operational criteria have to be established system by system. Not surprisingly, for many years working (i.e., operational) definitions, for testing hypotheses of historical homology between structures in the central nervous system of different species, were not well defined. Approaches and techniques used for comparison of other body structures, such as bones, were often not applicable to analysis of neural characters due to their unique attributes. In an effort to come to terms with the unique nature of neural characters, a recent

theoretical synthesis proposed by vertebrate paleoneurologists dealt with the problems associated with determination of homologies in brain structures (Campbell and Hodos, 1970). The position of these authors regarding phylogenetic versus structuralist concepts of homology was that they addressed different questions and, accordingly, did not represent mutually exclusive points of view. The following definition of homology was offered by Campbell and Hodos (1970: 358), citing Ghiselin (1966a, b) and Bock (1969): "Structures and other entities are homologous when they could, in principle, be traced back through a genealogical series to a stipulated common ancestral precursor irrespective of morphological similarity." However, this definition of historical homology presented a confusing admixture of theoretical and operational criteria and did not specifically deal with homoplasy.

For specific recognition of historical homology among nervous system characters in different species, several working criteria were suggested by Striedter & Northcutt (1991): 1) data from the fossil record were considered the most robust criteria in support of homology hypotheses since they provides the most direct evidence. However, as discussed above, these data are more limited in the information provided; 2) "minuteness of similarities" provides data regarding the "fineness" of detail in resemblance between purportedly homologous characters in different species; 3) "multiplicity of similarities", where a higher number of similarities provide greater support;

and 4) "ontogenetic similarities" where multiple similarities within inherited developmental patterns provide evidence. These multiple criteria are used within a framework provided by the specific tests for homology in the nervous system enumerated below.

Some of the most useful tests for homology in the nervous system involve comparisons of topology, topography, sulcal and gyral position, embryology, local neuroanatomy, histochemistry, immunocytochemistry (for chemical phenotype), electrophysiology, and behavioral outcome (from experimental modifications such as lesions and electrical stimulation). Tests for electrophysiology and behavioral outcome could be incorporated into the operational framework proposed by Bock for the functional-adaptive analysis of characters (Bock, 1981) as discussed below. For each of these tests used for establishing the probability of homologous relationships between similar structures in two species, there are of course, complicating factors which require an appreciation of mechanisms active during neural development and adult plasticity. Such mechanisms are thought to provide a substrate for evolutionary change, (e.g. Ebbesson, 1984; Northcutt, 1984; Kaas, 1989; Arbas et al., 1991; Frotscher, 1992; Nishikawa et al., 1992; Zilles, 1992). For example, many neurons project via their axon collaterals to multiple distal targets. However, if one of these targets does not provide an appropriate feedback signal to the principal neuron, perhaps due to underlying behavioral shifts or redundancy, axon collaterals to this target region may be

withdrawn during development. As this interactive phenomenon persists over successive generations a connection will no longer exist between these two regions in adult brains and the circuitry will have been effectively modified (Arbas et al., 1991). This, as with other such responsive developmental events, may represent the neural mechanisms which underlie adaptive evolutionary change. For example, only in anthropoid primates amongst mammals, do axonal projections from the cerebral cortex by-pass brainstem inter-neurons to terminate directly onto motoneurons innervating muscles of the head and neck (Sokoloff and Deacon, 1990). In macaques, all brainstem motoneuron groups (including those that innervate the facial, tongue and jaw musculature) receive direct cortical projections except for the nucleus ambiguus, the motor nucleus that innervates muscles of the larynx and pharynx. In chimpanzees, however, direct cortical projections terminate on cells of nucleus ambiguus (Kuypers, 1958b) as is also the case in humans (Kuypers, 1958a). This may represent an example of the "fine tuning" of neural interconnections with concomitant improvement of motor skills. This shift to direct cortico-motoneuronal connections is unique to anthropoid primates among mammals. For many tasks, these direct connections may provide a more refined and skilled capacity for complex motor behaviors like object manipulation or communicative facial gestures.

2.6.4. Evidence for homology of human brain language areas in the cerebral cortex of *Macaca*.

Many studies have supported the hypothesis that regions of the cerebral cortex in *Macaca* are homologous to brain regions in humans involved with speech and language (Galaburda and Pandya, 1982; Deacon, 1989). Evidence for homology of these brain regions come from data on neural topology, topography, sulcal position, and morphology. Although some experiments have involved the study of comparative physiology of these homologous regions, the evidence has been considered less supportive (Myers, 1972; Jürgens, 1979; Sutton, 1979). However, when this supposedly non-supportive physiologic data is placed within the framework of functional-adaptive concepts of evolutionary change, it does indeed provide important additional information. The criteria and evidence used to establish theories of homology between brain communication areas in humans and macaques are now presented.

Studies conducted by Brodmann in the early twentieth century first established "cytoarchitectonics" - the study of cellular type, structure and organization in the layers of the cerbral cortex - as a powerful method for comparing and defining similar patterns of regional neural cellular morphology present in different species (Brodmann, 1909; Le Brun Kemper and Galaburda, 1984). This anatomical method allowed for the parcellation or division of the cerebral cortex into distinct regions. These regions were, in

turn, thought to be the distinct neural substrates for specific behavioral functions.

Many subsequent studies based upon these cytoarchitectonic areas have further demonstrated that there is a consistent relationship between these areas and the cortical surface structures, such as sulci, that border and delimit them (Sanides, 1970). In nearly all cases the limits of these cytoarchitectonic fields were located at the deep portions of sulci, fissures and dimples on the cerebral cortex, both in humans and non-human primates. These definable anatomical relations allowed for cytoarchitectonic regions located deep to the surface of the brain to be related to the presence and relative position of features on the surface of the brain. Accordingly, these data allowed evidence from the fossil record, largely comprising anatomical features on the brain's surface, to be interpreted within the reliable framework of established patterns of regional anatomy and functional localization.

2.6.4.1. Evidence for homology of Broca's Area in human and macaque brains

A particularly important region relating to speech and language in humans is Brodmann's Area 44 (Brodmann, 1909) - commonly referred to functionally as Broca's anterior speech area. Subsequent to Brodmann, more detailed cytoarchitectonic studies have referred to this cortical area as "Area 6bα" (Vogt and Vogt, 1919) and "Area FCBm" (Von Bonin,G and Bailey,

1947). In *Macaca mulatta,* this well defined cytoarchitectonic region is located in the left hemisphere of the pre-motor agranular cortex on the postero-inferior border of the arcuate sulcus (Galaburda and Pandya, 1982). It was demonstrated that this area in macaques has a similar cellular organization to Broca's anterior speech area in humans (Galaburda, 1980). This cytoarchitectonic evidence strongly supported the hypothesis of a homologous relationship for this brain region in humans and macaques. Interestingly, the cytoarchitectonic morphology of Brodmann's Area 44 in humans was reported to be more differentiated and the cortical mantle thicker than that seen in macaques. However, the region was consistently similar in the following organizational pattern of cellular elements:

> *"Area 44 in the human pars opercularis in more specialized than adjacent area 45 because it contains larger IIIc pyramids and has a lesser degree of eulamination.... ...layer III contains large pyramids on the border with IV, which is indistinct; layer IV is narrow but clearly present; layer Va contains numerous large pyramids, often in rows, encroaching on the deeper border of layer IV; layer Vb is relatively sparse for this part of the frontal lobe; and layer VI is not easily separable from Vb"* (Galaburda and Pandya, 1982:211).

Galaburda and Pandya (1982) concluded that although the anatomical basis for homology between these regions in humans and macaques was well established, unfortunately, the biological role subserved by these regions in macaques was not known. However, the anatomical evidence was so compelling, it could be argued that these brain areas in macaques may well

subserve "scaled-down communicative functions" (Galaburda and Pandya, 1982: 211). Obviously though, whatever the communicative outcome and its modality, they are not scaled down from a macaque's perspective.

Since it has been previously demonstrated that lesions of Area 44 in the left hemisphere of non-human primates do not give rise to vocalization deficits, these "scaled down communicative functions" are apparently not related to neural vocalization pathways (Myers, 1972; Jürgens, 1979). They may, however, be related to gestural-visual communicative pathways in non-human primates. Experimental lesion studies have yet to address the possibility of gestural-visual primacy in non-human primate communication. The sole study of its kind, which lesioned Area 44 in macaques and then released the animals back into their social group, reported not only a major disruption of facial signaling patterns but an inability of the lesioned animal to re-establish itself within the social group to which it had belonged from birth (Myers, 1972). This outcome was reported to be not due to active rejection or negative responses from other members of the group but represented a failure of the lesioned individual to reaffirm social group relations. This may have been due to an inability of the lesioned animal to process and deliver appropriate communicative signals that may be critical for acceptance within the social group. This experimental situation may represent (behavioral) evidence of biological role equivalence, indicating a shift in the communicative modality subserved by these homologous regions

of the cerebral cortex. Such a perspective is in line with Bock's functional-adaptive criteria utilized for operational testing of homology hypotheses (Bock, 1981). In humans this cortical region, representing the more derived condition, subserves vocal-auditory function (speech and language), but in monkeys the same neural substrate may subserve gestural-visual communication involving facial expression and body gestures. Supportive evidence for this idea comes from studies of deaf humans using sign language. In these individuals it has been shown that the same cortical area is utilized for gestural-visual communication (i.e., sign language) as that used for spoken language (Bellugi et al., 1988). In essence, in different species, this region of the cerebral cortex may be specialized for inter-individual communication, regardless of the communicative modality used or its complexity.

2.6.4.2. Evidence for homology of Wernicke's Area in human and macaque brains

A second cerebrocortical area of great importance to the receptive modality of vocal-auditory communication in humans is Wernicke's "area" (Wernicke, 1874). This area is located in several adjacent regions of the posterior temporal and inferior parietal lobes. In both humans and macaques, the auditory fields of the superior temporal gyrus show similar patterns of cytoarchitectonic organization with a marked rostro-caudal trend of cortical laminar differentiation. This involves graded laminar

differentiation of cortical layer III and an increased breadth of layer V which reaches a maximum in Area PaAlt. The region just posterior to Area PaAlt, Area Tpt, shows a tendency towards eulamination (i.e., possessing all six layers of the cerebral cortex), similar to the neighboring inferior parietal association cortex (Galaburda and Pandya, 1982). In humans, this specific, cytoarchitectonically defined region of the posterior portion of the left hemisphere superior temporal gyrus, Area Tpt (i.e., the planum temporale - defined above), is included as a major part of Wernicke's posterior receptive speech area (Wernicke, 1874) (see also (Galaburda et al., 1978b; Geschwind and Galaburda, 1984)). Using cytoarchitectonic analysis, it was demonstrated that this region in humans was homologous to a similarly placed region in *Macaca mulatta* (Galaburda and Pandya, 1982). Further, the cytoarchitectonically defined region was shown to be significantly larger in the left hemisphere (Galaburda et al., 1978b). The cytoarchitectonic profile characterizing this region in human and macaques was as follows:

> *"The temporoparietal area Tpt appears as an additional field belonging to the auditory region in a broader sense. It lies caudal to the PaAe and extends toward the temporoparietal junction. It is not classified as a parakoniocortex because it lacks sufficient strength in Layer IV and the cell density in Layer V is too great. It is easily recognized by the appearance of sublayer IIIc whereby the pyramids offer an irregular border to Layer IV in an undulating fashion. In its inner margin Layer IV fuses somewhat with Layer VI, resulting in an indistinct border. Layer VI is densely populated with cells which frequently are disposed in branching columns reaching toward Layer V. As a whole, this area resembles the parietal integration cortex of the inferior parietal lobule,*

> *but is easily distinguished from it by virtue of the rigidly layered appearance of the latter.* (Galaburda and Sanides, 1980:605)

Finally, cytoarchitectonic studies of regions of the inferior parietal lobe in human brains (included within the concept of Wernicke's speech area in humans) showed parcellation into multiple discrete areas, each with homologies in the macaque brain (Eidelberg and Galaburda, 1984). Each of these sub-regions also closely paralleled the pattern of cortico-cortical inter-connectivity seen in macaques. The inferior parietal region differed between macaques and humans, however, in the relative overall size, greater differentiation into sub-areas, and a more pronounced morphologic inter-hemispheric asymmetry (Eidelberg and Galaburda, 1984).

2.6.4.3. Neural connectivity evidence for homology of Broca's and Wernicke's Areas in human and macaque brains

Once areas of the cerebral cortex in different species are shown to be homologous using cytoarchitectonic criteria, further differences and similarities can be ascertained by studying fiber connections. Furthermore, the discovery that areas determined to be homologous on cytoarchitectonic grounds also have similar connectional patterns with other brain regions strengthens the hypothesis that the areas are indeed homologous (Galaburda and Pandya, 1982). Examination of neural connectivity in non-human primates involves making discrete injections of a neural tract-tracing

substance (e.g., the enzyme horseradish peroxidase) into the cortical region of interest in live animals. This substance is taken up, either by local neuronal cell bodies and transported anterogradely via their axons to distal termination sites, or by local axon terminals and transported retrogradely back to their distally located cell bodies (Mesulam, 1982). In this manner, connections both to and from a particular cortical region can be mapped out with a great deal of certainty.

In humans, a major brain fiber tract, the "arcuate fasciculus", forms a connection between the posterior temporal and inferior parietal cortical regions collectively known as Wernicke's language area, and those regions in the inferior frontal lobe known as Broca's language area (Geschwind et al., 1968). Disruption of this tract in humans, caused by localized pathologic lesions, gives rise to a clinical phenomenon known as conduction aphasia. This condition is characterized by a normal understanding of spoken language (comprehension) in combination with relatively fluent, grammatic and meaningful speech but with markedly poor naming and word repetition (Geschwind, 1970; Bachman and Albert, 1991).

Neural tracing studies in *Macaca* have demonstrated that there is also a major fiber tract connecting Brodmann's area 44 of the inferior frontal lobe (Broca's area) and Area Tpt of the posterior temporal lobe (Wernicke's area) (Galaburda and Pandya, 1982). A similar pathway was also demonstrated in *Samiri* (Forbes and Moskowitz, 1977). However, unlike the condition in

humans, the homologous tract in macaques does not receive a major direct contribution from the inferior parietal polymodal association cortices, and instead passes anteriorly via a different more direct peri-insular route. Although this suggests a degree of connectional divergence between humans and macaques, extensive interconnections between the inferior parietal regions and Area Tpt have been demonstrated in macaques (Pandya and Seltzer, 1982). As such. these intrinsic connections in macaques could represent the basal substrate from which the more derived human condition evolved. Once again, an evolutionary shift of neural connectivity, involving axon collateral reorganization, could have given rise to the more derived condition present in humans. Unfortunately, the course of this major fiber tract is unknown for the great apes. However, as was the case for cortico-motoneuronal projections onto nucleus ambiguus (described above), great apes may show the more derived condition.

Other evidence involving neural connectivity pertaining to homology of Area Tpt in macaques and humans involves inter-connections with a sub-cortical structure, the parahippocampal gyrus, which is involved with memory circuits of the limbic system. In studies of this system, neural tract-tracers were injected into both the parahippocampal gyrus and Area Tpt of *Macaca mulatta* in order to map reciprocal connections. Results showed that there were in fact extensive reciprocal connections between these two regions which probably represented a neural system related to acoustic learning and

memory (Tranel et al., 1988). It was thus hypothesized that homologous systems in both humans and macaques may be involved in species-specific learning and language (communication) acquisition.

Extensive neural tract-tracing studies of areas of the frontal and temporal lobe in *Macaca fascicularis* homologous to human speech areas have recently been conducted by Deacon (1984, 1989, 1992b). His studies demonstrated that micro-injections of neural tracer into the macaque homologue of Broca's area in humans resulted in labeling of multiple distal sites. These sites included areas such as the inferior parietal cortex and the dorsal opercular bank of the sylvian fissure (Area Tpt) and proximal sites such as the precentral motor cortex (subserving cortical control of muscles of the face, tongue and larynx). As noted above, similar connections between these regions are also known to be present in humans. Further, the inferior peri-arcuate region of macaques, like Broca's area in humans, has extensive connections with both auditory and oral-vocal somatic (i.e., sensory feedback) information, projects to oral-vocal motor cortex, and has demonstrated laryngeal motor function (Deacon, 1992b).

Most of our current knowledge of speech/language area connectivity in humans is based on the limited evidence obtained by observation of functional deficits present after gross pathologic lesions or electrical stimulation. Conversely, the more comprehensive and detailed experimental data obtained from neural tract-tracing studies of homologous regions in Old

World monkeys has demonstrated that these circuits are considerably more complex than was originally thought. Based on extension of his tract-tracing studies in macaques to human language circuits, Deacon hypothesized that language areas (in humans) may be composed of heterogeneous functionally discrete sub-regions interconnected so as to comprise distinct language subsystems. (Deacon, 1988). To date, there is no way of testing Deacon's hypothesis in humans, although new advances in brain imaging such as functional magnetic resonance imaging may allow for this in the future.

2.6.5. Conclusions

In sum, the hypothesis that human language areas have homologs in the brains of Old World monkeys has been supported by a wealth of multidisciplinary evidence as outlined above. In light of this evidence, these areas in macaque and human brains could be represented by a mosaic of both static and transformational homologies (i.e., the macaque condition representing the antecedent condition to that in hominoids) which would apply at different levels of analysis. For example, static homology would incorporate the topographic evidence in which cortical sub-areas (defined by cytoarchitectonic similarities) maintain positional relationships, both to each other and to adjacent sulci and gyri. Supporting evidence of nerve fiber connections between these "anatomically homologous" brain regions may be represented both by the concept of stasis as well as transformation.

However, more data on humans are needed to establish the degree of evolutionary change that may have taken place in the neural circuitry underlying brain language mechanisms. Transformational homologies are indicated by data that concern the intrinsic cellular organization of these human language areas which have undergone significant reorganization and differentiation including gyrification by the expression of additional sulci. Likewise, the functional-adaptive data which indicate a major shift in both the complexity and primary modality of the communicative medium, is best described as supporting an interpretation as being the consequence of a transformational event.

Although the studies discussed here strongly support the hypothesis of a homologous relationship between human language areas and (tested) regions in macaque brains, many aspects of the exact nature of transformation of these regions from macaques to humans remain to be studied. This includes, cellular and sub-cellular physiological roles, neurochemical shifts, the dynamics of inter-hemispheric asymmetry, and finally, shifts in communicative modality and complexity.

CHAPTER 3

MATERIALS AND METHODS AND ANATOMY AND VARIATION OF CEREBRAL CORTEX IN *MACACA FASCICULARIS*

3.1. CHAPTER OVERVIEW

The materials and methods, involving choice of species and specimen acquisition and preparation, for the quantitative studies presented in subsequent chapters are described in Section 3.2. of this chapter. The subsequent section (Section 3.3.) presents a descriptive and semi-quantitative analysis of the anatomy and variation present in the cerebrocortical structures used in this study: 1) the arcuate and central sulci and post arcuate (pre-motor) cortex of the inferior frontal lobe, and 2) the sylvian fissure, superior temporal sulcus and superior temporal gyrus of the temporal lobe. This anatomic assessment provided a better understanding of the validity and usefulness of the quantitative methods used later.

Two key observations made in this analysis involved previously undescribed patterns of variation. Subdivision of the arcuate sulcus into vertical and horizontal limbs must be used with caution since in 14 of the 44 brains this was not feasible. With regard to ascertaining the exact position of the sylvian point, in 24 of 44 brains this important landmark was hidden deep to the surface by adjacent cortex.

3.2 ANATOMICAL METHODS

3.2.1 Choice of species

For the multiple reasons stated below, the cercopithecoid (Old World monkey) species *Macaca fascicularis* was chosen as the subject of this project.

The central hypothesis of this dissertation embraces the paradigm that specific regions of the cerebral cortex, already present in the common ancestor of hominoids and cercopithecoids, provided the neural substrate upon which was constructed the derived neural circuitry underlying modern human vocal-auditory communication and language. In support of this paradigm, it has been shown by several investigators that there are brain regions in macaques that are homologous to known human speech/language brain regions. These regions include Broca's area, located in the inferior frontal lobe, and Wernicke's area, located in the superior temporal and inferior parietal lobes. For example, studies by Galaburda and co-workers used cytoarchitectonic methods to compare the types and distribution of neurons in the cerebral cortex of macaques and humans. Using these criteria, they demonstrated that specific regions of the cerebral cortex in *Macaca mulatta* are homologous to Broca's and Wernicke's areas in the brains of humans (Galaburda, 1980). Furthermore, using neural pathway tracing techniques, they showed that the arcuate fasciculus, a major fiber pathway connecting Broca's and Wernicke's areas in humans, was also

present in macaques (Galaburda and Pandya, 1982). Similar neural pathway tracing work conducted by Deacon extended these preliminary observations. Deacon showed more extensive human-like similarities in the complexity of neural connections of these brain regions in another, closely related macaque species *Macaca fascicularis* (Deacon, 1984, 1988, 1989, 1992b).

Based on these data, it seems likely that the neural circuitry subserving language in *Homo sapiens* was present, in some basal form, in the brains of the common ancestor of cercopithecoids and hominoids. As such, the macaque brain may provide a model of the primitive condition upon which was constructed the more derived brain language circuitry present in humans. Whether these regions in the brains of monkeys show, as they do in humans, a marked asymmetric hemispheric representation, or a predominantly left hemisphere functional specialization, is as yet unclear.

The preliminary work conducted by Galaburda, Deacon and their co-workers, amongst others, utilized species of the genus *Macaca*, primarily the widespread and diverse species *Macaca fascicularis* (common names = cynomolgus monkey, crab eating macaque, long-tailed macaque). Fortunately, this species is used extensively in the United States for brain-related and other research, and a great deal of neural information is available. Likewise, the closely related species *Macaca mulatta* (common name = rhesus monkey) has also been used extensively for brain research,

and a great deal of relevant information is available. In addition, their ready availability, non-endangered status and the stringent basal requirement of this project: that the brains of live animals be fixed directly via the cerebral vasculature, under highly controlled conditions, by trans-cardiac perfusion (see below), made this widely used species the most logical and meaningful choice. As such, an adequate sample of adult individuals of both sexes could be readily procured. However, none of the animals used in this project was sacrificed for this project alone but all were obtained from other investigators after unrelated experimental research had been conducted (see below)

The species *Macaca fascicularis* is widely dispersed throughout a geographic range including Southeast Myanmar, South Thailand and Indochina, the Malay Peninsula, the Nicobar Islands, Sumatra, Java, Borneo, the Philippines, and the East Indies except Celebes (Fooden, 1976; Nowak and Paradiso, 1983). Although some populations of *Macaca fascicularis* spend a large proportion of their time traveling and foraging on a terrestrial substrate, it is generally considered as a primarily arboreal species (Wheatley, 1980) as well as being primarily diurnal. Population densities of *M. fascicularis* are in the region of 36-90 individuals per km^2 with an estimated group home range of 0.8 km^2 (Kurland, 1973; Angst, 1975) and a group sex composition ratio of approximately 2.1:1 - females:males. The social structure of *M. fascicularis* and *M. mulatta* are similar with dominance hierarchies in each sex which are usually based on age, kinship

and coalitions (Angst, 1975). The species group is usually made up of a central component with an alpha male and the majority of females and their young, as well as a peripheral component comprising the younger males and some females (Roonwal and Mohnot, 1977). The inter-social relationships between males in the group may be quite hostile but females tend to be relatively passive towards each other. This may be a result of the strict dominance hierarchy in which the social status of offspring is entirely dependent upon inheritance from the mother (Sade, 1967). Males lead and defend the group but females and their young form a central subgroup in which the young are reared. As with all primate groups except humans, the exposure of individuals in the group to novel social situations is extremely rare with the majority of such encounters being limited to aggressive inter-species interactions with individuals of neighboring groups usually during territorial encounters. As such, most individuals must be completely aware of the social profile and expectations of at least all individual animals within their own group.

3.2.2. Procurement of Animals

Perfusion-fixed brains of *Macaca fascicularis* were obtained from the laboratory of Dr William Doyle in the Otolaryngology Department of The Children's Hospital of Pittsburgh and from the laboratory of Dr Gay Holstein in the Department of Neurology of the Mount Sinai School of Medicine, New York. The individuals of *Macaca fascicularis* had been wild caught from

unknown locations in South East Asia and exported to the United States. Many of the animals had undergone long term experimental procedures in Dr Doyle's laboratory involving monitoring of middle ear and eustachian tube function. None of the long term procedures conducted in Dr Doyle's or Dr Holstein's laboratories were related to any peripheral system that could directly impact on the neural systems being assessed in this project. Upon termination of these investigators experiments, it was necessary to sacrifice the animals and collect pharyngeal and middle/inner ear tissues. Three trips were made to Pittsburgh during which 35 animals were trans-cardially perfusion-fixed and their brains secured (as described below). The remaining animals, obtained from Dr Holstein, were perfusion-fixed in my laboratory in the Department of Otolaryngology at Mount Sinai School of Medicine.

3.2.3. Brain tissue preparation

For all of the procedures performed in this multi-faceted study, it was critical that brain tissues be rapidly fixed in situ with freshly prepared solution, then maintained under specific conditions until processing was completed. This critical procedure limits fixation artifacts which can directly influence the measurements made in a study such as this. This is the first study of Old World monkey brain asymmetry in which the fixation conditions were controlled in this manner. All animals in this study were euthanized by fixation via trans-cardiac vascular perfusion while under deep barbiturate anesthesia. Animals were treated in compliance with the American

Association for Laboratory Animal Science (AALAS) Policy on the Humane Care and Use of Laboratory Animals, and that of the United States Department of Health and Human Services Guide for the Care and Use of Laboratory Animals. The specific procedures are described below:

3.2.4. Preparation of fixative

For all procedures the fix solution must be made up within 4-8 hours before use in order to obtain maximum preservation of brain tissues. The fixative agent, paraformaldehyde, forms unacceptably long polymeric chains over longer time periods. The resultant large molecular structures cannot access the tissue matrix as readily or as rapidly as the smaller chains of fresh fix solution. For this reason, the chemicals required for solution preparation were taken to the laboratory in Pittsburgh in dry form, then the solutions prepared 2-6 hours prior to perfusion. Approximately four litres of fix solution were perfused through each animal. The fresh fixative solution contained 4% paraformaldehyde and 0.1% magnesium sulfate in an 0.1 Molar phosphate buffer at pH 7.4.

3.2.5. Trans-cardiac perfusion method

3.2.5.1. Anesthesia

Animals were immobilized in a crush cage and injected intramuscularly (IM) with a mixture of Ketamine Hydrochloride (20 mg/kg) and Xylazine (6mg/kg). This anesthetic combination produces anesthesia with profound

analgesia within two to five minutes. Animals were removed from their cages, placed in the supine position and their hands and feet tethered loosely to a wooden board. The entire procedure was conducted under a fume hood from this point on.

3.2.5.2. Insertion of perfusion cannula

A midline skin incision extending from the upper thorax to the level of the mid abdomen was made and the skin retracted laterally on both sides. The abdominal cavity was entered by an incision made in the abdominal muscles just inferior to the thoracic margin, then the incision extended laterally on both sides. Care was taken not to violate the diaphragm and thoracic cavity at this time. The sternum was elevated and the diaphragm severed along its costal margin, exposing the thoracic cavity. Any fibrous attachments of the heart to the ventral thoracic wall were severed so that it fell dorsally. The left lung was elevated and the descending aorta clamped with a hemostat. The pericardial sac was opened and the heart pushed out. An incision was made into the right atrium to provide an outflow for blood and perfusion fluids. An incision was made into the left ventricle, then the cannula passed into it and via the aortic valve into the ascending aorta. The perfusion pump (Masterflex) was now turned on. To prevent fluid backflow, the body of the left ventricle was clamped around the cannula using a large sponge clamp.

3.2.5.3. Perfusion regime

Initially, 150-200mls of buffered physiological saline (0.85% sodium chloride in 0.1 Molar phosphate buffer) at body temperature (37°C) was perfused at a flow rate of ~150mls/min until the solution exiting from the right atrium was relatively clear. This step purged all blood from the vasculature thus facilitating the action of the fix solution. This vascular flush was not allowed to exceed a time period of one minute regardless of the clarity of the exiting perfusate. The perfusion pump was briefly stopped and the inlet tube transferred to the fix solution (described above) at 20°C. The fix solution was perfused at a flow rate of ~150mls/min for 5mins then reduced to 75mls/min and continued for a further 25 minutes.

3.2.6. Removal of brain from skull

The skin and musculature overlying the cranium was removed by gross dissection. Using bone rongeurs, the removal of cranial bone was initiated at the supero-lateral aspect of the foramen magnum. Bone was removed anterolaterally on both sides until the vault was freed. The dura mater overlying the brain was separated from the cranial vault by blunt dissection, then the vault was removed and the brain exposed. The fibrous dura mater was incised along the midline then reflected laterally on both sides. The brainstem was transected at the level of the obex then the brain was elevated away from the cranial base allowing visualization of the cranial nerves.

Starting posteriorly, the cranial nerves were severed on both sides until the brain was freed from the endocranial skull base.

3.2.7. Post-fixation of brain

The entire brain was now removed and post-fixed by immersion in fix solution at 4°C for 4-6 hours on a rotating table. The purpose of this step was to continue the fixation process of stabilizing molecules by cross-linking. The relatively short post-fixation period was a compromise solution which reduces the potential for fix-induced transformation of molecular structure and integrity which can occur over longer time periods. The reduction of post-fix solution temperature also facilitated this.

After post-fixation the brain was transferred to phosphate buffered 20% sucrose solution (20% sucrose in 0.1 Molar phosphate buffer) at 4°C and placed on a shaking table in the cold room. The intact brain was left in this solution until it sank, usually about 24-36 hours, indicating complete infiltration with sucrose solution. This solution served as a tissue cryoprotectant which considerably lessened damage to tissue cellular elements upon subsequent freezing for sectioning. It achieves this by forming ice crystals in the tissue (upon freezing with dry ice to -65°C), that are much smaller, and significantly less destructive to cellular structure, than those formed by water alone. After measurements were made, brains were frozen at -70°C for archival storage.

3.2.8. Potential for fixation induced artifacts

A concern that had to be addressed in studies such as this was the potential for differential effects of fixation on brain tissues that might have given rise to unreliable data and results. For example, since the brain shrinks a certain amount during the fixation process, regions that are not as well fixed or are not fixed at equal rates may not shrink to the same degree. Most previous studies of non-human primate brain asymmetry have used data derived from post-mortem immersion-fixed brains (e.g., see Heilbroner, 1987). Immersion fixation does not allow for equal access of fixative solution throughout the brain at the same time as does perfusion fixation. As such, this gives rise to the potential for differential shrinkage. In all animals used for this study, maximal access of the fix solution, by trans-cardiac perfusion fixation through the cerebral vasculature, with adequate and homogeneous brain tissue fixation, was assessed by gross visual assessment of the cortical mantle after perfusion.

After a good perfusion fixation, the cerebral cortex was an even yellow-tan color throughout. In the case of a poor perfusion or other problems (such as vascular blockage) that may differentially compromise fixative access to various local brain regions of interest, a pink blush over the region indicated poor local fixation due to retention of vascular contents. If this occurred, the brain was not used for further analysis since unevenness of fixation-induced

shrinkage and cytoarchitecture may have given rise to aberrant data on hemispheric asymmetry patterns.

In only two cases, gross inspection of freshly perfused brains showed a pink blush over parts of the cortical surface. These two brains were not included in this study. In no cases did subsequent microscopic analysis of those brains selected for production of brain sections reveal significant retention of vascular elements.

3.2.9 Brain Volume Measurement

A 500ml measuring cylinder with 5 ml divisions was filled to exactly 250ml with phosphate buffered sucrose (20% sucrose in 0.1 Molar phosphate buffer). The intact brain was removed from phosphate buffered sucrose, quickly drained of excess fluid, then placed in the fluid-filled measuring cylinder. When the brain was completely submerged, fluid was removed from the cylinder until it was at its previous level. This removed fluid was transferred to a more accurate 100ml cylinder with 2ml divisions. The volume of fluid removed represented the fluid displaced by the brain, hence, brain volume. This brain volume value is used in some aspects of the data analysis to scale and compare various measures of brain dimensions.

It should be noted that fluid present in the cerebral ventricular system was not drained by this technique, and as such, accounted for part of the total volume determined. Likewise, the fluid present in the cerebral

vasculature was not drained and also accounted for part of the total volume. Since the dura mater had already been removed, it did not contribute.

3.2.10. Archival Photography of Brain

3.2.10.1. Equipment and materials

To provide an accurate photographic record of cerebrocortical morphology each intact brain was photographed using an Olympus OM-2 camera with a 50mm macro lens capable of 1:1 magnification, using Kodak 100 ASA daylight color print film. A millimeter scale bar was included in all photographs to provide an exact scaling reference for subsequent image analysis of surface cerebrocortical morphology. A black velvet background was used to clearly contrast and delineate brain margins. A fiber optic light source with two flexible arms was used to light the brain with a standardized even illumination pattern directed at 45^{0} to the vertical axis on both sides. A rigid vertical copy stand (Zeiss Orthoplan) was used to photograph the brain in a series of standardized positions.

3.2.10.2. Standardized views of brain

Standard orientation of brain position was achieved by aligning bilateral structures into the same vertical plane, relative to the longitudinal axis of the camera, both by visual observation and by measurement of bilateral

correspondence. The standard anatomical brain positions used for archival photographic recording were as follows:

i) Low magnification photograph of superior aspect of entire brain with basal surface of brain in horizontal plane (Figure 3-1a).

ii) Low magnification photograph of inferior aspect of entire brain with basal surface of brain in horizontal plane (Figure 3-1b).

iii) Low magnification photograph of lateral aspect of entire left hemisphere of the brain (Figure 3-2a).

iv) Low magnification photograph of lateral aspect of entire right hemisphere of the brain (Figure 3-2b).

v) High magnification close-up photograph of left-side cerebrocortical region in the frontal lobe posterior to the arcuate sulcus and anterior to the central sulcus (Figure 3-3a).

vi) As for v), above, but of the homotypic region in the right cerebrocortical hemisphere. (Figure 3-3b).

vii) High magnification close-up photograph of left-side cerebrocortical region in the posterior aspect of the superior temporal gyrus of the temporal lobe (Figure 3-4a).

viii) As for vii), above, but of the homotypic region in the right cerebrocortical hemisphere (Figure 3-4b).

ix) High magnification close-up photograph of left-side cerebrocortical region in the anterior aspect of the superior temporal gyrus of the temporal lobe (Figure 3-5a).

x) As for ix) but of the homotypic region in the right cerebrocortical hemisphere (Figure 3-5b).

After photography, 4" x 6" color photographic prints were produced, labeled appropriately, and stored in archival quality plastic protective sleeves. All negatives were stored for future use in a similar manner.

Figure 3-1. Low magnification photographs of the brain of *Macaca fascicularis*. **a)** Superior aspect of brain with brain base in horizontal orientation. **b)** Inferior aspect of brain with brain base in horizontal orientation.

KEY: FL = frontal lobe; PL = parietal lobe; OL = occipital lobe; TL = temporal lobe; CE = cerebellum; BR = brainstem. Scale = 10mm

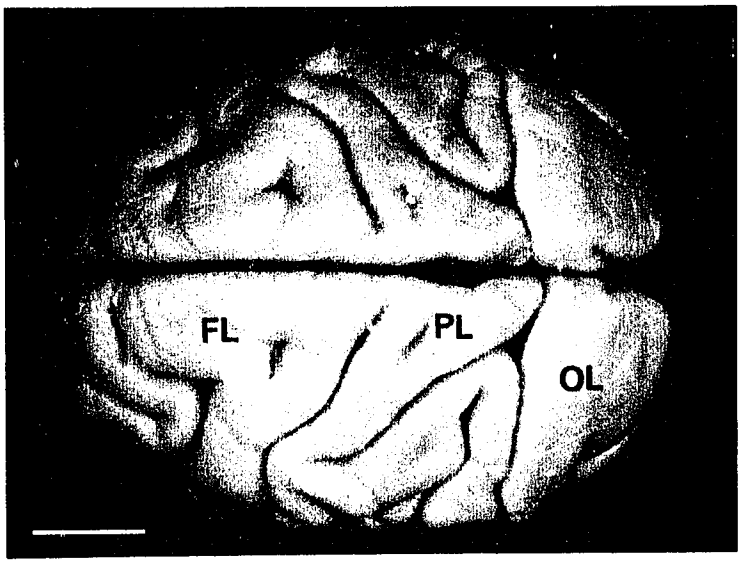

a

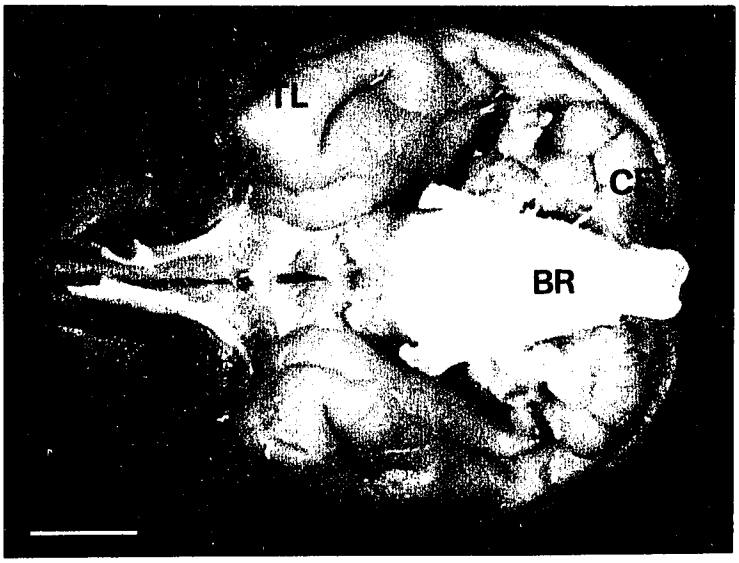

b

Figure 3-2. Low magnification photographs of the brain of *Macaca fascicularis*. **a)** Lateral aspect of left cerebral hemisphere. **b)** Lateral aspect of right cerebral hemisphere.

KEY: FL = frontal lobe; PL = parietal lobe; OL = occipital lobe; TL = temporal lobe; BR = brainstem. Scale = 10mm

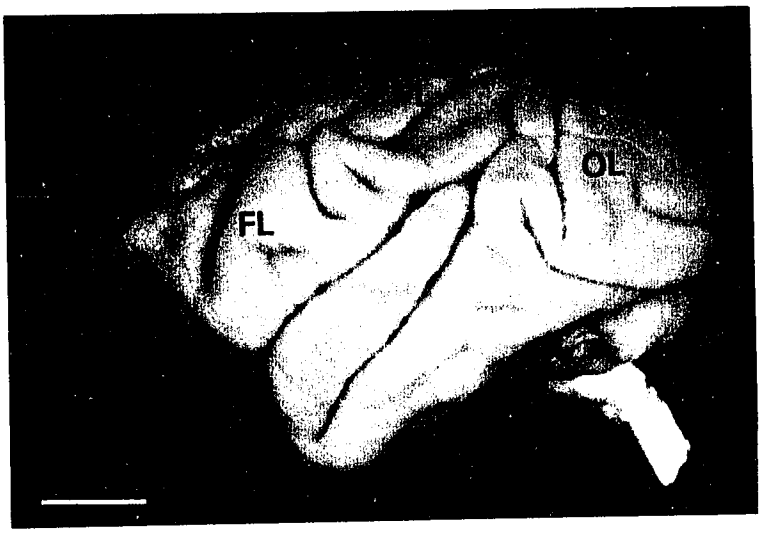

a

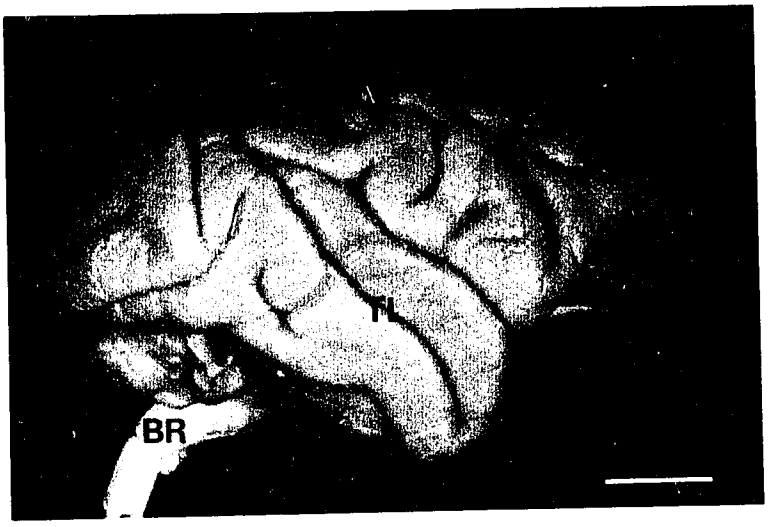

b

Figure 3-3. High magnification photographs of the frontal lobe of *Macaca fascicularis*. a) Post arcuate pre-motor region (PA) and pre-central motor region (MO) of cortex in the left hemisphere. b) Corresponding region in right hemisphere.

KEY: AS = arcuate sulcus; CS = central sulcus; SCD = sub-central dimple. Scale = 5mm

a

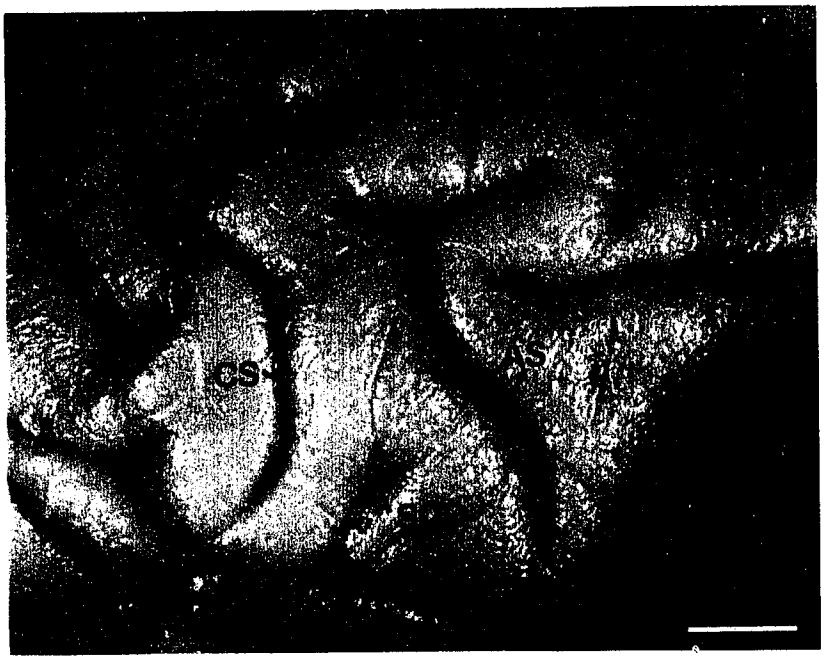

b

Figure 3-4. High magnification photographs of the brain of *Macaca fascicularis*. **a)** Posterior temporal / inferior parietal region of left cerebral hemisphere. **b)** Same region in right hemisphere.

KEY: SF = sylvian fissure; STS = superior temporal sulcus; STG = superior temporal gyrus; arrow = sylvian point. Scale = 5mm

a

b

Figure 3-5. High magnification photographs of the brain of *Macaca fascicularis*. **a)** Anterior region of the temporal lobe in left cerebral hemisphere. **b)** Corresponding region on the right hemisphere.

KEY: . SF = sylvian fissure; STS = superior temporal sulcus; STG = superior temporal gyrus; MTG = middle temporal gyrus. Scale = 5mm

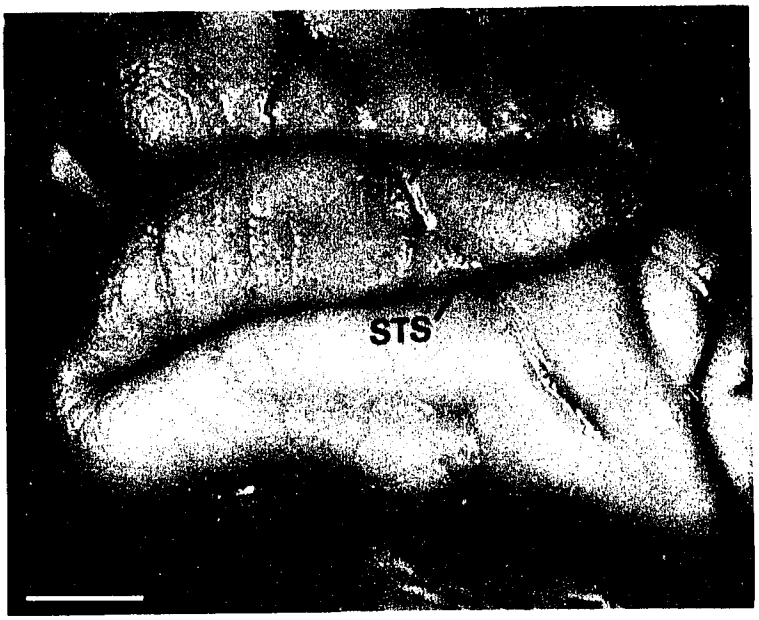

a

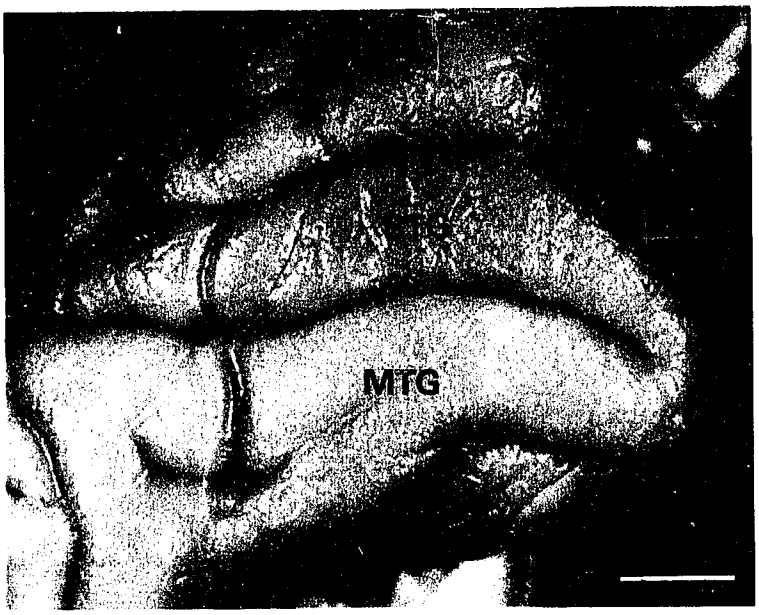

b

3.3 CEREBRAL ANATOMY AND VARIATION

This section presents anatomic descriptions and semi quantitative analyses of selected surface anatomical features on the frontal and temporal lobes of *Macaca fascicularis* brains. The type and degree of variation in the inter-hemispheric extent and the course of structures such as sulci and gyri are considered. This initial comprehensive survey provided a framework upon which a better understanding of both intra- and inter-individual differences, and the presence and degree of sexual dimorphism, was based. Within this basal anatomical framework the subsequent quantitative morphometric analyses presented in chapters 4 and 5 were undertaken.

The term "semi-quantitative analysis" refers to assignment of an arbitrary value of e.g. Pattern I, II or III to represent the degree of variation within a structure. For example, Pattern I = not present, Pattern II = present - small, and Pattern III = present - large. For each of the three structures evaluated in this manner below, structure-specific criteria used for arbitrary value assignment are stated.

3.3.1 Frontal lobe structures

Surface structures of the frontal lobe included in this study are the "vertical" and "horizontal" limbs of the arcuate sulcus and the subcentral dimple (Figures 3-6 and 3-7). These structures are compared on the left and

right hemispheres in a total sample of 44 individuals comprising 20 females and 24 males of *Macaca fascicularis*.

The "vertical limb" of the arcuate sulcus (*inferior ramus* of the arcuate sulcus (Von Bonin,G and Bailey, 1947b)) extends from the infero-lateral portion of the frontal lobe. It continues superiorly and merges into the horizontal limb of the arcuate sulcus (*superior ramus* of the arcuate sulcus (Von Bonin,G and Bailey, 1947b)). The horizontal limb extends anteriorly almost parallel to the principal sulcus. A posterior extension, or "spur", (Von Bonin,G and Bailey, 1947b) of the horizontal limb of the arcuate sulcus is present in some individuals, but this is highly variable, and may be absent or quite large as described below (Figures 3-6, 3-7, and Table 3-1). The distinction between the "vertical limb" or "inferior part" of the arcuate sulcus and its antero-superior horizontal extension is not as clear in brains of *Macaca fascicularis* as has been previously suggested (e.g., Von Bonin,G and Bailey, 1947a; Heilbroner and Holloway, 1989). Within the large sample of freshly perfusion-fixed brains used for this study, much variation was evident, and several morphological patterns were noted, as described below. Within each pattern there was further variation within parameters such as magnitude, course and relations.

3.3.1.1. Arcuate sulcus, Pattern I

In the morphological condition represented here as "Pattern I of the arcuate sulcus", there is no anatomical indication of a posterior extension of the sulcus towards the post-arcuate / pre-central region (region marked by arrows in Figure 3-6a). Hemispheric distribution of Pattern I is represented in Figure 3-9. In Pattern I, the vertical portion of the arcuate sulcus (ASv) courses supero-anteriorly as an arc shaped continuum with the anteriorly directed horizontal portion of the arcuate sulcus (Figure 3-6a). In individuals showing Pattern I, there was not even a rudimentary cerebrocortical landmark that allowed the arcuate sulcus to be unequivocally subdivided into vertical and horizontal "limbs".

Within the 44 individuals included in this study, 14 individual brains, representing ~32% of the total sample, showed co-occurrence of Pattern I of the arcuate sulcus on both the left and right hemispheres (Figure 3-9 and Table 3-1). This sub-population with bilateral representation of Pattern I comprised nine males, representing 38% of the male sub-population and five females, representing 25% of the female sub-population. As such, the corresponding bilateral representation of Pattern I of the arcuate sulcus appears to be considerably more prevalent in male brains. A further seven individuals, representing ~16% of total sample (four females and three males), showed Pattern I of the arcuate sulcus on the left hemisphere but a different pattern on the right hemisphere (Table 3-1 and Figure 3-9). In all

of these individuals, the corresponding right hemispheres showed the slightly more differentiated condition described below as Pattern II of the arcuate sulcus. Conversely, 7 more individuals (2 females, 5 males) showed Pattern I of the arcuate sulcus on the right hemisphere but a different pattern on the left hemisphere (Table 3-1 and Figure 3-9). The corresponding left hemispheres of these (right hemisphere Pattern I) individuals all manifested the more differentiated condition, Pattern II of the arcuate sulcus. In no cases was Pattern I in either hemisphere complemented on the contralateral hemisphere by the most differentiated condition, Pattern III of the arcuate sulcus, described below.

Within the sample of 44 brains representing a total of 88 cerebral hemispheres, Pattern I was present on 42 hemispheres, representing 48% of the total hemispheric sample. The hemispheric distribution of Pattern I (regardless of corresponding hemispheric representation patterns) was equal at a total of 21 cases on the left hemisphere (10 females & 11 males) and 21 cases on the right hemisphere (8 females & 13 males). The total sex distribution of Pattern I was 18 females versus 24 males (3:4 ratio), indicating a possible male preponderance of this morphological pattern. Since Pattern I is the least differentiated condition, it may also represent a less derived morphologic condition. In this event, females are considerably more derived with regard to their morphologic expression of this neural character.

Figure 3-6. Macro-photographs of the frontal lobe in the left hemisphere of *Macaca fascicularis*. **a)** Illustrates "Pattern I" of the arcuate sulcus; small arrows show region lacking a posterior spur (Section 3.3.1.1.); **b)** Illustrates "Pattern II" of the arcuate sulcus; large arrow indicates small posterior spur (Section 3.3.1.2.).

KEY: AS = arcuate sulcus; CS = central sulcus, scd = sub-central dimple; PS = principal sulcus. Scale = 5mm

a

b

Figure 3-7. Photographs of the frontal lobe in the left hemisphere of *Macaca fascicularis*. **a)** Arrow indicates maximum (<3mm) condition of "Pattern II" of the arcuate sulcus (Section 3.3.1.1.); **b)** Arrows indicate "Pattern III" of the arcuate sulcus (Section 3.3.1.2.).

KEY: ASv = "vertical limb" - and ASh = "horizontal limb" - of arcuate sulcus; CS = central sulcus, PS = principal sulcus; scd = sub-central dimple Scale = 5mm

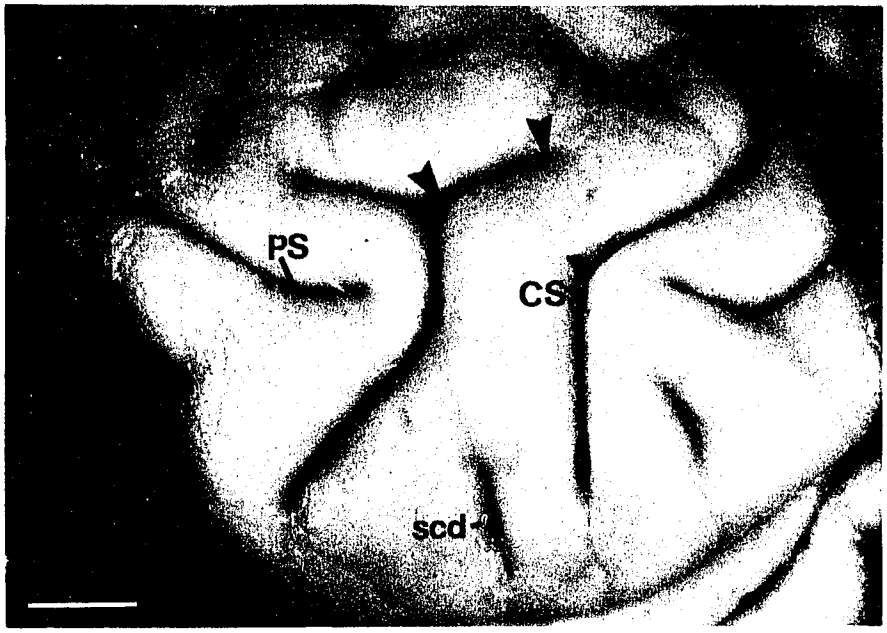

a

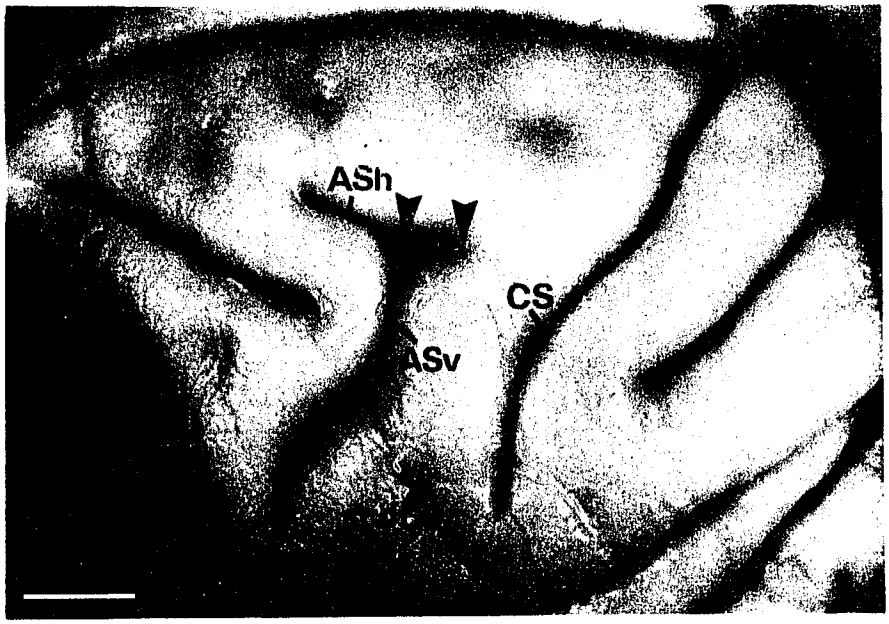

b

3.3.1.2. Arcuate sulcus, Pattern II

In the morphological condition categorized here as "Pattern II of the arcuate sulcus" a posterior extension of the horizontal portion of the arcuate sulcus or "arcuate spur", described above in section 3.3.1., was present (arrows in Figures 3-6b and 3-7a). The minimum requirement for inclusion within this group was that at least a distinct rudimentary region of sulcal differentiation with posterior extension be evident, as shown by the arrow in Figure 3-6b. The upper range of morphological expression included within Pattern II required that the antero-posterior length of this "arcuate spur", be three millimeters or shorter, as measured from the longitudinal axis of the vertical portion of the arcuate sulcus to its posterior termination (Figure 3-7a). The maximum length of three millimeters was chosen as an arbitrary pattern distinguishing character, after observing the distribution of morphological variation throughout the total sample.

Within the total sample of 44 brains, 12 individuals, representing ~27% of the total sample, showed co-occurrence of Pattern II of the arcuate sulcus on both the left and right hemispheres (Figure 3-9 & Table 3-1). This sub-population comprised five females and seven males. Without regard to bilateral hemispheric representation, Pattern II occurred in the left hemisphere in a total of 20 individuals (9 females and 12 males) and on the right hemisphere in a total of 21 individuals (10 females and 11 males). This

corresponded to ~47% of the total sample of individual hemispheres (n=88). Interestingly, this value is similar to that for the distribution of Pattern I throughout the sample of individual hemispheres. There were no apparent sex differences in the distribution of Pattern II within the sample population.

With regard to co-occurrence of other patterns in the contralateral hemisphere to those manifesting Pattern II, the following distributions were apparent. In 3 females, the presence of Pattern II in the left hemisphere was complemented by the more differentiated morphologic condition, Pattern III, in the right hemisphere (Figure 3-9 & table 3-1). In all cases where Pattern II was present in the right hemisphere, Pattern II was also present on the left hemisphere (Figure 3-9, Table 3-1) but not the reverse condition.

Similar to Pattern I of the arcuate sulcus, Pattern II accounted for ~47% of the total morphologic diversity within this large sample of cerebral hemispheres of both sexes.

3.3.1.3. Arcuate sulcus, Pattern III

The morphological pattern classified here as "Pattern II of the arcuate sulcus" included all hemispheres where the posterior spur of the horizontal limb of the arcuate sulcus was larger than three millimeters (Figure 3-7b). In cases where this large spur occurred, the corresponding region of the adjoining central sulcus, was markedly pushed posteriorly into a sweeping

arc-like configuration (Figure 3-7b) in contrast to its usual vertical orientation (compare "CS" in Figures 3-6a and 3-7b).

This morphologic condition occurred rarely in *Macaca fascicularis* being evident in ~6% (5 of 88) of the cerebral hemispheres used for this study. In 2 females, Pattern III was present only on the right cerebral hemisphere, with the complementary left hemispheres showing Pattern II. In one female, Pattern III on the left hemisphere was complemented by Pattern II on the right. One male showed extremely large posterior spurs of the horizontal limb of the arcuate sulcus (Pattern III) on both hemispheres (Figure 3-8b, Table 3-1). Once again, these data suggest that females may be more derived in their expression of this character

3.3.1.4. Subcentral dimple, Patterns I, II and III

The subcentral dimple, or "sulcus sub-centralis anterior" (Von Bonin,G and Bailey, 1947a), is located on the inferior part of the frontal lobe in the region of the frontal operculum. It represents an important brain surface landmark that clearly distinguishes two distinct cytoarchitectonic regions of the inferior post-arcuate cortex, Area FBA and FCBm (Von Bonin,G and Bailey, 1947a). For purposes of this study, Area FCBm corresponds to the main region of interest in the post arcuate area since it is considered to be homologous to Broca's area in humans.

The morphologic size of the subcentral dimple on both hemispheres was assessed using an arbitrary, three level, subjective visual assessment in which: *small = Pattern I* (e.g. Figure 3-6b), *medium = Pattern II* (e.g. Figure 3-7a), *and large = Pattern III* (e.g. Figure 3-7b).

On both the left and the right hemispheres Pattern I of the sub-central dimple was evident in 24 of 44 individuals, representing 55% of total individual cerebral hemispheres, n=88 (Figure 3-9, Table 3-1). In 20 of these 24 individuals, representing 83% of this sub-population, Pattern I of the subcentral dimple was present at an equal level on both hemispheres. This population included 13 females and seven males. The remaining four individuals within this sub-sample included: i) one male and one female showing Pattern I in the right hemisphere and Pattern II in the left; ii) one male showing Pattern I on the left hemisphere and Pattern II on the right; and finally, iii) an unusual condition in which one male showed Pattern I on the right hemisphere and Pattern III on the left.

3.3.2. Temporal lobe structures

3.3.2.1. Sylvian fissure and sylvian point

In order to make accurate, meaningful measures of the antero-posterior length of the sylvian fissure, it was necessary to unambiguously identify the exact anteroposterior position of its posterior termination. This posterior landmark is commonly referred to as the "Sylvian Point" (Witelson and

Kigar, 1992). As such, it is critical to have a good understanding of the variation present in this morphological character. Within this sample of 44 perfusion-fixed *Macaca fascicularis* brains, it was not always possible to view the precise location of the sylvian point on the surface of the brain. The reason for this was that it was often located deep to the surface and its position masked by adjacent overlapping cortical tissues such as the inferior parietal and superior temporal gyri. By spreading open the sylvian fissure superiorly and the superior temporal sulcus inferiorly, however, the precise antero-posterior location of the sylvian point was readily determined. This method was used to formulate an arbitrary semi-quantitative scale in which the following patterns or anatomical configurations were taken into account:

3.3.2.2. Sylvian point, Pattern I

The morphological configuration designated here as P*attern I*, refers to the condition in which the posterior region of the superior temporal gyrus and the adjoining posterior termination of the sylvian fissure (sylvian point) were covered (operculated) by adjacent regions of the inferior parietal and middle temporal gyri (Figure 3-8a). The antero-posterior level at which the superior temporal sulcus merged with the sylvian fissure (anterior to the sylvian point) was quite variable as can be seen in the difference between measures of sylvian fissure length made by this method and those made from lateral brain photographs. This point of fissural-sulcal merging has been

used in the past to represent the position of the sylvian point (Heilbroner, 1987) and was used in this study to estimate the two-dimensional length of the sylvian fissure from photographs. Unlike the arcuate sulcus and sub-central dimple, above, a total sample size of 43 brains was used for the sylvian point since the region was obliterated in one brain

In 16 of 43 brains, representing ~37% of the total sample, Pattern I of the sylvian point (the fully operculated condition) was present on both the left and right hemispheres of the same brains (Table 3-1 & Figure 3-9). This sub-population included 7 males and 9 females. Three other individuals (1 male and 2 females) with Pattern I in the left hemisphere showed Pattern II on the right.

3.3.2.3. Sylvian point, Pattern II

In contrast to Pattern I, above, in which the sylvian point was hidden deep to the surface of the brain, Pattern II refers to the condition in which the sylvian point was located in a cleft formed by the inferior parietal cortex and the middle temporal gyrus. As with Pattern I, the posterior portion of the superior temporal gyrus was also partly masked and was positioned deep to the surface of the brain. In comparison to Pattern I which was the "fully operculated" condition, Pattern II is defined here as the "partly operculated" condition of the sylvian point (Figure 3-8b). In Pattern II, this point of fissural-sulcal merging was more posteriorly located than with Pattern I.

This allowed the sylvian point to be viewed from the brain's surface without the having to spread the sylvian fissure and superior gyrus apart. It is important to note that this discrete morphologic pattern may be observed on fresh brains but could not be distinguished from Pattern I on brain endocasts. The width of the superior temporal gyrus was larger in specimens with Pattern II than those with Pattern I (compare plates a & b in Figure 3-8), which may reflect the generally lesser degree of operculation evident in these Pattern II individuals. Such a difference may be more easily measured on brain endocasts.

In 8 of 43 individuals, representing 19% of the total sample, Pattern II of the sylvian point was present on both the left and right hemispheres in corresponding brains (Table 3-1 & Figure 3-9). This sub-sample comprised five male and three female brains. In a further two male brains, representing 4.7% of the total sample, Pattern II in the right hemisphere was complemented by Pattern III on the left hemisphere. In a further one male brain and one female brain, also representing 4.7% of the total sample, Pattern II in the left hemisphere was complemented by Pattern III on the right. Finally, in two female brains and one male brain, representing ~7.0% of the sample, Pattern II on the right hemisphere was complemented by Pattern I on the left hemisphere (Table 3-1 & Figure 3-9).

Figure 3-8 Photographs of the left hemispheres of *Macaca fascicularis* brains. **a)** arrows = "Pattern I"- fully operculated sylvian point; **b)** arrows = "Pattern II" - partly operculated sylvian point, and **c)** "Pattern III" - fully exposed sylvian point. SF = sylvian fissure; STS = superior temporal sulcus; SP = sylvian point. Scale = 10mm

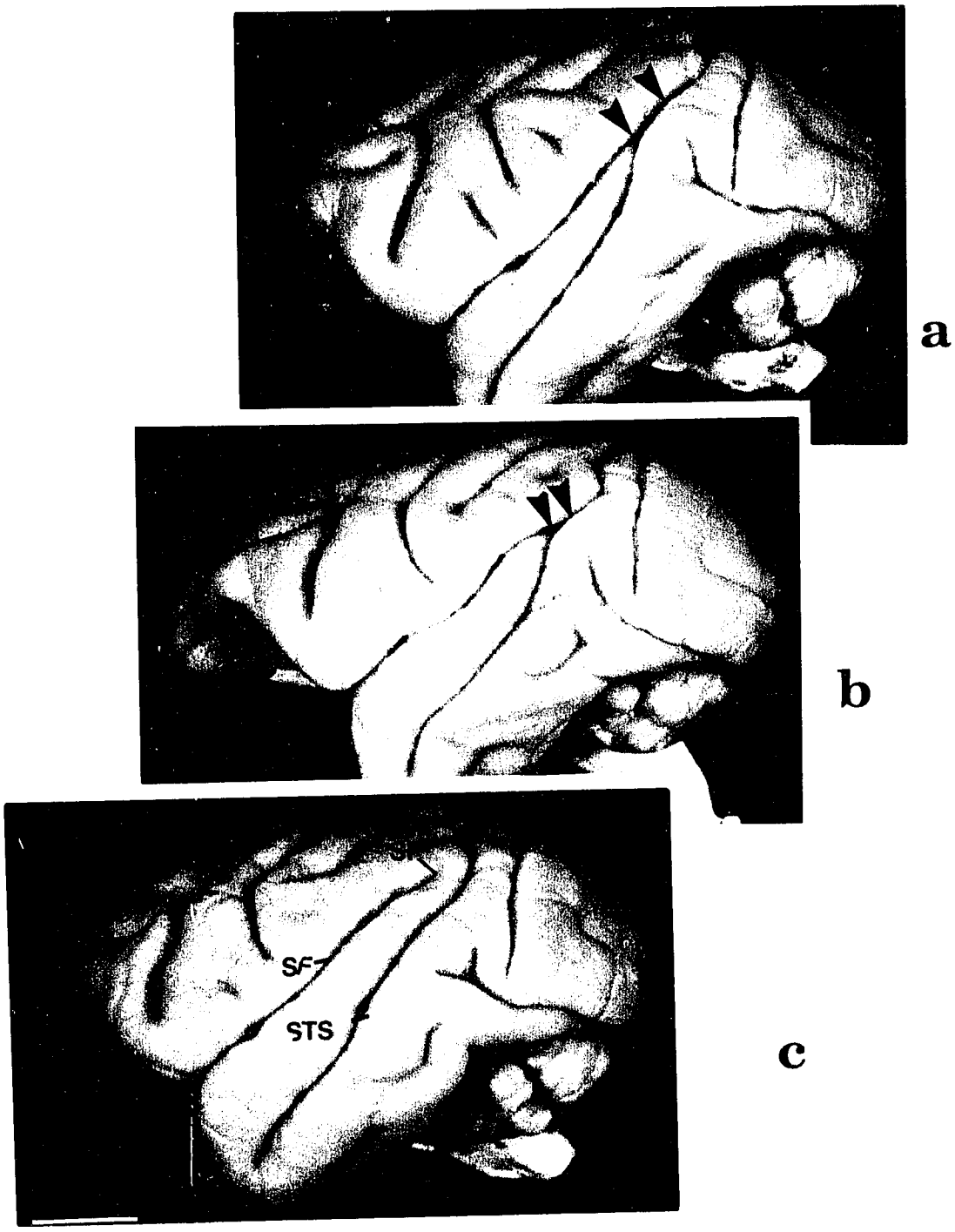
a
b
SF
STS
c

3.3.2.4. Sylvian point, Pattern III

Unlike Pattern I and II of the sylvian point described above, Pattern III refers to those brains in which the posterior portion of the superior temporal gyrus and the posterior point of termination of the sylvian fissure, the sylvian point, are clearly and unambiguously exposed in their position on the external surface of the brain (Figure 3-8c).

In 12 of 43 individuals, representing 28% of the total sample, Pattern III was apparent on both the left and right cerebral hemispheres of corresponding brains (Table 3-1, Figure 3-8c). This sub-sample comprised seven male and five female brains. In a further two male individuals, Pattern III on the left hemisphere was complemented by Pattern II on the right. Likewise, in a further two individuals, comprising one male and one female brain, Pattern III in the right hemisphere was complemented by Pattern II on the left hemisphere. Within the total sample of 86 hemispheres, Pattern III was present in 16 hemispheres, representing 20% of the total hemispheric sample. The ratio of 10:6 males to females may indicate a predominance of this less differentiated, and possibly less derived, morphological character, in males.

Table 3-1 Semi-quantitative analysis of comparative anatomy and variation of the arcuate sulcus, sub-central dimple, and sylvian point. See text sections 3.3.1. and 3.3.2 for details

Comparative Anatomy and Variation of the Arcuate Sulcus, Sub-central Dimple, and Sylvian Point

	ARCUATE SULCUS						SUB-CENTRAL DIMPLE						SYLVIAN POINT					
	LEFT			RIGHT			LEFT			RIGHT			LEFT			RIGHT		
M#	I	II	III	I	II	III	I	II	III	I	II	III	I	II	III	I	II	III
1	*			*					*	*					*			*
2			*			*		*			*		*			*		
3	*			*				*			*				*			*
4		*		*				*			*			*			*	
5		*			*			*				*		*			*	
6		*		*				*			*			*			*	
7		*				*	*				*			*			*	
8		*				*	*				*		*				*	
9		*		*				*			*		*				*	
10	*			*				*			*		*			*		
11	*				*		*			*					*			*
12		*			*		*			*				NA			NA	
13	*			*					*			*	*			*		
14	*			*			*			*					*		*	
15		*		*					*		*			*			*	
16		*			*			*		*					*			*
17	*			*			*			*			*			*		
18		*			*		*			*			*			*		
19	*				*			*		*			*			*		
20	*			*			*			*			*			*		
21	*				*		*			*				*				*
22	*			*			*				*				*			*
23	*			*			*			*			*			*		
24		*			*		*			*				*				*
25	*			*			*			*			*			*		
26		*			*				*			*		*			*	
27		*		*					*		*		*				*	
28		*			*			*			*		*			*		
29		*		*				*			*				*			*
30	*				*			*			*		*			*		
31	*				*		*			*					*			*
32		*		*			*			*					*		*	

Table 3-1, continued on next page

Table 3-1 continued from previous page

	ARCUATE SULCUS						SUB-CENTRAL DIMPLE						SYLVIAN POINT					
	LEFT			RIGHT			LEFT			RIGHT			LEFT			RIGHT		
M#	I	II	III	I	II	III	I	II	III	I	II	III	I	II	III	I	II	III
33	*			*			*			*			*			*		
34	*			*				*				*		*			*	
35		*			*		*			*			*			*		
36	*				*		*				*		*			*		
37	*				*		*			*					*			*
38		*			*			*			*		*			*		
39			*		*			*		*					*			*
40		*			*		*			*					*			*
41	*			*			*			*					*			*
42		*			*		*			*					*			*
43	*			*			*			*			*			*		
44		*			*		*			*				*			*	
totals	21	21	2	21	20	3	24	15	5	24	16	4	19	10	14	16	13	14
males	11	11	1	13	9	1	8	10	5	9	10	4	8	6	9	7	8	7
females	10	10	1	8	11	2	16	5	0	15	6	0	11	4	5	9	5	7

KEY

ARCUATE SULCUS

I	NO POSTERIOR SPUR
II	SMALL POSTERIOR SPUR
III	LARGE POSTERIOR SPUR

SUB-CENTRAL DIMPLE

I	SMALL
II	MEDIUM
III	LARGE

SYLVIAN POINT

I	OPERCULATED SYLVIAN POINT
II	INTERMEDIATE SYLVIAN POINT
III	PRESENT ON SURFACE

Figure 3-9 Graphic depiction of anatomical variation within the arcuate sulcus, sub-central dimple, and sylvian point in *Macaca fascicularis* brains (n=44). Refer to text sections 3.3.1. & 3.3.2. for details of anatomical variation assigned to Patterns I, II, and II for each structure.

NA = structure not available

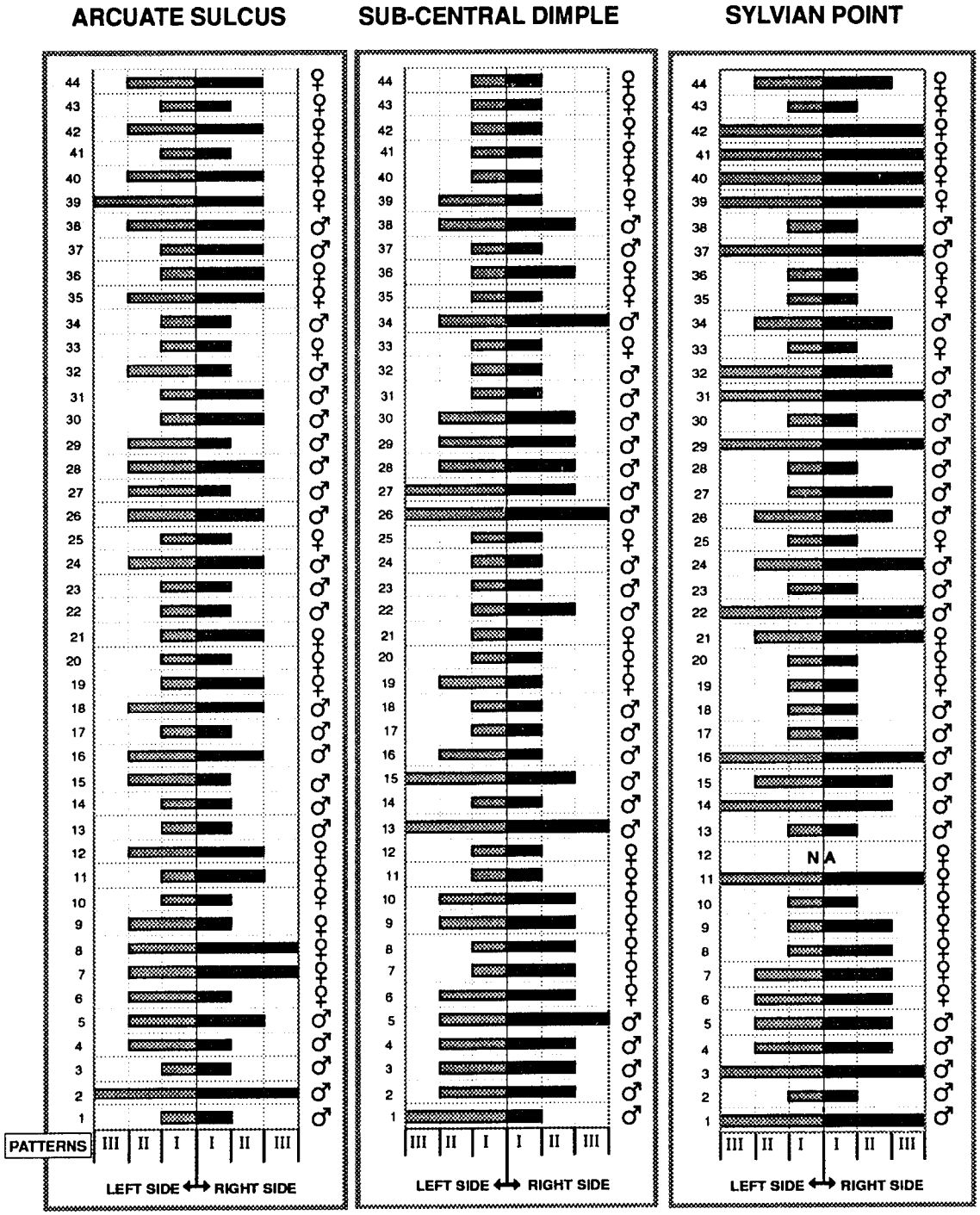
ARCUATE SULCUS
SUB-CENTRAL DIMPLE
SYLVIAN POINT
PATTERNS
III II I I II III
LEFT SIDE ↔ RIGHT SIDE
NA

3.3.2.5. The posterior temporal gyrus, inferior parietal gyrus and the supra-sylvian dimple

The inferior parietal/posterior temporal cerebrocortical area in humans contains the brain regions known as the supra-marginal gyrus and the angular gyrus (Kappers et al., 1967). These cortical regions are thought to be involved in processing polymodal information and play a role in the receptive language functions subserved by the multi-faceted functional paradigm subsumed under Wernicke's area (Damasio,AR and Geschwind, 1984). The corresponding regions were assessed in this sample of 44 *Macaca fascicularis* brains.

Within this sample of *Macaca fascicularis* brains, the gross anatomic patterns within the posterior temporal and inferior parietal regions show evidence of a great deal of inter-individual variation. However, at least one consistent morphological pattern observed in this study was the occurrence of a small but distinct bulbous gyrus, referred to here as the "supra-sylvian gyrus". This prominent brain surface structure is located on the inferior parietal lobe immediately superior and posterior to the sylvian point. The supra-sylvian gyrus is in most cases associated with a small sulcal dimple located immediately superior to it (Figure 3-10). This dimple was referred to by Falk in 1978 as a "small unnamed sulcus" which she labeled "BRTS" (Falk, 1978b). The suprasylvian gyrus described here is bounded

Figure 3-10. Low magnification macrophotographs of the posterior region of the posterior temporal and inferior parietal lobes in the right hemisphere of *Macaca fascicularis*. **a)** A pronounced suprasylvian dimple (large arrow) and associated, bulging "supra-sylvian gyrus (small arrows). **b)** Smaller "BRTS" dimple but with bulging supra-sylvian gyrus.

KEY: SF = sylvian fissure; STS = superior temporal sulcus, IPS = inter-parietal sulcus. Scale = 5mm

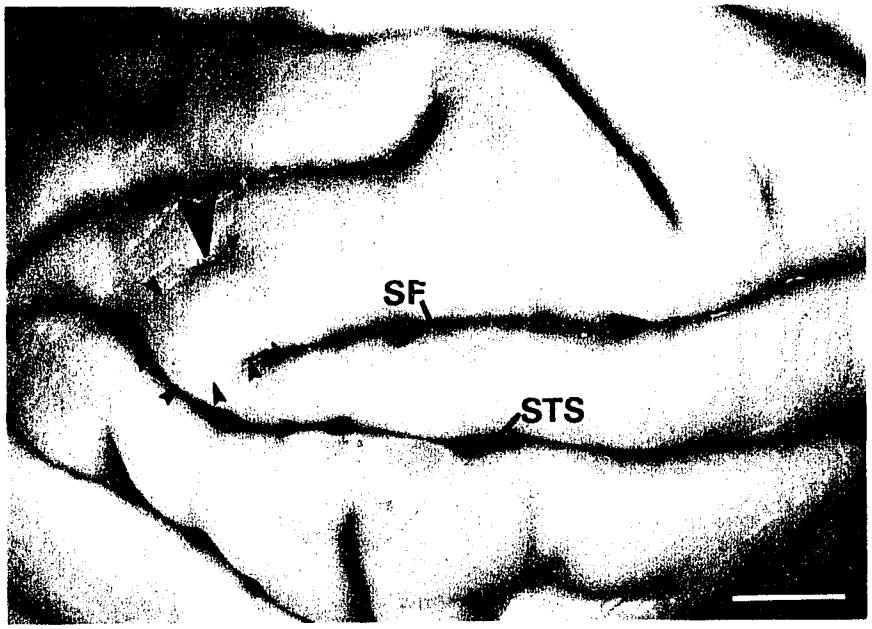

a

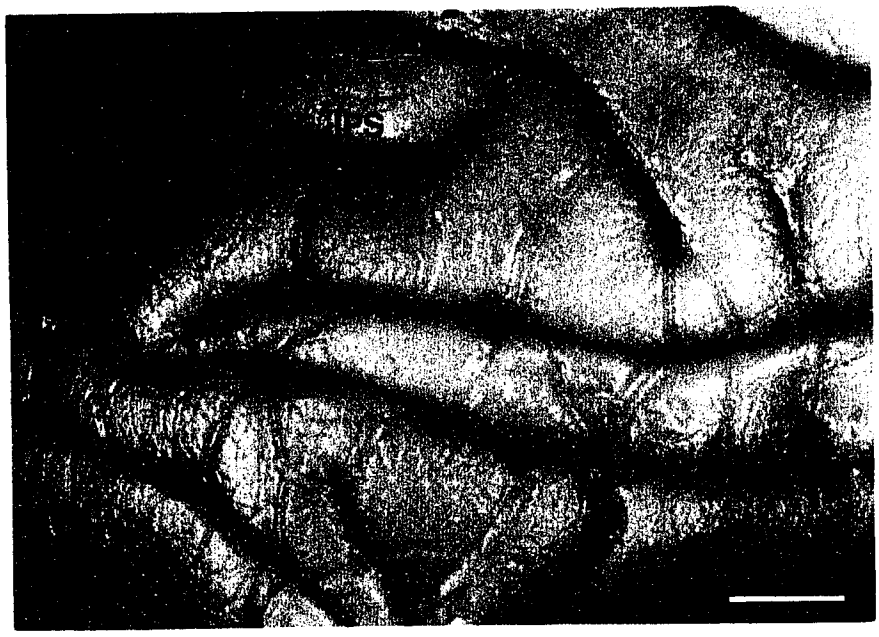

b

inferiorly and posteriorly by the superior temporal sulcus and superiorly by Falk's sulcus BRTS or the "suprasylvian dimple". In brains where the superior temporal gyrus and sylvian point are fully exposed on the surface of the brain (Figure 3-8c and Figure 3-10), the region posterior to the sylvian point curved around medially and superiorly then anteriorly to join with the horizontally oriented suprasylvian dimple (Figure 3-10a). The differentiation of the suprasylvian dimple as a anterior sulcal bifurcation originating from the posterior aspect of the superior temporal sulcus was clearly apparent on ten of the 44 brains studied (Figure 3-10b). Although the bulbous, laterally projecting, condition of the suprasylvian gyrus was evident on all of the brains used in this study, the presence of the suprasylvian dimple was not always apparent. Unfortunately, it was not possible to adequately quantify these characters further from the two-dimensional sample of lateral brain photographs since the three-dimensional nature of these structures was not sufficiently represented.

CHAPTER 4

"3-DIMENSIONAL" MORPHOMETRY OF BRAIN SURFACE STRUCTURES

4.1. CHAPTER OVERVIEW

This chapter analyses measures of lengths of the arcuate sulcus, central sulcus, sylvian fissure and superior temporal sulcus as they course over the surface of the brain in a sample of 18 (or 17) brains (females n = 9 [or 8], males n=9) using a precise new measurement method. Each measure of specific homotypic structures was made on the left and the right hemispheres.

These brain surface features, such as the arcuate sulcus and the superior temporal sulcus, course extensively through three-dimensions (3-D). As such, a quantitative method had to be devised to assess and compare this critical morphological aspect. A method was used which involved measuring contoured distances by intimate association, directly on the external surface of the cerbral cortex. Although structures were measured as they coursed across the three dimensional surface of the brain, values are not represented by a three dimensional (3-D) coordinate data matrix (i.e., x, y, and z coordinates). Instead, *curvilinear* measures, which were made directly from

the surface of brains, were transposed into two-dimensional (2-D) linear values for subsequent quantitation and statistical analysis. However, since these transposed values reflect directly the length of the complex 3-D contour (and thus contain potentially critical information beyond a 2-D assessment) they will be referred to in this dissertation as "three-dimensional" measures.

Using type 1, paired sample t-Tests, values were analyzed for patterns of interhemispheric asymmetry. Due to the large number of t-Tests being conducted it should be noted that an α - error will be present in proportion to the level of the significance value used here ($P = <0.05$).

No significant hemispheric differences were evident in the 3-D length of the arcuate sulcus although males only showed a slight trend ($P = 0.2$) for the arcuate sulcus to be both longer and to predominate in the right hemisphere. In contrast, arcuate sulcus length values in females were equally distributed as a size continuum throughout both hemispheres ($P = 0.7$).

Results of 3-D central sulcus length also showed no significant difference between the left and right hemispheres. As for the arcuate sulcus, a slight trend towards right hemisphere predominance was seen in males only although this was not reflected by the statistical analysis ($P = 0.9$)

Results of 3-D length of the sylvian fissure showed no significant difference between the left and right hemispheres. However, there was a trend in males only for the sylvian fissure to be longer more often in the left

hemisphere in six of the nine individuals.

Results of 3-D length of the superior temporal sulcus showed no significant difference between the left and right hemispheres. However, in this case there was a trend, in females only, for the superior temporal sulcus to be longer more often in the right hemisphere in seven of the nine individuals.

4.2. 3-D MEASUREMENT METHOD

The three-dimensional measures were made by applying thick (0.5mm diameter) flexible braided surgical suture material (Dexon Plus-0), bilaterally along the surface extent of a sulcus on the surface of the brain. Using fine micro-forceps (V. Mueller NL-1401), the suture material was first carefully laid in the gradual cleft formed by the end zone of a sulcus so that it closely approximated the termination point. The material was then laid along the sulcus as it coursed over the three dimensional surface of the brain. Due to its braided structure and circular profile, the material flexed easily throughout all 3-D planes along the course of the sulcus. The material was carefully maintained in the cleft formed by the two adjacent cortical walls and was not allowed to fall into the deeper parts of a sulcus. Finally, great care was taken to position the material in the distal sulcal termination zone.

At this point, the suture material was removed from the sulcus, laid straight and one end carefully aligned, using a dissecting microscope, to a

thin black line drawn on a piece of plasticized white paper. The end was held down to the line using the forceps, then the suture material was fully straightened, without stretching, and its other end marked with a small dot on the piece of paper. A straight line was drawn between the two end points of the suture material marked on the paper. The 2-D length of the line on the paper was measured with a digitizing pad quantitation system (Zeiss Videoplan 2) and an absolute value in millimeters obtained. This two-dimensional linear value represented exactly the same value for absolute length as its three dimensional equivalent. Preliminary studies showed the accuracy of this method to be < 0.2mm in repeated measures.

4.3. 3-D LINEAR MEASURES OF FRONTAL LOBE STRUCTURES

4.3.1. Method for measuring 3-D length of arcuate sulcus

Previous reports have measured the vertical limb and horizontal "limbs" of the arcuate sulcus (Heilbroner & Holloway, 1989) as distinct entities. Analysis of morphometric variation in the 44 brains used for parts of this project (section 3.2.1.1.) demonstrated that in 32% of individuals the arcuate sulcus presented as a continuum with no apparent distinction between its vertical and horizontal components (e.g. Figure 3-6a). For this reason, the length of the arcuate sulcus measured here did not consider the vertical and

horizontal limbs:

(3-D Linear Distance "AS-3d") Three dimensional linear distance from the infero-lateral point of termination of the vertical portion of the arcuate sulcus to the antero-medial point of termination of the horizontal section of the arcuate sulcus on the left and right hemispheres.

4.3.2. Results of 3-D arcuate sulcus measures

4.3.2.1. Left hemisphere arcuate sulcus, 3-D length

The average three-dimensional length of the medio-lateral extent of the arcuate sulcus in the *left cerebral hemispheres* in the total sample (n = 17), was 19.77 ± 1.87mm (max = 23.86mm; min = 16,87mm; median = 19.34mm). For the sub-sample comprising 8 females, the average length of left hemisphere *AS-3d* was slightly less than the total sample average at 18.38 ± 0.8mm (max = 19.358; min = 16.87; median = 18.262). For the sub-sample comprising 9 males, the average length of *AS-3d* in the left hemisphere was considerably larger than the total sample average at 21.0 ± 1.66mm (max = 23.86; min = 18.5; median = 21.33). See Table 4-1 for all primary data.

4.3.2.2. Right hemisphere arcuate sulcus, 3-D length

The average three dimensional length of the arcuate sulcus in the *right cerebral hemisphere*, in the total sample (n = 17) was marginally larger than that of the left hemisphere at 20.24 ± 3.04mm (max = 27.7mm; min =

Table 4-1 **a)** Three-dimensional linear measures of the length of the vertical and horizontal portions of the arcuate sulcus (AS-3d) on the left and right hemispheres. **b)** Type 1 (paired sample) t-Tests of hemispheric differences in *AS-3d* in total sample and male and female sub-samples.

3-D Measures of Arcuate Sulcus Length

n=	ARCUATE SULCUS		LARGEST SIDE	SIDE DIFFS	SORTED DIFFS	PGM#	SEX
	LEFT	RIGHT					
1	19.28	20.87	R>L	1.59	5.31	38	F
2	19.34	18.78	L>R	-0.57	2.38	39	M
3	21.70	20.36	L>R	-1.34	2.02	40	M
4	22.40	27.71	R>L	5.31	1.99	41	M
5	20.96	22.24	R>L	1.27	1.59	42	M
6	21.90	21.52	L>R	-0.38	1.27	43	M
7	23.86	25.86	R>L	1.99	1.26	44	M
8	20.51	19.01	L>R	-1.50	0.13	45	M
9	18.17	19.42	R>L	1.26	0.07	46	F
10	18.50	20.88	R>L	2.38	-0.28	47	M
11	18.20	16.47	L>R	-1.73	-0.37	48	F
12	19.87	21.89	R>L	2.02	-0.38	52	M
13	18.33	18.45	R>L	0.13	-0.57	53	F
14	19.36	17.49	L>R	-1.87	-1.34	54	F
15	16.88	16.60	L>R	-0.28	-1.50	55	F
16	18.87	18.93	R>L	0.07	-1.73	56	F
17	17.94	17.57	L>R	-0.37	-1.87	57	F
MEAN	*19.77*	*20.24*					
STDEV	*1.87*	*3.04*					
MAX	*23.86*	*27.71*					
MIN	*16.88*	*16.47*					
MEDIAN	*19.34*	*19.42*					

t-Test: Paired Two Sample for Means

	TOTAL SAMPLE		MALES ONLY		FEMALES ONLY	
	AS (L)	AS (R)	AS (L)	AS (R)	AS (L)	AS (R)
Mean	19.77	20.24	21.01	22.03	18.38	18.22
Variance	3.49	9.24	2.74	8.87	0.65	2.24
Observations	17	17	9	9	8	8
Pearson Correlation	0.82		0.69		0.57	
Hypoth Mean Diff	0.00		0.00		0.00	
df	16.00		8.00		7.00	
t Stat	-1.04		-1.39		0.35	
P(T<=t) one-tail	0.16		0.10		0.37	
t Critical one-tail	1.75		1.86		1.89	
P(T<=t) two-tail	**0.31**	**N/S**	**0.20**	**N/S**	**0.74**	**N/S**
t Critical two-tail	2.12		2.31		2.36	

16.47mm; median = 19.42mm). For the sub-sample comprising 8 females, the average length of *AS-3d* in the right hemisphere was 18.22 ± 1.5mm (max = 20.87mm; min = 16.47mm; median = 18.01mm).). In the sub-sample comprising 9 males, the average length of *AS-3d* in the right hemisphere was larger than that on the left hemisphere at 22.03 ± 2.98mm (max = 27.7mm; min = 18.78mm; median = 21.7mm). However, this larger right hemisphere male sub-sample mean for *AS-3d* was inflated by one male individual in which the right hemisphere arcuate sulcus was (compared to the rest of the total sample), much larger than the corresponding value in the left hemisphere (left = 22.4mm vs right = 27.71mm, ~19% larger). When this highly variable individual was temporarily removed from the sample, the mean length of *AS-3d* on the right hemisphere was still larger than that on the left (L = 20.83mm) at 21.32mm. See Table 4-1 for all primary data

4.3.2.3. Hemispheric differences in 3-D arcuate sulcus length

The arcuate sulcus on the left hemisphere was larger than that on the right in 8 of 17 individuals, comprising 4 males and 4 females (Figure 4-1, Table 4-1). The arcuate sulcus on the right hemisphere was larger than that on the left in 9 of the 17 individuals, comprising 5 males and 4 females. Values less than 0.1 mm are considered to represent symmetry of this measure.

Figure 4-1 Scatter plots of 3-D linear measures of the length of the arcuate sulcus (*AS-3d*) on the left and right hemispheres. Hemispheric distribution of measures in: **a)** total sample (n=17) **b)** female sub-sample (n=8), and **c)** male sub-sample (n=9). In each case, the diagonal line represents a reference for hemispheric symmetry.

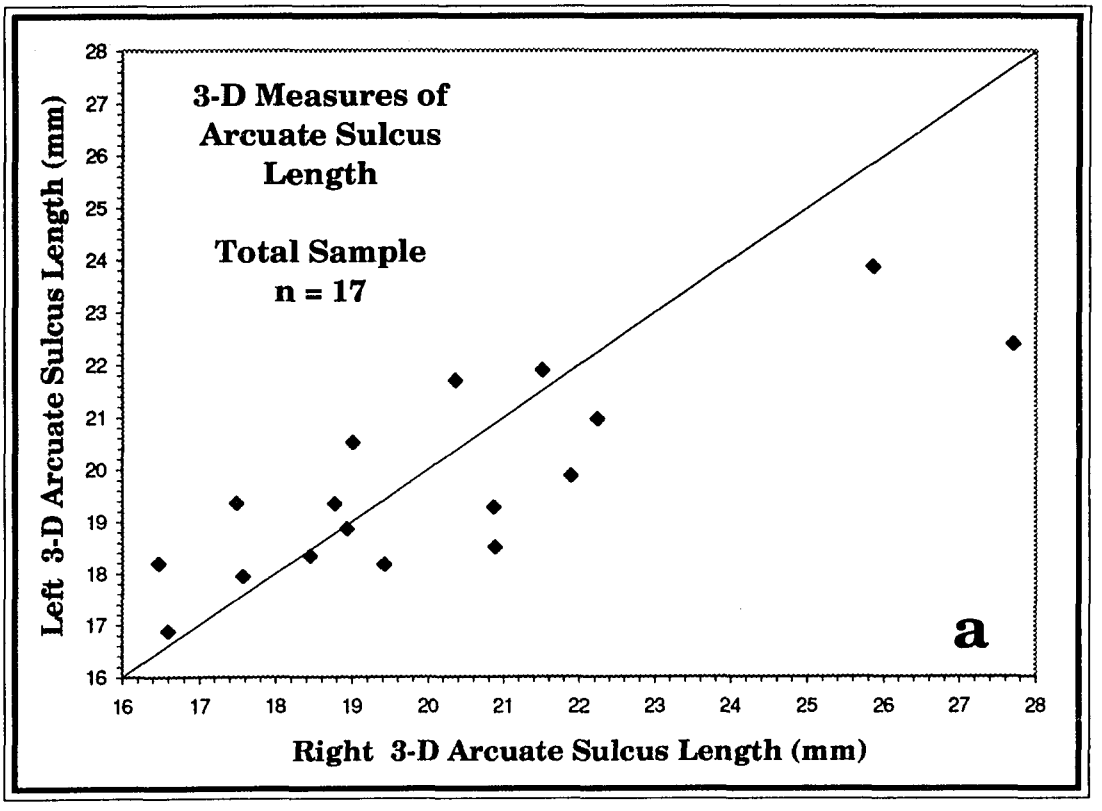
3-D Measures of Arcuate Sulcus Length
Total Sample
n = 17
Left 3-D Arcuate Sulcus Length (mm)
Right 3-D Arcuate Sulcus Length (mm)
a
16 17 18 19 20 21 22 23 24 25 26 27 28

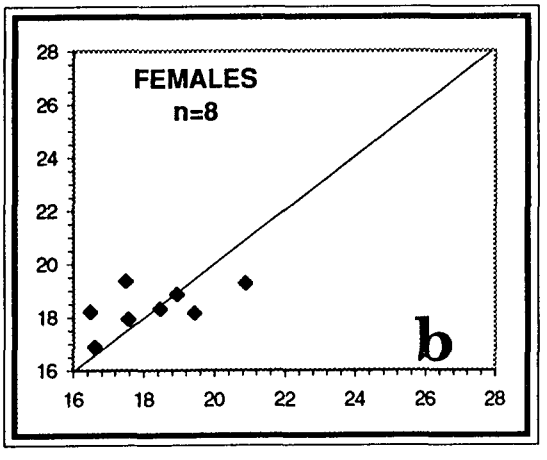
FEMALES
n=8
b
16 18 20 22 24 26 28

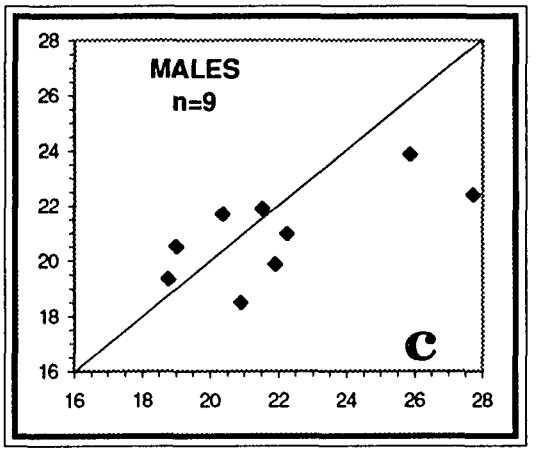
MALES
n=9
c
16 18 20 22 24 26 28

Figure 4-2 Plot of hemispheric differences in the length of the arcuate sulcus (*AS-3d*). Values (in millimeters) represent the difference in length between corresponding sulci on the left and right individuals, plotted for the largest side: **a)** total sample (n=17) **b)** female sub-sample (n=8), and **c)** male sub-sample (n=9).

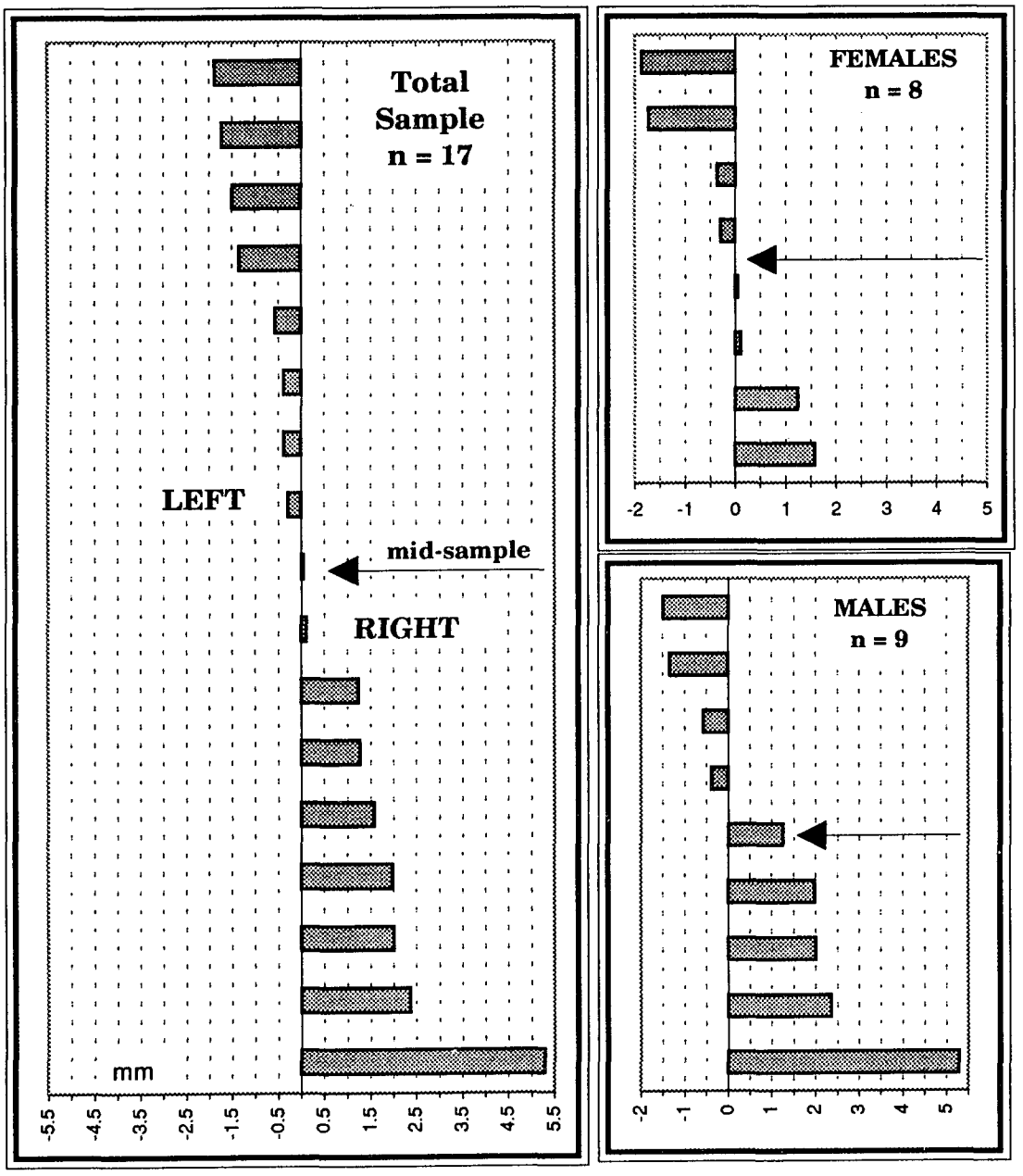
Total
Sample
n = 17
LEFT
mid-sample
RIGHT
mm
-5.5
-4.5
-3.5
-2.5
-1.5
-0.5
0.5
1.5
2.5
3.5
4.5
5.5
FEMALES
n = 8
-2
-1
0
1
2
3
4
5
MALES
n = 9
-2
-1
0
1
2
3
4
5

4.3.2.4. Statistical analysis

Using a type 1 (paired sample) two-tailed t-Test, it was shown that there were no significant differences between the length of the arcuate sulcus in the right and left cerebral hemispheres in the total sample of 17 individuals ($P = 0.31$, Table 4-1). When males and females were considered separately, it was also shown that there were no significant hemispheric differences of this measure between the left and right cerebral hemispheres; males ($P = 0.20$) and females ($P = 0.74$). There was, however, a suggestion of a trend in the 9 males for the arcuate sulcus to be larger predominantly in the right hemisphere as can be seen in Figures 4-1c and 4-2c. Further, although the probability value for left vs right hemisphere 3-D arcuate sulcus length was not significant at $P = 0.2$, the value is much lower than that for females or the total sample. As such, an increased sample size may bring out this potentially subtle pattern of right hemisphere dominated asymmetry.

4.3.3. Method for measuring 3-D length of central sulcus

As for the arcuate sulcus above, this measure was made by applying braided flexible suture material along the supero-inferior extent of the central sulcus on both the left and right cerebrocortical hemispheres. This measure of central sulcus length was made in a total sample of 17 brains comprising 8 female and 9 male individuals of *Macaca fascicularis*. Since the

superior portions of the central sulcus are quite medially placed, it was not possible to reliably make this measure from lateral photographs of the intact brain. Therefore, as for the arcuate sulcus, comparisons between two-dimensional and three dimensional measures were not able to be performed. The specific measure is defined as follows:

> *(3-D Linear Distance "CS-3d")* The three-dimensional linear distance from the infero-lateral point of termination of the of the central sulcus to the supero-medial point of termination on the left and right hemispheres.

4.3.4. Results and analysis of 3-D length measures of central sulcus

4.3.4.1. Left hemisphere central sulcus, 3-D length

The average 3-D length of the central sulcus on the left hemisphere in the total sample (n = 17) was 26.7 ±1.9mm (max = 29.4mm; min = 23.7mm; median = 27mm); Table 3-8. In the females (n = 8), the average length of the left central sulcus was smaller than the total sample average at 25.5 ±1.6mm (max = 28.4mm; min=23.7mm; median = 25.1mm). In the male sub-sample (n = 9), the average length of the left central sulcus was larger than the total sample average at 27.8 ±1.3 mm (max = 29.4mm; min = 25.9mm; median = 28.2mm). See table 4-2 for primary data.

4.3.4.2. Right hemisphere central sulcus, 3-D length

The average length of the central sulcus in the right hemisphere of the total sample (n =17) was similar to that of the left at 26.9 ±2.1mm (max = 30.1mm; min = 23.5mm; median = 26.8mm). In the female sub-sample (n = 8), the average length of the left central sulcus was, as in the left hemisphere, slightly smaller than the total sample average (26.7mm) at 25.9 ±2.1mm (max = 29.3mm; min = 23.5mm; median = 26mm). In the male sub-sample (n = 9), the average length of the left central sulcus was, as for the left hemisphere, larger than the total sample average at 27.8 ±1.8 mm (max = 30.1mm; min = 24.4mm; median = 28mm). See Table 4-2 for primary data, and Figures 4-3 & 4-4.

4.3.4.3. Hemispheric differences in 3-D central sulcus length

The central sulcus was longer on the left hemisphere in 6 of 17 individuals in the total sample, comprising 2 males and 4 females. The central sulcus was larger on the right hemisphere in 11 brains, comprising 7 males and 4 females (Figures 4-3 and 4-4, Table 4-2).

4.3.4.4. Statistical analysis

Using a type 1 (paired sample) two-tailed t-Test, it was shown that there were no significant differences between the length of the central sulcus in the right and left cerebral hemispheres in the total sample ($P = 0.63$, Table 4-2).

Table 4-2 **a)** Three-dimensional linear measures of the length of the central sulcus (CS-3d) on the left and right hemispheres of 17 brains. **b)** Type 1 (paired sample) t-Tests of hemispheric differences in *"CS-3d"* in total sample and male and female sub-samples.

3-D Measures of Central Sulcus Length

n=	CENTRAL SULCUS		LARGEST SIDE	SIDE DIFFS	SORTED DIFFS	PGM#	SEX
	LEFT	RIGHT					
1	26.46	29.29	R>L	2.83	3.00	38	F
2	25.94	26.72	R>L	0.78	2.78	39	M
3	28.43	28.54	R>L	0.12	2.77	40	M
4	29.18	29.83	R>L	0.65	2.04	41	M
5	27.43	24.39	L>R	-3.04	0.90	42	M
6	27.96	26.82	L>R	-1.14	0.21	43	M
7	29.44	30.14	R>L	0.71	0.10	44	M
8	27.02	27.52	R>L	0.50	-0.08	45	M
9	25.35	25.50	R>L	0.14	-0.30	46	F
10	25.87	26.92	R>L	1.05	-0.53	47	M
11	27.01	26.50	L>R	-0.51	-0.93	48	F
12	28.98	29.10	R>L	0.12	-1.07	52	M
13	28.42	27.74	L>R	-0.68	-1.19	53	F
14	24.36	24.11	L>R	-0.25	-1.22	54	F
15	24.08	23.45	L>R	-0.64	-1.38	55	F
16	24.87	26.59	R>L	1.72	-1.60	56	F
17	23.70	23.86	R>L	0.16	-2.82	57	F
MEAN	*26.73*	*26.88*					
STDEV	*1.85*	*2.11*					
MAX	*29.44*	*30.14*					
MIN	*23.70*	*23.45*					
MEDIAN	*27.01*	*26.82*					

a

t-Test: Paired Two Sample for Means

	TOTAL SAMPLE		MALES ONLY		FEMALES ONLY	
	CS (L)	CS (R)	CS (L)	CS (R)	CS (L)	CS (R)
Mean	26.73	26.88	27.80	27.78	25.53	25.88
Variance	3.43	4.44	1.79	3.31	2.67	4.18
Observations	17	17	9	9	8	8
Pearson Correlation	0.81		0.70		0.79	
Hypoth Mean Diff	0.00		0.00		0.00	
df	16.00		8.00		7.00	
t Stat	-0.48		0.07		-0.77	
P(T<=t) one-tail	0.32		0.47		0.23	
t Critical one-tail	1.75		1.86		1.89	
P(T<=t) two-tail	**0.63**	**N/S**	**0.95**	**N/S**	**0.46**	**N/S**
t Critical two-tail	2.12		2.31		2.36	

b

Figure 4-3 Scatter plots of 3-D linear measures of the length of the central sulcus (*CS-3d*) on the left and right hemispheres. Hemispheric distribution of measures in: **a)** total sample (n=17) **b)** female sub-sample (n=8), and **c)** male sub-sample (n=9). In each case, the diagonal line represents a reference for hemispheric symmetry.

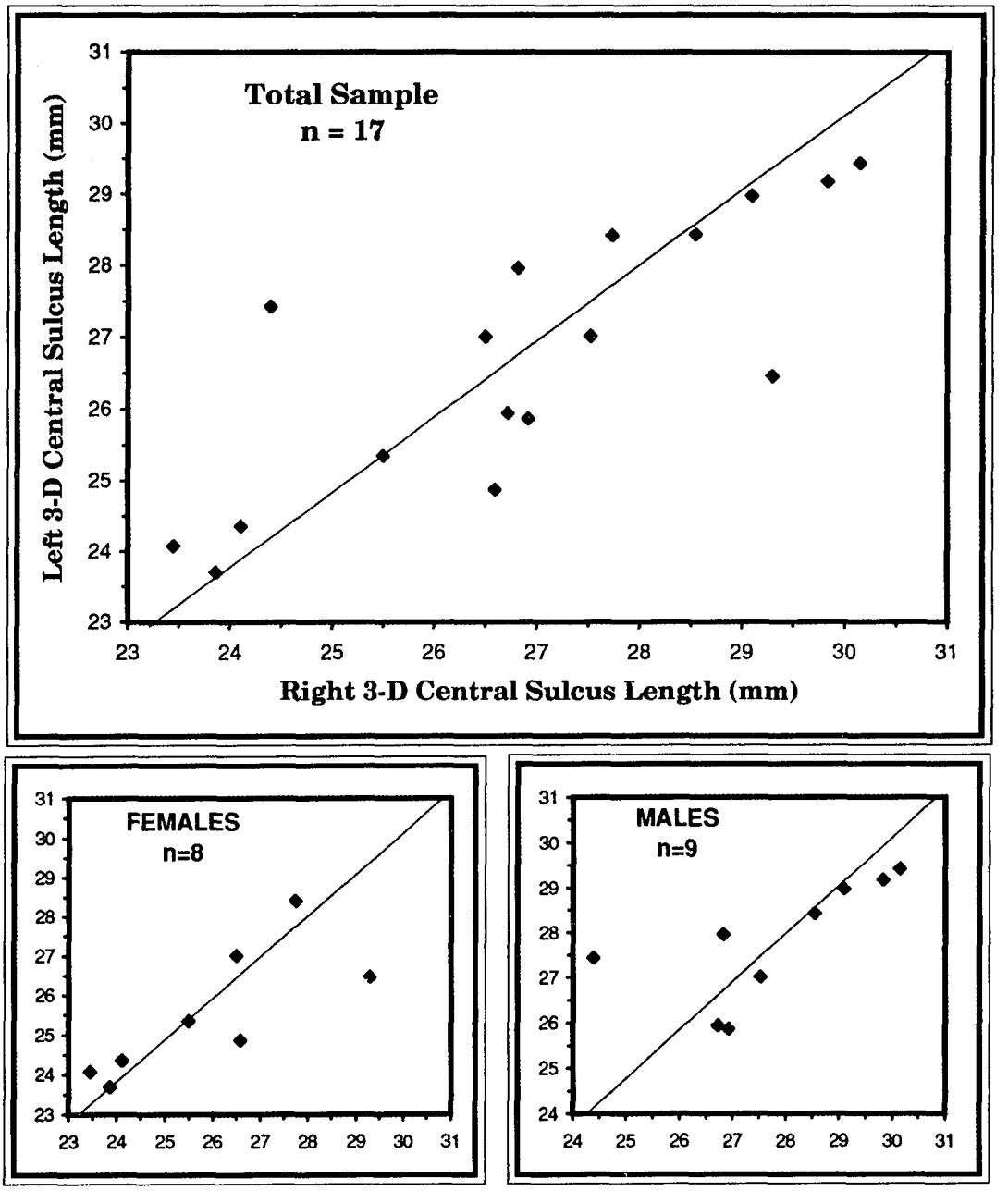
Total Sample
n = 17
Left 3-D Central Sulcus Length (mm)
Right 3-D Central Sulcus Length (mm)
FEMALES
n=8
MALES
n=9

Figure 4-4 Plot of hemispheric differences in the length of the central sulcus (*CS-3d*). Values (in millimeters) represent the difference in length between corresponding sulci on the left and right individuals, plotted for the largest side: **a)** total sample (n=17) **b)** female sub-sample (n=8), and **c)** male sub-sample (n=9).

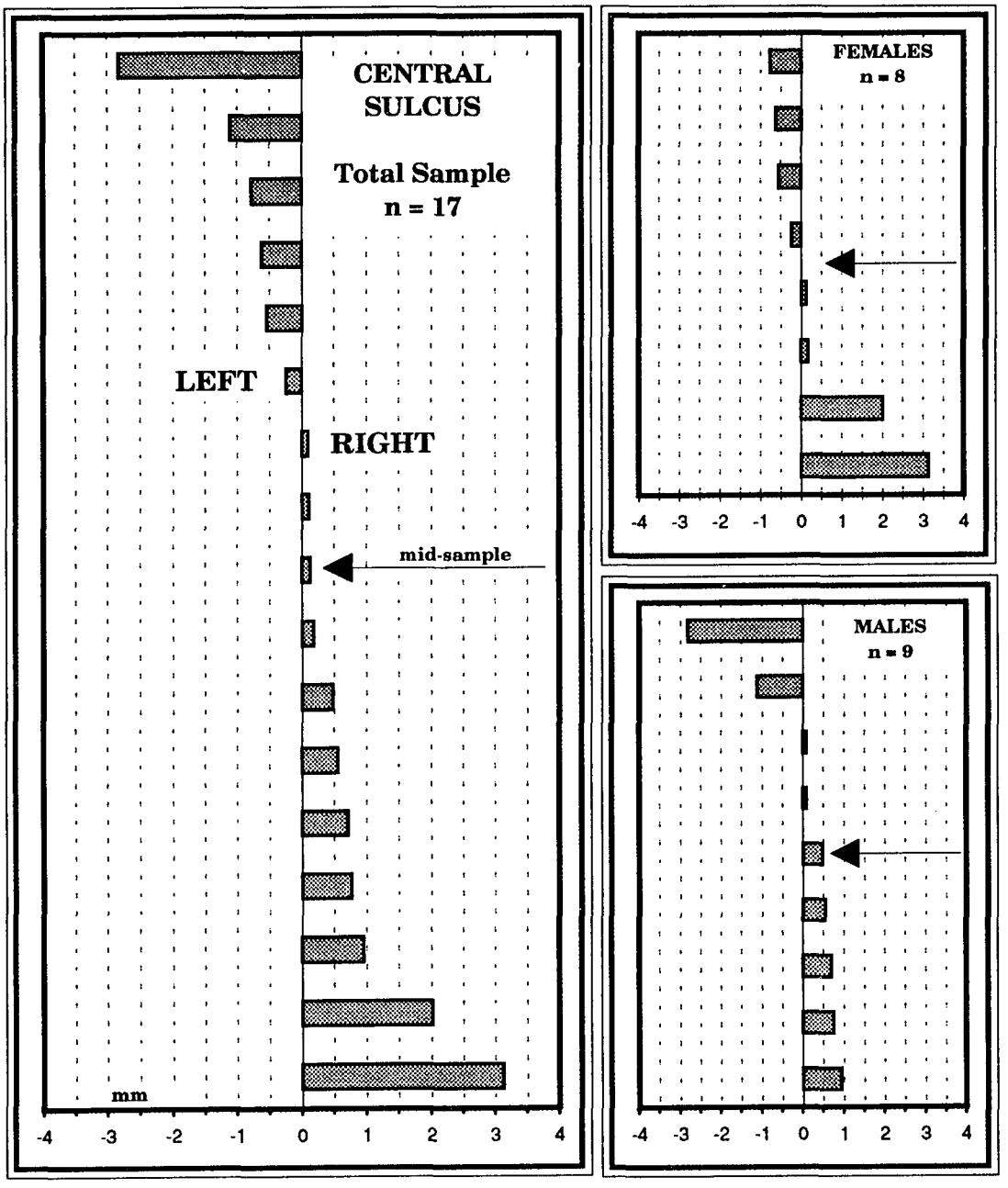
CENTRAL SULCUS
Total Sample n = 17
LEFT
RIGHT
mid-sample
mm
-4 -3 -2 -1 0 1 2 3 4
FEMALES n = 8
-4 -3 -2 -1 0 1 2 3 4
MALES n = 9
-4 -3 -2 -1 0 1 2 3 4

There were also no significant hemispheric differences of 3-D central sulcus lengths in the female sub-sample (n = 8) at $P = 0.46$ or in the male sub-sample (n = 9) at $P = 0.95$ (Table 4-2b). As was the case for the arcuate sulcus there was, however, a suggestion of a possible trend in males, for the central sulcus to be larger more often in the right hemisphere since 7 of the 9 males in the sample showed a longer central sulcus on the right side (Figure 4-4). This slight trend for right hemisphere predominance in males is similar to that reported for the arcuate sulcus above.

4.4. 3-D LINEAR MEASURES OF TEMPORAL LOBE STRUCTURES

4.4.1. Method for measuring 3-D linear length of the sylvian fissure

Previously, the length of the sylvian fissure has been measured on fossil endocasts, endocasts of extant primates, from lateral photographs of immersion fixed brains as well as directly from the surface of immersion-fixed brains (see Chapters 2 & 7). However, there are many problems with determining the exact position of the sylvian point on the brains surface. In the analysis of brain surface anatomy and variation, presented in Chapter 3 (section 3.3.2.), it was determined that the posterior termination of the sylvian fissure, or "sylvian point" (Witelson & Kigar, 1992), was completely obscured, being buried deep to the brain's surface on both cerebral

hemispheres in 37% (16 of 43) of individuals. In a further 19% (8 of 43) individuals, the sylvian point was visible from the surface but was at the bottom of a deep cleft. In all of these latter individuals, the superior temporal and inferior parietal gyri come together a variable distance anterior to the sylvian point (see Figure 3-8a & b). Some previous measures of sylvian fissure length, on endocasts for example, have used the point of joining of the sylvian fissure and superior temporal sulcus as an estimation of sylvian point position (Falk, 1978b).

For reasons stated above, in this analysis the entire antero-posterior length of the sylvian fissure was measured as an absolute value regardless of the position of the sylvian point and was not estimated by the point of convergence of the sylvian fissure and superior temporal sulcus. In cases where the sylvian point was located deep to the surface of the brain, the inferior parietal and superior temporal gyri were spread apart allowing direct placement of the measuring cord. This provided for definitive localization and more precise measurement of this important temporal lobe landmark. The method used to measure the 3-D length of the sylvian fissure is described in Section 4.2. The specific measure is defined as:

(3-D Linear Distance :SF-3d") Three dimensional linear distance of the sylvian fissure on the left and right hemispheres measured from the most anterior point on the lateral surface of the brain to its posterior termination

point, or "sylvian point" (regardless of surface or deep position).

4.4.2. Results of 3-D sylvian fissure length measures

4.4.2.1. Left hemisphere sylvian fissure, 3-D length

The average value for 3-D length, or antero-posterior extent, of the sylvian fissure in the left cerebrocortical hemisphere of the total sample (n = 18), was 32.05 ±2.7mm (max = 36.6mm, min = 26.9mm, median = 32.5mm (Table 4-3). For females (n = 9), the average length of the left hemisphere sylvian fissure was smaller than the total sample average at 30.73 ±2.83mm (max = 43.5mm, min = 26.9mm, median = 30.7mm); Table 3-14. For males (n = 9), the average length of the left hemisphere sylvian fissure was larger than the total sample average at 33.4 ±1.7mm (max = 36.6mm, min = 31.6mm, median = 32.9mm); Table 4-3, Figures 4-5 & 4-6.

4.4.2.2. Right hemisphere sylvian fissure, 3-D length

The average length of the sylvian fissure in the right hemisphere of the total sample was almost identical to that on the left (32.05mm) at 32.04 ±2.1mm (max = 37.5mm, min = 29mm, median = 31.93). The average length of the right hemisphere sylvian fissure in females (n = 9) was similar to the left side value (of 30.7mm) at 30.9 ±1.6mm (max = 33.3mm, min = 29mm, median = 30.7mm. In males(n = 9) the average length of the right sylvian

Table 4-3 **a)** Three-dimensional linear measures of the length of the sylvian fissure (SF-3d) on the left and right hemispheres. **b)** Type 1 (paired sample) t-Tests of hemispheric differences in the measure "*SF-3d*" in total sample and separately in the male and female sub-samples.

3-D Measures of Sylvian Fissure Length

n=	SYLVIAN FISSURE		LARGEST	SIDE	SORTED	PGM#	SEX
	LEFT	RIGHT	SIDE	DIFFS	DIFFS		
1	26.91	28.95	2.04	R>L	3.00	38	F
2	32.25	31.95	-0.30	L>R	2.78	39	M
3	31.64	30.05	-1.60	L>R	2.77	40	M
4	36.57	37.48	0.90	R>L	2.04	41	M
5	32.92	31.91	-1.00	L>R	0.90	42	M
6	31.56	34.33	2.77	R>L	0.21	43	M
7	34.21	33.13	-1.07	L>R	0.10	44	M
8	32.71	32.63	-0.08	L>R	-0.08	45	M
9	34.50	31.68	-2.82	L>R	-0.30	46	F
10	33.31	32.77	-0.53	L>R	-0.53	47	M
11	29.16	29.37	0.21	R>L	-0.93	48	F
12	27.73	30.73	3.00	R>L	-1.00	51	F
13	35.47	34.27	-1.19	L>R	-1.07	52	M
14	34.31	33.09	-1.22	L>R	-1.19	53	F
15	33.18	33.28	0.10	R>L	-1.22	54	F
16	30.74	29.81	-0.93	L>R	-1.38	55	F
17	28.56	31.34	2.78	R>L	-1.60	56	F
18	31.26	29.89	-1.38	L>R	-2.82	57	F
MEAN	*32.05*	*32.04*					
STDEV	*2.66*	*2.13*					
MAX	*36.57*	*37.48*					
MIN	*26.91*	*28.95*					
MEDIAN	*32.48*	*31.93*					

a

t-Test: Paired Two Sample for Means

	TOTAL SAMPLE		MALES ONLY		FEMALES ONLY	
	SF (L)	SF (R)	SF (L)	SF (R)	SF (L)	SF (R)
Mean	32.05	32.04	33.40	33.17	30.70	30.90
Variance	7.08	4.54	2.94	4.30	8.00	2.46
Observations	18	18	9	9	9	9
Pearson Correlation	0.78		0.76		0.72	
Hypoth Mean Diff	0.00		0.00		0.00	
df	17.00		8.00		8.00	
t Stat	-0.04		0.52		-0.30	
P(T<=t) one-tail	0.48		0.31		0.39	
t Critical one-tail	1.74		1.86		1.86	
P(T<=t) two-tail	**0.97**	**N/S**	**0.62**	**N/S**	**0.78**	**N/S**
t Critical two-tail	2.11		2.31		2.31	

b

fissure was, similar to that for the total sample and the female sub-sample as well as being similar to the corresponding left hemisphere average value (of 33.4mm) at 33.2 ±2.07mm (max = 37.5mm, min = 30.1mm, median = 32.8mm); Table 4-3 and Figures 4-5 & 4-6.

4.4.2.3. Hemispheric differences in 3-D sylvian fissure length

The sylvian fissure was longer in the left hemisphere in a total of 11 individuals, including males (n = 7) and females (n = 4). Conversely, the sylvian fissure was longer in the left hemisphere in a total of 7 individuals including males (n = 2) and females (n = 5), Figure 4-5 & 4-6.

4.4.2.4. Statistical analysis

Using these absolute values for 3-D length of the sylvian fissure, type 1 (paired sample) t-Tests were performed to assess left versus right hemisphere differences in the total sample and the sex sub-samples. In the total sample (n = 18), there were no significant differences between the length of the sylvian fissure on the left and right hemispheres, at $P = 0.97$, Table 4-3. In females (n = 9) and males (n = 9), there were also no significant hemispheric asymmetry of this measure, at $P = 0.77$, and $P = 0.62$ respectively (Table 4-3).

The difference in millimeters of absolute values for sylvian fissure length were calculated to graph the extent and direction of hemispheric

Figure 4-5 Scatter plots of 3-D linear measures of the length of the sylvian fissure (*SF-3d*) on the left and right hemispheres. Hemispheric distribution of measures in: **a)** total sample (n=18); **b)** female sub-sample (n=9); and **c)** male sub-sample (n=9). In each case, the diagonal line represents a reference for hemispheric symmetry.

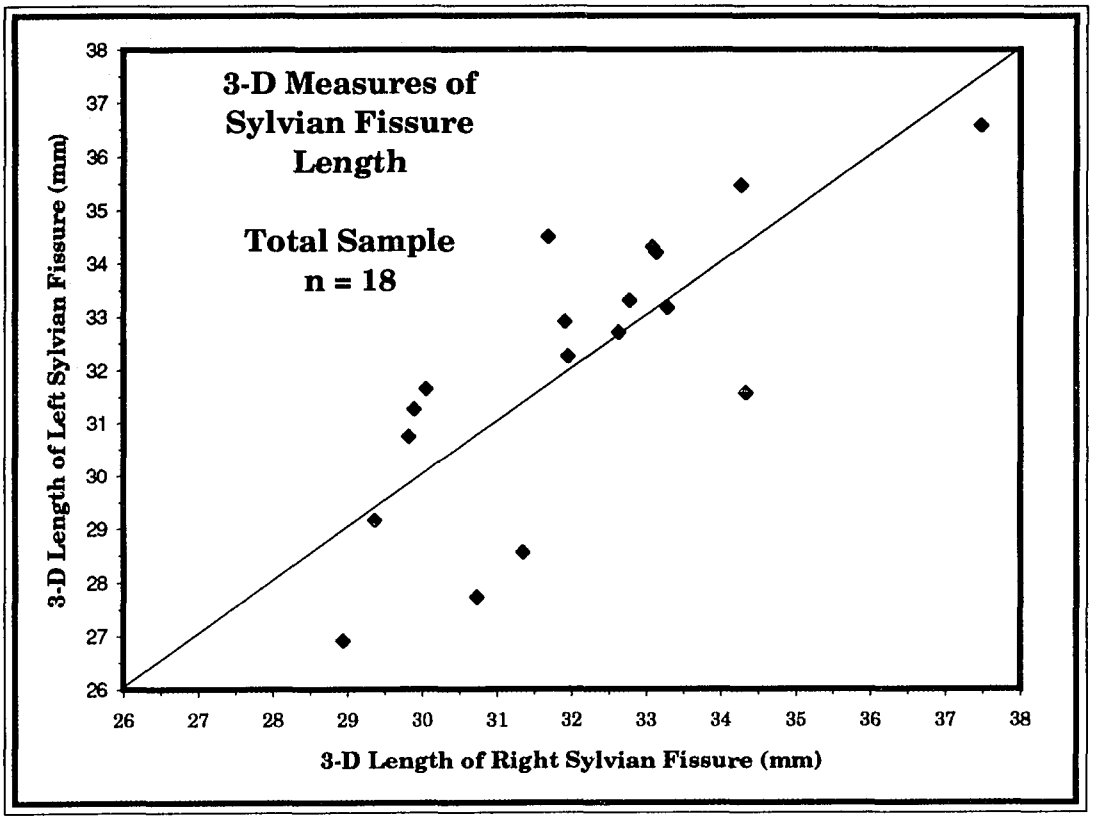
3-D Measures of Sylvian Fissure Length
Total Sample n = 18
3-D Length of Left Sylvian Fissure (mm)
3-D Length of Right Sylvian Fissure (mm)
26 27 28 29 30 31 32 33 34 35 36 37 38

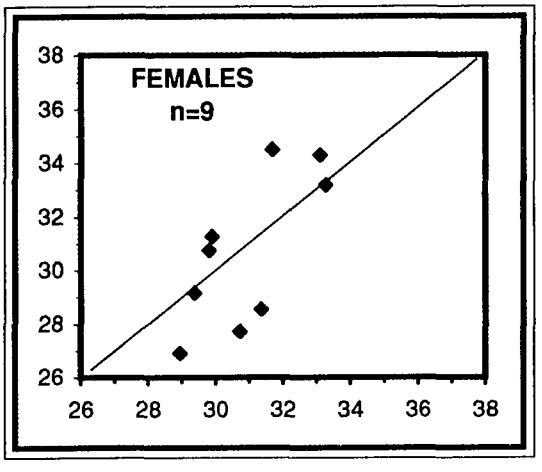
FEMALES
n=9
26 28 30 32 34 36 38

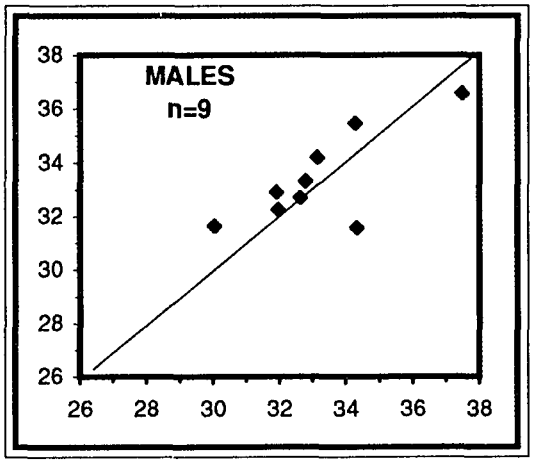
MALES
n=9
26 28 30 32 34 36 38

Figure 4-6 Plot of hemispheric differences in the 3-D length of the sylvian fissure (*SF-3d*). Values (mm) represent the difference in length between corresponding sulci on the left and right hemispheres plotted for the largest side: **a)** total sample (n=18); **b)** female sub-sample (n=9); and **c)** male sub-sample (n=9)

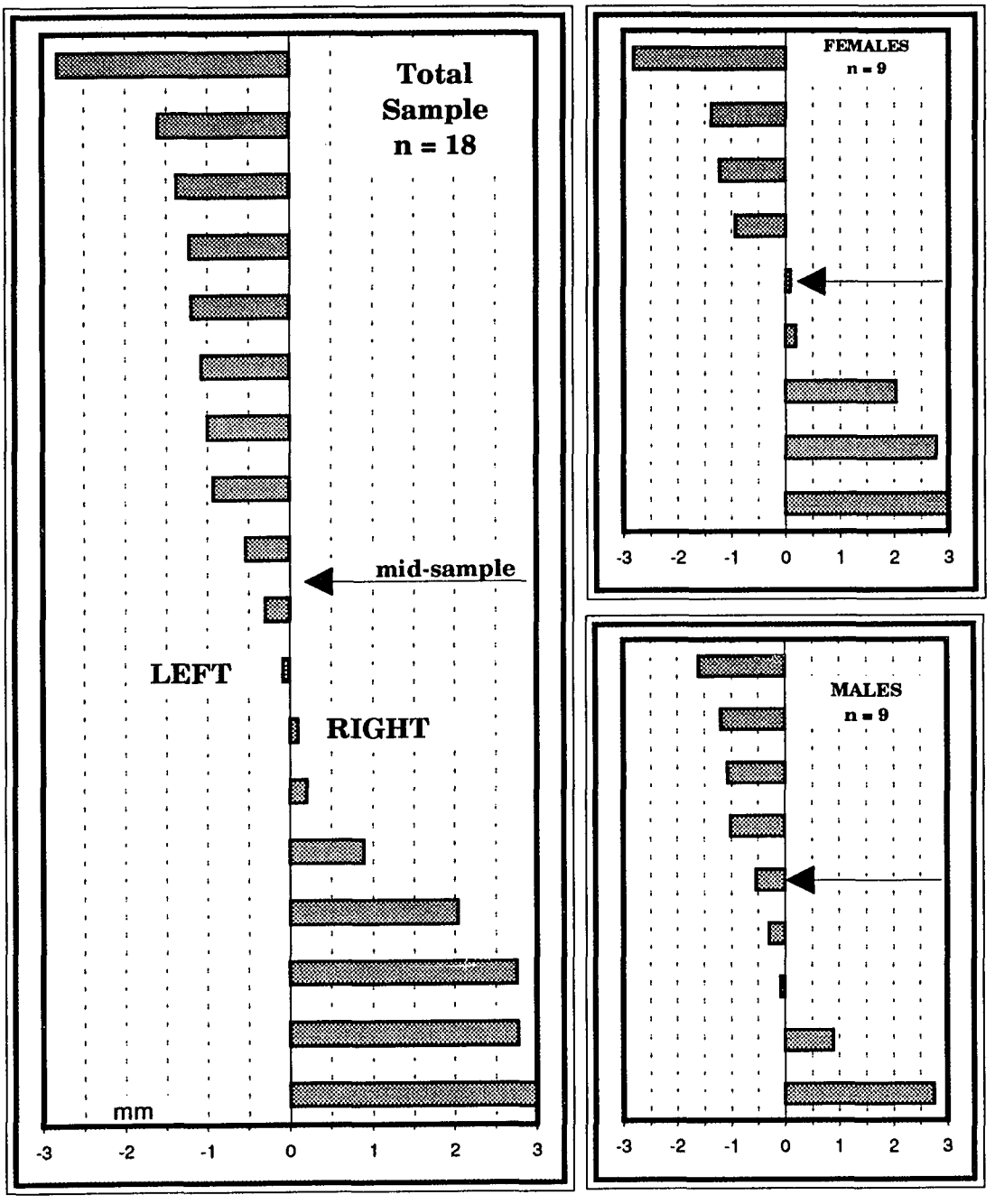
Total
Sample
n = 18
mid-sample
LEFT
RIGHT
mm
-3
-2
-1
0
1
2
3
FEMALES
n = 9
MALES
n = 9

predominance, both within the total sample and between the sexes. In Figure 4-5, absolute values are presented as a scatter-plot (for the total sample 4-5a, females 4-5b and males 4-5c) to compare the distribution and sex differences in hemispheric asymmetry of the sylvian fissure as compared to symmetry (represented by the diagonal line in all 3 plots). A second comparison of absolute values involved calculation of a value for the difference in size between the two hemispheres. These were plotted as a bar graph for the total sample, females only and males only in Figure 4-6.

4.4.3. Method for measuring 3-D length of superior temporal sulcus

Of the four sulci measured in this three-dimensional study, the superior temporal sulcus presents the most extensive and multi-planar course along the surface of the brain. It extends from its anterior termination on the lateral aspect of the brain, between the superior and middle temporal gyri, to its posterior termination on the medial aspect of the posterior parietal lobe, on the dorsal surface of the brain (see Figures 3-1a & 3-2a). For this reason, it is not possible to capture the full extent of the sulcus from either lateral or dorsal photographs of the brain in two dimensions.

The method used here to measure the 3-D length of the superior temporal sulcus was essentially the same as that used for the other structures (see section 4.2.). Since the course of this sulcus was so long and tortuous, special

care had to be taken to ensure that placement of the braided suture material was on the surface of the brain and not within the sulcus at any point.

The specific measure is defined as follows:

> *(3-D Linear Distance "STS-3d")* *The three dimensional linear distance from the antero-lateral point of termination of the superior temporal sulcus on the temporal lobe to its postero-medial point of termination on the parietal lobe, on the left and right hemispheres.*

4.4.4. Results of 3-D measures of superior temporal sulcus length

4.4.4.1. Left hemisphere superior temporal sulcus, 3-D length

The mean value for 3-D length of the antero-posterior extent of the superior temporal sulcus in the left cerebrocortical hemisphere of the total sample (n=18), was 46.5 ±3.3mm (max = 54.5mm, min = 41.5mm, median = 46.0mm), see Table 4-4. For the female sub-sample (n = 9), the average length of the left hemisphere superior temporal sulcus was smaller, at 45.2 ±2.6mm (Table 4-4). For the male sub-sample (n = 9), the average length of the left hemisphere superior temporal sulcus was larger than the total sample average at 47.9 ±3.4mm (Table 4-4).

4.4.4.2. Right hemisphere superior temporal sulcus, 3-D length

The average length of the superior temporal sulcus in the right hemisphere of the total sample (n = 18) was 47.0 ±3.1mm (max = 53.2, min =

41.8, median = 47.4, (Table 4-4). The average length of the right superior temporal sulcus in females (n = 9) was smaller than that of the total sample, at 45.9 ±2.7. In the males (n = 9), the average length of the right superior temporal sulcus was larger than the total sample value, at 48.1 ±3.2mm (Table 4-4).

4.4.4.3. Hemispheric differences in 3-D length of superior temporal sulcus

The superior temporal sulcus was longer in the left hemisphere in a total of 6 individuals (males, n = 4 and females, n = 2). Conversely, the superior temporal sulcus was longer in the right hemisphere in a total of 12 individuals (females, n = 6, and males, n = 6) (Figures 4-7 and 4-8). This represented a surprisingly large inter-hemispheric size dominance distribution ratio of 1:3 for left vs right. In the total sample largest side distribution graph (Figure 4-8), the right hemisphere dominated by three individuals past the mid-sample point. The male sub-sample showed an offset distribution favoring the right hemisphere by one individual with an inter-hemispheric ratio of 1:2.25 (left:right). The female sub-sample showed a more striking right hemisphere predominance with an offset distribution favoring the right hemisphere by three individuals, with an inter-hemispheric ratio of 1:4.5.

The difference in millimeters of absolute values for superior temporal sulcus

length were calculated in order to visualize the extent and direction of hemispheric preponderance both within the total sample and between the sexes. In Figure 4-7 absolute values are presented as scatter-plots for the total sample, female sub-sample, and male sub-sample in order to compare the distribution and sex differences in hemispheric asymmetry of superior temporal sulcus as compared to hemispheric symmetry (represented by the diagonal line in all 3 plots). A second comparison of absolute values involved calculation of a value for the difference in size between the two hemispheres. These were plotted as a bar graph for the total sample, females only and males only in Figure 4-8

4.4.4.4. Statistical analysis:.

Using absolute size values Type 1 (paired sample) t-Tests were used to assess left versus right hemisphere differences in superior temporal sulcus length. In the total sample of 18 individuals, there were no significant differences between the length of the superior temporal sulcus on the left and right hemispheres ($P = 0.42$, Table 4-4). In the female sub-sample (n = 9) there was also no significant difference between the left and right hemispheres although the P value was lower than that for the total sample at $P = 0.35$ (Table 4-4). This probably reflects the right hemisphere predominance seen in the female sub-sample distribution pattern (Figures 4-7 & 4-8). In the male sub-sample (n = 9), there was also no significant difference between the

Table 4-4 **a)** Three-dimensional linear measures of the length of the superior temporal sulcus (STS-3d) on the left and right hemispheres. **b)** Type 1 (paired sample) t-Tests of hemispheric differences in *STS-3d* in total sample and male and female sub-samples.

3-D Measures of Superior Temporal Sulcus Length

n=	SUP. TEMP. SULC.		SIDE	LARGER	SORTED	PGM#	SEX
	LEFT	RIGHT	DIFFS	SIDE	DIFFS		
1	41.49	41.80	0.31	R>L	3.94	38	F
2	45.39	43.85	-1.54	L>R	2.75	39	M
3	46.27	45.12	-1.15	L>R	2.66	40	M
4	50.39	53.15	2.75	R>L	2.06	41	M
5	46.82	49.48	2.66	R>L	1.96	42	M
6	48.02	50.08	2.06	R>L	1.81	43	M
7	48.86	47.21	-1.65	L>R	1.59	44	M
8	42.19	44.00	1.81	R>L	1.58	45	M
9	45.68	47.27	1.59	R>L	1.29	46	F
10	48.21	49.79	1.58	R>L	1.17	47	M
11	43.84	47.77	3.94	R>L	0.72	48	F
12	43.68	44.41	0.72	R>L	0.31	51	F
13	54.51	49.84	-4.67	L>R	-1.15	52	M
14	48.44	49.61	1.17	R>L	-1.54	53	F
15	49.76	47.44	-2.32	L>R	-1.65	54	F
16	45.45	42.85	-2.59	L>R	-2.32	55	F
17	45.66	47.61	1.96	R>L	-2.59	56	F
18	42.77	44.05	1.29	R>L	-4.67	57	F
MEAN	*46.52*	*46.96*					
STDEV	*3.26*	*3.06*					
MAX	*54.51*	*53.15*					
MIN	*41.49*	*41.80*					
MEDIAN	*45.97*	*47.35*					

a

t-Test: Paired Two Sample for Means

	TOTAL SAMPLE		MALES ONLY		FEMALES ONLY	
	STS(L)	STS(R)	STS(L)	STS(R)	STS(L)	STS(R)
Mean	46.52	46.96	47.85	48.06	45.19	45.87
Variance	10.65	9.38	11.70	10.22	6.95	7.02
Observations	18	18	9	9	9	9
Pearson Correlation	0.75		0.70		0.70	
Hypoth Mean Diff	0.00		0.00		0.00	
df	17.00		8.00		8.00	
t Stat	0.82		-0.24		-0.99	
P(T<=t) one-tail	0.21		0.41		0.18	
t Critical one-tail	1.74		1.86		1.86	
P(T<=t) two-tail	**0.42**	**N/S**	**0.82**	**N/S**	**0.35**	**N/S**
t Critical two-tail	2.11		2.31		2.31	

b

Figure 4-7 Scatter plots of 3-D linear measures of the length of the superior temporal sulcus (*STS-3d*) on the left and right hemispheres. Hemispheric distribution of measures in: **a)** total sample (n=18), **b)** female sub-sample (n=9), and **c)** male sub-sample (n=9). In each case, the diagonal line represents a reference for hemispheric symmetry.

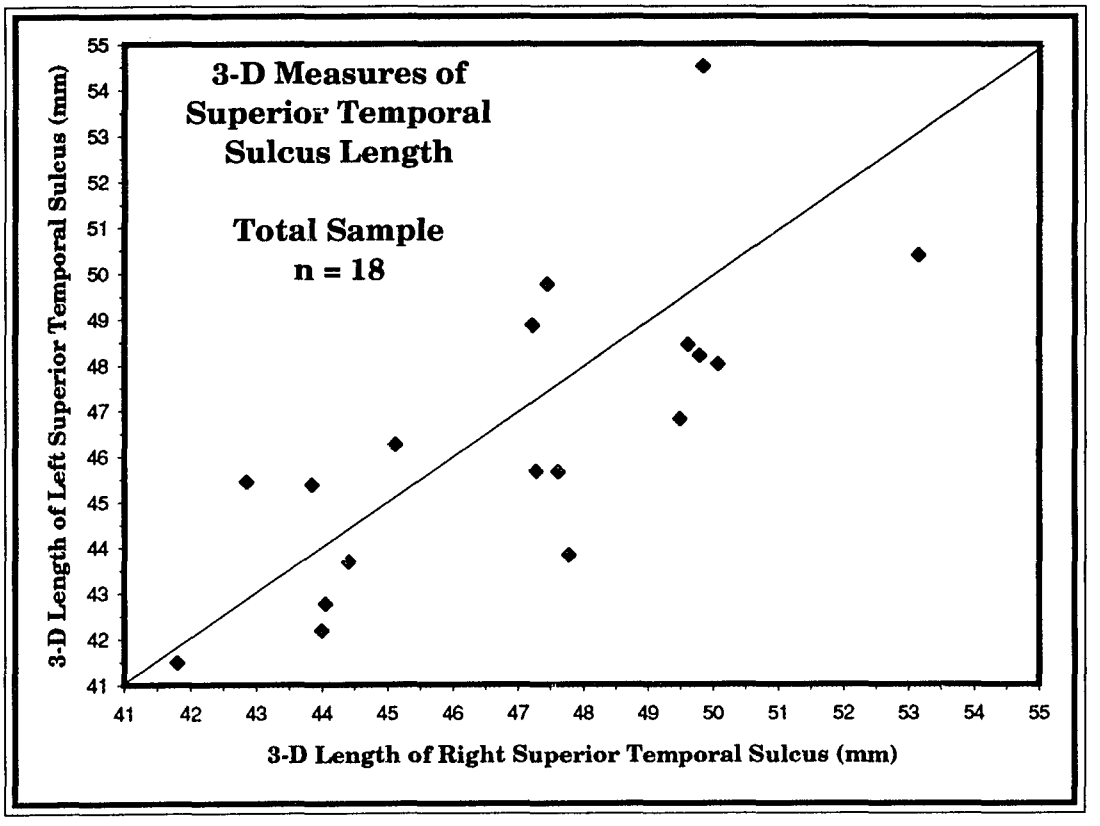
3-D Measures of Superior Temporal Sulcus Length
Total Sample
n = 18
3-D Length of Left Superior Temporal Sulcus (mm)
3-D Length of Right Superior Temporal Sulcus (mm)
41 42 43 44 45 46 47 48 49 50 51 52 53 54 55

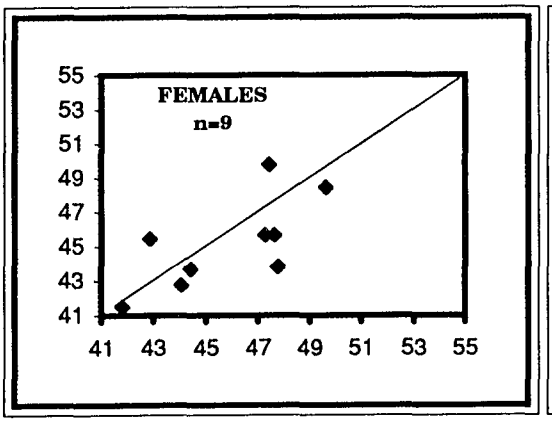
FEMALES
n=9
41 43 45 47 49 51 53 55

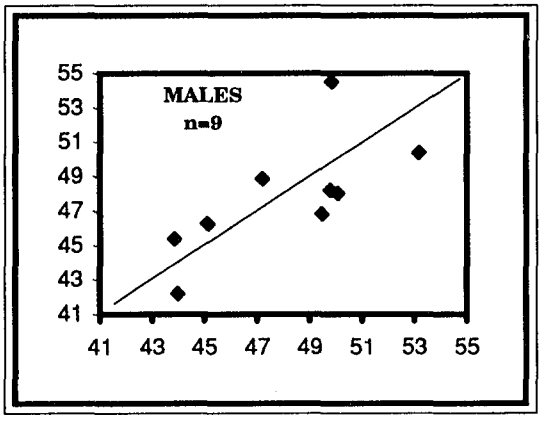
MALES
n=9
41 43 45 47 49 51 53 55

Figure 4-8 Plot of hemispheric differences in the length of the superior temporal sulcus (*STS-3d*). Values (millimeters) represent the difference in length between corresponding sulci on the left and right individuals, plotted for the largest side: **a)** total sample (n=18), **b)** female sub-sample (n=9), and **c)** male sub-sample (n=9).

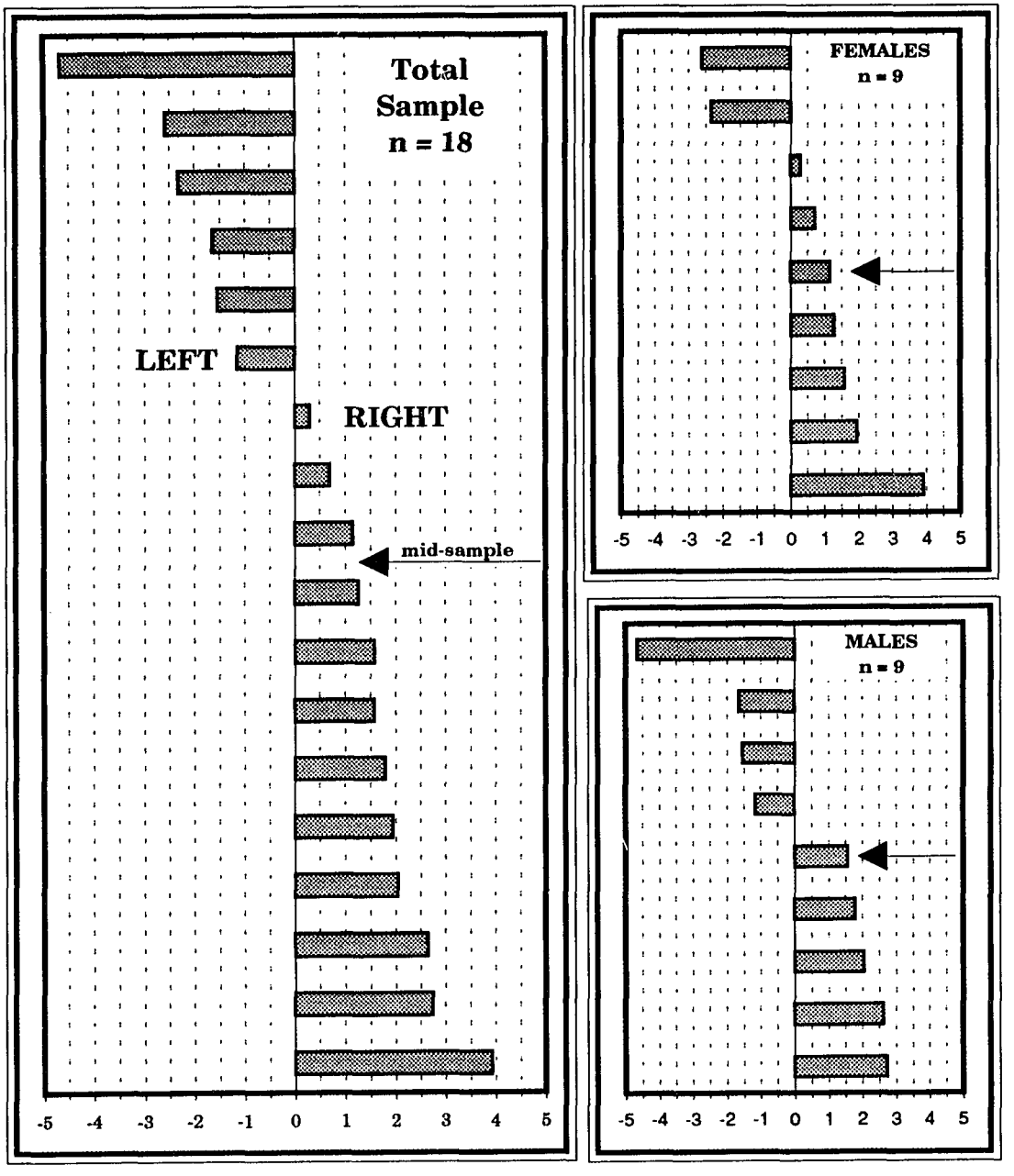
Total
Sample
n = 18
LEFT
RIGHT
mid-sample
-5 -4 -3 -2 -1 0 1 2 3 4 5
FEMALES
n = 9
-5 -4 -3 -2 -1 0 1 2 3 4 5
MALES
n = 9
-5 -4 -3 -2 -1 0 1 2 3 4 5

3-D length of the superior temporal sulcus in the left and right hemispheres at $P = 0.82$ (Table 4-4).

CHAPTER 5

2-DIMENSIONAL MORPHOMETRY OF BRAIN SURFACE STRUCTURES

5.1 CHAPTER OVERVIEW

This chapter presents the results of 2-D linear and area measures made directly from archival photographs of brains on a digitizing pad system. The three distinct sections present data from morphometric analysis of: ***1)*** frontal lobe structures in the region homologous to Broca's area in humans (Section 5.3, Figure 5-1); ***2)*** temporal lobe structures in the region homologous to Wernicke's area in humans (Section 5.4, Figures 5-12 & 5-13); and ***3)*** Frontal and occipital petelias and inter-hemispheric widths for comparison to human patterns (Section 5-5, Figure 5-24).

Methods used and a definition of the measures utilized are presented in Sections 5.3.1. and 5.3.2. for the frontal lobe, Sections 5.4.1. & 5.4.2. for the temporal lobe, and Sections 5.5.1. & 5.5.2. for petelias and inter-hemispheric widths.

Results from frontal lobe measures (Section 5.3.3.):

In most cases, measures of sulcal length and areas on the surface of the

brain in the inferior frontal cortical regions in the left and right hemispheres showed size predominance in the right hemisphere. This distinct trend was evident, for example, in ***1)*** measures of arcuate sulcus height (AS-v); ***2)*** both the antero-posterior linear distances (A-C i to v, and brain surface areas (A-Ci^2 and A-Cii^2), between the arcuate and central sulci, and ***3)*** the distance from the arcuate sulcus to the sub-central dimple (A-SCD).

In some cases marked sex differences were apparent which were not evident in the combined sex sample. For example, the measure A-SCD was significantly larger in the right hemisphere in females ($P = 0.01$) whereas in males ($P = 0.6$) and the combined sample ($P = 0.24$) no significant difference was indicated. Likewise, the 2-D linear measure AS-v was significantly larger in the right hemisphere of males ($P = 0.04$) but not in females ($P = 0.81$).

Results from temporal lobe measures (Section 5.4.3.)

In contrast to previous studies of inter-hemispheric lengths of the sylvian fissure (SF-ap) and superior temporal sulcus (STS-ap), results from the 2-D linear measures used in this study showed there to be no significant differences between the left and right hemispheres. There was however, an indication of a trend in both cases to be longer more often in the right hemisphere.

Measures of area and width of the posterior region of the superior

temporal gyrus (STG i-v, STG-Tpt[2] and STG-tot[2]) were either significantly larger in the right hemisphere, or showed a distinct trend in that direction. Interestingly, total area measures of the STG showed hemispheric symmetry, whereas similar measures of the posterior region of the STG showed right hemisphere predominance. Sex differences were not as apparent for temporal lobe structures as they were for measures of frontal lobe structures although sex-specific trends towards right hemisphere predominance were indicated in some of the measures.

Results from petelia and hemispheric width measures (5.5.3. and 5.5.4.):

Results of frontal pole petelial extension showed hemispheric asymmetry both in representation and degree. In females, left hemisphere predominance was indicated, whereas in males the right hemisphere predominated. In contrast, for occipital lobe petelial extension, a left hemisphere predominance was indicated for all groups.

Co-occurence of right frontal with left occipital petelias, the common human condition, was present in 27% of the sample. The opposite configuration, cooccurence of left frontal and right occipital petelias was present in 23% of individuals.

There were no significant hemispheric differences between the multiple measures of frontal and parietal lobe width in the left and right hemispheres. However, there was an indication of a slight trend in all measures in males

for left hemispheric predominance.

Conclusions:

The majority of the results presented here from linear and area measures of both inferior frontal lobe and posterior temporal lobe structures clearly and consistently demonstrate a predominance in the right cerebral hemisphere. These results contrast with the basic hypothesis of this dissertation that left hemisphere frontal lobe structures on the brain's surface would predominate in the left hemisphere. Other notable findings include demonstration of major sex differences in both the degree and pattern of hemispheric distribution for some measures. This serves to illustrate the critical need, in studies such as this, to critically assess sex-related differences in patterns of brain asymmetry.

5.2. 2-D MEASUREMENT METHOD

As described in Chapter 3, Section 3.2.10., a complete archival photographic record of the external morphology of the each brain was made (Figures 3-1, to 3-5). For measurement purposes, a millimeter scale bar was included in each photograph. A Zeiss Videoplan II connected to a 12" x 12" digitizing pad and an electronic digitizing stylus was used for this measuring procedure. Using the MOP-Videoplan software package, both 2-D linear dimensions and 2-D areas of brain surface cerebro-cortical structures were measured by tracing the linear dimensions or outlines of structures directly from the archival photographs. In each case, the digitizing software was scaled to the magnification of the photograph using the scale bar included on every photograph. This was repeated for each photograph by calibrating a linear distance of 20mm on the photograph millimeter scale to the software scaling factor. The resultant output in millimeters represented absolute values and required no further transformation. The digitizing pad had a resolution of <0.01mm, allowing for good measurement accuracy. A series of linear and surface area measurements were made, from each brain, of specific homotypic structures on both the left and the right cerebrocortical hemispheres. In cases where reference lines had to be constructed on the cortex, the photograph was first fixed to the surface of the digitizing pad

using masking tape. Then, a sheet of plain copier transparency film (Universal office products Cat # 65020) was placed over the photograph and taped into position. Extremely fine lines were scratched onto the transparency film using a sharp tipped steel scribe while viewing the area under a dissecting microscope at 20x magnification. This technique allowed for extremely high accuracy of line placement relative to brain structures, and high accuracy and resolution of measured linear dimensions. A preliminary study using a series of different measures demonstrated that the accuracy of repeatability for this digitizing system was <0.1mm.

5.3. FRONTAL LOBE STRUCTURES

5.3.1. 2-D Linear measures of frontal lobe structures

5.3.1.1. (Linear Distance "A-C_v", Figure 5-1a)

Linear distance from the inferior point of termination of the vertical limb of the arcuate sulcus to the inferior point of termination of the central sulcus on the left and right hemispheres.

5.3.1.2 (Linear Distance "A-C_i", Figure 5-1a)

Linear distance from the most superior point of the vertical limb of the arcuate sulcus to the corresponding part of the central sulcus on the left and right hemispheres. This line is drawn parallel the line

produced by measure A-Cv described above.

5.3.1.3. (Linear Distances "A-Cii", "A-Ciii", and "A-Civ", Figure 5-1a)

A series of 3 linear distances between the vertical limb of the arcuate sulcus and the central sulcus on the left and right hemispheres.. These lines are made by measuring the distance between the two measures A-Ci and A-Cv which correspond to the most inferior and most superior aspects of the vertical limb of the arcuate sulcus) then calculating the position of 3 equidistant points between them. Lines parallel to those already drawn for A-Ci and A-Cv are then plotted.

5.3.1.4. (Linear Distance "A-SCD", Figure 5-1a)

The linear distance between the most inferior part of the vertical limb of the arcuate sulcus and the vertical midpoint of the subcentral dimple.

5.3.1.5. (Linear Distance "C-SCD", Figure 5-1a)

The linear distance between the most inferior part of the central sulcus and the vertical midpoint of the subcentral dimple.

5.3.1.6. (Line Length "AS-v", Figure 5-1a)

The length (not linear distance) of the vertical section of the arcuate sulcus measured along its contours.

Note: For the linear measures A-Ci, and Asv, described above, precise determination of the dorsal termination of the "vertical limb" of the arcuate sulcus was required. This point, when present, is characterized by the presence of a posterior extension, of the "horizontal limb". This study determined that the posterior extension is not present in 48% of cerebral hemispheres (Chapter 3, Section 3.3.1.). In these specimens the superior point of termination was estimated by the following method. First, a line was drawn on the plastic overlay corresponding to the longitudinal axis of the horizontal portion of the arcuate sulcus. A line was also drawn corresponding to the vertical portion of the arcuate sulcus. The point of intersection of these two lines was used as the superior termination of the vertical section of the arcuate sulcus.

5.3.2. 2-D Area measures of frontal lobe structures

5.3.2.1. (Area "A-Ci²", Figure 5-1b)

The area of surface cerebral cortex within the margins confined by the central sulcus posteriorly, the vertical limb of the arcuate sulcus anteriorly, and the two lines A-Ci superiorly and A-Cv (see 5.3.1.1. & 5.3.1.2., above) inferiorly.

5.3.1.2. (Area "A-Cii²", Figure 5-1b)

The area of surface cerebral cortex within the margins confined by the

central sulcus posteriorly, the vertical limb of the arcuate sulcus anteriorly, and the lines A-C_{ii} (see 5.3.1.3.) superiorly and A-C_v (see 5.3.1.1.) inferiorly. This second area measure provided a comparison with that of the total post arcuate/precentral cortical region (Area "A-Ci^2", Figure 5-1b), described above, but limits the comparison to the more inferior region which includes the homologue of Broca's area and does not include the more unpredictable superior region where the course of the arcuate and central sulci can be highly variable (described in Chapter 3, Section 3.3.1.).

Note: For measures A-C_{i-v}, A-SCD, C-SCD, A-Ci^2 and A-Cii^2 the high magnification macrophotographs of the left and right post arcuate / precentral motor cortex were used. (see photographs in Figures 3-3a & b and diagrams in Figures 5-1a & 5-1b)

Figure 5-1 2-D linear and area measures: **a)** Linear measures (mm): A-Ci, A-Cii, A-Ciii, A-Civ, A-Cv, & AS-v (Sections 5.3.1.1. to 5.3.1.6.); **b)** Area measures (mm^2): $A\text{-}Ci^2$ & $A\text{-}Cii^2$ (5.3.2.1. and 5.3.2.2.)

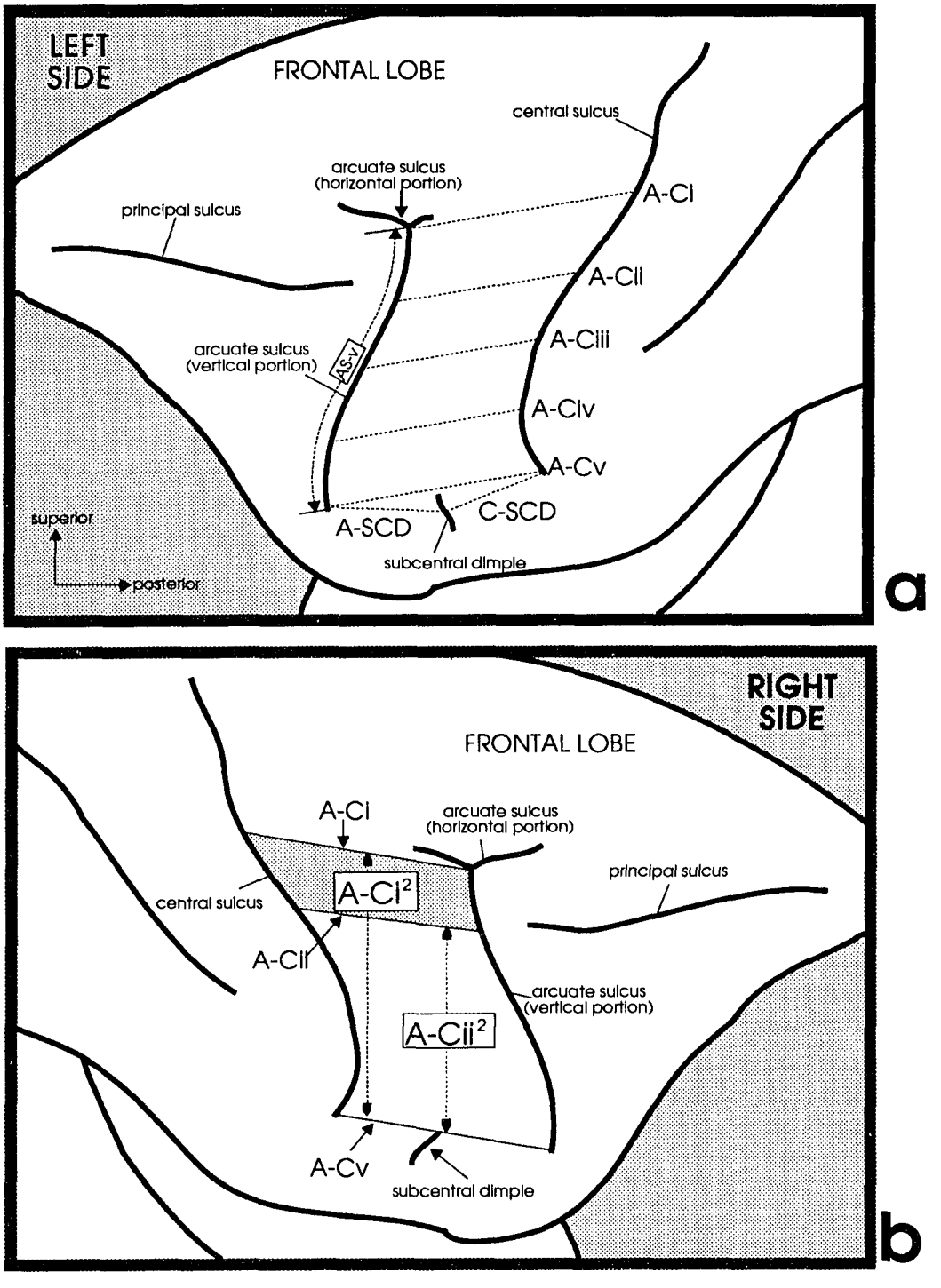
LEFT SIDE
FRONTAL LOBE
central sulcus
arcuate sulcus (horizontal portion)
principal sulcus
A-CI
A-CII
A-CIii
arcuate sulcus (vertical portion)
AS-v
A-CIv
A-Cv
C-SCD
A-SCD
subcentral dimple
superior
posterior
a
RIGHT SIDE
FRONTAL LOBE
A-CI
arcuate sulcus (horizontal portion)
principal sulcus
central sulcus
A-CI²
A-CII
arcuate sulcus (vertical portion)
A-CII²
A-Cv
subcentral dimple
b

5.3.3. Results of 2-D measures of frontal lobe structures

5.3.3.1. 2-D Linear measures of the vertical portion of the arcuate sulcus ("AS-v") on the left and right hemispheres

These measures were made from close up photographs (Figures 3-3a & 3-3b) of the left and right frontal lobes in the region posterior to the arcuate sulcus and anterior to the central sulcus. The parameters used to define the measure are presented in Section 5.3.1. This measurement series represented brain surface linear dimensions of the left hemisphere cerebrocortical region (referred to as area FCBm in *Macaca*; see Von Bonin & Bailey, 1947) which is homologous to Broca's area in *Homo* (cytoarchitectonic area 44; see Brodmann, 1909).

Inter-hemispheric dimensions of 2-D linear measure AS-v:

The total sample (n = 33) used for this measure included females (n = 19) and males (n = 14). The mean length of the vertical portion of the arcuate sulcus (AS-v) in the left hemisphere of the total sample was 15.5 ±1.6mm (max = 19.0, min = 11.4). The corresponding length in the right hemisphere was 15.9 ±1.9mm (Table 5-1).

In females (n = 19), the mean length of AS-v in the left hemisphere was 15.2 ±1.31, and in the right 15.27 ±1.55mm.

In males (n = 14), the mean length of AS-v on the left hemisphere was 15.9 ±1.8mm and on the right, larger at 16.2 ±1.9mm (Table 5-1).

Table 5-1 **a)** Table of lengths of the vertical portion of the arcuate sulcus (ASv) on the left and right hemispheres in total sample (n = 33). **b)** Bar graph of means and standard deviation for total sample, and sex-specific sub-samples. **c)** Paired sample t-Tests comparing AS-v on the left and right hemispheres in total sample and sub-samples (see Section 5.3.3.1.)

Length of Vertical Limb of Arcuate Sulcus

n=	AS-v		PG	SEX
	LEFT	RIGHT	M#	
1	15.2	14.6	14	F
2	15.5	13.5	15	F
3	14.5	13.1	16	F
4	14.6	16.2	17	F
5	14.6	14.8	18	F
6	13.1	14.7	19	F
7	17.3	17.7	23	M
8	11.4	12.0	24	M
9	17.6	16.5	25	M
10	14.6	17.1	26	F
11	15.2	15.6	27	F
12	13.2	13.9	29	F
13	15.1	13.6	30	F
14	17.2	16.0	31	M
15	16.2	17.8	32	M
16	17.6	16.4	37	M
17	15.0	14.1	38	F
18	14.9	17.3	39	M
19	17.7	18.1	40	M
20	17.5	19.1	41	M
21	16.0	16.4	42	M
22	14.9	17.2	43	M
23	15.1	17.2	44	M
24	14.0	14.4	45	M
25	19.0	19.2	46	F
26	17.0	15.0	48	F
27	16.4	17.6	49	F
28	15.9	19.9	52	M
29	15.9	16.5	53	F
30	15.3	15.0	54	F
31	14.1	15.3	55	F
32	15.4	16.2	56	F
33	15.1	14.2	57	F
Mean	*15.5*	*15.9*	total	
Stdev	*1.6*	*1.9*	sample	
Max	*19.0*	*19.9*		
Min	*11.4*	*12.0*		
Mean	*15.2*	*15.3*	females	
Stdev	*1.3*	*1.6*		
Mean	*15.9*	*16.9*	males	
Stdev	*1.8*	*1.9*		

a

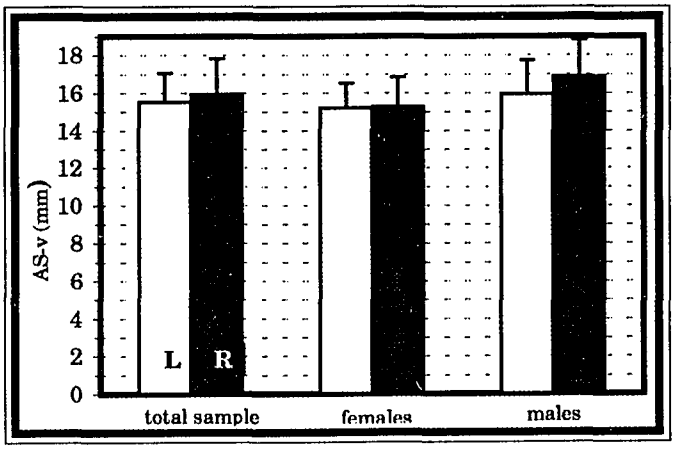

b

AS-v

	Total		Females		Males	
	left	right	left	right	left	right
Mean	15.5	15.9	15.2	15.3	15.9	16.9
Variance	2.4	3.5	1.7	2.4	3.2	3.8
Observations	33	33	19	19	14	14
Pearson Correl'n	0.67		0.61		0.67	
Hypoth Mean Diff	0		0		0	
df	32		18		13	
t Stat	-1.73		-0.24		-2.26	
P(T<=t) one-tail	0.05	***	0.40	N/S	0.02	***
t Critical one-tail	1.69		1.73		1.77	
P(T<=t) two-tail	0.09	A/S	0.81	N/S	0.04	***
t Critical two-tail	2.04		2.10		2.16	

c

The pattern of hemispheric distribution for the largest side of measure AS-v, showed considerable variation between the total sample and the sex-specific sub-samples. For example, within the total sample (n = 33), 11 individuals, representing ~33% of the total sample, showed a larger AS-v in the left hemisphere. This included eight females (42% of sub-sample), and three males (21% of sub-sample).

On the right hemisphere, 22 of 33 individuals, representing ~67% of the total sample, showed a larger AS-v on the right hemisphere. This included 11 females (58% of sub-sample) and 11 males (79% of sub-sample), (see Figure 5-2).

In the total sample, and particularly in the male sub-sample, the distribution of asymmetry in the measure of length of the vertical portion of the arcuate sulcus showed a distinct tendency to be longer more frequently in the right hemisphere. This can be clearly seen in Figure 5-2 where the right hemisphere larger values extend well beyond the mid-sample point indicated by the arrow.

Statistical analysis of 2-D linear measure AS-v:

Using the paired sample t-Test, data were subjected to statistical analysis for hemispheric differences as a total sample (n = 33), as a female sub-sample (n = 19) and as a male sub-sample (n = 14) as presented in Table 5-1.

Figure 5-2 Plot of hemispheric differences in the length of the arcuate sulcus (*AS-v*). Values in millimeters represent the difference in length between corresponding sulci on the left and right individuals, plotted for the largest side: **a)** total sample (n=33), **b)** female sub-sample (n=19), and **c)** male sub-sample (n=14). See text, Section 5.3.3.1. for details

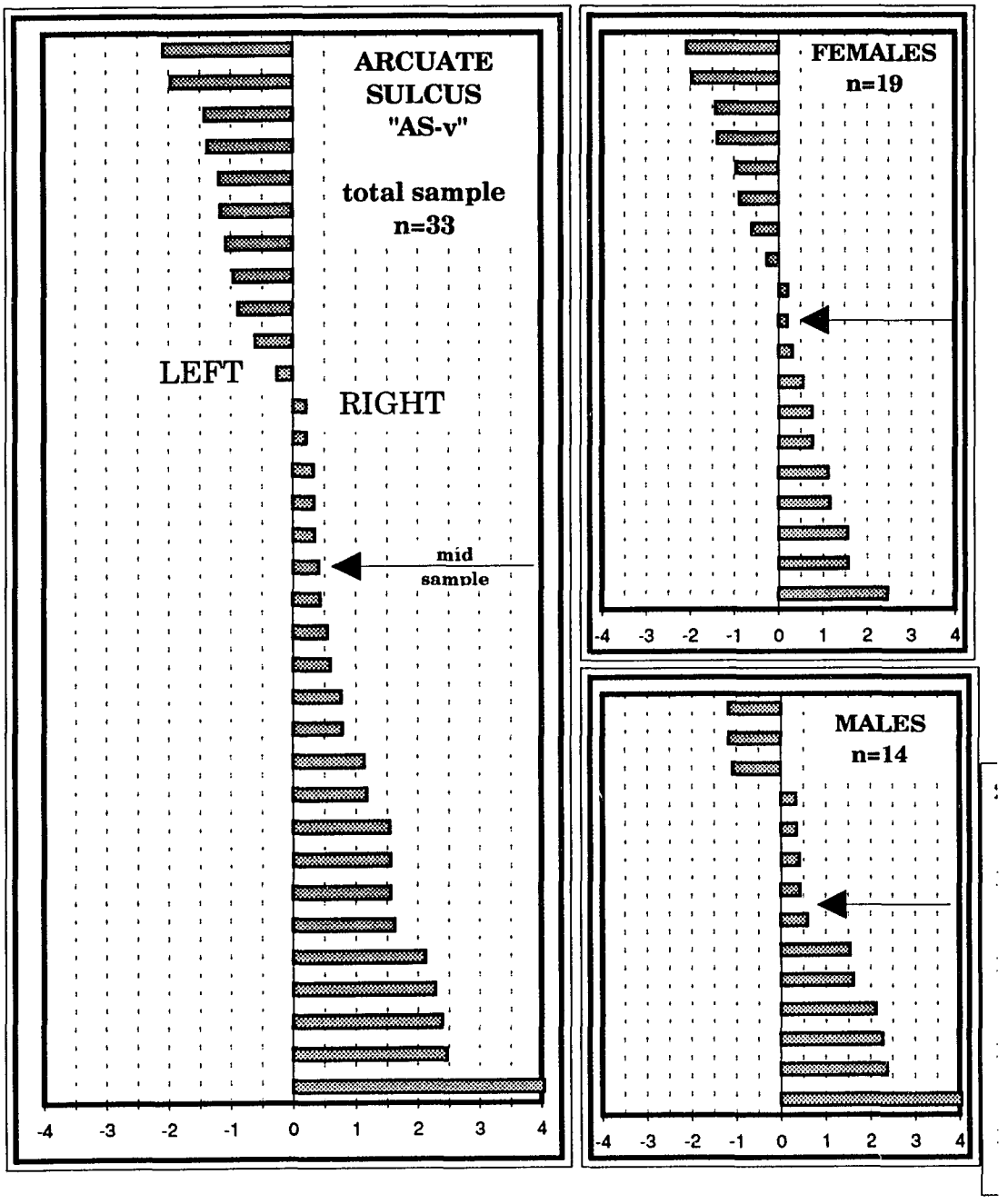
ARCUATE
SULCUS
"AS-v"
total sample
n=33
LEFT
RIGHT
mid
sample
-4 -3 -2 -1 0 1 2 3 4
FEMALES
n=19
-4 -3 -2 -1 0 1 2 3 4
MALES
n=14
-4 -3 -2 -1 0 1 2 3 4

Using the *P* value for a two-tailed t-Test, there was no significant difference between the length of the vertical portion of the arcuate sulcus (AS-v) in the left and right hemispheres in the total sample ($P = 0.09$). However, the one tailed value ($P = 0.05$) indicated that AS-v was significantly larger in the right hemisphere in the total sample; see Table 5-1c. The use of a one-tailed t-Test *P* value may be appropriate in this case where the distribution of hemispheric asymmetry predominates in the right hemisphere (Figure 5-2).

In the females (n = 19) there were no significant differences in the length of the vertical portion of the arcuate sulcus ($P = 0.81$). Conversely, in the male sub-sample (n = 14), AS-v in the right hemisphere was significantly larger than that on the left hemisphere at $P = 0.04$ (or one-tailed $P = 0.02$); see Table 5-1c.

A highly significant right hemisphere predominance of AS-v was seen only in the male sub-sample ($P < 0.05$). This was markedly distinct from that seen for females, where even though the sub-sample was 36% larger than that for males, not even a trend towards hemispheric asymmetry was indicated due to the extremely low probability value of $P = 0.81$. As such, the trend for right hemisphere predominance in the total sample, indicated by an almost significant *P* value, was entirely due to data contributed from the male sub-sample.

5.3.3.2. 2-D linear measures of the distance from the arcuate sulcus to the central sulcus: (A-Ci, A-Cii, A-Ciii, A-Civ and A-Cv)

This section comprised a series of five 2-D linear measures, A-Ci, A-Cii, A-Ciii, A-Civ, and A-Cv which represented the extent of the antero-posterior distance between the vertical part of the arcuate sulcus anteriorly and the central sulcus posteriorly on both the left and right cerebral hemispheres (Figure 5-1). The five measures were spaced equally between the entire vertical extent of cortex immediately posterior to the arcuate sulcus. This region of the cerebral cortex in monkeys contains the homologue of Broca's area in humans. The sample comprised a total of 33 individuals of *Macaca fascicularis*, including females (n = 19) and males (n = 14).

Inter-hemispheric dimensions of 2-D linear measure A-Ci:

The 2-D linear distance, A-Ci, was the most superior of the five measures, originating from the region where the post-arcuate "spur", or posterior extension of the horizontal portion of the arcuate sulcus, when present (see Chapter 3, Section 3.3.1.) coursed posteriorly. In cases where the spur was not present other means were used to estimate this position on the arcuate sulcus (see Section 3.3.1.).

In the total sample (n = 33) the 2-D linear distance A-Ci was 9.5 ±1.4mm (max = 12.8mm, min = 6.8mm, median = 9.2mm) on the left hemisphere and 10.1 ±1.7mm (max = 13.1, min = 6.6, median = 10.2) on the right.

Figure 5-3 Histograms of means and standard deviations for the series of five 2-D linear distance between the arcuate and central sulci on the left and right hemispheres A-Ci, A-Cii, A-Ciii, A-Civ & A-Cv. Values for total sample, female sub-sample and male sub-sample are plotted separately. (see Section 5.3.3.2.)

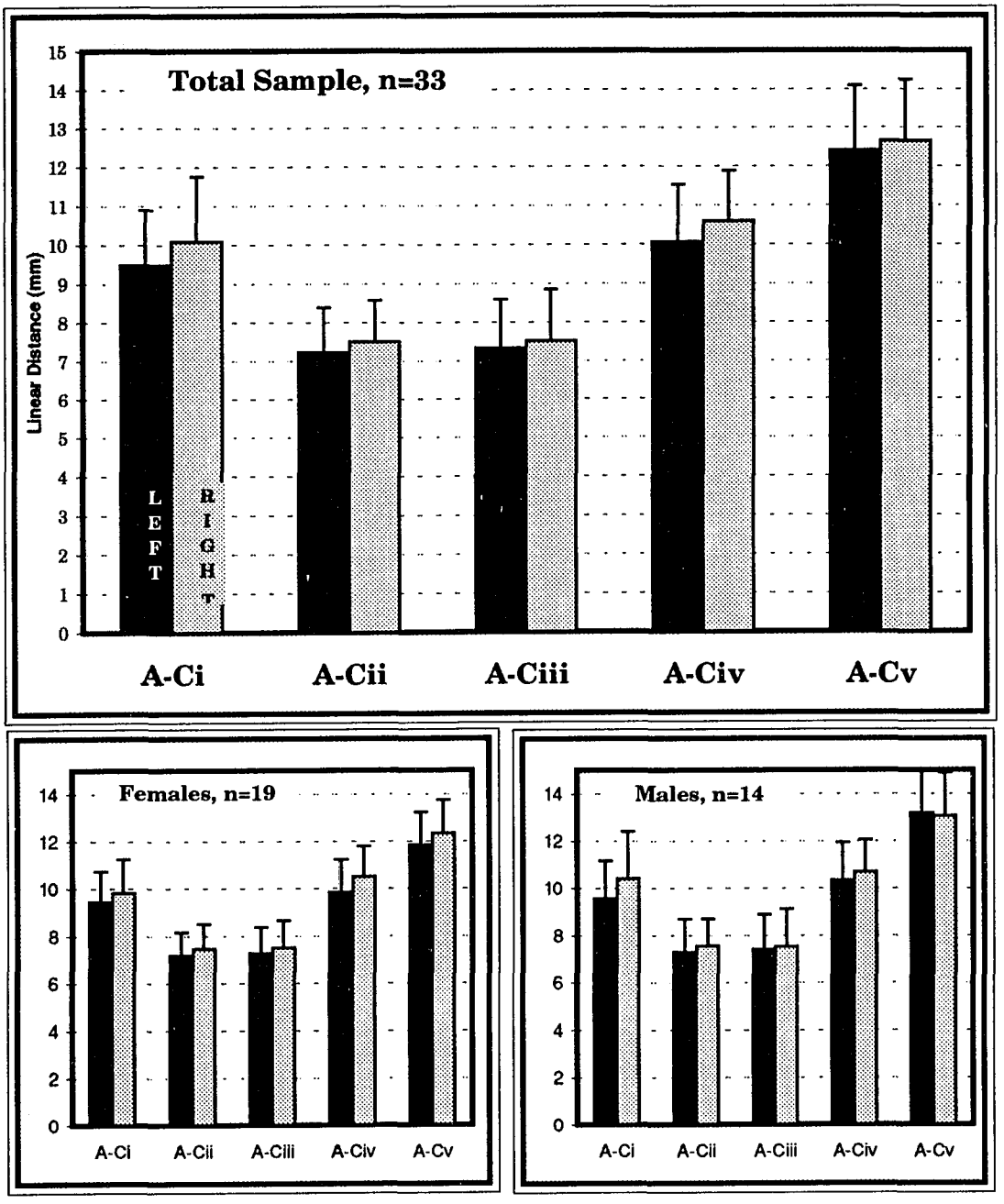
Total Sample, n=33
Linear Distance (mm)
LEFT
RIGHT
A-Ci
A-Cii
A-Ciii
A-Civ
A-Cv
Females, n=19
Males, n=14

In females (n =19) A-Ci was 9.4 ±1.3mm (max = 12.3mm, min = 7.3mm, median = 9.2mm) on the left hemisphere and 9.8 ±1.4mm (max = 11.8mm, min = 6.6mm, median = 10.2mm) on the right hemisphere (Figure 5-3 & Appendix 5-1).

In males (n =14) A-Ci was 9.6 ±1.6mm (max = 12.8mm, min = 6.8m, median = 9.4m) on the left hemisphere and 10.4 ±2.0 max = 13.1m, min = 7.6mm, median = 10.1m) on the right (Figure 5-3 & Appendix 5-1).

As was seen for the length of the vertical portion of the arcuate sulcus (AS-v) described above in Section 5.3.3.1., there appeared to be a slight right hemisphere predominance of measure A-Ci (Figure 5-4). Within the total sample (n = 33), 22 individuals (~67% of total sample) showed a larger value for A-Ci in the right hemisphere. In females (n = 19), 12 individuals (~63% of sub-sample) showed a larger A-Ci in the right hemisphere. Likewise, in males (n = 14) 10 individuals (~71% of sub-sample) showed a strikingly larger distribution of values for A-Ci in the right hemisphere (Figure 5-4)

Statistical analysis of 2-D linear measure A-Ci:

Using the type 1 t-Test on values for A-Ci on both left and right hemispheres in the total sample (n = 33), it was shown that A-Ci was significantly larger on the right hemisphere ($P = 0.01$), (Appendix 5-2). In females (n = 19), there was no significant difference between the two

hemispheres in this measure ($P = 0.12$). Conversely, in males (n = 14), the linear measure A-Ci was significantly larger on the right hemisphere ($P = 0.04$; see Appendix 5-1).

Although the female sub-sample did not show significant right hemisphere predominance of the measure A-Ci at the $P<0.05$ level, the probability value was low ($P = 0.12$), suggesting at least a trend. Further, the total sample showed a probability value much less than that for males alone ($P = 0.01$ vs $P = 0.04$) indicating a significant contribution from the female sub-sample to the total sample probability.

Inter-hemispheric dimensions of linear measure A-Cii:

This measure represented a second 2-D measure of the distance between the arcuate sulcus and the central sulcus that was inferior to the distance measured by A-Ci, above (see Figure 5-1).

In the total sample (n = 33) the 2-D linear distance on the left hemisphere of A-Cii was 7.2 ±1.2mm (max = 10.3mm, min = 5.6mm, median = 7.2mm), and 7.5 ±1.1mm (max = 10.2, min = 5.2, median = 7.7) on the right (Figure 5-3; Appendix 5-1).

In females (n = 19), A-Cii was 7.2 ±1.0mm (max = 8.8mm, min = 5.6mm, median = 7.2mm) on the left hemisphere and 7.5 ±1.0mm (max = 9.1mm, min = 5.2mm, median = 7.7mm) on the right (Figure 5-3; Appendix 5-1).

Figure 5-4 Plot of hemispheric differences in lengths from the arcuate sulcus to the central sulcus (*A-Ci*). Values represent differences in length (mm) between sulci on the left and right hemispheres, plotted for the largest side: **a)** total sample (n=33), **b)** female sub-sample (n=19), and **c)** male sub-sample (n=14). See text, Section 5.3.3.2.

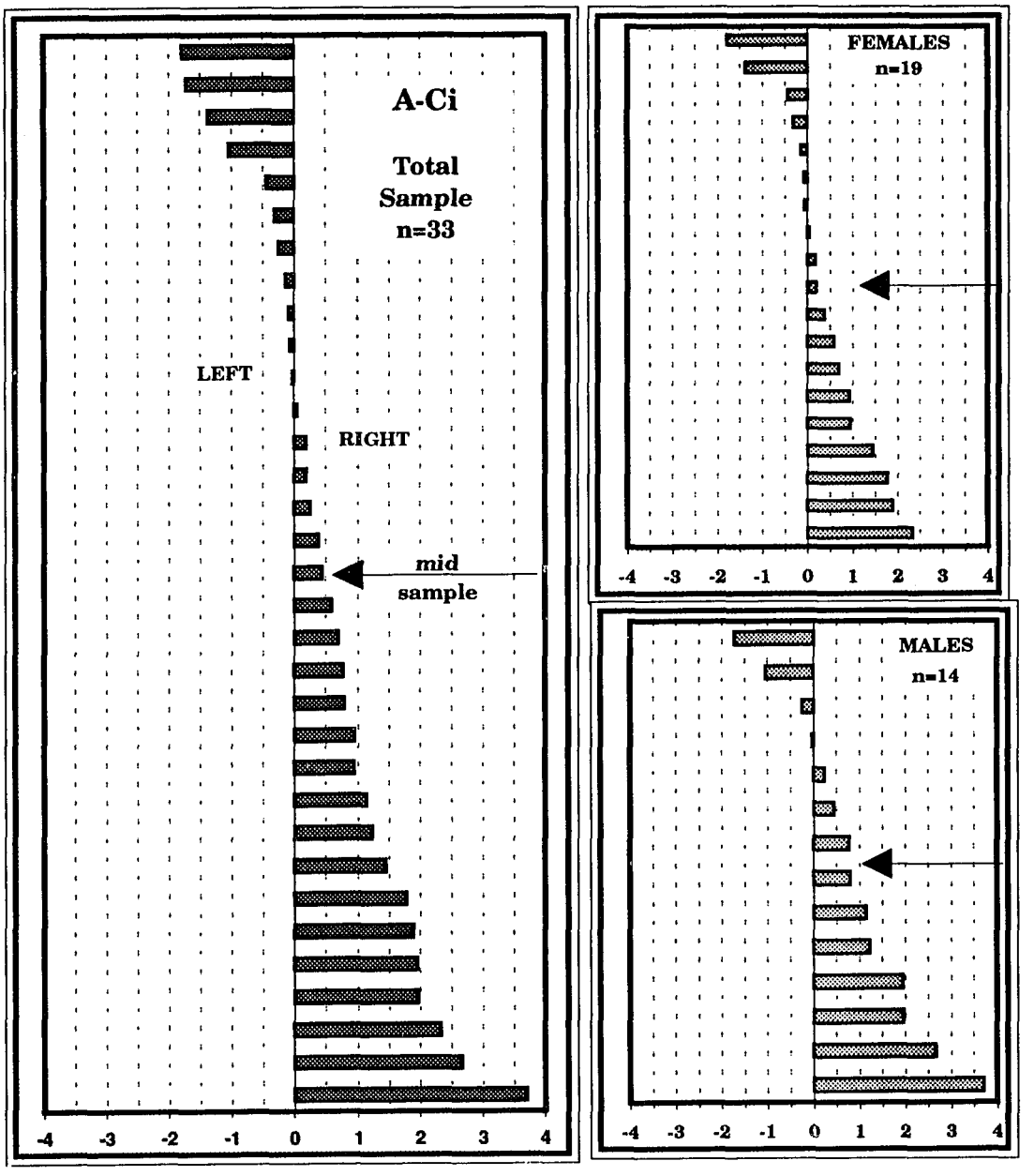
A-Ci
Total
Sample
n=33
LEFT
RIGHT
mid
sample
-4 -3 -2 -1 0 1 2 3 4
FEMALES
n=19
-4 -3 -2 -1 0 1 2 3 4
MALES
n=14
-4 -3 -2 -1 0 1 2 3 4

In the male sub-sample (n = 14) the 2-D linear distance A-Cii was 7.3 ±1.4mm (max = 10.3mm, min = 5.6mm, median = 6.9mm) on the left hemisphere and 7.5 ±1.2mm (max = 10.3mm, min = 5.8mm, median = 7.5mm) on the right (Figure 5-3; Appendix 5-1).

As for A-Ci, a slight right hemisphere predominance was seen for linear measure A-Cii (Figure 5-5). In the total sample (n = 33), 22 individuals (~67% of sample) showed a larger value for A-Cii on the right hemisphere. In females (n = 19), 12 individuals (~63% of sub-sample), and in males (n = 14) 10 individuals (~71% of sub-sample), showed a larger value for A-Cii on the right hemisphere (Figure 5-5) .

Statistical analysis of measure A-Cii:

Using the paired sample t-Test on data from the total sample (n = 33), it was shown that A-Cii was significantly larger on the right hemisphere than on the left ($P = 0.038$), (Appendix 5-2). In females (n = 19) A-Cii on the right hemisphere was significantly larger than the left ($P = 0.03$), (Appendix 5-2). In males (n = 14) however, there was no significant difference between A-Cii in the left and right hemispheres ($P = 0.33$); see Appendix 5-2.

These results are quite different from those of measure A-Ci in that the inter-hemispheric significance values are reversed, with males showing no significant size difference between hemispheres as opposed to females.

Figure 5-5 Plot of hemispheric differences in length from the arcuate sulcus to the central sulcus (*A-Cii*). Values represent differences in length (mm) between sulci on the left and right hemispheres, plotted for the largest side: **a)** total sample (n=33), **b)** female sub-sample (n=19), and **c)** male sub-sample (n=14). See text, Section 5.3.3.2.

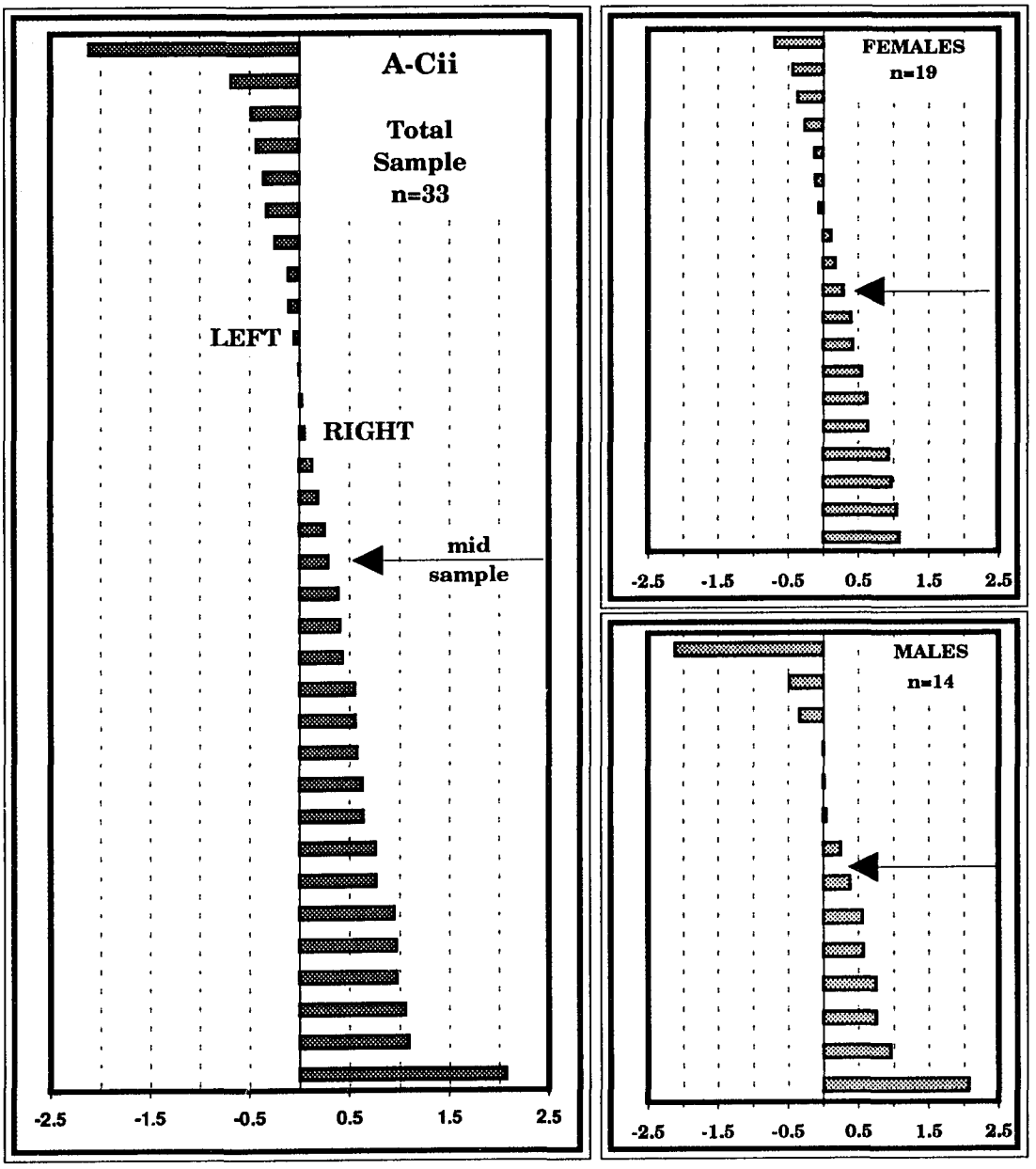
A-Cii
Total
Sample
n=33
LEFT
RIGHT
mid
sample
-2.5
-1.5
-0.5
0.5
1.5
2.5
FEMALES
n=19
-2.5
-1.5
-0.5
0.5
1.5
2.5
MALES
n=14
-2.5
-1.5
-0.5
0.5
1.5
2.5

Inter-hemispheric dimensions of linear measure A-Ciii:

The measure A-Ciii represents the 2-D linear distance between the arcuate sulcus and the central sulcus at the supero-inferior level situated at the median of the arcuate sulcus and the midline of measures A-Ci & A-Cv.

In the total sample (n = 33) the 2-D linear measure A-Ciii was 7.3 ±1.3mm (max = 10.2mm, min = 5.5mm, median = 7.2mm), on the left hemisphere and 7.51 ±1.33mm (max = 11.9, min = 5.34, median = 7.4) on the right (Figure 5-3 & Appendix 5-1).

In females (n =19) A-Ciii was 7.3 ±1.1mm (max = 8.9mm, min = 5.6mm, median = 7.2mm) on the left hemisphere and 7.5 ±1.1mm (max = 10.0mm, min = 5.3mm, median = 7.8mm) on the right. In males (n = 14) A-Ciii was 7.4 ±1.5mm (max = 10.2mm, min = 5.5mm, median = 7.2mm) on the left hemisphere and 7.5 ±1.6mm (max = 11.3mm, min = 5.6mm, median = 7.1mm) on the right hemisphere.

A similar, though less pronounced trend, (compared to A-Ci and A-Cii), was evident in the 2-D linear measure A-Ciii, to be larger more often in the right hemisphere (Figure 5-6). In the total sample (n = 33), 20 individuals (~61% of sample) were larger in the right hemisphere (Figure 5-6). In females (n = 19), the trend was less pronounced, in which 11 individuals (~58% of sub-sample) were right hemisphere dominant (Figure 5-6). In males (n = 14). 9 individuals (64% of sub-sample) were larger in the right

hemisphere for the measure A-Ciii (Figure 5-6)

Statistical analysis of measure A-Ciii:

Using the type 1 t-Test on 2-D linear measures of A-Ciii it was shown that there were no significant size differences between the length of A-Ciii on the left and right hemispheres, in either the total sample ($P = 0.31$), the female sub-sample ($P = 0.2$), and the male sub-sample ($P = 0.74$); see Appendix 5-2.

For the measure A-Ciii, neither the total sample or the sex-specific sub-samples showed statistically significant inter-hemispheric size or distribution differences at the $P < 0.05$ level. However, the female sub-sample showed a slight trend to be larger in the right hemisphere at $P < 0.2$.

Inter-hemispheric dimensions of linear measure A-Civ:

This is the fourth in a series of five independent measures of the 2-D distance between the arcuate sulcus and the central sulcus in the left and right hemispheres. Unlike the three measures described above (A-Ci, A-Cii and A-Ciii), this measure, A-Civ and the subsequent measure A-Cv, described below, are situated in the area of macaque cortex that is homologous to Broca's speech area in humans (see Figure 5-1 and section 5.3.1.3. for a description and placement of this measure).

Figure 5-6 Plot of hemispheric differences in length from the arcuate sulcus to the central sulcus (*A-Ciii*). Values represent differences in length (mm) between sulci on the left and right hemispheres, plotted for the largest side: **a)** total sample (n=33), **b)** female sub-sample (n=19), and **c)** male sub-sample (n=14). See text, Section 5.3.3.2.

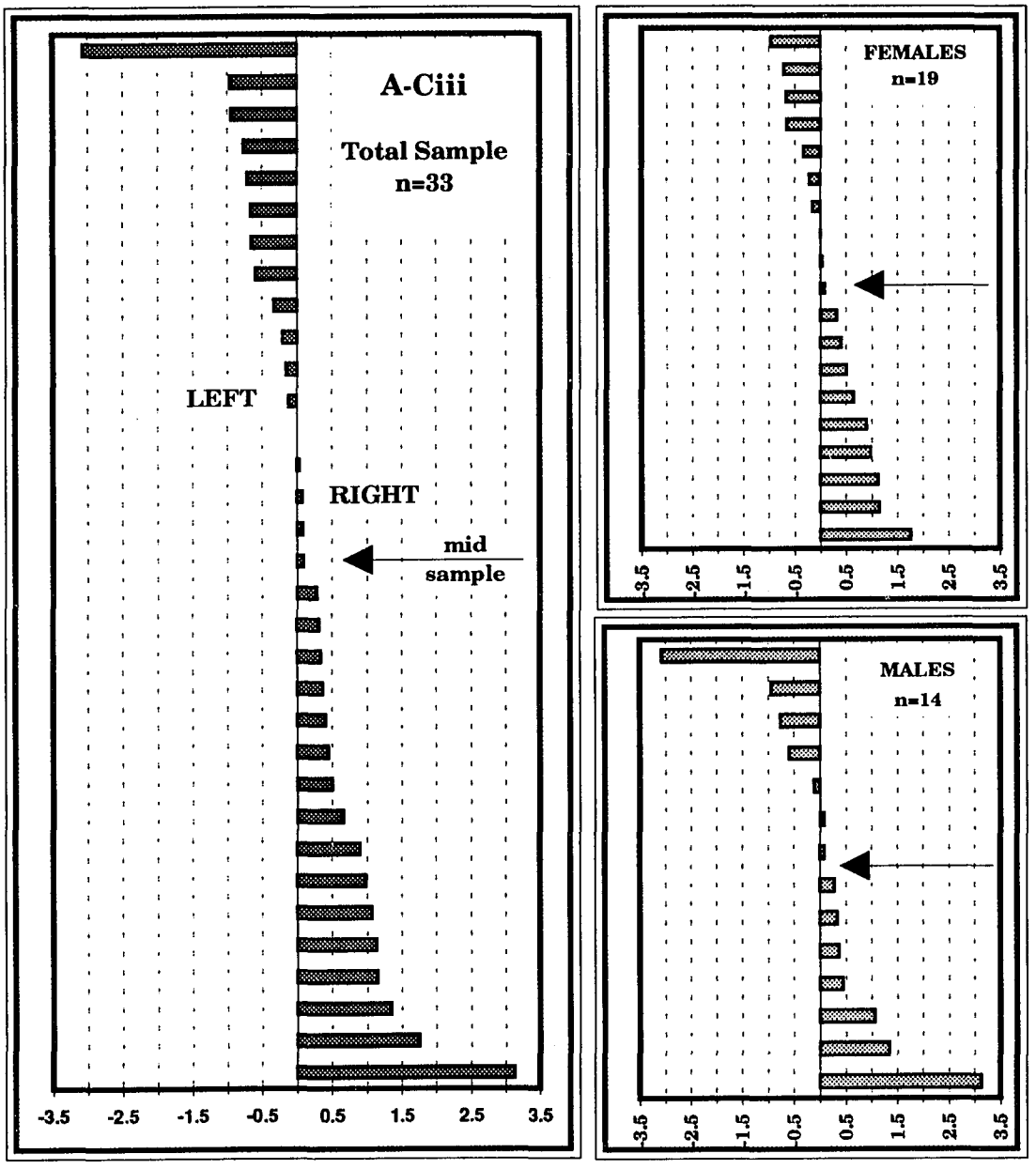
A-Ciii
Total Sample
n=33
LEFT
RIGHT
mid
sample
-3.5
-2.5
-1.5
-0.5
0.5
1.5
2.5
3.5
FEMALES
n=19
MALES
n=14

In the total sample (n = 33) the 2-D linear distance A-Civ was 10.1 ±1.5mm (max = 13mm, min = 7.2mm, median = 9.8mm), on the left hemisphere, and somewhat larger, 10.6 ±1.3mm (max = 14.0, min = 8.2, median = 10.6mm) on the right hemisphere (Appendix 5-1).

In females (n = 19), A-Civ was 9.9 ±1.4mm (max = 11.8mm, min = 7.2mm, median = 9.8mm) on the left and again, larger at 10.5 ±1.3mm (max = 13.4mm, min = 8.2mm, median = 10.6mm) on the right hemisphere.

In males (n = 14) A-Civ was 10.3 ±1.6mm (max = 13.0m, min = 8.2m, median = 10.0mm) on the left hemisphere and slightly larger, at 10.7 ±1.4mm (max = 14.0mm, min = 8.7mm, median = 10.5mm), on the right. As for the more superiorly placed 2-D linear measures of the distance between the arcuate sulcus and the central sulcus described above, the more inferiorly placed measure, A-Civ, predominated in the right hemisphere. In the total sample (n = 33), 23 individuals (70% of sample) showed a larger value for A-Civ in the right hemisphere (Figure 5-7). In females (n = 19), 14 individuals (74% of sub-sample), and in males (n = 14) nine individuals (64% of sub-sample), showed a larger value for A-Civ on the right hemisphere (Figure 5-7).

Figure 5-7 Plot of hemispheric differences in length from the arcuate sulcus to the central sulcus (*A-Civ*). Values represent differences in length (mm) between sulci on the left and right hemispheres, plotted for the largest side: **a)** total sample (n=33), **b)** female sub-sample (n=19), and **c)** male sub-sample (n=14). See text, Section 5.3.3.2.

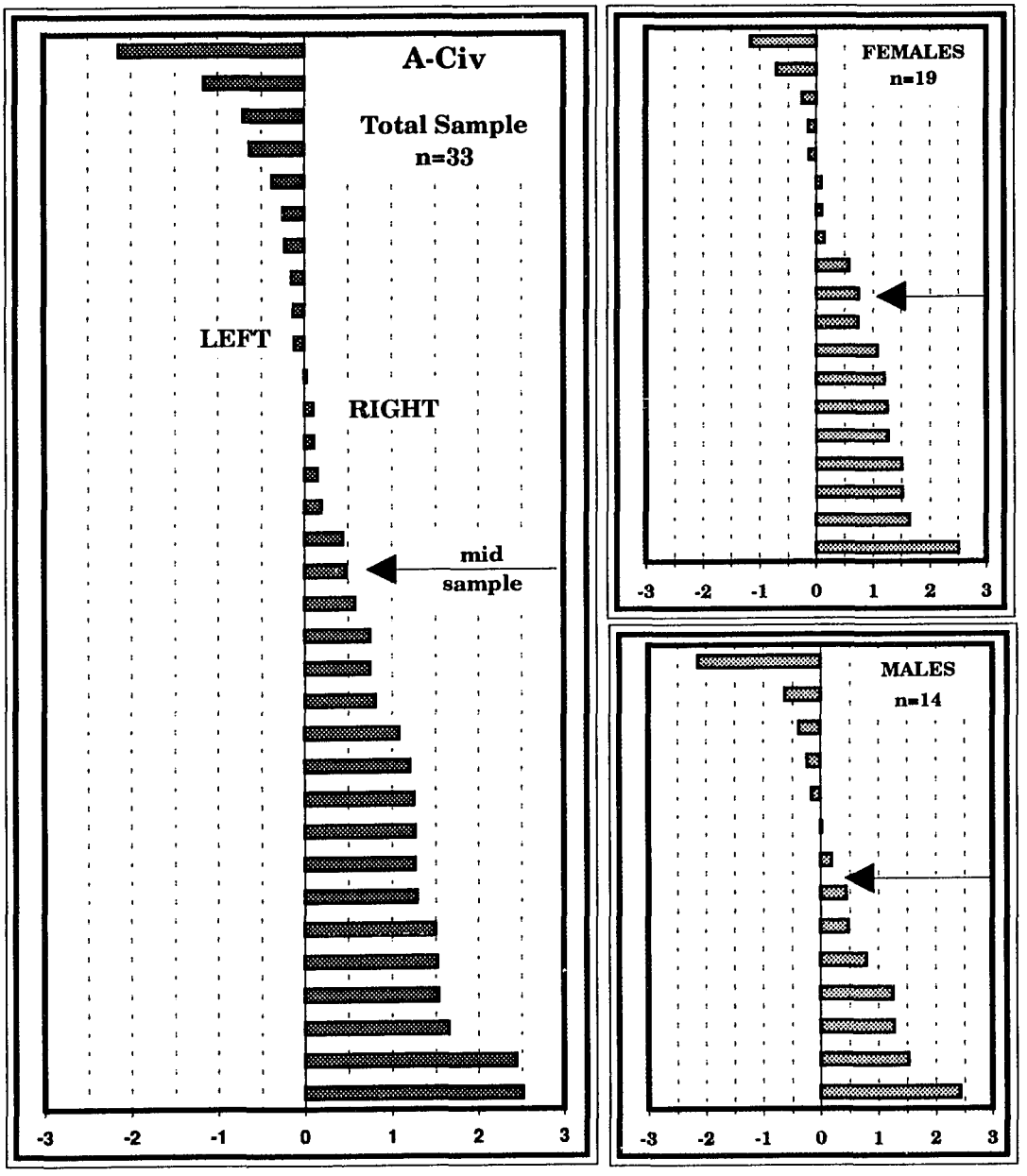
A-Civ
Total Sample
n=33
LEFT
RIGHT
mid
sample
-3
-2
-1
0
1
2
3
FEMALES
n=19
MALES
n=14

Statistical analysis of measure A-Civ:

Using the type 1 t-Test, it was shown that the 2-D linear measure A-Civ in the total sample (n = 33) was significant larger on the right hemisphere than it was on the left ($P = 0.005$). In females (n = 19) the right hemisphere was also significantly larger on the right hemisphere ($P = 0.007$). In males (n = 14) there were no significant differences between the measure A-Civ on the left and right hemispheres ($P = 0.25$). See Appendix 5-3 for t-Test output tables.

Inter-hemispheric dimensions of linear measure A-Cv:

This 2-D linear measure of the distance between the arcuate sulcus and the central sulcus, A-Cv, was the most inferiorly placed of the five independent measures described above. It was located on the inferior points of termination of both the arcuate and central sulci (see Figure 5-1 and Section 5.3.1.1. for positioning and details of this measure). As for the similar measure positioned immediately above (A-Civ), A-Cv was situated on the area of cortex posterior to the arcuate sulcus which is homologous to Broca's speech area in humans.

In the total sample (n = 33), the mean value for the 2-D linear distance A-Cv was 12.4 ±1.7mm (max = 16.8mm, min = 9.7mm, median = 12.3mm) on the left hemisphere, and 12.6 ±1.6mm (max = 15.8, min = 9.7, median = 12.3mm) on the right hemisphere (Figures 5-3 and Appendix 5-1).

In females (n = 19), A-Cv was 11.8 ±1.4mm (max = 14.2mm, min = 9.7mm, median = 11.9mm) on the left hemisphere, and 12.3 ±1.4mm (max = 15.8mm, min = 10.3mm, median = 12.2mm) on the right hemisphere (Figures 5-3 and Appendix 5-1). In males (n = 14), A-Cv was 13.2 ±1.8mm (max = 16.8mm, min = 10.2mm, median = 13.1mm) on the left hemisphere, and 13.1 ±1.8mm (max = 15.8mm, min = 9.7mm, median = 12.9mm) on the right hemisphere (Figures 5-3 and Appendix 5-1).

As for all the measures of the distance between the arcuate sulcus and central sulcus in the left and right hemispheres, this most inferiorly placed measure predominated in the right hemisphere (Figure 5-8). In the total sample (n = 33), 22 individuals (~67% of sample) showed a larger value for A-Cv on the right hemisphere. Likewise, in females (n = 19), 13 individuals (68% of sub-sample) and in males (n = 14), 9 individuals (~64% of sub-sample) showed a larger value for A-Cv on the right hemisphere (Figure 5-8).

Statistical analysis of measure A-Cv:

Using the type 1 t-Test, it was shown that there were no significant differences between the size of A-Cv on the left and right hemispheres, either in the total sample ($P = 0.25$), in the female sub-sample ($P = 0.055$) or in the male sub-sample ($P = 0.77$). However, the almost significant, 2-tailed P value for the female sub-sample ($P = 0.055$), and the highly significant 1-tailed P value ($P = 0.028$) showed that A-Cv was larger in the right

Figure 5-8 Plot of hemispheric differences in length from the arcuate sulcus to the central sulcus (A-Cv). Values represent differences in length (mm) between sulci on the left and right hemispheres, plotted for the largest side: **a)** total sample (n=33), **b)** female sub-sample (n=19), and **c)** male sub-sample (n=14). See text, Section 5.3.3.2, and Figure 5-1

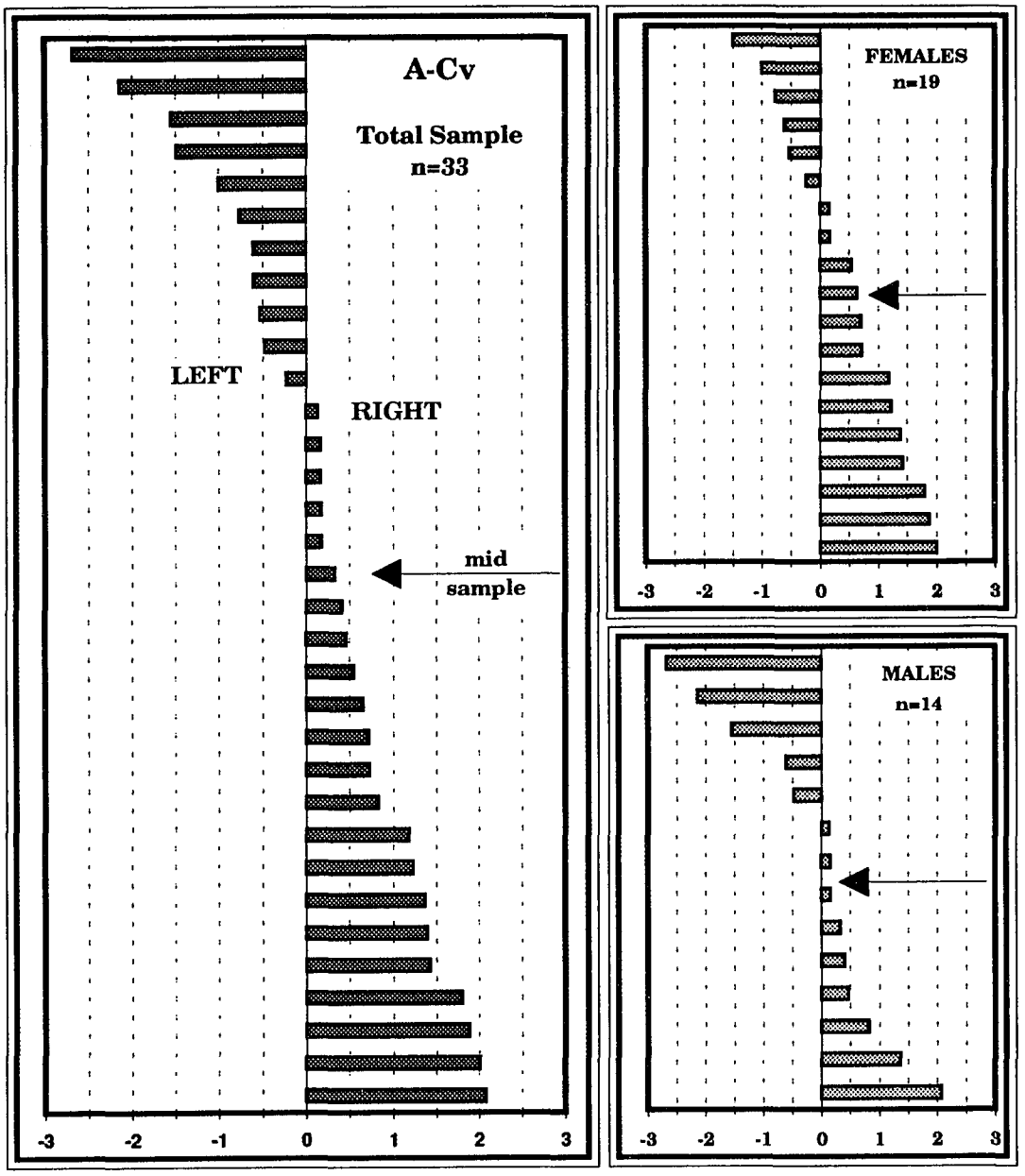
A-Cv
Total Sample
n=33
LEFT
RIGHT
mid
sample
-3
-2
-1
0
1
2
3
FEMALES
n=19
MALES
n=14

hemisphere in females only. Interestingly, males showed a significant right hemisphere predominance in only the most superiorly placed of the five measures (A-Ci).

Analysis of pooled data from the five independent measures A-Ci, A-Cii, A-Ciii, A-Civ and A-Cv:

The five independent measures described above were made in order to see if there was a specific region along the supero-inferior extent of the cortex located posterior to the arcuate sulcus where asymmetry was more pronounced. This segmented approach was designed to test the central hypothesis of this dissertation, that regions of the cortex homologous to human speech-language areas would show the most asymmetry. As such, it was predicted that the more inferior measures on the left hemisphere would be significantly larger on the left hemisphere. However, three of the five measures, including one inferiorly placed measure, A-Civ, showed a significant predominance in the right hemisphere. In no case were the measures significantly larger on the left hemisphere.

In an effort to see the total inter-hemispheric distribution pattern of this measure, the values for the five measures A-Ci - A-Cv were pooled and considered as a whole. This data then can be compared to the area measures of the same cortical region (A-Ci^2 and A-Cii^2), presented below.

Inter-hemispheric distribution of pooled A-C measures:

The total sample (n = 165) of the five combined measures A-C i-v was larger on the right hemisphere in 110 cases, representing ~67% of the expanded sample (Figures 5-9 & 5-10). In measures of the female sub-sample (n = 95), 63 measures representing 66% of the expanded sub-sample, were larger on the right hemisphere (Figure 5-9). In combined measures of the male sub-sample (n = 70), 47 values, representing 67% of the expanded sub-sample, were larger in the right hemisphere.

The mean of these pooled independent values for A-Ci-v in the left hemisphere of the total sample (n = 165) was 9.3 ± 2.4mm and on the right hemisphere, 9.7 ± 2.4mm (Appendix 5-4). The mean for females (n = 95) on the left hemisphere was 9.1 ±2.1 and for the right 9.5 ±2.2mm. For males (n = 70) the mean value for the left hemisphere was 9.6 ±2.6mm and for the right 9.9 ±2.6.

When the mean of each of the five values A-Ci-v were calculated, the resultant mean of means was identical to that for the data considered separately at 9.3 ±1.12 for the left hemisphere, and 9.7 ±1.1mm for the right. However, standard deviations were lower when data were so manipulated

Statistical analysis of pooled measures A-Ci to A-C-v:

For statistical analysis, two approaches were used for comparison of left versus right hemisphere differences in the pooled measures of A-C i-v. First, every paired data point for the left and right hemispheres was considered as

Figure 5-9 Plot of hemispheric differences in length from the arcuate sulcus to the central sulcus for five combined values (*A-C i-v*). Values represent differences in length (mm) between sulci on the left and right hemispheres, plotted for the largest side: **a)** total sample (n=33), **b)** females (n=19), and **c)** males (n=14). Section 5.3.3.2, & Figure 5-1.

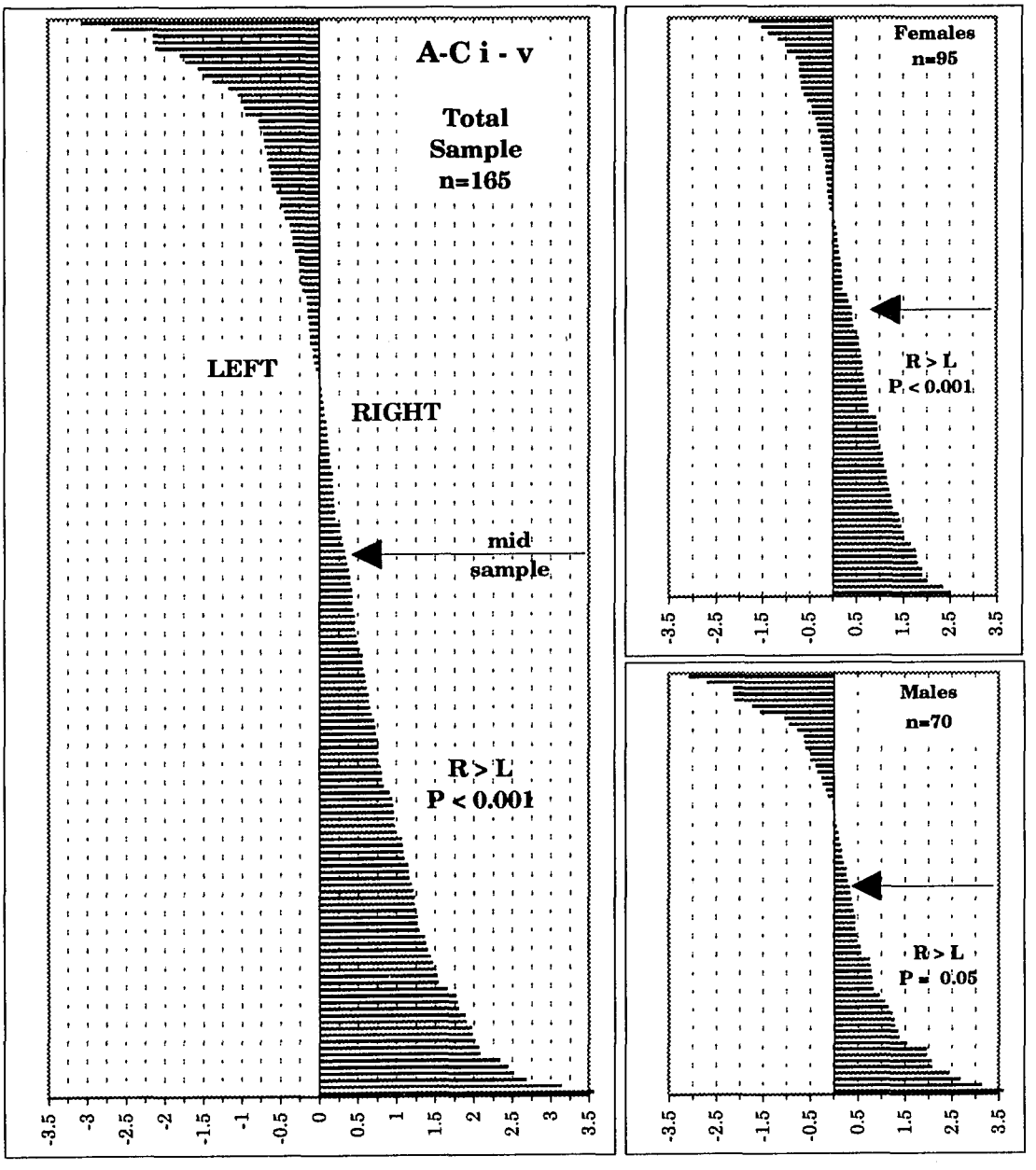
A-C i - v
Total
Sample
n=165
LEFT
RIGHT
mid
sample
R > L
P < 0.001
-3.5
-3
-2.5
-2
-1.5
-1
-0.5
0
0.5
1
1.5
2
2.5
3
3.5
Females
n=95
R > L
P < 0.001
Males
n=70
R > L
P = 0.05

an independent value. As such, each individual animal was represented by five separate pairs of data-points with a total n = 165. Second. the means of data-points A-C i-v on the left and right hemispheres were considered as individual points, with a resultant n = 33.

Using the type 1 t-Test on the first data-set, it was shown that the pooled values for A-Ci-v (n = 165), showed that the measures in the total sample were significantly larger on the right hemisphere ($P < 0.001$). In the pooled values for A-C i-v in females (n = 95), the right hemisphere was also larger at a highly significant level ($P < 0.001$); see Appendix 5-4.

Using the type 1 t-Test on the second data-set, it was also shown that in the total sample of mean values (n = 33) the right hemisphere was significantly larger than the left ($P < 0.001$).

5.3.3.3. 2-D linear measures of the sub-central dimple to the arcuate and central sulci (A-SCD and C-SCD)

The sub-central dimple was present to some degree in the inferior frontal lobe in all of the brains used for this study although its size was quite variable (see Chapter 3, Section 3.3.1.4.). The amount of cortex between the sub-central dimple and the arcuate sulcus anteriorly and the central sulcus posteriorly was estimated by measuring the linear distances between these structures on the left and right hemispheres (see Figures 3-6 & 5-1a).

Inter-hemispheric dimensions of linear measure A-SCD:

In the total sample used for this measure (n = 29) the mean value for the linear measure of the arcuate sulcus to the sub-central dimple (A-SCD) was 7.9 ±1.3mm (max = 11.8mm, min = 6.1mm, median = 7.7mm) on the left hemisphere and slightly larger at 8.1 ±1.2mm (max = 10.4mm, min = 8.1mm, median = 8.0mm) on the right hemisphere (Appendix 5-5 & 5-6).

In females (n = 18), A-SCD was smaller than the total sample mean at 7.5 ±0.9mm on the left hemisphere and 8.1 ±1.1mm on the right (Appendix 5-5 & 5-6). In males (n = 11) the mean values for A-SCD were larger than the total sample mean at 8.4 ±1.7mm on the left hemisphere and 8.2 ±1.4mm on the right hemisphere (Appendix 5-5 & 5-6).

The inter-hemispheric distribution pattern of the total sample appeared to predominate on the right hemisphere as can be seen in Figure 5-9. In the total sample (n = 29), 18 individuals (62% of sample) showed a value for A-SCD that was larger on the right hemisphere than on the left.

In females (n = 18), the value for A-SCD in 13 individuals (72% of sub-sample) was larger on the right hemisphere. In males (n = 11), the right hemisphere did not appear to predominate since only five individuals (45% of sub-sample) showed a larger value for A-SCD on the right hemisphere (Figure 5-9). This may have been due to the relatively small sample size however.

Figure 5-10 Plot of hemispheric differences in length from the arcuate sulcus to the sub-central dimple (*A-SCD*). Values represent differences in length (mm) between sulci on the left and right hemispheres, plotted for the largest side: **a)** total sample (n=29), **b)** female sub-sample (n=18), and **c)** male sub-sample (n=11). See text, Section 5.3.3.3, and Figure 5-1.

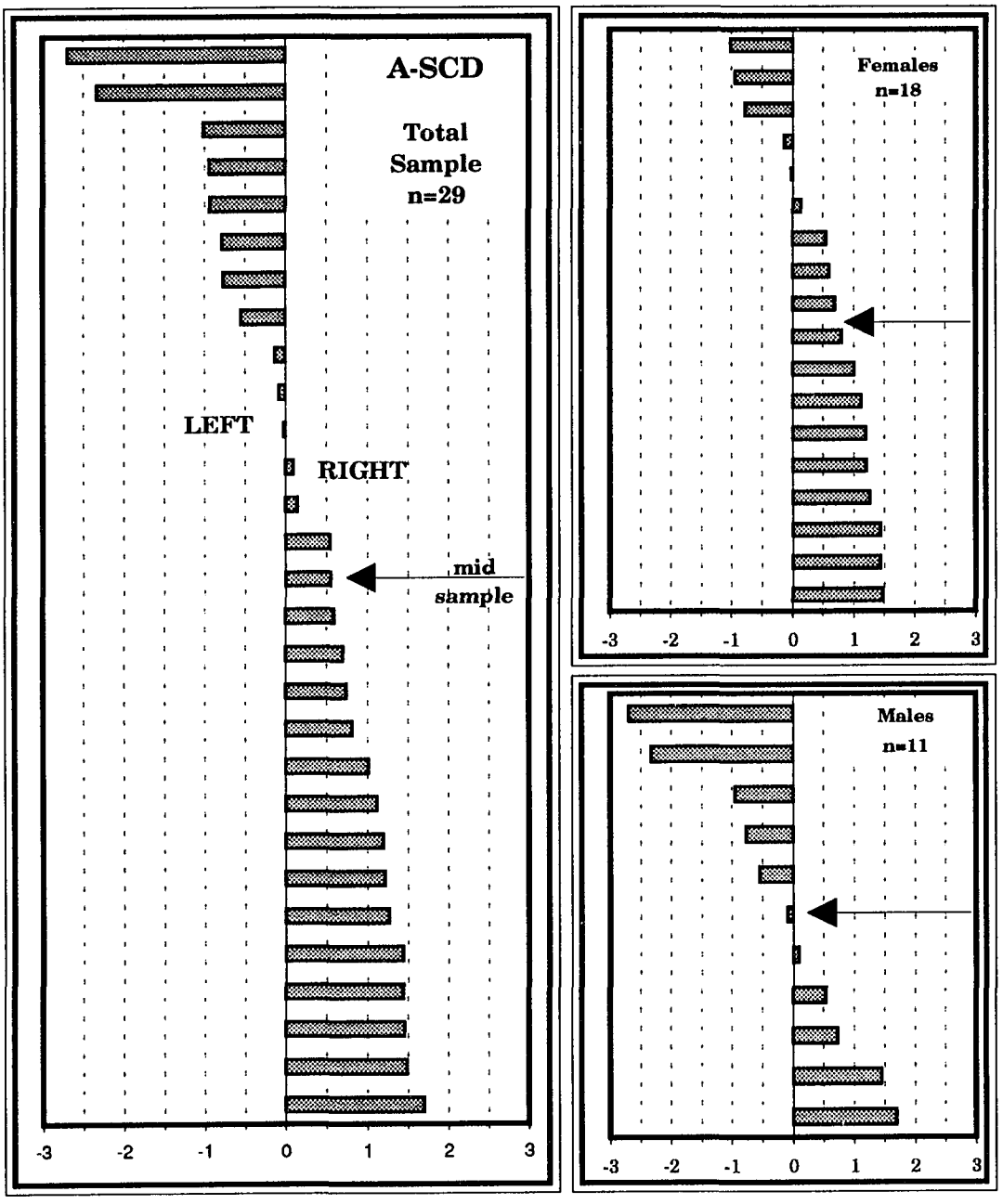
A-SCD
Total
Sample
n=29
LEFT
RIGHT
mid
sample
-3
-2
-1
0
1
2
3
Females
n=18
-3
-2
-1
0
1
2
3
Males
n=11
-3
-2
-1
0
1
2
3

1 *Statistical analysis of 2-D linear measure A-SCD*

Using the type 1 t-Test on data for the 2-D linear measure A-SCD in the total sample (n = 29) it was shown that there were no significant size differences between the left and right hemispheres ($P = 0.24$). In females (n = 19) however, A-SCD was significantly larger on the right hemisphere($P = 0.01$). In males (n = 11), there was no significant difference between A-SCD in the left and right hemispheres ($P = 0.56$); see Appendix 5-6.

The low probability value seen for the total sample may have been due to the influence of the highly significant hemispheric difference seen only in females. Although the sample sizes are relatively small for this measure it provides yet another example of the striking differences that may be apparent when the sexes are considered separately and may not be evident in a combined sex sample.

Inter-hemispheric dimensions of linear measure C-SCD:

In a total sample (n = 29) the mean value for the linear measure of the central sulcus to the sub-central dimple (C-SCD) was 4.5 ±0.8mm (max = 6.8mm, min = 3.2mm, median = 4.5mm) on the left hemisphere and 4.5 ±0.9mm (max = 7.6mm, min = 4.4mm, median = 4.41mm) on the right (Appendix 5-7 & 5-8).

In females (n = 18), C-SCD was slightly smaller than the total sample mean at 4.4 ±0.7mm on the left hemisphere and 4.3 ±0.7mm on the right (Appendix 5-7 & 5-8).

Figure 5-11 Plot of hemispheric differences in length from the central sulcus to the sub-central dimple (*C-SCD*). Values represent differences in length (mm) between sulci on the left and right hemispheres, plotted for the largest side: in the total sample (n=29), the female sub-sample (n=18), and the male sub-sample (n=11). See text, Section 5.3.3.3, and Figure 5-1.

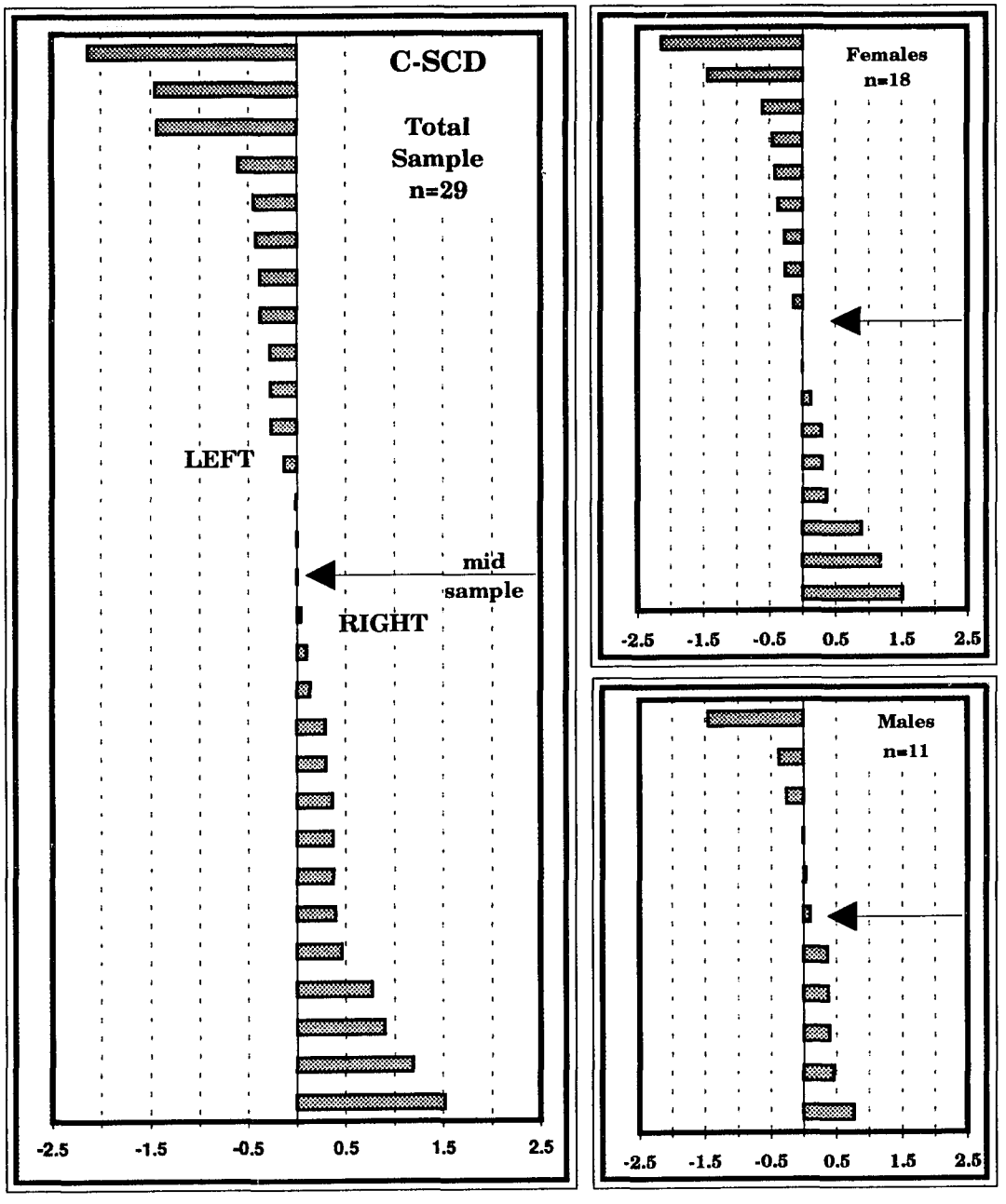
C-SCD
Total
Sample
n=29
LEFT
mid
sample
RIGHT
-2.5
-1.5
-0.5
0.5
1.5
2.5
Females
n=18
-2.5
-1.5
-0.5
0.5
1.5
2.5
Males
n=11
-2.5
-1.5
-0.5
0.5
1.5
2.5

In males (n = 11) the mean values for C-SCD was 4.8 ±0.9mm on the left hemisphere and 4.8 ±1.1mm on the right hemisphere (Appendix 5-7 & 5-8).

In comparison to most of the other 2-D linear measures of the frontal lobe described above, C-SCD did not show an obvious right hemisphere predominance in either the total sample or the sex-specific sub-samples (Figure 5-11). For example, in the total sample (n = 29), only 16 individuals (55% of sample) were larger on the right hemisphere. In females (n = 19), although nine individuals were larger on the right hemisphere, two of these values were close to zero. As such, only seven individuals (of 16, = 44% of sample) were larger on the right hemisphere. As can be seen in Figure 5-11, a similar situation was also the case for males (n = 11). The smaller sample size used for this measure may also have contributed to this equivocal outcome.

Statistical analysis of 2-D linear measure C-SCD:

Using the type 1 t-Test, it was shown that there were no significant size differences between C-SCD on the left and right hemispheres, in either the total sample (n = 29) where $P = 0.84$, in males (n = 11) where $P = 0.73$, and in females (n = 18) where $P = 0.82$, (Appendix 5-8).

5.3.3.4. 2-D area measures of the arcuate sulcus to central sulcus (A-Ci² and A-Cii²)

Two separate 2-D area measures (A-Ci² and A-Cii²), representing the amount of brain surface cerebral cortex located between the arcuate sulcus and central sulcus on both the left and right hemispheres, were used in this analysis for the reasons discussed in Section 5.3.2. (see Figure 5-1). The exact criteria used for consistent inter-hemispheric and inter-individual placement of these two area measures made from lateral photographs of the brain are described in Section 5.3.2.

Inter-hemispheric dimensions of 2-D area measure A-Ci²:

In the total sample (n = 33), the mean value for the larger 2-D area measure A-Ci² was 116.1 ±20.5mm² (max = 168.6mm², min = 72.0mm²) on the left hemisphere and 118.9 ±24.2mm² (max = 196.1mm², min = 74.8mm²) on the right hemisphere (Appendix 5-9).

In females (n = 19), A-Ci² was smaller than the total sample mean at 111.9 ±16.9mm² on the left hemisphere and 112.1 ±20.5mm² on the right (Appendix 5-9). In males (n = 14), A-Ci² was 121.9 ±24.1mm² on the left hemisphere and 128.2 ±26.5mm² on the right hemisphere (Appendix 5-9).

The overall inter-hemispheric distribution pattern of the 2-D area measure A-Ci² showed a distinct tendency to be right hemisphere predominant both in the total sample and in the sex-specific sub-samples as can be seen in Figure 5-11). In the total sample (n = 33), 22 individuals (67%

Figure 5-12 Plot of hemispheric differences in 2-D area from the arcuate sulcus to the central sulcus ($A\text{-}Ci^2$). Values represent differences in area (mm^2) between this measure on the left and right hemispheres, plotted for the largest side, in: the total sample (n=33), the female sub-sample (n=19), and the male sub-sample (n=14). See text, Section 5.3.3.4, and Figure 5-1

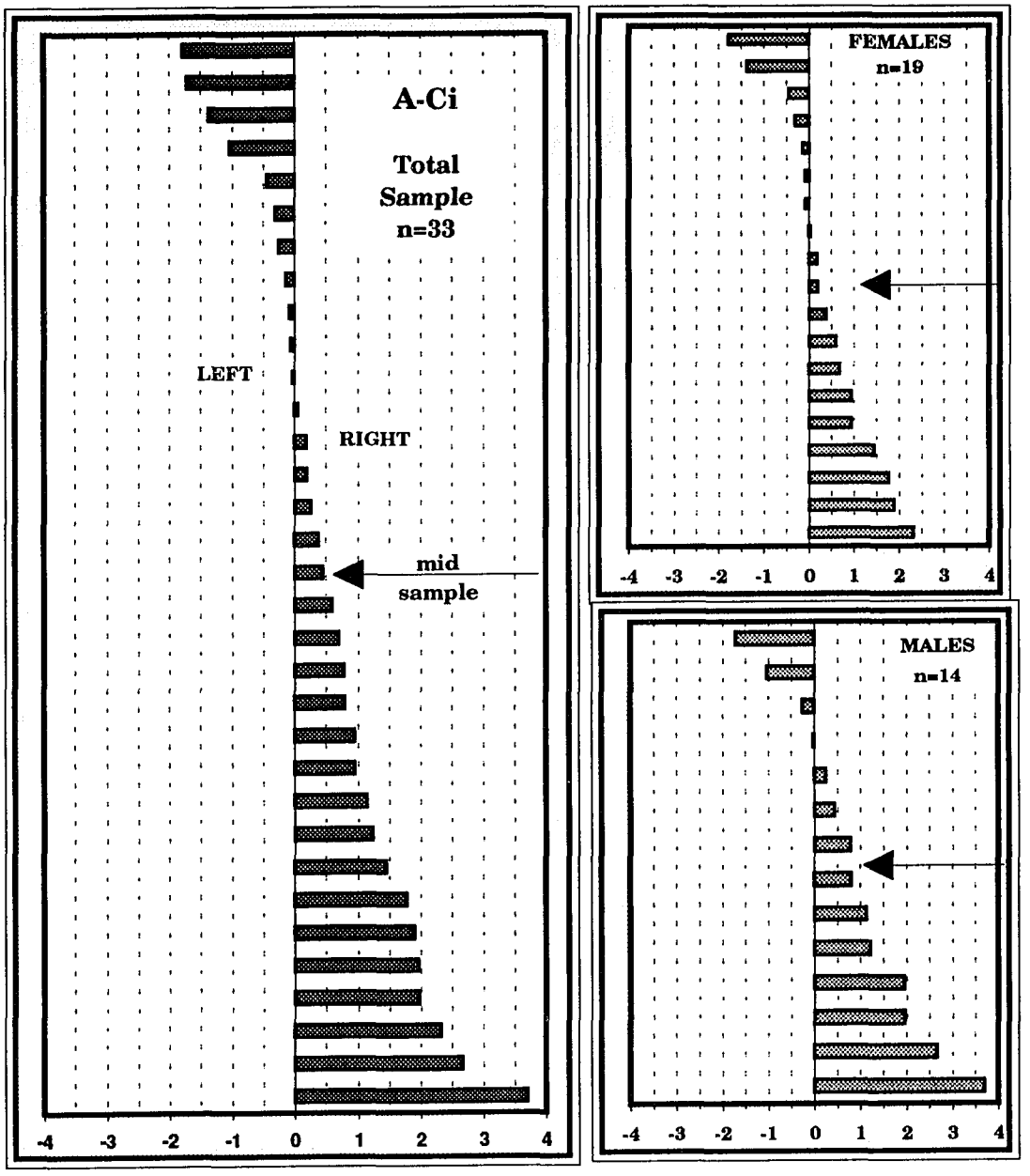
A-Ci
Total
Sample
n=33
LEFT
RIGHT
mid
sample
-4 -3 -2 -1 0 1 2 3 4
FEMALES
n=19
-4 -3 -2 -1 0 1 2 3 4
MALES
n=14
-4 -3 -2 -1 0 1 2 3 4

of sample) showed a larger value for A-Ci^2 in the right hemisphere. In females (n = 19), 11 individuals (58% of sub-sample), and more strikingly, in males (n = 14), 11 individuals (79% of sub-sample), showed a larger value for A-Ci^2 in the right hemisphere.

Statistical analysis of 2-D area measure A-Ci^2:

Using the type 1 t-Test it was shown that there were no significant size differences between A-Ci^2 on the left and right hemispheres, in either the total sample (P = 0.41), the female sub-sample (P = 0.96) or the male sub-sample (P = 0.16), (Appendix 5-10).

Although there were no apparent significant differences between the two hemispheres in the total sample or the sex-specific sub-samples, the results do indicate some difference between the sexes in which males (P = 0.16) but not females (P = 0.96), show a distinct tendency to be larger on the right hemisphere (Appendix 5-10). This is in marked contrast to those sex differences seen for the pooled 2-D linear measures A-C i-v (Section 5.3.3.2.) of the same area of cortex.

Inter-hemispheric dimensions of 2-D area measure A-Cii^2:

In the total sample (n = 33), the mean value for the smaller and more inferiorly placed second cortical 2-D area measure between the arcuate sulcus and central sulcus A-Cii^2 (Figure 5-1), was 91.9 ±17.1mm^2 (max = 150.8mm^2, min = 59.3mm^2, median = 91.4mm^2) on the left hemisphere, and

90.0 ±15.9mm^2 (max = 123.3mm^2, min = 57.6mm^2, median = 89.2mm^2) on the right hemisphere (Appendix 5-9).

In females (n = 19), the mean value for A-Cii^2 was 87.3 ±13.9mm^2 on the left hemisphere and 87.4 ±14.8mm^2 on the right hemisphere (Appendix 5-9). In males (n = 14), the mean value for the 2-D area of A-Cii^2 was 98.1 ±19.5mm^2 on the left hemisphere and 93.5 ±17.2mm^2 on the right hemisphere (Appendix 5-9).

As was seen for the complementary 2-D area measure A-Ci^2, the inter hemispheric distribution pattern of the second area measure A-Cii^2 showed a tendency to be larger more often in the right hemisphere, particularly in males as can be seen in Figure 5-13. In contrast, females tended to show a more even inter-hemispheric distribution pattern, both in the range of absolute sizes, and in distribution of the largest side (Figure 5-13). In males (n = 14) for example, 11 individuals (79% of sub-sample), showed a larger value for A-Cii2 on the right hemisphere. In contrast, 9 of 19 females (47% of sub-sample) were larger on the right.

Statistical analysis of 2-D area measure A-C^{ii2}:

Using the type 1 t-Test, it was shown that there were no significant differences between the 2-D area measure A-Cii^2 in the left and right hemispheres in the total sample (P = 0.41), in females (P = 0.98) or in males (P = 0.20); see Appendix 5-10.

Figure 5-13 Plot of hemispheric differences in the second measure of 2-D area from the arcuate sulcus to the central sulcus (*A-Cii*^{2}). Values represent differences in area (mm^2) between the left and right hemispheres, plotted for the largest side, in: the total sample (n=33), females (n=19), and males (n=14). See text, Section 5.3.3.4, and Figure 5-1

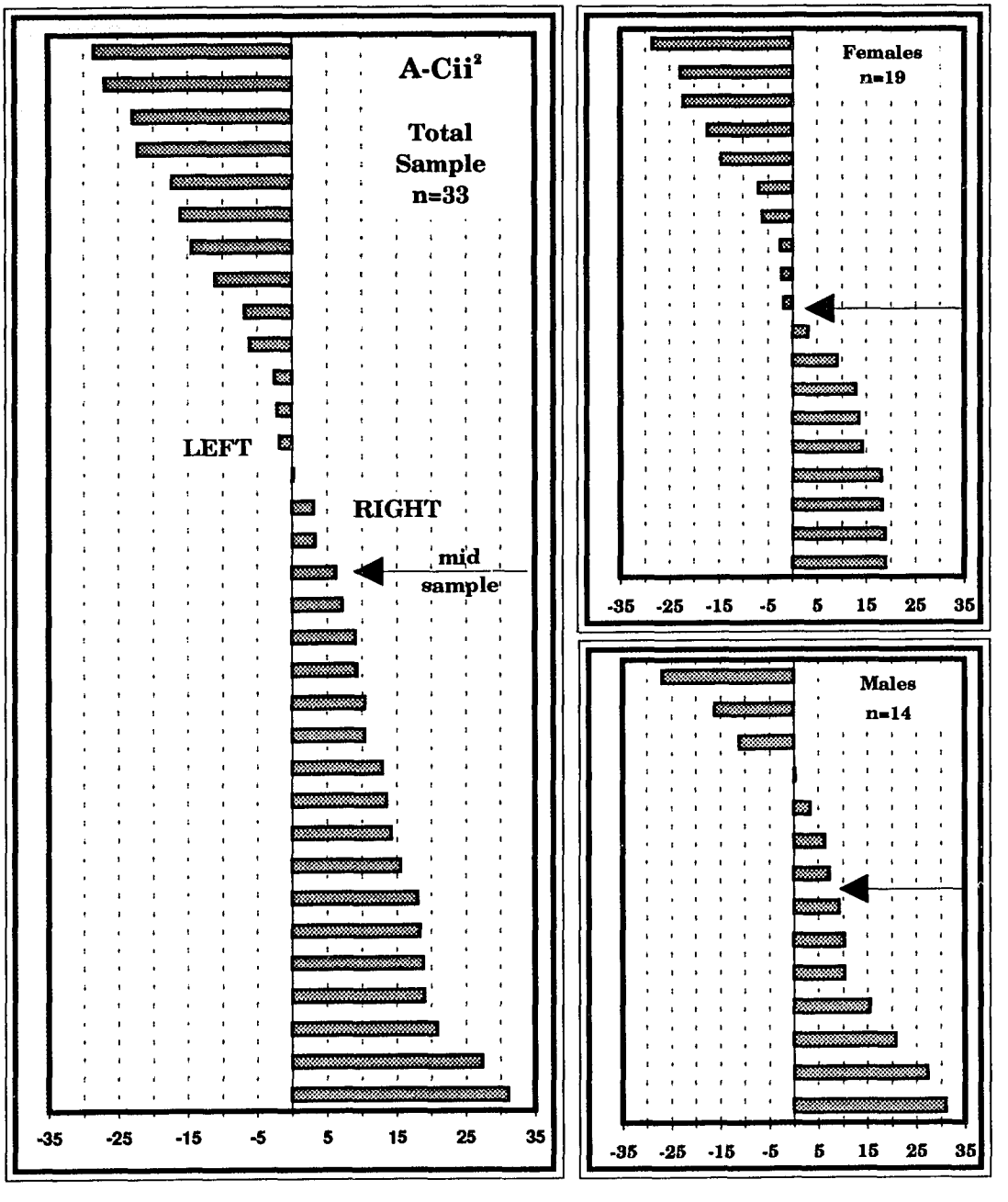
A-Cii²
Total
Sample
n=33
LEFT
RIGHT
mid
sample
-35 -25 -15 -5 5 15 25 35
Females
n=19
-35 -25 -15 -5 5 15 25 35
Males
n=14
-35 -25 -15 -5 5 15 25 35

As for the complementary larger measure of cortical area between the arcuate and central sulci, A-Ci^2, the more inferiorly placed A-Cii^2 showed some evidence of sex related differences in the pattern of inter-hemispheric distribution. For example, males at $P = 0.20$ showed a distinct tendency for A-Cii^2 to be larger in the left hemisphere. However, this outcome was in marked contrast to corresponding male values for measure A-Ci^2 in which there was a sex-specific tendency to be larger in the left, not the right hemisphere. In both of these complementary area measures, females showed no tendency to be larger in either the left or right hemispheres at $P = 0.96$ and $P = 0.98$ respectively (Appendix 5-10).

5.4. TEMPORAL LOBE STRUCTURES

5.4.1. 2-D linear measures of temporal lobe structures

5.4.1.1. (Linear Length "SF-ap", Figure 5-14a)

The antero-posterior length of the left and right sylvian fissure; commencing anteriorly at the point where a v-shaped divergence ("a" in Figure 5-14a) defines the lower cortex of the inferior frontal gyrus and the anterior border of the superior temporal gyrus, and terminating posteriorly where the superior temporal gyrus joins the inferior parietal gyrus (Figure 5-14a). In some brains the posterior

portion of the superior temporal gyrus and the corresponding sylvian point, are located deep to the cortical surface under an operculating portion of the inferior parietal gyrus (Section 3.2.1.). For this analysis, in such cases the posterior border of the sylvian fissure was estimated as the point of convergence of the superior temporal sulcus and sylvian fissure. In all cases, the distance was measured on the low power lateral view macrophotographs (Figure 3-2 and Figure 5-14). In order to include any inherent 2-D curvature, the sylvian fissure was measured by following its entire length with the cursor and not by measuring the distance of a straight line between two points.

5.4.1.2. (Linear Length "STS-ap", Figure 5-14a)

The antero-posterior length of the left and right superior temporal sulcus; commencing anteriorly at the point where the superior temporal gyrus combines with the middle temporal gyrus, and terminating posterior to the sylvian fissure, at the point where the superior temporal gyrus curves superiorly towards the inferior parietal gyrus (Figures 3-4 and 3-5).

Note: In order to include any inherent curvature, the superior temporal sulcus was measured by following its entire length with the digitizing cursor. As such, the measure did not represent the length of a straight line between these two points

5.4.1.3. (Linear Distance "STG-v", Figure 5-15a)

The 2-D linear distance, on the superior temporal gyrus, between the sylvian fissure and the superior temporal sulcus, corresponding to a line extended inferiorly from the central sulcus (CS-ext) on Figure 5-15a). This line is at right angles to line A-B (Figure 5-15a) which represents the longitudinal axis of the superior temporal gyrus. Line A-B (Figure 5-15a) is made by connecting points "a" (= the intersection of the extension of the central sulcus with the sylvian fissure; Figure 5-15a & b) with the posterior termination of the sylvian fissure, the sylvian point (Figure 5-15a).

Note: Although the position of this line was a construction, its position was reproducible because it was independent of brain size. Further, it served as an anterior delimiter, posterior to which included the cytoarchitectonic area of interest on the superior temporal gyrus, Area Tpt, which is homologous to Wernicke's area in humans. It also served as the anterior delimiter for the following series of four complementary linear measures STG-ii - STG-v (Figure 5-15a). The position of this initial line was determined on the left hemisphere, and the anterior-posterior distance from the posterior termination of the sylvian fissure measured. This distance was then used to place a similar line on the opposite hemisphere. This precautionary measure

took into account, and prevented any data skewing, that may have resulted from hemispheric differences in the position of the inferior central sulcus.

5.4.1.4. (Linear Distances "STG-i", "STG-ii", "STG-iii"' and "STG-iv", Figure 5-15a)

Complementary linear distances to STG-v (above) representing the width of the superior temporal gyrus in the region containing the cytoarchitectonic homologue of Wernicke's area in humans, Area Tpt (Figure 5-15b). Using the posterior termination of the sylvian fissure, the sylvian point, as the posterior delimiter, and the constructed line STG-v (Section 5.4.1.3.) as the anterior delimiter, a series of four equidistant lines were created, extending from the sylvian fissure to the superior temporal sulcus. These lines were created parallel to the initial line STG-v (Section 5.4.1.3.), and at right angles to the constructed line A-B (Figure 5-15a), which represented the longitudinal axis of the superior temporal gyrus.

5.4.2. 2-D Area measures of the temporal lobe

5.4.2.1. (Area "STG-Tpt^2", Figure 5-154)

The area of surface cerebral cortex on the posterior part of the superior temporal gyrus containing the cytoarchitectonic area Tpt (homologous to Wernicke's area in humans). It was defined as being delimited anteriorly, by the constructed line "STG-v" (Section 5.4.1.3. &

Figure 5-15a) and posteriorly, by the termination of the sylvian fissure (Figure 5-15a & b, point "b"). This measure was taken from the high power regional macro-photograph (Figures 3-4a and 3-4b)

5.4.2.2. (Area "STG-tot^2", Figure 5-14b)

The area of surface cerebral cortex on the entire anteroposterior extent of the superior temporal gyrus. Posteriorly it was defined by the termination of the sylvian fissure, superiorly by the sylvian fissure, and inferiorly by the superior temporal sulcus, which is extended anteriorly to bisect the confluence of the superior and middle temporal gyri (line "STS-ext" in Figure 5-14). These measures are made from the low power macrophotographs of the lateral aspect of the brain (Figure 3-2).

Figure 5-14 2-D linear and area measures from lateral brain photographs. **a)** Linear measures (mm) "SF-ap" & "STS-ap" (Sections 5.4.1.1. & 5.4.1.2.); **b)** Area measure (mm^2) "STG-tot^{2}" (Section 5.4.2.2.)

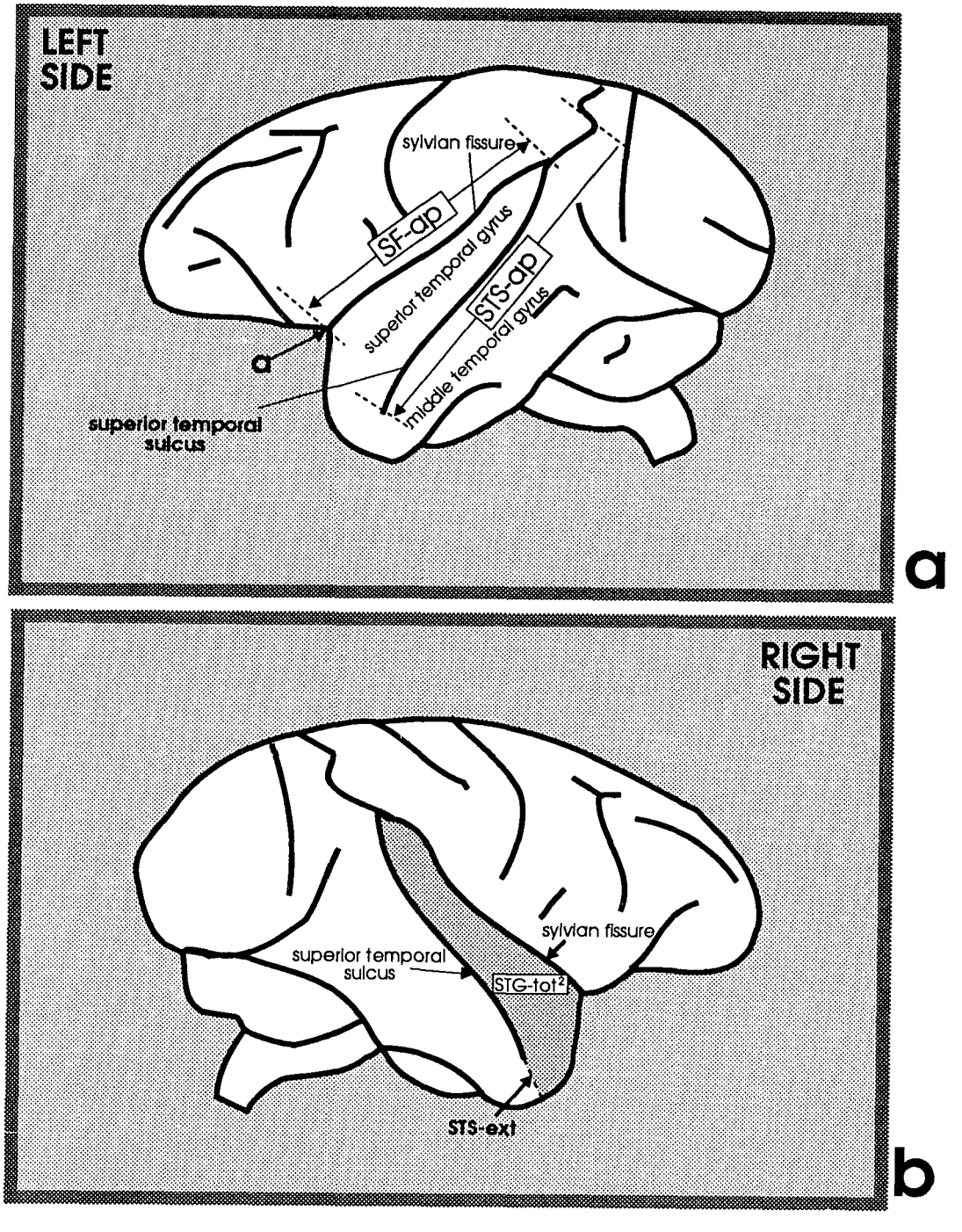
LEFT
SIDE
sylvian fissure
SF-ap
superior temporal gyrus
STS-ap
middle temporal gyrus
a
superior temporal
sulcus
a
RIGHT
SIDE
sylvian fissure
superior temporal
sulcus
STG-tot²
STS-ext
b

Figure 5-15 2-D linear and area measures made from close up lateral brain photographs of the temporal lobe region. **a)** Linear measures (mm) "STG-i", "STG-ii", "STG-iii", "STG-iv" & "STG-v". (Sections 5.3.1.3. & 5.3.1.4.); **b)** Area measure (mm^2) "STG-Tpt^2" (Section 5.3.2.1.)

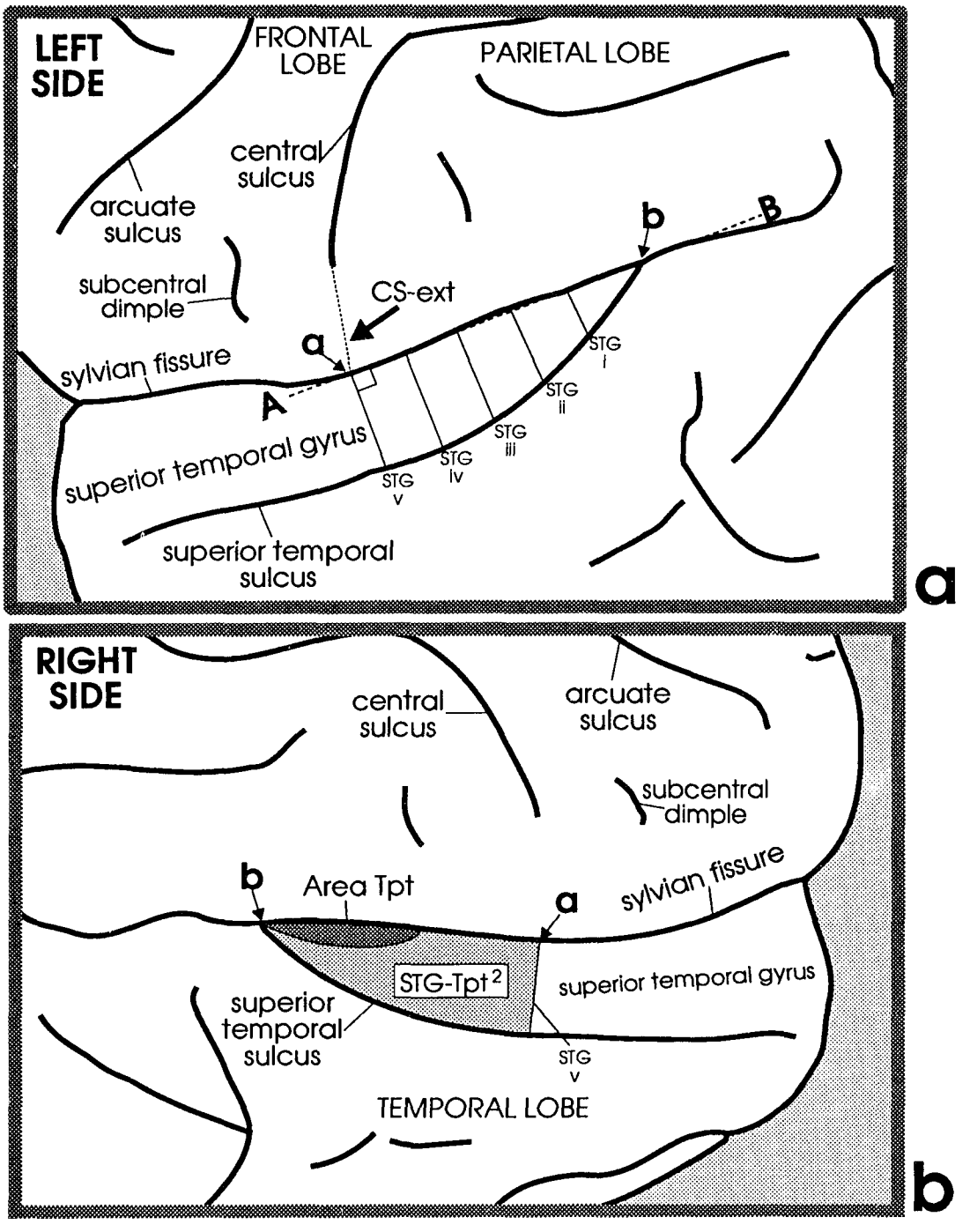
LEFT SIDE
FRONTAL LOBE
PARIETAL LOBE
central sulcus
arcuate sulcus
b
B
subcentral dimple
CS-ext
a
sylvian fissure
A
STG i
STG ii
STG iii
STG iv
STG v
superior temporal gyrus
superior temporal sulcus
a
RIGHT SIDE
central sulcus
arcuate sulcus
subcentral dimple
b
Area Tpt
a
sylvian fissure
STG-Tpt 2
superior temporal gyrus
superior temporal sulcus
STG v
TEMPORAL LOBE
b

5.4.3. Results of 2-D measures of temporal lobe structures

5.4.3.1. 2-D linear measures of the antero-posterior length of the sylvian fissure (SF-ap) in the left and right hemispheres.

This measure of sylvian fissure antero-posterior length in millimeters was made from lateral photographs of the brain using a quantitative digitizing system. As mentioned above, if the sylvian point was not present on the surface of the brain, the posterior confluence of the sylvian fissure and superior temporal sulcus was used as the posterior delimiter.

Inter-hemispheric dimensions of 2-D linear measure SF-ap:

In the total sample (n = 34), the mean value for the antero-posterior length of the left hemisphere sylvian fissure (SF-ap) was 28.3 ±3.8m (max = 36.1mm, min = 21.2mm, and median = 27.6mm) and on the right hemisphere 28.51 ±4.02mm (max = 38.3mm, min = 22.0mm, and median = 27.3mm) (Appendix 5-11). In females (n = 16), the 2-D linear measure SF-ap on the left hemisphere was smaller than the total sample mean at 25.8 ±2.2mm as was the value for the right hemisphere at 26.2 ±2.4mm (Appendix 5-11). In males (n = 18), the mean length of SF-ap on the left hemisphere was 30.5 ±3.6mm, and on the right, 30.6 ±4.1mm (Appendix 5-11).

The sylvian fissure was longer in the left hemisphere in 13 individuals (38% of the total sample) comprising females (n = 5; 31.% of the sub-sample) and males (n = 8; 44% of sub-sample), (Figure 5-15). The sylvian fissure was

Figure 5-16 Plot of hemispheric differences antero-posterior 2-D length of the sylvian fissure (*SF-ap*). Values represent differences in length (mm) between the left and right hemispheres, plotted for the largest side, in: the total sample (n=34), females (n=16), and males (n=18). Section 5.4.3.1.

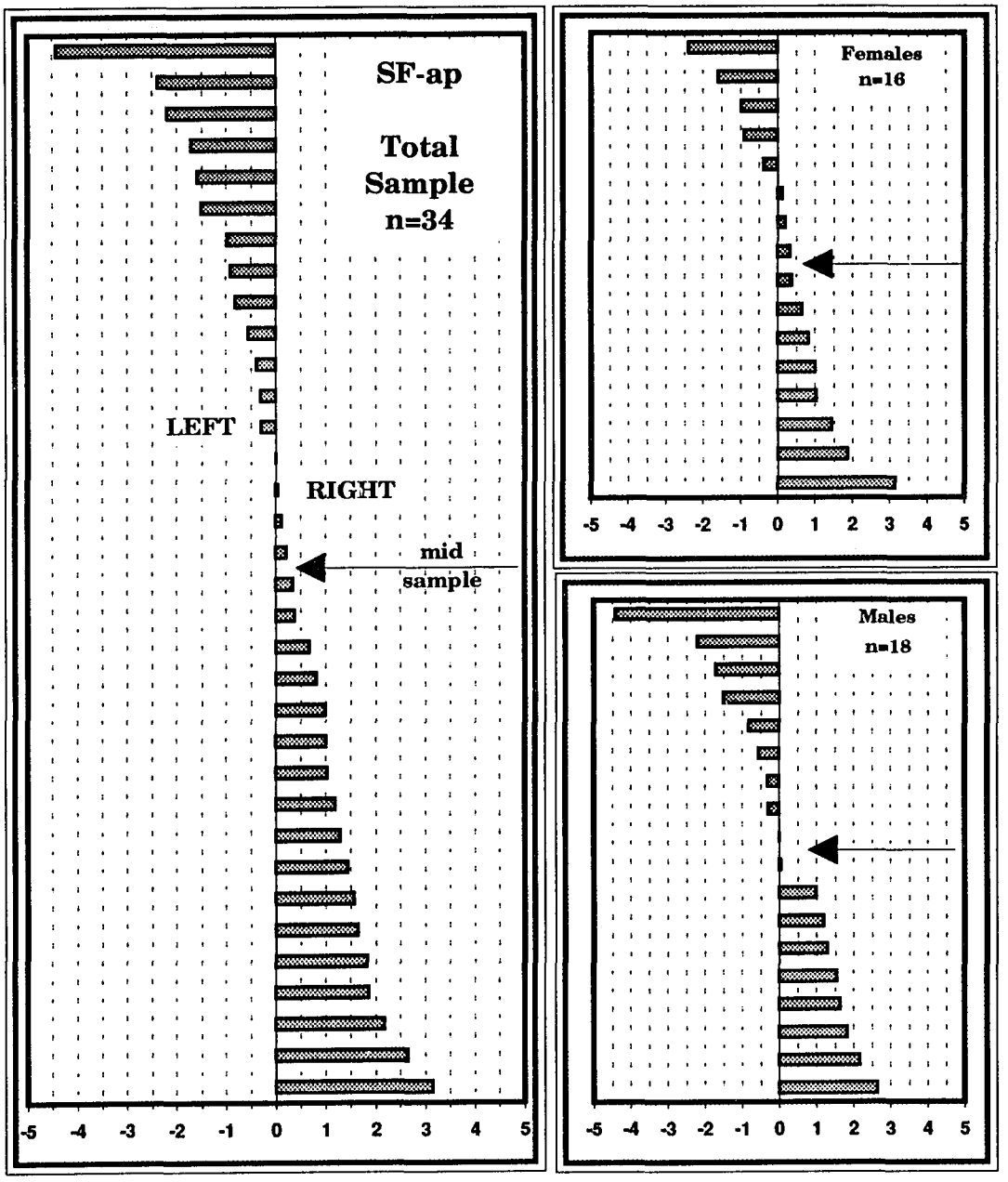
SF-ap
Total
Sample
n=34
LEFT
RIGHT
mid
sample
-5 -4 -3 -2 -1 0 1 2 3 4 5
Females
n=16
-5 -4 -3 -2 -1 0 1 2 3 4 5
Males
n=18
-5 -4 -3 -2 -1 0 1 2 3 4 5

longer in the right hemisphere in 21 individuals (62% of the total sample), comprising females (n = 11) which were 69% of the sub-sample, and males (n =10) which were 56% of the sub-sample, (Figure 5-16).

Statistical analysis of 2-D linear measure, SFa-p:

Using the Type 1 t-Test, it was shown that there were no significant differences between the length of the sylvian fissure on the left and right hemispheres in either the total sample ($P = 0.48$), the female sub-sample ($P = 0.38$) or the male sub-sample ($P = 0.82$); see Appendix 5-12.

5.4.3.2. 2-D linear measures of the antero-posterior length of the superior temporal sulcus (STS-ap) in the left and right hemispheres.

These measures of superior temporal sulcus antero-posterior length (STS-ap) in millimeters were made from lateral photographs of the brain. For this 2-D analysis, the most posterior termination point of the superior temporal sulcus was unable to be located on lateral photographs. This was because the posterior part of the sulcus coursed medially and became effectively out of view (e.g. see Figure 3-8). However, area Tpt, the homologue of Wernicke's area in humans, is located anterior to this medialization point. For this reason, it was decided to measure the extent of the superior temporal sulcus from its anterior origin to the point, just posterior to the sylvian point, where it turns medially through almost 90° (see Figure 3-4). This measure was not affected, as was the sylvian point, by variation in morphology of the posterior superior temporal gyrus, since its

course on the brain surface continued unhindered. The anterior margin of STS-ap was determined by the cutoff point provided by the 2-D perspective of the lateral photograph (e.g. see Figure 3-2) .

Inter-hemispheric dimensions of 2-D linear measure STS-ap:

In the total sample (n = 34), the antero-posterior length of the left hemisphere superior temporal sulcus (STS-ap) was 37.5 ±3.9mm (max = 45.2mm, min = 32.6mm, and median = 36.8mm, Appendix 5-13). On the right hemisphere, SF-ap was at 37.8 ±4.2mm (max = 45.9mm, min = 30.6mm, and median = 36.9mm, Appendix 5-13).

In females (n = 16), the mean value for STS-ap was smaller than that of the total sample at 35.1 ±1.7mm. On the right hemisphere, STS-ap was smaller than the total sample mean and similar to its own left side value, at 35.3 ±2.4mm (Appendix 5-13). In males (n = 18), the mean length of the STS-ap on the left hemisphere was larger than the total sample mean at 39.7 ±4.0mm (Appendix 5-13). The mean length of STS-ap on the right hemisphere was larger than the total sample mean, but close to its own left side value, at 40.1 ±4.2mm (Appendix 5-13a).

The superior temporal sulcus was longer in the left hemisphere in 11 individuals (32.4% of the total sample,) comprising 4 females (22.2% of sub-sample) and 7 males (43.8% of sub-sample); see Figure 5-17. The superior temporal sulcus was longer in the right hemisphere in a total of 23 individuals (68% of the total sample) comprising 12 females (75% of sub-

Figure 5-17 Plot of hemispheric differences in antero-posterior 2-D length of the superior temporal sulcus (*STS-ap*). Values represent differences in length (mm) between the left and right hemispheres, plotted for largest side, in the total sample (n=34), females (n=16), & males (n=18). Section 5.4.3.2

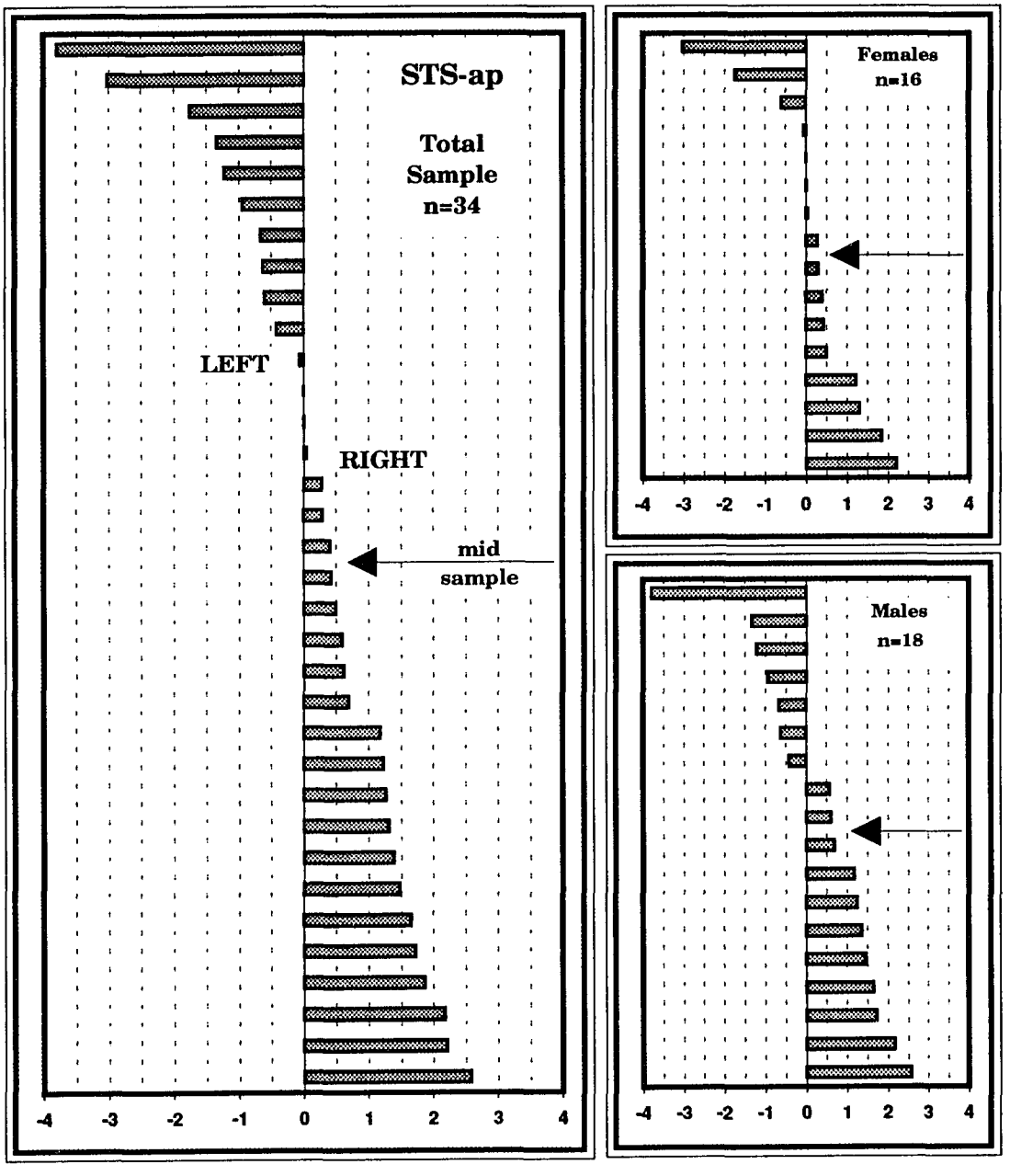
STS-ap
Total
Sample
n=34
LEFT
RIGHT
mid
sample
-4 -3 -2 -1 0 1 2 3 4
Females
n=16
-4 -3 -2 -1 0 1 2 3 4
Males
n=18
-4 -3 -2 -1 0 1 2 3 4

sample) and 11 males (68.6% of sub-sample); see Figure 5-17.

Statistical analysis of 2-D linear measure, STSa-p:

Using the Type 1 t-Test, it was shown that there were no significant differences in the 2-D length of the superior temporal sulcus on the left and right hemispheres in either the total sample ($P = 0.25$), the female sub-sample ($P = 0.53$) or the male sub-sample ($P = 0.35$); see Appendix 5-12. However, as can be seen in Figure 5-17, in both males and females, the superior temporal sulcus showed a tendency to be longer in the right hemisphere in ~61-75% of individuals.

5.4.3.3. *2-D Linear measures of superior temporal gyrus width ("STG-i", "STG-ii", "STG-iii", "STG-iv" & "STG-v")*

This series of five independent 2-D linear measures (STG i-v) represented the width of the superior temporal gyrus between the sylvian fissure and the superior temporal sulcus (Figure 5-15a). These measures included only that portion of the superior temporal gyrus situated caudal to the central sulcus. Located within this posterior region in macaques is the temporal lobe cortical area "Area Tpt", shown to be homologous to Wernicke's area in humans (Figure 5-15b). These 2-D linear measures were made directly from close-up lateral photographs of the posterior temporal lobe (Figure 3-4) using an image analysis system and a digitizing pad.

Inter-hemispheric dimensions of 2-D linear measure STG-i:

In the total sample (n = 27) the mean value for the most posterior measure of superior temporal gyrus width STG-i, (located just anterior to the sylvian point) on the left hemisphere was 2.5 ±1.1mm (max = 4.2mm, min = 1.0mm, median = 2.3mm). On the right hemisphere the mean value was 2.6 ±0.8mm (max = 4.1mm, min = 1.1mm, median = 2.7mm); see Appendix 5-14.

In females (n =14), the mean value for STG-i on the left hemisphere was 2.3 ±1.0mm and on the right hemisphere 2.3 ±0.9mm (see Appendix 5-14). In males (n = 13), the mean value for STG-i on the left hemisphere was 2.7 ±1.0, and for the right hemisphere 2.8 ±0.6 (see Appendix 5-14).

Values for this most posterior measure of superior temporal sulcus width were larger in the right hemisphere in 18 individuals (67% of sample) which included nine females (64% of sub-sample), and 9 males (69% of sub-sample); see Figure 5-18 for inter-hemispheric distribution graph.

Statistical analysis of 2-D linear measure, STG-i:

Using the type 1 t-Test it was shown that there were no significant differences between the measure STG-i in the left and right hemispheres in the total sample (n = 27) in which $P = 0.62$, the female sub-sample (n = 14) where $P = 0.95$, and in the male sub-sample (n = 13) where $P = 0.56$ (Appendix 5-15). However, it can be seen from Figure 5-18 that there was a tendency for this measure to be larger more often in the right hemisphere.

Figure 5-18 Plot of hemispheric differences in measure 1 of the width of the superior temporal gyrus (*STG-i*). Values represent differences in length (mm) between the left and right hemispheres, plotted for the largest side, in: the total sample (n=27), females (n=14), and males (n=13). Section 5.4.3.3.

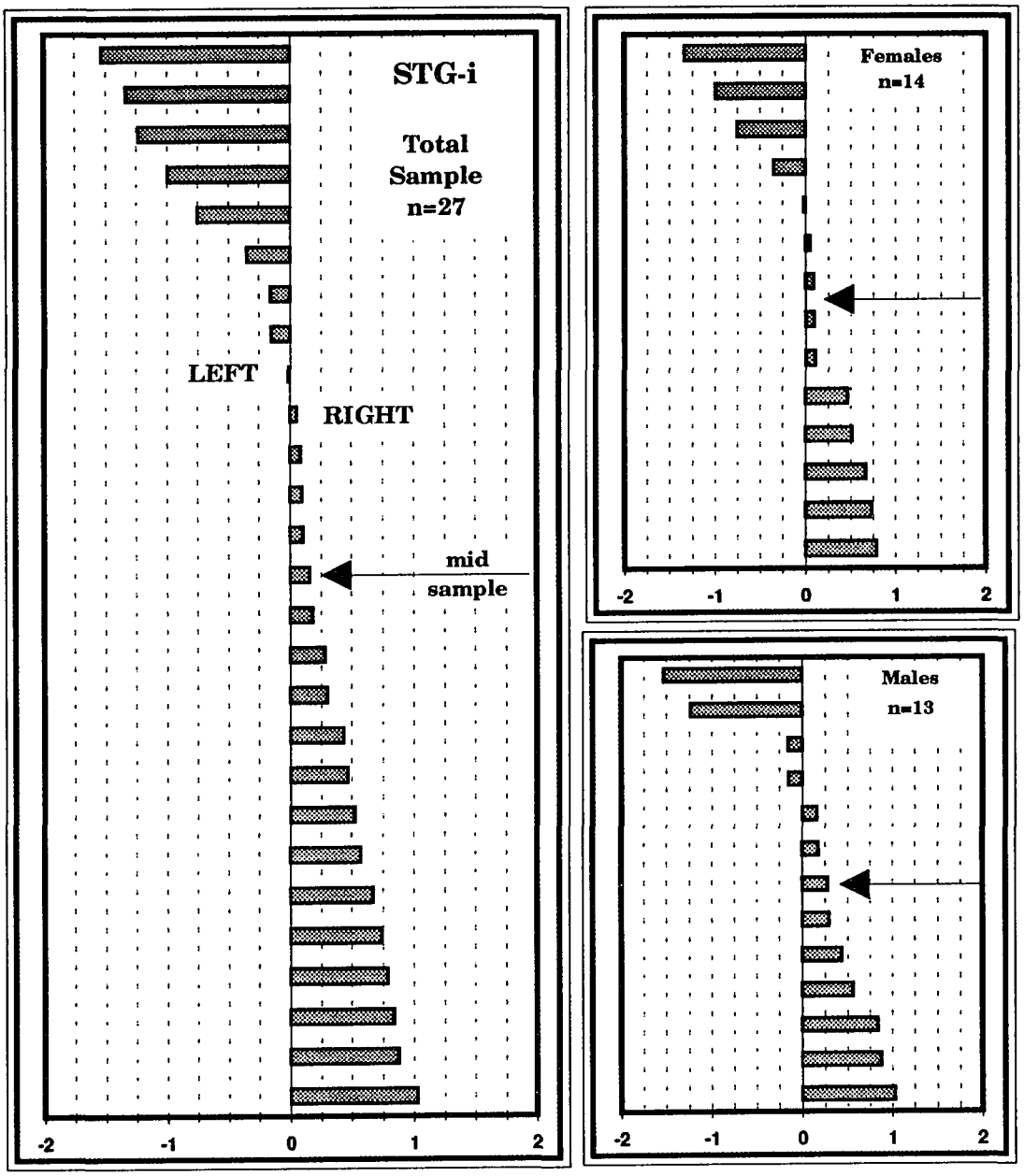
STG-i
Total
Sample
n=27
LEFT
RIGHT
mid
sample
-2
-1
0
1
2
Females
n=14
-2
-1
0
1
2
Males
n=13
-2
-1
0
1
2

Inter-hemispheric dimensions of 2-D linear measure STG-ii:

In the total sample (n = 27) the mean value for the measure of superior temporal gyrus width immediately anterior to STG-i, "STG-ii", was 3.6 ±0.7mm (max = 5.4mm, min = 2.5mm, median = 3.7mm) on the left hemisphere. On the right hemisphere the mean value was 3.9 ±0.7mm (max = 5.1mm, min = 2.9, median = 3.8mm); see Appendix 5-14.

In females (n = 14), the mean value for STG-ii on the left hemisphere was 3.6 ±0.6mm and on the right hemisphere 3.8 ±0.7mm (Appendix 5-14). In males (n = 13), the mean value for STG-ii was 3.6 ±0.7mm on the left hemisphere, and considerably larger, at 3.96 ±0.7mm, on the right hemisphere (Appendix 5-14).

As for the previous, more posterior measure of superior temporal gyrus width (STG-i, above), the measure STG-ii also showed a tendency to be larger more often in the right hemisphere. For example, in the total sample (n = 27), 17 individuals (63% of sample) were larger in the right hemisphere. This distribution for the total sample represented 57% of the female (8 of 14) and 69% of the male (9 of 13) sub-samples (Figure 5-19).

Statistical analysis of 2-D linear measure, STG-ii:

Using the type 1 t-test it was shown that there were no significant differences for the measure STG-ii between the left and right hemispheres in the total sample ($P = 0.06$), the female sub-sample ($P = 0.34$) or the male sub-sample ($P = 0.12$). However, the low, almost significant two-tailed P value

Figure 5-19 Plot of hemispheric differences in measure 2 of the width of the superior temporal gyrus (*STG-ii*). Values represent differences in length (mm) between the left and right hemispheres, plotted for the largest side, in: the total sample (n=27), females (n=14), and males (n=13). Section 5.4.3.3.

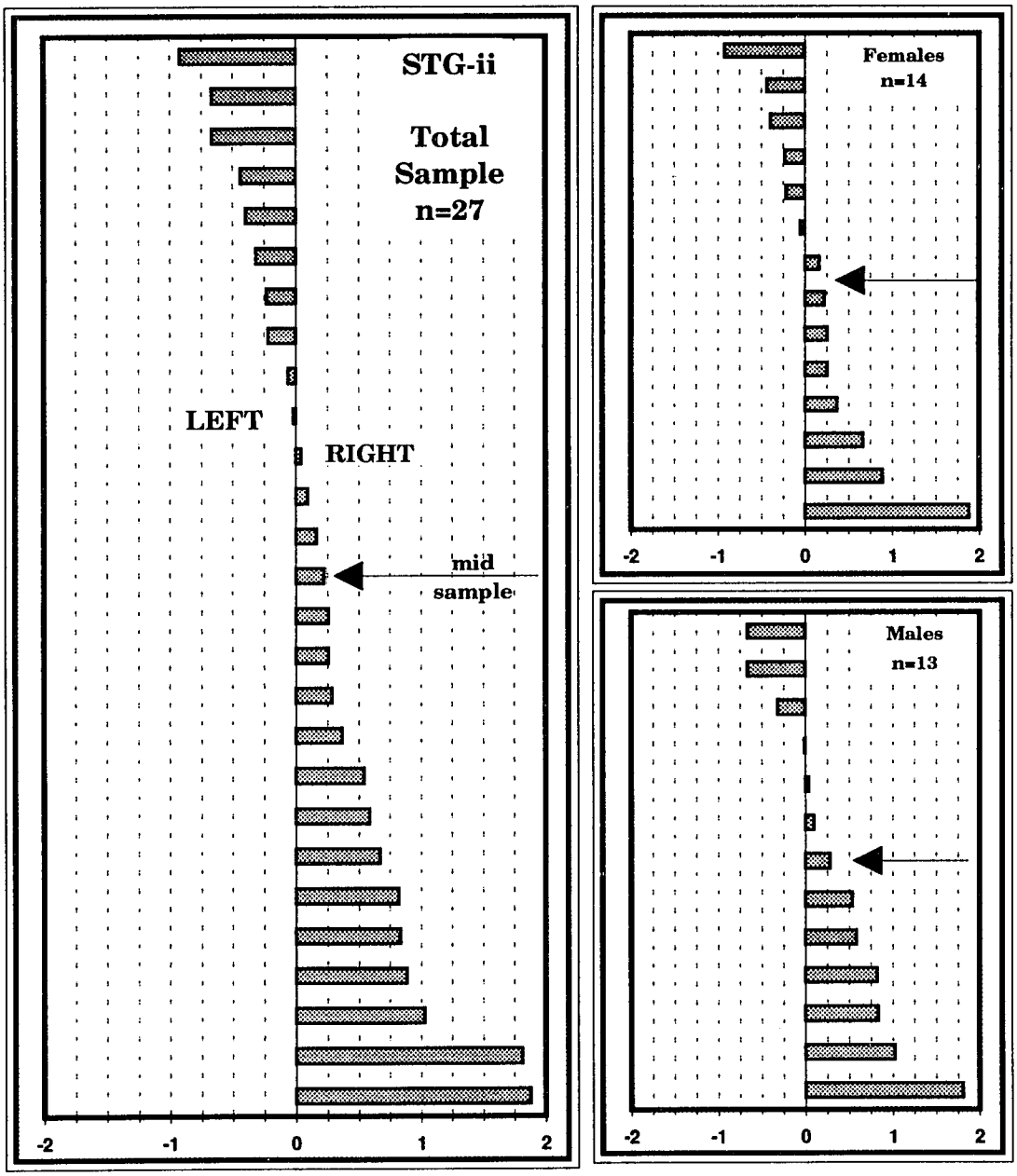
STG-ii
Total
Sample
n=27
LEFT
RIGHT
mid
sample
-2
-1
0
1
2
Females
n=14
-2
-1
0
1
2
Males
n=13
-2
-1
0
1
2

for the total sample (P = 0.06), indicated that the right hemisphere showed a strong tendency to be larger on the right hemisphere than on the left (means L = 3.6mm vs R = 3.9mm). The P value for males (P = 0.11) was much smaller than that for females (P = 0.34), but since the total sample P value (P = 0.06) was smaller than that for males and females, both sub-samples must have contributed to the outcome (Appendix 5-15).

Inter-hemispheric dimensions of 2-D linear measure STG-iii:

This third value for the 2-D linear width of the posterior portion of the superior temporal gyrus, STG-iii, represented the mid-point of this series of five independent measures (Figure 5-15a).

In the total sample (n = 27), the mean value for STG-iii on the left hemisphere was 4.5 ±0.7mm (max = 7.18mm, min = 3.57mm, median = 4.47mm) and on the right hemisphere 4.7 ±0.6mm (max = 5.8mm, min = 3.9mm, median = 4.7mm); see Appendix 5-14 & 5-15.

In females (n = 14), the mean value for STG-iii was 4.5 ±0.5mm on the left hemisphere, and 4.64 ±0.51mm on the right. In males (n = 13), the mean value for STG-iii was 4.5 ±0.9mm on the left hemisphere and 4.6 ±0.5mm on the right hemisphere (see Appendix 5-14 & 5-15).

As for the previous two more posterior measures of superior temporal gyrus width, there was a tendency for the measure STG-iii to be larger more often on the right hemisphere (Figure 5-90). In the total sample (n = 27), 21 individuals (78% of sample) were larger on the right hemisphere. This

Figure 5-20 Plot of hemispheric differences in the third measure of superior temporal gyrus width (*STG-iii*). Values represent differences in length (mm) between the left and right hemispheres, plotted for the largest side; total sample (n=27), females (n=14), and males (n=13). Section 5.4.3.3.

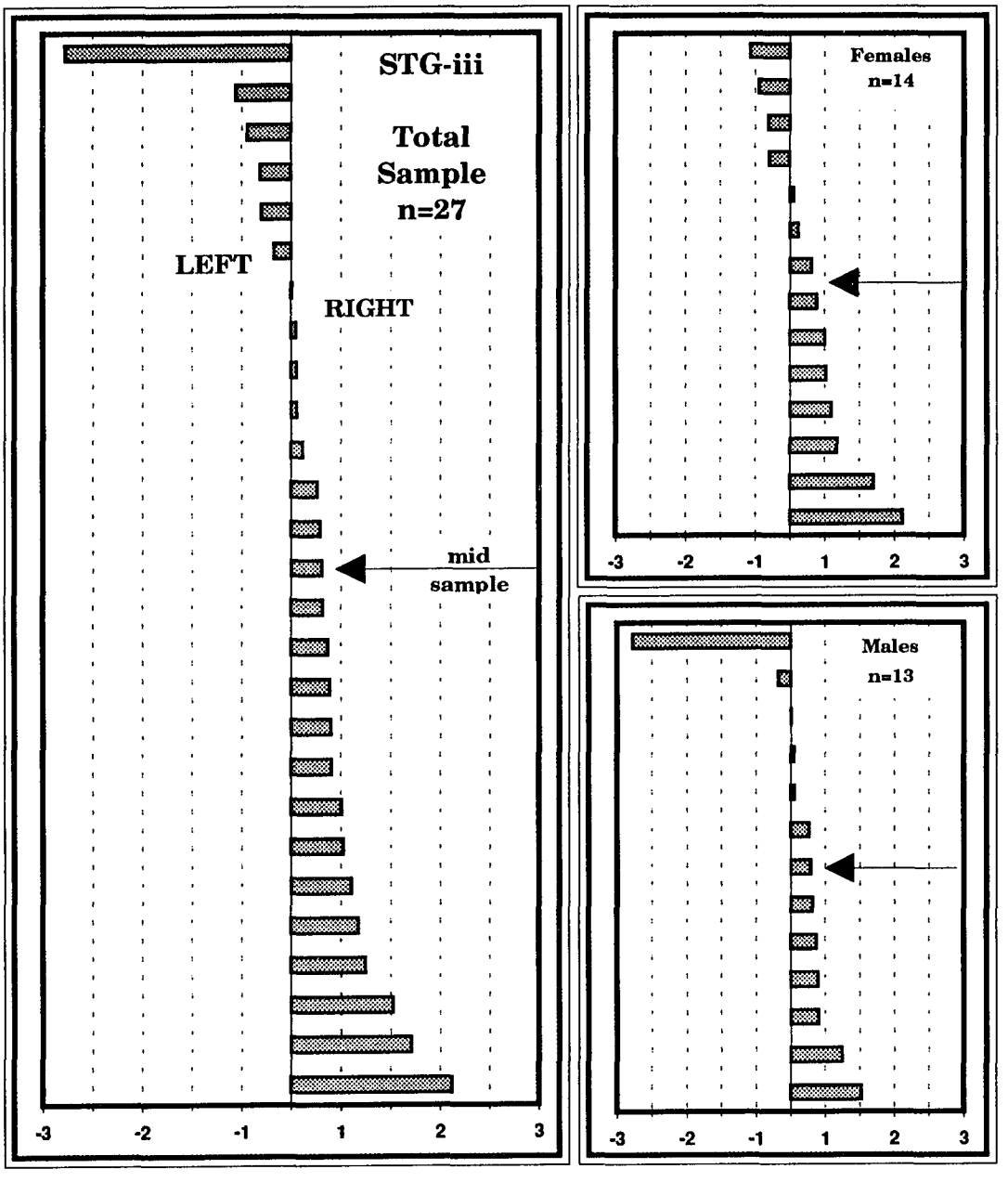
STG-iii
Total
Sample
n=27
LEFT
RIGHT
mid
sample
-3
-2
-1
1
2
3
Females
n=14
Males
n=13

included 71% of the female sub-sample (10 of 14) and 85% of the male sub-sample (11 of 13); see Figure 5-20.

Statistical analysis of 2-D linear measure, STG-iii:

Using the type 1 t-Test, it was shown that there were no significant differences between the length of STG-iii on the right and left hemispheres in the total sample ($P = 0.11$), in the female sub-sample ($P = 0.08$) or in the male sub-sample ($P = 0.59$); see Appendix 5-15.

As was the case for the previous measure of superior temporal gyrus width (STG-ii), the two-tailed value for the female sub-sample ($P = 0.08$) indicated a strong trend for this measure to be larger, once again, in the right hemisphere (mean values, L = 4.5mm vs R = 4.8mm; the one tailed t-Test was significant at $P = 0.04$. The larger P value in the total sample ($P = 0.12$) was influenced largely by the high P value for males (see Appendix 5-15).

Inter-hemispheric dimensions of 2-D linear measure STG-iv:

This was the fourth in a series of five independent measures of the 2-D linear width of the superior temporal gyrus between the sylvian fissure and superior temporal sulcus (see Figure 5-21).

In the total sample (n = 27) the mean value for STG-iv on the left hemisphere was 4.7 ±0.7mm (max = 6.8mm, min = 3.7mm, median = 4.6mm) and almost identical on the right hemisphere at 4.7 ±0.6mm (max = 6.1mm, min = 3.7mm, median = 4.5mm); see Appendix 5-14 & 5-16. In females (n =

Figure 5-21 Plot of hemispheric differences in measure 4 of the width of the superior temporal gyrus (*STG-iv*). Values represent differences in length (mm) between the left and right hemispheres, plotted for the largest side; total sample (n=27), females (n=14), & males (n=13). Section 5.4.3.3

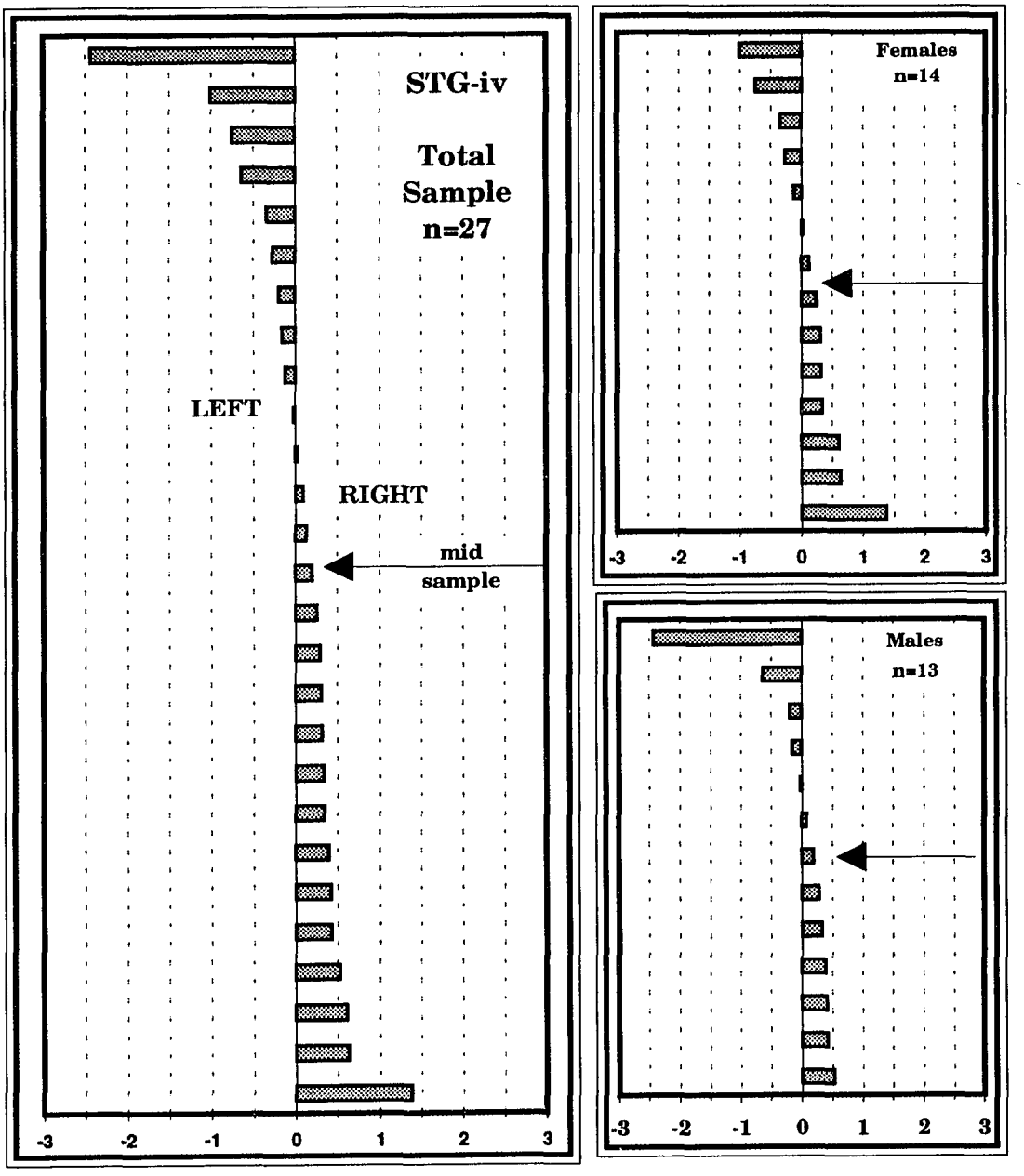
STG-iv
Total
Sample
n=27
LEFT
RIGHT
mid
sample
-3
-2
-1
0
1
2
3
Females
n=14
Males
n=13

14), the mean value for STG-iv on the left hemisphere was 4.7 ±0.6mm and on the right hemisphere, 4.8 ±0.7mm (Appendix 5-14 & 5-16). In males (n = 13), the mean value for STG-iv on the left hemisphere was, unusually, smaller than that for females, at 4.6 ±0.74mm and on the right hemisphere, 4.5 ±0.5mm (Appendix 5-14 & 5-16).

In the total sample (n = 27), 17 individuals (63% of sample) showed a larger value for STG-iv on the right hemisphere. This sample included nine females (64% of sub-sample) and eight males (62% of sub-sample); see Figure 5-21.

Statistical analysis of 2-D linear measure, STG-iv:

Using the type 1 t-Test it was shown that there were no significant differences between the measure STG-iv between the left and right hemispheres in either the total sample ($P = 0.8$), the female sub-sample ($P = 0.49$) or the male sub-sample ($P = 0.82$); see Appendix 5-16.

Inter-hemispheric dimensions of 2-D linear measure STG-v:

This was the final measure in the series of five independent measures of the width of the superior temporal gyrus between the sylvian fissure and superior temporal sulcus. This measure was the most anterior of the series and was located immediately inferior to the central sulcus.

The mean value for STG-v on the left hemisphere in the total sample (n = 27), was 4.8 ±0.7mm (max = 6.6mm, min = 3.7mm, median = 4.8mm) and on

Figure 5-22 Plot of hemispheric differences in measure 5 of the width of the superior temporal gyrus (*STG-v*). Values represent differences in length (mm) between the left and right hemispheres, plotted for the largest side, in: the total sample (n=27), females (n=14), and males (n=13). Section 5.4.3.3

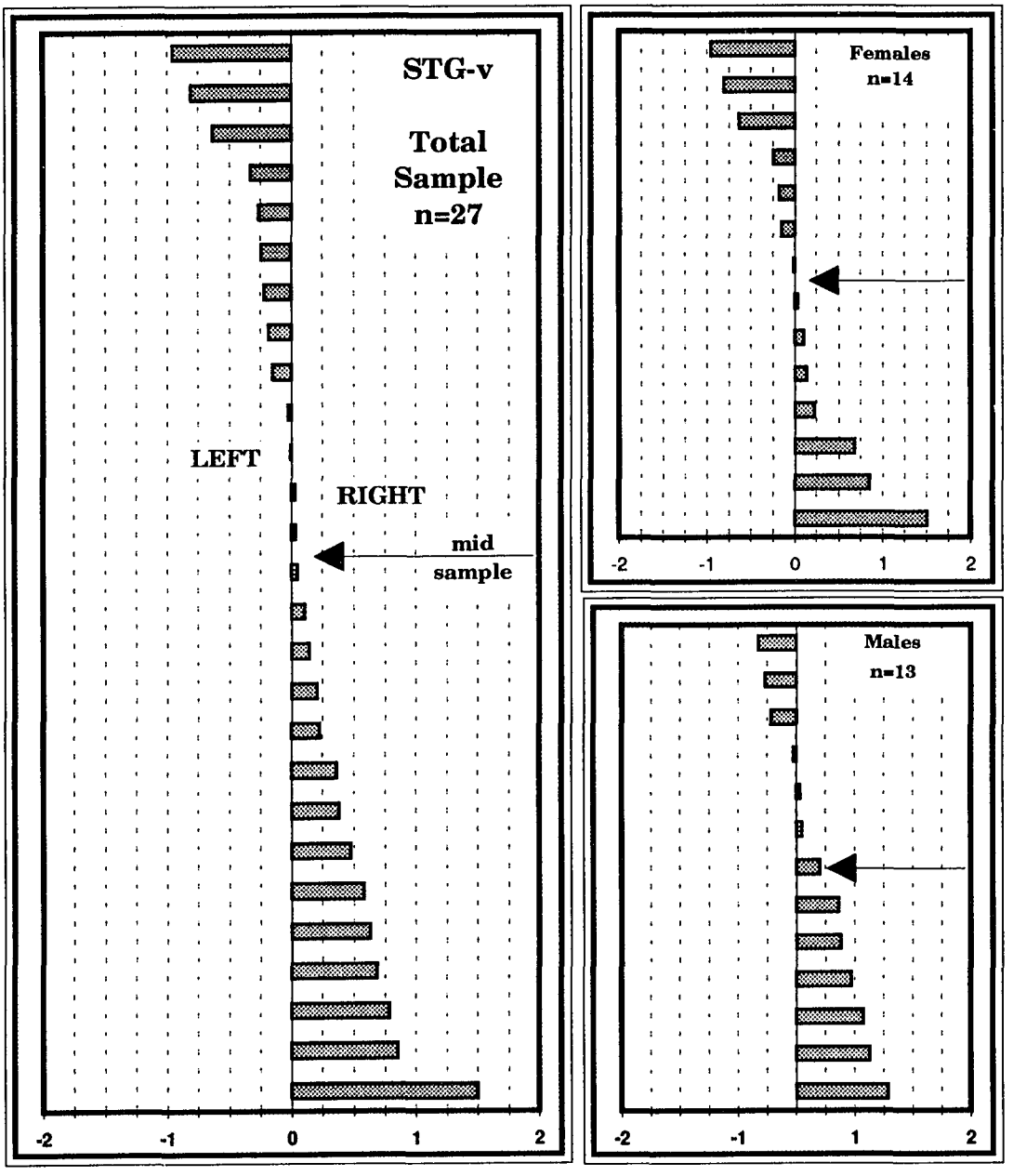
STG-v
Total
Sample
n=27
LEFT
RIGHT
mid
sample
-2
-1
0
1
2
Females
n=14
-2
-1
0
1
2
Males
n=13
-2
-1
1
2

the right hemisphere, 4.9 ±0.7mm (max = 6.2mm, min = 3.7mm, median = 4.9mm); (Appendix 5-14).

In females (n = 14), the mean value for STG-v length in the left hemisphere was 5.02 ±0.9mm and for the right hemisphere 5.1 ±0.8mm; (Appendix 5-14). In males (n = 13), the mean value for STG-v length in theleft hemisphere was 4.6 ±0.5mm and on the right hemisphere, 4.8 ±0.6mm (Appendix 5-14). In males (n = 13), the mean value for STG-v length in the left hemisphere was 4.6 ±0.5mm and on the right hemisphere, 4.8 ±0.6mm (Appendix 5-14).

In the total sample, 16 individuals (59% of sample) showed a value for STG-v that was larger in the right hemisphere. In females, 7 individuals (50% of sub-sample) and in males 9 individuals (69% of sub-sample) showed a larger value for STG-v in the right hemisphere. In this most anterior measure, a right hemisphere preponderance was not as dramatic as in the other four more posterior measures in the series (Figure 5-22).

Statistical analysis of 2-D linear measure, STG-v:

Using the type 1 t-Test, it was shown that in the total sample (n = 27) there was no significant difference between the length of STG-v in the left and right hemispheres ($P = 0.24$); see Appendix 5-16. In females, there was also no significant difference for this measure between the left and right hemispheres ($P = 0.8$). In males however, STG-v was close to being significantly larger on the right hemisphere at $P = 0.06$. The one-tailed P

value for this measure showed a significantly larger right hemisphere (P = 0.03). Interestingly, the lower P value for the total sample was influenced by the male sub-sample alone. This distinction is important since, although the sub-sample size was relatively small to adequately describe such a subtle effect, the sex difference in hemispheric asymmetry was striking.

Analysis of pooled data from the five independent measures STG-1, STG-ii, STG-iii, STG-iv, & STG-v:

The five independent measures of superior temporal gyrus width were made in an attempt to localize the exact antero-posterior location of maximum inter-hemispheric asymmetry. For this final analysis, the values were pooled in order to assess the global distribution in the total sample (n = 135) of the overall pattern of inter-hemispheric asymmetry (Figure 5-23).

In the total sample of the combined measures STG-i - STG-v (n = 135), 89 measures (66% of total sample) were larger in the right hemisphere. This value for the pooled sample is quite similar to values for right hemisphere preponderance seen in most of the previous measures (Figure 5-23).

Statistical analysis of pooled 2-D linear measure, STG-i - STG-v:

Using the type 1 t-Test on pooled data for the total sample of five independent measures, STG-i to STG-v (n = 135), it was shown that this measure was highly significantly larger in the right hemisphere (P = 0.014 two-tailed ; and P = 0.007 one-tailed) with mean values of L = 4.01mm vs R = 4.15mm; (Figure 5-23).

Figure 5-23 Plot of hemispheric differences in five pooled measures of the width of the superior temporal gyrus (STG-i-v). Values represent differences in length (mm) between the left and right hemispheres, plotted for the largest side, in the total pooled sample (n=135). Section 5.4.3.3

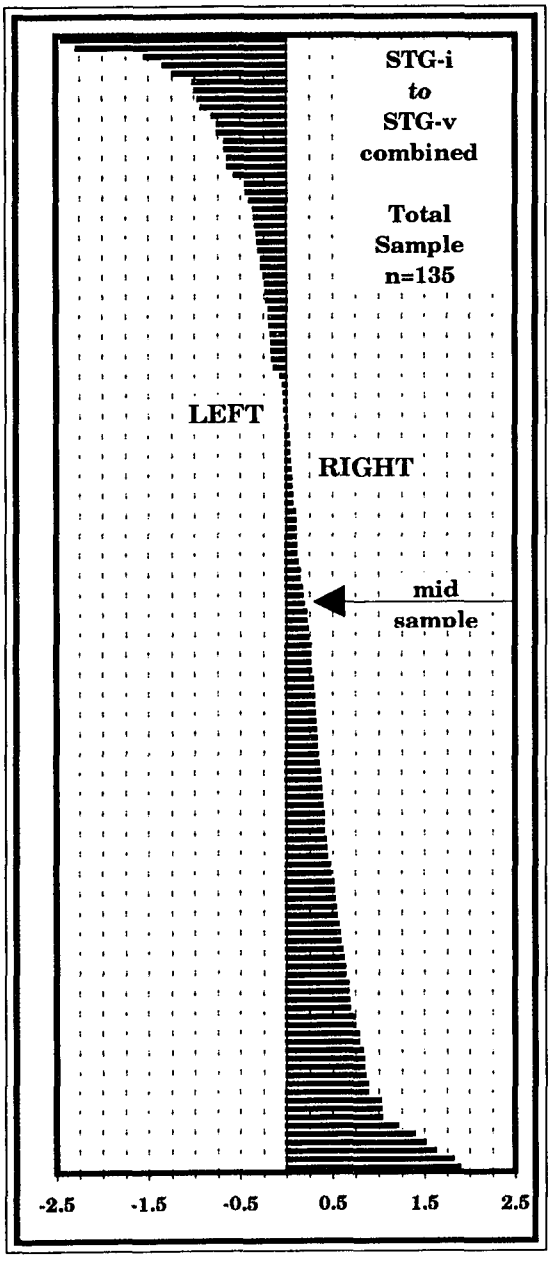

Paired t-Test of combined sample

	STGi-v	
	LEFT	*RIGHT*
Mean	4.01	4.15
Variance	1.34	1.20
Observations	135	135
Pearson Correl'n	0.83	
Hypoth Mean Diff	0	
df	134	
t Stat	-2.49	
P(T<=t) one-tail	0.007	***
t Critical one-tail	1.66	
P(T<=t) two-tail	0.014	***
t Critical two-tail	1.98	

R > L (P < 0.01)

5.4.3.4. 2-D measures of the total area of the superior temporal gyrus on the surface of the brain (STG-tot²)

This measure of superior temporal gyrus total area (STG-tot) in square millimeters was made from archival photographs of the lateral aspect of the entire brain using a quantitative digitizing pad and stylus system (Figure 5-14, Section 5.4.2.2.).

The most posterior point of the sylvian fissure, the sylvian point, could not be definitively located on a number of photographs. This was because the region was either totally or partially obscured by overlapping parietal cortex. In these cases, the posterior boundary of STG-tot² was the confluence of the sylvian fissure and the superior temporal sulcus. In most cases a similar condition of this anatomical variation was present bilaterally (see Section 3.3.2.1. for details).

In cases of where the sylvian point was visible, the posterior border of the superior temporal gyrus was defined as the region, just posterior to the sylvian point, where the superior temporal sulcus turned through almost 90° supero-medially (Figure 3-4). The anterior border of STG-tot² was defined by the definitive cutoff margin determined by the lateral viewpoint perspective of the 2-D photograph (Figure 3-2).

Inter-hemispheric dimensions of 2-D area measure STG-tot²:

In the total sample for this measure (n = 33) the mean value for the total brain surface area of the superior temporal gyrus (STG-tot²) on the left

hemisphere was 190.1 ±39.7mm^2 (max = 305.3mm^2, min = 115.9mm^2, median = 186.4mm^2). On the right hemisphere, the mean value for STG-tot^2 on the right hemisphere was almost identical at 190.3 ± 37.9mm^2 (Appendix 5-17 & 5-18).

In females (n = 15) the mean value for STG-tot^2 on the left hemisphere was smaller than the total sample mean at 172.3 ±28.7mm^2. On the right hemisphere, STG-tot^2 was smaller than the left at 169.3 ±29.3mm^2. In males (n = 18), the mean length of STG-tot^2 was larger than the total sample mean at 205 ±42.2mm^2 in the left hemisphere, and even larger in the right hemisphere at 207.7 ±35.8mm^2 (see Appendix 5-17 & 5-18).

The 2-D area of the superior temporal gyrus was larger in the left hemisphere in a total of 16 individuals (48.5% of the total sample). This included eight females (53.3% of sub-sample) and eight males (44.4% of sub-sample; see Figure 5-24). The area of the superior temporal gyrus was larger in the right hemisphere in a total of 17 individuals (51.5% of total sample). this included seven females (46.7% of sub-sample) and 10 males (55.6% of sub-sample); see Figure 5-24. Essentially, unlike the majority of previous measures, there was no indication of a right hemisphere predominance of the 2-D area of the superior temporal gyrus (Figure 5-24).

Statistical analysis of 2-D area measure, STG-tot^2:

Using the Type 1 t-Test, it was shown that there were no significant differences in the area of the superior temporal gyrus on the left and right

Figure 5-24 Plot of hemispheric differences in the 2-D area of the superior temporal gyrus (*STG-tot*^{2}). Values represent differences in area (mm^2) between the left and right hemispheres, plotted for the largest side, in the total sample (n = 33), females (n = 15) and males (n = 18). Section 5.4.3.4

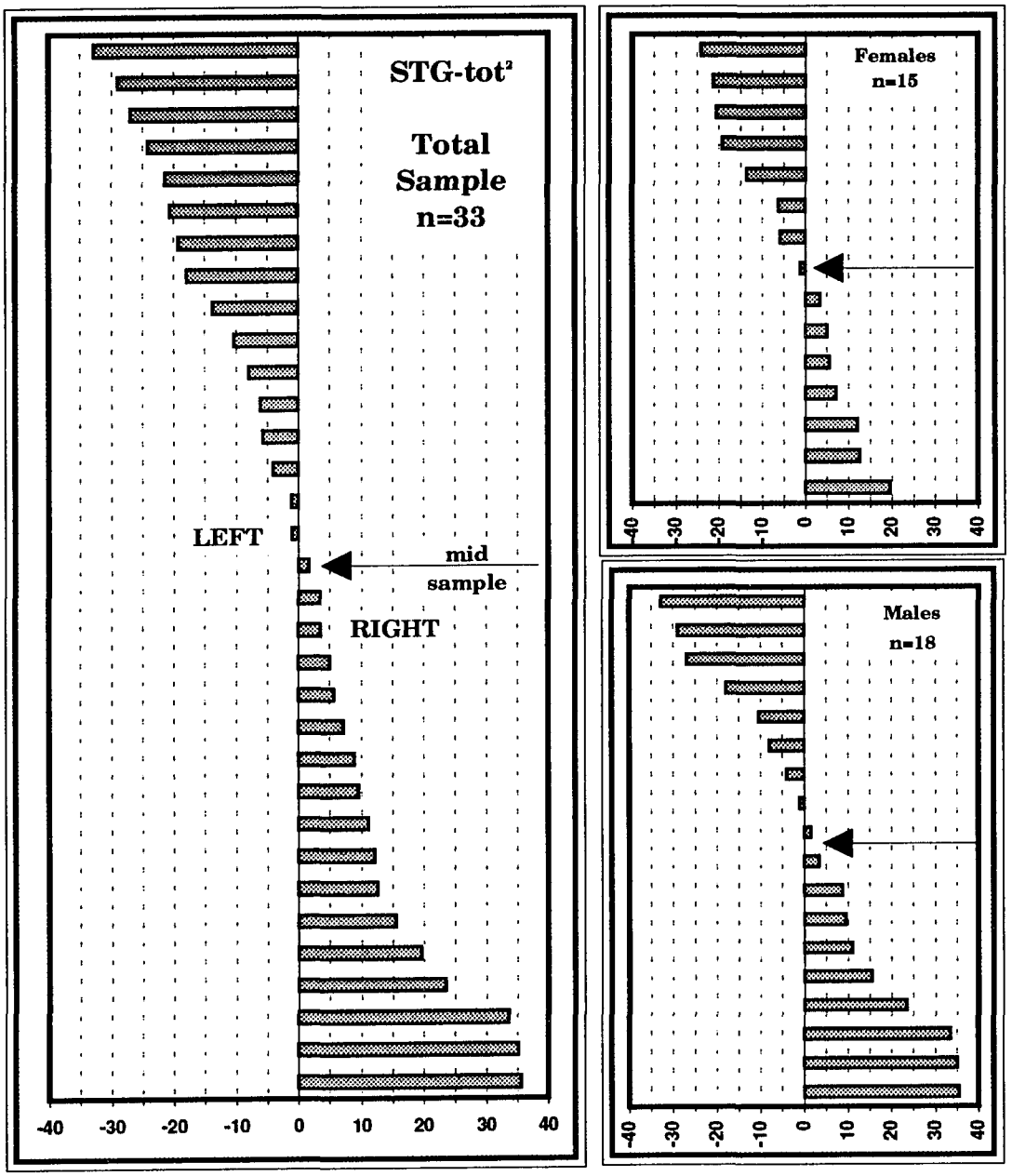
STG-tot²
Total Sample n=33
LEFT
mid sample
RIGHT
-40 -30 -20 -10 0 10 20 30 40
Females n=15
-40 -30 -20 -10 0 10 20 30 40
Males n=18
-40 -30 -20 -10 0 10 20 30 40

hemispheres in either the total sample (n = 33) where $P = 0.97$, the female sub-sample (n = 15) where $P = 0.42$, or the male sub-sample (n = 18) where $P = 0.59$; see Appendix 5-18. As can be seen in Figure 5-24, in both males and females, there was no indication of a trend towards hemispheric asymmetry in this measure of superior temporal gyrus area. In fact, the pattern showed an even distribution between the two hemispheres, with no tendency towards right hemisphere dominance as seen for the superior temporal sulcus and the majority of other measures.

5.4.3.5. 2-D measure of the area of the posterior region of the superior temporal gyrus (STG-Tpt^2)

These measures of the surface area of a sub-region of the superior temporal gyrus area, located posterior to the central sulcus (STG-Tpt^2), were made from lateral photographs of the brain using a quantitative digitizing system (Figure 5-15b). The anterior border of this measure was defined as the constructed line STG-v (Section 5.4.2.2.). The posterior border was the same as that described for area measure STG-tot^2 (Section 5.4.3.4.). This posterior region of the superior temporal gyrus in macaques contains the cytoarchitectonic area (Area Tpt) that is homologous to Wernicke's area in humans.

Inter-hemispheric dimensions of 2-D area measure STG-Tpt^2:

In the total sample (n = 26) the mean value for the brain surface area of the posterior region of the superior temporal gyrus, STG-Tpt^2, on the left

Figure 5-25 Plot of hemispheric differences in the 2-D area of the posterior region of the superior temporal gyrus (*STG-Tpt*^{2}). Values represent differences in area (mm^2) between the left and right hemispheres, plotted for the largest side, in the total sample (n = 26), females (n = 13) and males (n = 13); Section 5.4.3.5.

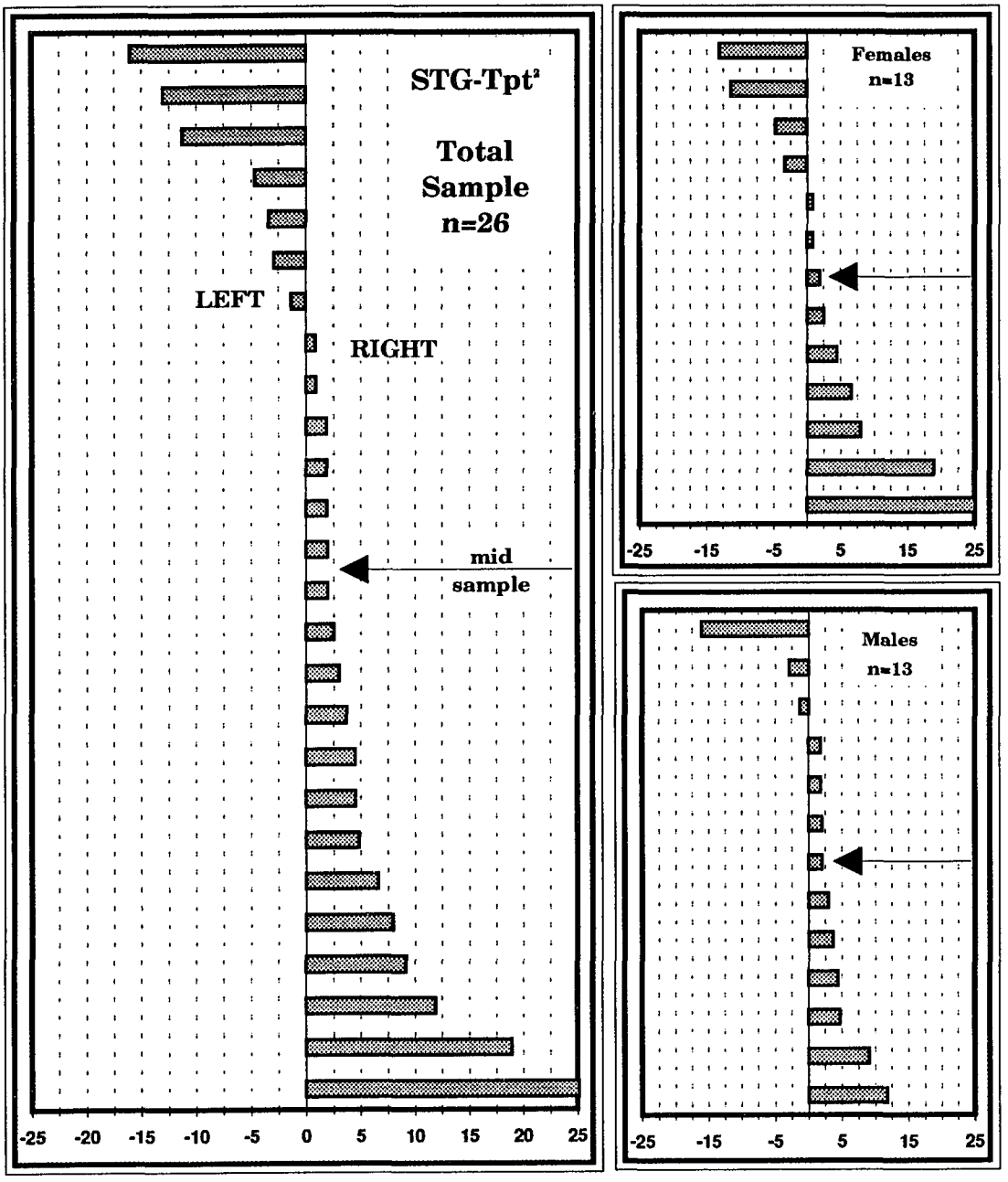
STG-Tpt²
Total Sample n=26
LEFT
RIGHT
mid sample
-25 -20 -15 -10 -5 0 5 10 15 20 25
Females n=13
-25 -15 -5 5 15 25
Males n=13
-25 -15 -5 5 15 25

hemisphere was 58.3 ±13.1mm^2 (max = 88.7mm^2, min = 40.03mm^2, median = 55.52mm^2). On the right hemisphere, the mean value for STG-Tpt^2 was slightly larger at 60.7 ±13.1 (max = 90.8mm^2, min = 42.8mm^2, median = 59.5mm^2 (Appendix 5-19).

In females (n = 13) the mean value for STG-Tpt on the left hemisphere was smaller than the total sample mean at 57.0 ±13.5mm^2 and on the right hemisphere somewhat larger at 59.9 ±13.0mm^2 (Appendix 5-19).In males (n = 13), the mean area for STG-Tpt on the left hemisphere was larger than the total sample mean at 59.6 ±13.1mm^2, and on the right hemisphere 61.5 ±13.6mm^2 (Appendix 5-19).

Individual values for area of the posterior region of the superior temporal gyrus (STG-Tpt^2) in the total sample (n = 26) were larger in the left hemisphere in seven individuals (27% of sample), including four females (31% of sub-sample) and three males (23% of sub-sample), (Figure 5-25). Conversely, STG-Tpt^2 was larger in the right hemisphere in 19 individuals (73% of total sample) including nine females (69% of sub-sample) and ten males (77% of sub-sample).

As can be seen in Figure 5-25, the distribution of hemispheric asymmetry predominated in the right hemisphere in the total sample as well as the male and female sub-samples. In all cases, larger values for the right side extend well past the arrow denoting the sample mid-range.

Statistical analysis of 2-D area measure, STG-Tpt²:

Using the Type 1 t-Test, it was shown that there were no significant differences in the area of the posterior region of the superior temporal gyrus between the left and right hemispheres in either the total sample (n = 26) at $P = 0.17$, the female sub-sample (n = 13) at $P = 0.35$, or the male sub-sample (n = 13) at $P = 0.31$ (Appendix 5-20).

However, the P value for the total sample was quite low ($P = 0.17$) and was much lower than the sex-specific sub-samples suggesting a contribution to total sample P value from both sub-samples. Furthermore, if indeed the offset distribution of R>L hemispheric asymmetry represents an offset distribution, the almost significant 1-tailed P value for the total sample ($P = 0.08$, Appendix 5-20) indicates a marked trend towards STG-Tpt2 being larger in the right hemisphere. This result is in marked contrast with the unequivocal symmetry shown for the total area of the total superior temporal gyrus (Figure 5-24).

5.5. FRONTAL AND OCCIPITAL PETELIAS AND WIDTHS OF THE CEREBRAL HEMISPHERES

5.5.1. 2-D linear measures of hemispheric petelial projections

Petelial projection refers to the asymmetric projection of the frontal or occipital pole of one hemisphere beyond that of the contralateral hemisphere,

in the longitudinal axis. The standard pattern in humans is a combination of right frontal and left occipital petelial projections.

This section quantified the dimensions, and assessed the inter-hemispheric patterns, of anterior projections of the frontal lobes and posterior projections of the occipital lobe in *Macaca fascicularis* brains (n = 23). The dimensions of left and right frontal and occipital projection asymmetry were determined by linear measures taken from the low power archival macro-photographs of the dorsal surface of the brain (Figure 3-1a). Refer to Section 5.2. for an overview of the method used here.

5.5.1.1. (Linear distance "FR-pet", Figure 5-26)

This measure represented the distance by which the frontal pole of one hemisphere projected anteriorly beyond the opposite hemisphere.

A line "A-B" (Figure 5-26) was drawn along the midline between the two cerebral hemispheres (along the longitudinal cerebral fissure), and extended beyond its margins posteriorly and anteriorly. Using a dissecting microscope (20x magnification) a drafting square and steel scribe were used to scratch two extremely fine lines (onto the plastic overlay) at right angles to line "A-B" corresponding to where they transect the distal-most points on the poles of the left and right frontal lobes (Figure 5-26). The anteroposterior distance between these lines was measured using a digital caliper while viewing it under the dissecting microscope. The distance and the hemisphere projecting

beyond the other was noted. If the distance was too small to be measured by the digital caliper, the plastic film was viewed on a light microscope at 63x magnification and measurements made using an ocular micrometer. These ocular measures were translated to absolute values (mm) by calibration to a 2mm scale stage micrometer with divisions of 0.01mm. This method allowed for a high level of accuracy (<0.1mm)

5.5.1.2. (Linear distance "OC-pet", Figure 5-26)

This measure represented the distance by which the occipital pole of one hemisphere projected posteriorly beyond the opposite hemisphere.

Two lines were drawn at right angles to line A-B (see Section 5.4.1.2., above and Figure 5-26) corresponding to where they transected the posterior distal-most points on the poles of the left and right occipital lobes. The anteroposterior distance between the two lines, measured along line A-B (Figure 5-26), and the hemisphere projecting beyond the other, was noted. The measurement methods used were the same as that described for FR-pet (Section 5.5.1.1.)

5.5.2. 2-D linear measures of hemispheric widths

5.5.2.1. (Linear distance "FRw-a", Figure 5-26)

Anterior frontal lobe width on the left and right hemispheres.

The medial to lateral distance of the width of the left and right frontal lobes at the anteroposterior level immediately anterior to the arcuate sulcus (points "a" and "b" on Figure 5-26). This distance is measured at right angles to line A-B (Figure 5-26). The medial border of this measure was defined as the most medial part of the hemisphere and not the constructed line A-B (Figure 5-26). This precaution took into account those cases where the longitudinal fissure was an open cleft.

5.5.2.2. (Linear distance "FRw-p", Figure 5-26)

Posterior frontal lobe width on the left and right hemispheres.

This measure represented the medial to lateral width of the left and right frontal lobes at the anteroposterior level between the lateral margins of the arcuate sulci and the central sulci (points "c" and "d" on Figure 5-26). The anteroposterior distance between these two landmarks was measured then divided to arrive at the midpoint. The medial-lateral distance (FRw-p) was measured from this midpoint at right angles to line A-B.

5.5.2.3. (Linear distance "PAw-a", Figure 5-26)

Anterior parietal lobe width on the left and right hemispheres.

The medial to lateral distance of the width of the left and right parietal lobes at the anteroposterior level between the lateral margins of the central sulcus and the superior temporal sulcus (points "e" and

"f" on Figure 5-26). The distance between these two landmarks was measured and divided to arrive at the midpoint. The hemispheric medial-lateral width was measured along this anteroposterior midpoint at right angles to line A-B.

5.5.2.4. (Linear distance "PAw-p", Figure 5-26)

Posterior parietal lobe width on the left and right hemispheres.

The medial to lateral width of the left and right parietal lobes was measured at the anteroposterior level intermediate between the lateral margins of the superior temporal sulcus anteriorly and the parieto-occipital (lunate) sulcus posteriorly (points "g" and "h" on Figure 5-26). The distance between the two sulcal landmarks was measured then divided to find the midpoint. Hemispheric width was measured along this antero-posterior midpoint at right angles to line A-B

Figure 5-26 2-D linear and area measures made from archival photographs of the dorsal surface of the brain, including: ***1)*** Linear measures (mm) of frontal and occipital pole petelial projections (FR-pet & OC-pet) Section 5.4.1.; and ***2)*** Anterior and posterior frontal and parietal lobe widths (FRw-a, FRw-p, PAw-a, & PAw-p). Section 5.5.2.

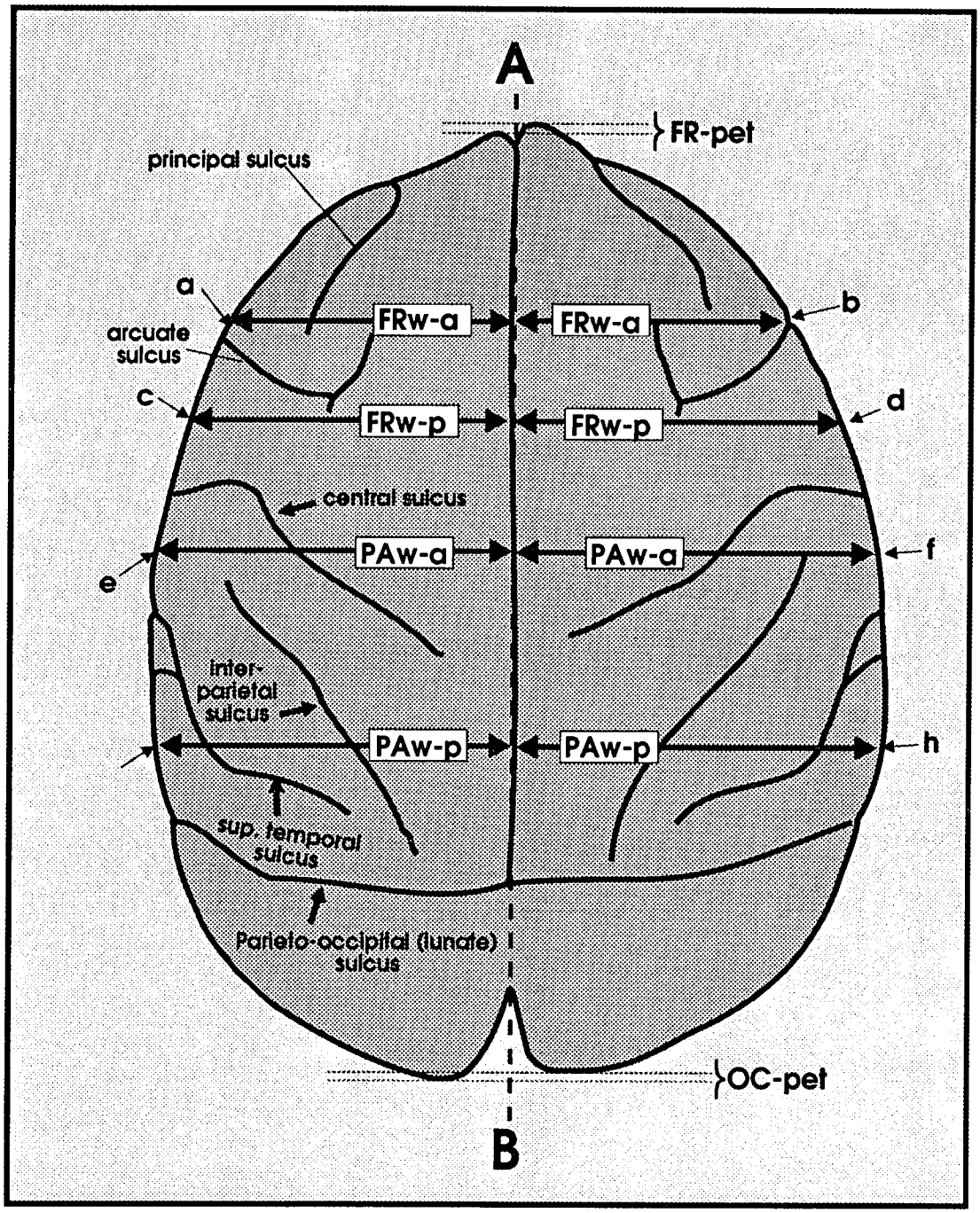
A
FR-pet
principal sulcus
a
b
arcuate sulcus
FRw-a
FRw-a
c
d
FRw-p
FRw-p
central sulcus
PAw-a
PAw-a
e
f
inter-parietal sulcus
PAw-p
PAw-p
h
sup. temporal sulcus
Parieto-occipital (lunate) sulcus
OC-pet
B

5.5.3. Results of 2-D linear measures of occipital and frontal lobe petelias

5.5.3.1. 2-D linear measures of frontal lobe petelial projection

In the total sample (n = 22), ten individuals (45.5% of total sample) showed anterior petelial extension of the left frontal lobe beyond that of the right frontal lobe. This included females (n = 8, - 57% of sub-sample), and males (n = 2 - 25% of sub-sample). The mean value for this left hemisphere extension was 0.25 ±0.05mm (max = 0.37mm, min = 0.18mm, median = 0.23mm).

A further nine individuals (41% of total sample), showed petelial extension of the right frontal pole, anterior to that of the left side, with a mean value slightly larger than that of the left hemisphere, of 0.27 ±0.09mm (max = 0.77mm, min = 0.11mm, median = 0.24mm). This included five females (35.7% of sub-sample), and four males (50% of sub-sample). See Figure 5-27 for the size range and distribution of left vs right frontal petelial extensions. Three individuals (1 female and 2 males) showed no difference between the most anterior point of the left or right frontal poles.

In sum, 10 of 22 individuals showed a petelial extension of the left hemisphere frontal lobe beyond that of the right, while 9 of 22 individuals showed extension of the right hemisphere beyond the left. Three individuals did not show any petelial extension of either hemisphere (Figure 5-27). In females the predominance appeared to be in the left hemisphere (Figure 5-

Figure 5-27 Plot of hemispheric differences in petelial projections of the frontal lobes (FR-pet). Values represent the distance (mm) by which one frontal lobe projects beyond that in the contralateral hemisphere. Total sample (n = 19/22; 3 showed no difference), females (n = 13/14) and males (n = 6/8). Section 5.5.3.1; Appendix 5-21 & 5-22.

FRONTAL LOBE PETELIAL PROJECTION

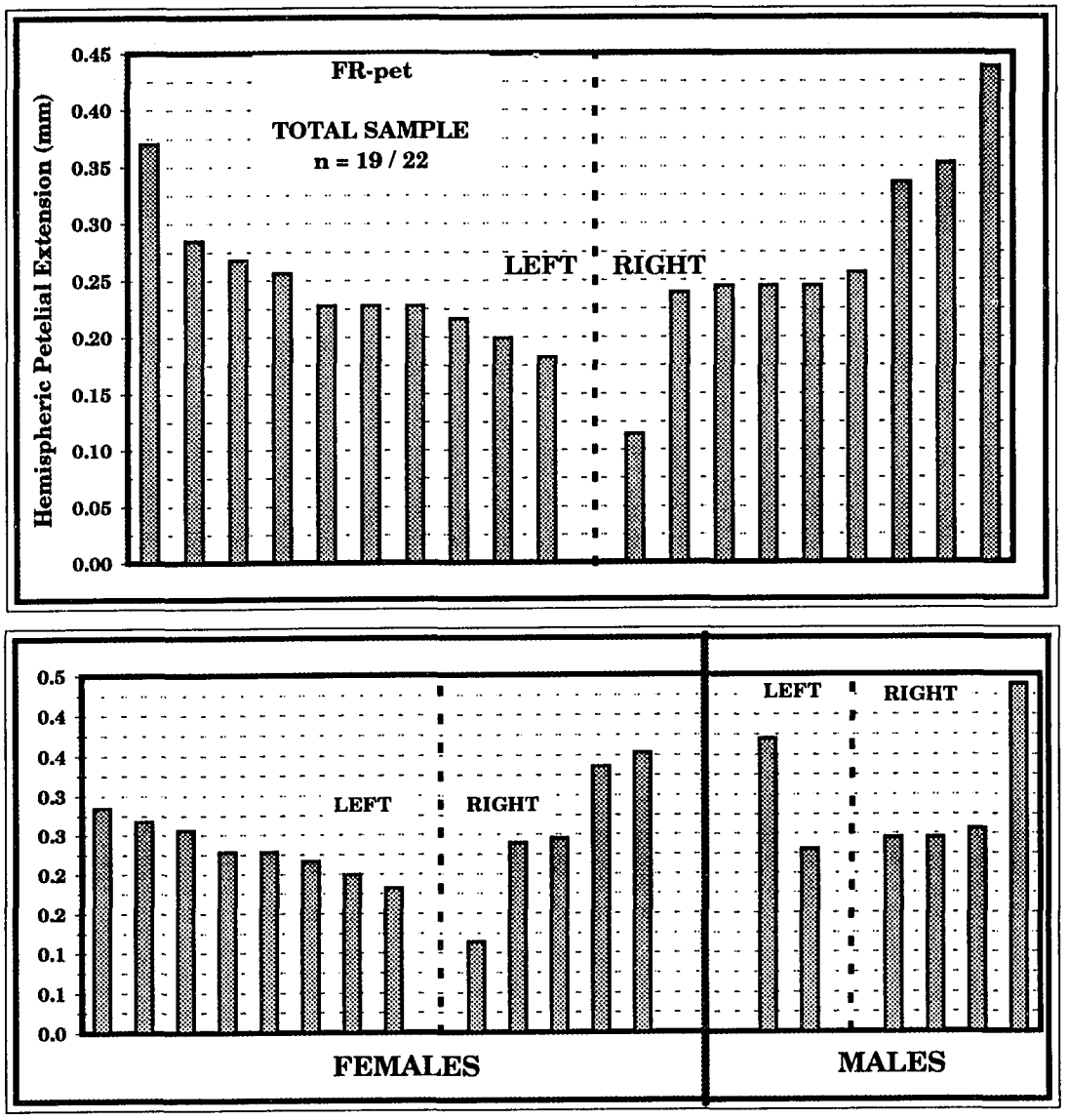

27) with a ratio of L:R of 1.6:1. In males the predominance appeared to be towards the right hemisphere with a ratio of 1:2. However, sample sizes were too small to make definitive statements regarding sex-specific differences at this stage.

Statistical analysis of frontal lobe petelial projection:

Using the Type 2 t-Test (assuming equal variance), it was shown that there were no significant differences between the extent of petelial extension of the frontal pole on the left and right hemispheres in the sample of 19 (10L:9R) individuals that showed this feature ($P = 0.41$).

5.5.3.2. 2-D Linear measures of occipital lobe petelial projection

In the total sample (n = 22), 13 individuals (59% of sample) showed petelial extension of the left occipital lobe beyond that of the right. This included nine females (64% of sub-sample), and four males (50% of sub-sample). The mean value for this left hemisphere posterior extension was 0.36 ±0.26mm (max = 0.77mm, min = 0.11mm, median = 0.22mm).Six individuals (27.3% of sample), showed petelial extension of the right occipital lobe posterior to that of the left side with a mean value of 0.53 ±0.55mm (max = 1.51mm, min = 0.09mm, median = 0.3mm). This right hemisphere group included four females (29% of sub-sample) and two males (25% of sub-sample). A further three individuals (1 female and 2 males) showed no hemispheric difference between the most posterior point of the occipital poles.

Figure 5-28 Plot of hemispheric differences in petelial projections of the occipital lobes (OC-pet). Values represent the distance (mm) by which one occipital lobe projects beyond that in the contralateral hemisphere. Total sample (n = 19/22; 3 showed no difference), females (n = 13/14) and males (n = 6/8). Section 5.5.3.2; Appendix 5-21 & 5-23.

OCCIPITAL LOBE PETELIAL PROJECTION

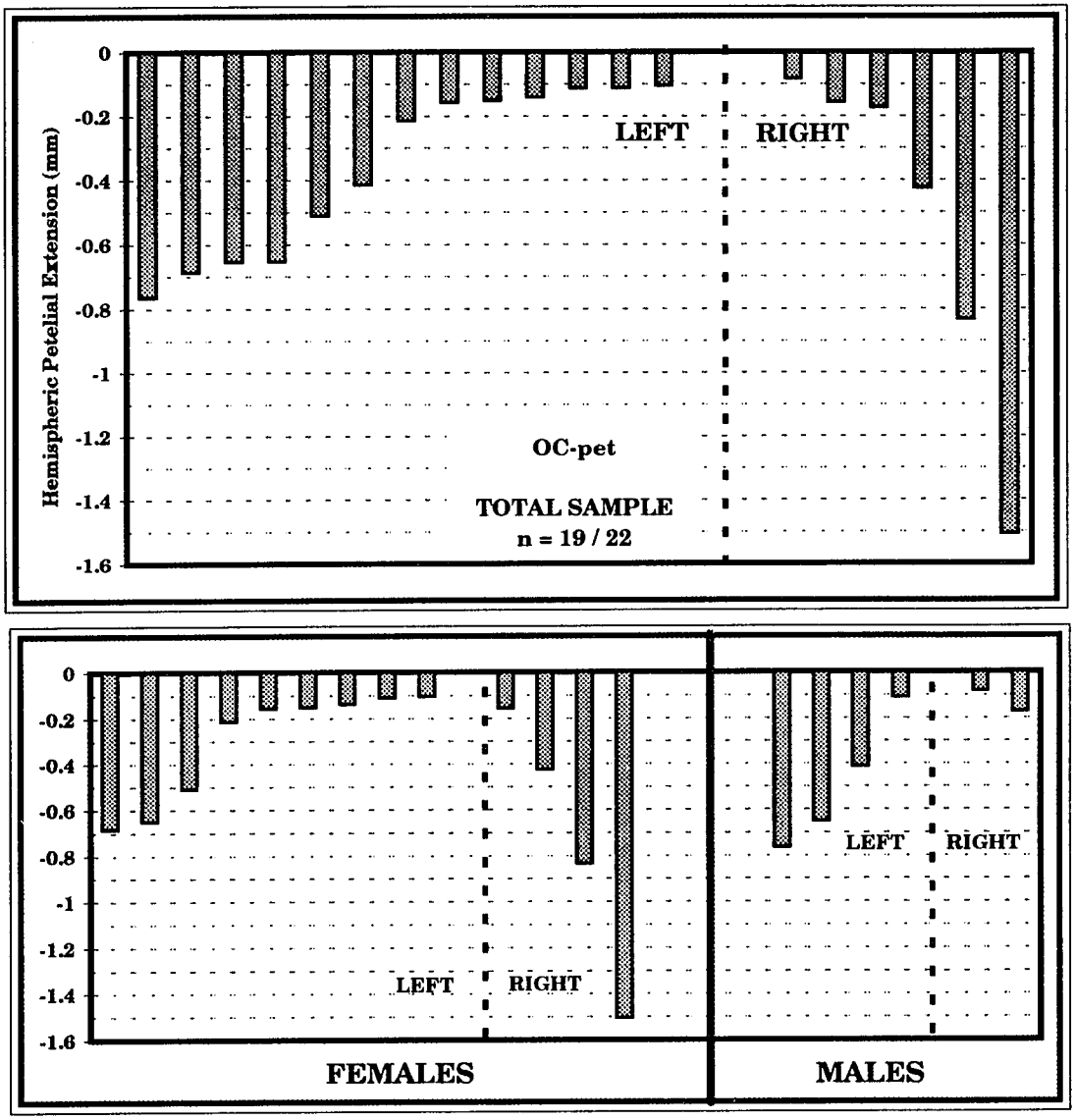

The petelial projection of the occipital pole in this sample appeared to predominate in the left hemisphere with 13 of 19 individuals projecting further posteriorly on this side with a ratio of 2.2:1. This was also apparent in the sex-specific sub-samples with females showing a ratio for L:R of 2.25:1 and for males 2:1 (Figure 5-28).

Statistical analysis of occipital lobe petelial projection:

Using the Type 2 t-Test, it was shown that there were no significant differences between the extent of petelial extension of the occipital pole on the left and right hemispheres in the total sample (n = 19 of 22 , 13L vs 6R) at P = 0.36; see Appendix 5-23. Likewise, in females (n = 13 of 14, 9L vs 4R) although the mean value for the right hemisphere was more than double that for the left, no significant difference was indicated at $P = 0.26$ (Appendix 5-23). Only in males (n = 6 of 8) did the one-tailed P value ($P = 0.08$) approach significance for a larger left hemisphere occipital lobe petelia (Appendix 5-23). This was in marked contrast to the distribution data which indicated twice as many left hemisphere occipital petelias than on the right hemisphere (Total sample L vs R = 13 vs 6); see histogram in Appendix 5-23.

5.5.3.3. Co-occurrence of frontal and occipital lobe petelias

In addition to the common petelial pattern seen in humans, right frontal petelia in combination with left occipital petelia, there are nine distinct alternative patterns of co-occurrence for frontal lobe and occipital lobe petelias; these are:

Pattern 1)	No petelia of either the frontal or occipital lobe
Pattern 2)	Petelial extension of right frontal only
Pattern 3)	Petelial extension of left frontal only
Pattern 4)	Petelial extension of right occipital only
Pattern 5)	Petelial extension of left occipital only
Pattern 6)	Petelial extension of right frontal & right occipital
Pattern 7)	Petelial extension of left frontal & left occipital
Pattern 8)	Petelial extension of right frontal & left occipital
Pattern 9)	Petelial extension of left frontal & right occipital

Distribution of patterns of co-occurrence in this sample:

Within this sample (n = 22) the co-expression of frontal and occipital petelias was represented by the following patterns:

Pattern 1	(none)	*Pattern 2*	(n = 2)
Pattern 3	(n = 1)	*Pattern 4*	(none)
Pattern 5	(n = 3)	*Pattern 6*	(n = 1)
Pattern 7	(n = 4)	*Pattern 8*	(n = 6)
Pattern 9	(n = 5)		

Pattern 8, seen in most humans (Hennenberg & Symons, 1992), in which right frontal and left occipital petelias co-occur was also the most common petelial pattern seen in this study. It was present in six of the 19 individuals

Figure 5-29 Plot of left versus right hemispheric differences and co-occurrence of petelial projections of the frontal (FR-pet) and occipital lobes (OC-pet). Values represent absolute distances (mm) by which one frontal or occipital lobe projected beyond that in the contralateral hemisphere. Total sample (n = 22), females (n = 14) and males (n = 8). Section 5.5.3.3.

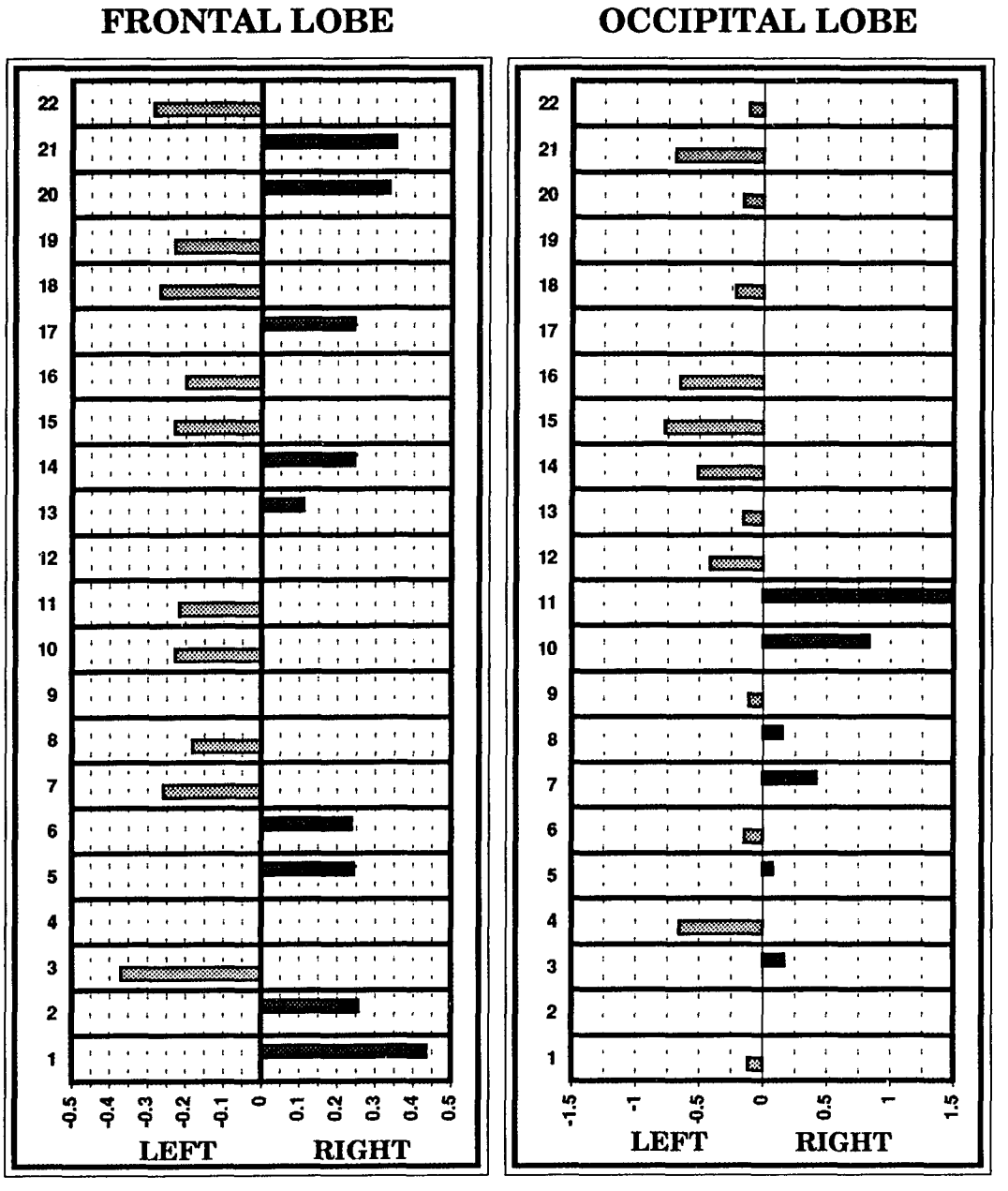
FRONTAL LOBE
OCCIPITAL LOBE
22
21
20
19
18
17
16
15
14
13
12
11
10
9
8
7
6
5
4
3
2
1
-0.5
-0.4
-0.3
-0.2
-0.1
0
0.1
0.2
0.3
0.4
0.5
LEFT
RIGHT
-1.5
-1
-0.5
0
0.5
1
1.5
LEFT
RIGHT

manifesting petelias, representing an overall occurrence of ~27.3% in the total sample (n = 22); See Figure 5-29 for comparison chart.

The second most common combination was Pattern 9 (n = 5) which represents the opposite petelial combination (to Pattern 8) with co-occurrence of left frontal and right occipital petelias. The occurrence of pattern 9 represented 22.7% of the total sample (n = 22). Although Pattern 8 was present in one more individual than Pattern 9, these preliminary results indicate that the occurrence of these two opposite patterns is equal and in combination account for half the total expression of petelias (Figure 5-29).

However, if the analysis is taken a step further by considering the three possible variations on the basic human pattern (co-occurrence of right frontal and left occipital petelias), i.e. Pattern 2 - right frontal only, Pattern 5 - left occipital only, and Pattern 8 - right frontal with left occipital, the outcome is 11 individuals, again representing 50% of the population (Figure 5-29). Likewise, if the opposite conditions are combined (i.e. Patterns 3, 4, and 9) the outcome is six individuals, almost half the previous outcome. This seems more in line with the human-like pattern and suggests the inception of the more derived state in *Macaca fascicularis*.

The hemispheric differences in petelial projection were in most cases very small, especially in the frontal lobe where all values were less than 0.5mm. Although values for occipital petelial extension were somewhat larger, all values but one were less than 0.9mm.

5.5.4. Results of 2-D linear measures of hemispheric width

These measures of frontal lobe width on the left and right hemispheres (in millimeters) were made from photographs of the superior surface of the brain as described in Section 5.5.2. and illustrated in Figure 5-26).

5.5.4.1. 2-D Linear measures of anterior frontal lobe width (FRw-a)

Inter-hemispheric distribution of measure FRw-a:

In the total sample (n = 22) the mean value for the width of the anterior region of the frontal lobe in the left hemisphere was 17.5 ±1.8mm (max = 20.5mm, min = 13.8mm, and median = 17.5mm) and smaller on the right hemisphere at 17.4 ±1.5mm (max = 20.7mm, min = 14.1mm, median = 17.7mm), (Appendix 5-24 & 5-25).

In females (n = 14), FRw-a on the left hemisphere was 16.8 ±1.7mm and on the right hemisphere 16.5 ±1.2mm (Appendix 5-24 & 5-25). In males (n = 8), FRw-a on the left hemisphere was 18.9 ±1.3mm and on the right hemisphere 18.7 ±0.9mm (Appendix 5-24 & 5-25). In the total sample (n = 22) the anterior portion of the frontal lobe was wider in the left hemisphere in a total of 11 individuals (50% of sample, Figure 5-30). This included six females (43% of sub-sample) and five males (62% of sub-sample); see Figure 5-30.

Figure 5-30 Plot of hemispheric differences in the 2-D linear width of the anterior portion of the frontal lobe (*FR-w-a*). Values represent differences in width (mm) between the left and right hemispheres, plotted for largest side, in total sample (n = 22), females (n = 14) & males (n = 8). Section 5.5.4.1.

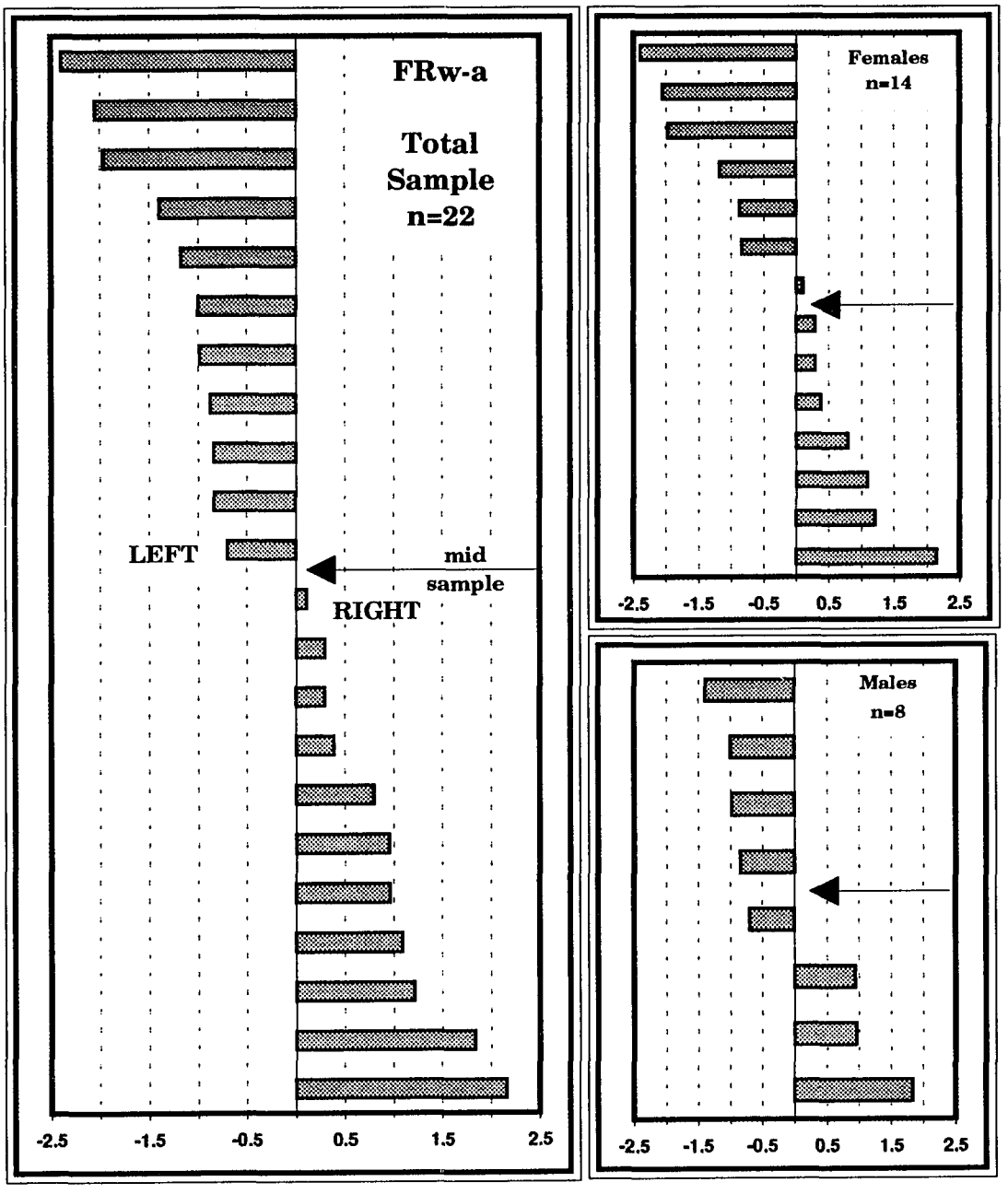
FRw-a
Total
Sample
n=22
LEFT
mid
sample
RIGHT
-2.5
-1.5
-0.5
0.5
1.5
2.5
Females
n=14
-2.5
-1.5
-0.5
0.5
1.5
2.5
Males
n=8
-2.5
-1.5
-0.5
0.5
1.5
2.5

The anterior region of the frontal lobe was also wider in the right hemisphere in the total sample (n = 22) in 11 individuals (50% of the total sample, Figure 5-30). This included eight females (57% of sub-sample, Figure 5-30) and three males (37% of sub-sample, Figure 5-30). The distribution pattern for this measure of frontal lobe width appeared to be symmetric (Figure 5-30), with equal representation in both hemispheres and no major tendency towards hemispheric predominance on either side. This applied both to the absolute number of left vs right hemisphere larger values (1:1) as well as the overall extent of the individual values (Figure 5-30 & Appendix 5-25). In the total sample and the sex-specific sub-samples, however, mean values for FRw-a in the left hemisphere were slightly larger (Appendix 5-25)

Statistical analysis of 2-D linear measure FR-w-a:

Using the Type 1 t-Test, it was shown that there were no significant differences in the width of the anterior portion of the frontal lobe on the left and right hemispheres in either the total sample ($P = 0.51$), the female sub-sample ($P = 0.58$) or the male sub-sample ($P = 0.75$); see Appendix 5-25.

5.5.4.2. 2-D Linear measures of posterior frontal lobe width (FRw-p)

Inter-hemispheric distribution of measure FRw-p:

In the total sample (n = 22) the mean value for FRw-p on the left hemisphere posterior was 20.9 ±2.3mm (max = 24.4m, min = 15.5mm, and

median = 21.1mm. On the right hemisphere, FRw-p was 20.97 ±1.9mm (max = 25.4mm, min = 17.6mm, median = 20.97mm), (Appendix 5-24 & 5-26).

In females (n = 14), the mean of values for FRw-p on the left hemisphere was 19.9 ±2.1mm and on the right hemisphere 20.1 ±1.6mm (Appendix 5-24 & 5-26). In males (n = 8), the mean of values for FRw-p on the left hemisphere was 22.6 ±1.4mm and on the right hemisphere 22.5 ±1.4mm (Appendix 5-24 & 5-26).

As can be seen in Figure 5-31, for the total sample (n = 22) the posterior region of the frontal lobe was wider in the left hemisphere in 10 individuals (45% of sample). This included five females (36% of sub-sample) and five males (63% of sub-sample). Two inter-hemispheric values in females were very small and as such were essentially symmetric.

The posterior region of the frontal lobe was wider in the right hemisphere of the total sample (n = 22) in 10 individuals (46% of the sample). This included seven females (50% of sub-sample) and three males (38% of sub-sample); see Figure 5-31.

As for the measure of anterior frontal lobe width above (Section 5.4.4.1), this 2-D linear measure of posterior frontal lobe width (FRw-p) did not show any tendencies to be either larger or to predominate in either the left or the right hemispheres (Figure 5-31 & Appendix 5-36).

Figure 5-31 Plot of hemispheric differences in the 2-D linear width of the posterior portion of the frontal lobe (*FR-w-p*). Values represent differences in width (mm) between the left and right hemispheres, plotted for largest side, in total sample (n = 22), females (n = 14) & males (n = 8). Section 5.4.4.2.

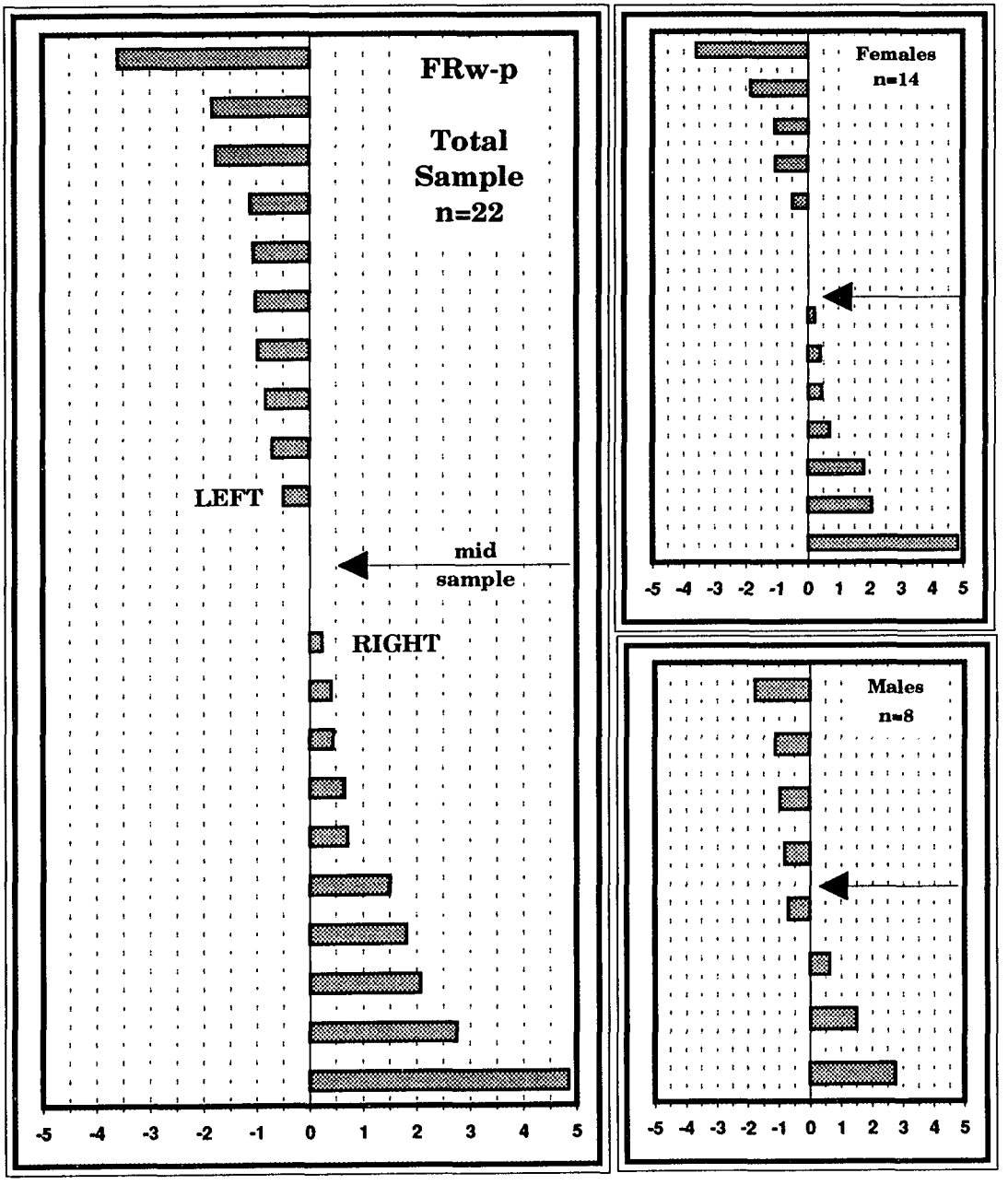
FRw-p
Total
Sample
n=22
LEFT
mid
sample
RIGHT
-5 -4 -3 -2 -1 0 1 2 3 4 5
Females
n=14
-5 -4 -3 -2 -1 0 1 2 3 4 5
Males
n=8
-5 -4 -3 -2 -1 0 1 2 3 4 5

Statistical analysis of 2-D linear measure FR-w-p:

Using the Type 1 t-Test, it was shown that there were no significant differences in the width of the posterior portion of the frontal lobe on the left and right hemispheres in either the total sample ($P = 0.8$), the female sub-sample ($P = 0.73$) or the male sub-sample ($P = 0.93$), (Appendix 5-26)

5.5.4.3. 2-D Linear measures of anterior parietal lobe width (PAw-a)

Inter-hemispheric distribution of measure PAw-a:

In the total sample (n = 22) the mean value for the width of the anterior region of the parietal lobe in the left hemisphere (PAw-a) was 23.0 ±2.2mm (max = 26.8m, min = 18.5mm, median = 23.0mm). On the right hemisphere, PAw-a was 23.1 ±2.0mm (max = 27.5mm, min = 19.2mm, median = 23.3mm), (Appendix 5-27 & 5-28).

In females (n = 14), the mean value for PAw-a on the left hemisphere was 21.9 ±1.9mm and on the right hemisphere 22.1 ±1.5 (Appendix 5-27 & 5-28). In males (n = 8), the mean of values for PAw-a on the left hemisphere was 24.9 ±1.3mm and on the right hemisphere 24.9 ±1.2 (Appendix 5-27 & 5-28).

The anterior region of the parietal lobe was wider in the left hemisphere in 12 individuals representing ~55% of the total sample (Figure 5-32). This included seven females (50% of sub-sample) and five males (63% of sub-sample, Figure 5-32). The anterior region of the parietal lobe was wider in the right hemisphere in 10 individuals (45% of sample). This included seven females (50% of sub-sample) and three males (37% of sub-sample),

Figure 5-32 Plot of hemispheric differences in the 2-D linear width of the anterior portion of the parietal lobe (*PA-w-a*). Values represent differences in width (mm) between the left and right hemispheres, plotted for largest side, in total sample (n = 22), females (n = 14) & males (n = 8). Section 5.5.4.3.

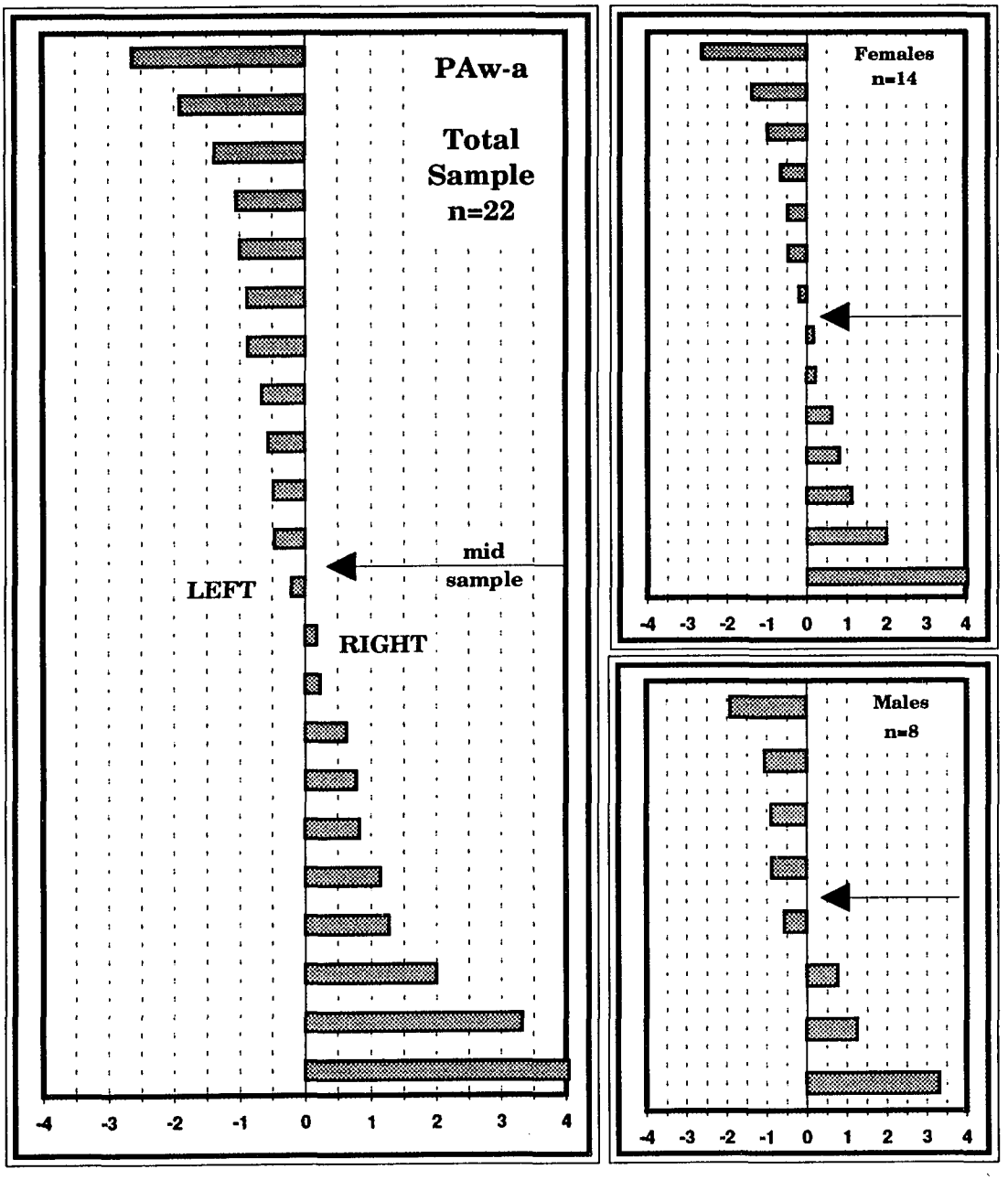
PAw-a
Total
Sample
n=22
mid
sample
LEFT
RIGHT
-4 -3 -2 -1 0 1 2 3 4
Females
n=14
-4 -3 -2 -1 0 1 2 3 4
Males
n=8
-4 -3 -2 -1 0 1 2 3 4

(Figure 5-32). As for the measures of frontal lobe width above (Sections 5.5.4.1. & 5.5.4.2), there was no overt tendency for the anterior portion of the parietal lobe (PA-w-a) to predominate or to be wider in either the left or the right hemisphere. However, although the size was small for the sex-specific male sub-sample (n = 8) there did appear to be a slight indication of a tendency to be larger more often in the left hemisphere (Figures 5-30, 5-31, & 5-32) as opposed to total symmetry in females (n = 14)

Statistical analysis of 2-D linear measure PA-w-a:

Using the Type 1 t-Test, it was shown that there were no significant differences in the width of the anterior portion of the parietal lobe (PAw-a) on the left and right hemispheres in either the total sample ($P = 0.75$), the female sub-sample ($P = 0.71$) or males ($P = 0.98$), Appendix 5-28.

5.5.4.3. 2-D Linear measures of posterior parietal lobe width (PAw-p)

Inter-hemispheric distribution of measure PAw-p

In the total sample (n = 22) the mean value for the measure of medial - lateral width of the posterior portion of the parietal lobe in the left hemisphere was 23.0 ±2.3mm (max = 28.1mm, min = 19.0mm, median = 23.1mm), see Appendix 5-27 & 5-28.

In females (n = 14), the mean value for PAw-p on the left hemisphere was 21.9±1.7mm and 21.8 ±1.5mm on the right. In males (n = 8), the mean value for PAw-p on the left hemisphere was 25.0 ±1.7mm and 24.8 ±1.0mm on the right; see Appendix 5-27 & 5-28.

Figure 5-33 Plot of hemispheric differences in the 2-D linear width of the posterior portion of the parietal lobe (*PA-w-p*). Values represent differences in width (mm) between left and right hemispheres, plotted for largest side, in the total sample (n = 22), females (n = 14) & males (n = 8). Section 5.5.4.4.

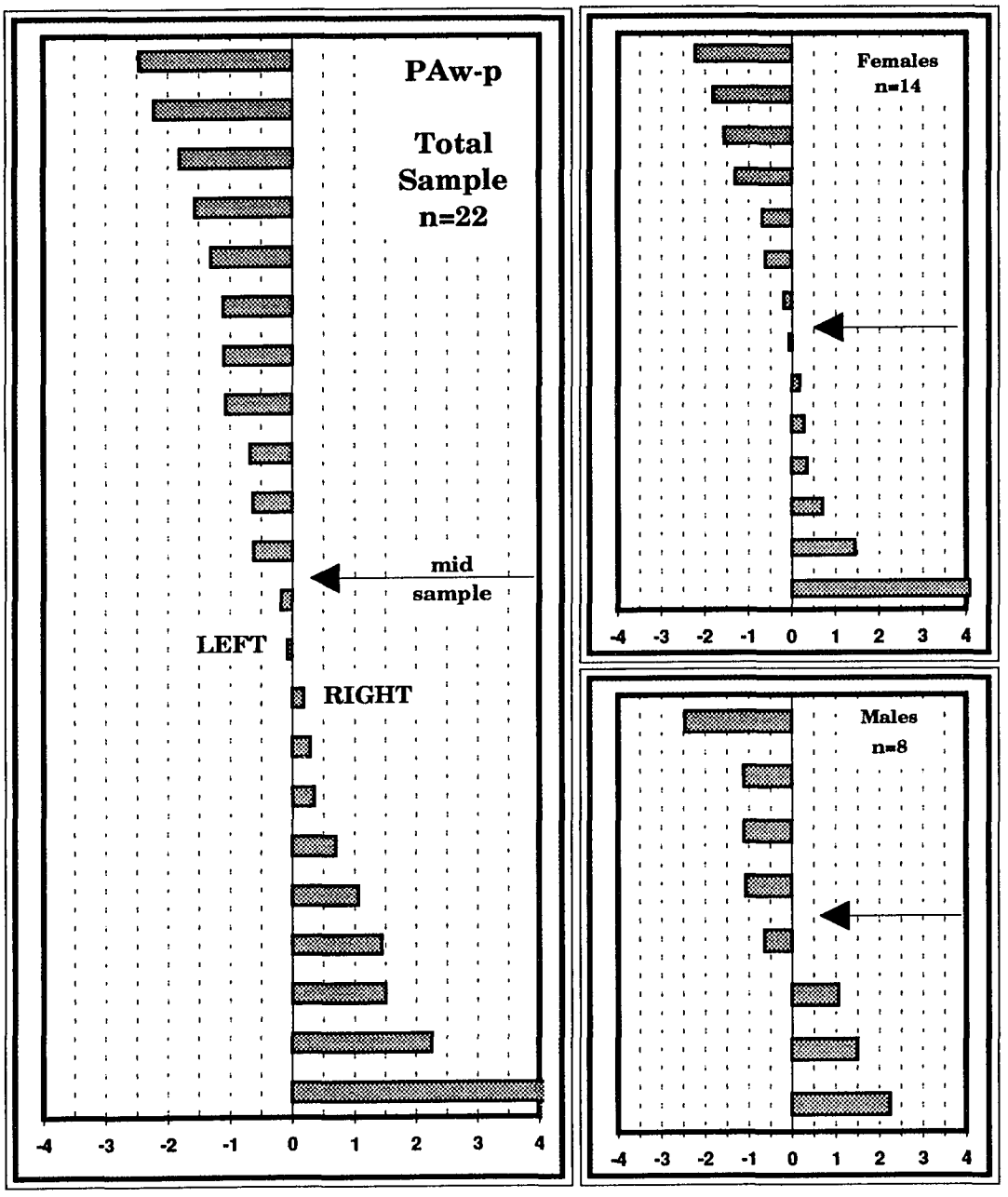
PAw-p
Total
Sample
n=22
mid
sample
LEFT
RIGHT
-4 -3 -2 -1 0 1 2 3 4
Females
n=14
-4 -3 -2 -1 0 1 2 3 4
Males
n=8
-4 -3 -2 -1 0 1 2 3 4

In the total sample (n = 22), the posterior portion of the parietal lobe (PAw-p) was wider in the left hemisphere in 13 individuals representing ~59% of the sample. This included eighth females (~57% of sub-sample) and five males (~63% of sub-sample); see Figure 5-32. The posterior region of the parietal lobe was wider in the *right hemisphere* in nine individuals representing ~41% of the total sample. Included within this group were six 6 females (~43% of sub-sample) and three males (~37% of sub-sample); see Figure 5-33.

As for the measures of frontal lobe and parietal lobe width above, there was no indication of hemispheric predominance in any sample except possibly in the male sub-sample. Although the sample size for males is small, there was a consistent tendency, seen in all four of the measures FRw-a, FRw-p, PAw-a, and here in PAw-p, for the width measure to predominate in the left hemisphere (see male sub-sample distribution pattern in Figures 5-30, 5-31, 5-39 & 5-33).

Statistical analysis of 2-D linear measures PA-w-p:

Using the Type 1 t-Test (paired sample), it was shown that there were no significant differences in the width of the posterior portion of the frontal lobe on the left and right hemispheres in either the total sample ($P = 0.7$), the female sub-sample ($P = 0.83$) or the male sub-sample ($P = 0.75$); see Appendix 5-29.

CHAPTER 6

MORPHOMETRY OF STRUCTURES DEEP TO THE SURFACE OF THE BRAIN

6.1 CHAPTER OVERVIEW:

This chapter presents a quantitative analysis of a new measure of inter-hemispheric cerebral asymmetry in *Macaca fascicularis*, that of the dimensions of deep brain structures. Previously, studies of macaque cortical regions adjacent to regions homologous to Broca's and Wernicke's area in humans, have focused on brain surface features. Examples of this approach are presented in Chapters 4 & 5 of this dissertation. Since the principal evidence for primate brain evolution, fossil endocasts, are limited to brain surface features, this latter approach has, and continues to, make use of important direct evidence. However, a better understanding of the morphological variation present in these same surface structures, as they course deep within the brain, is important. This will allow for a more complete assessment and understanding of the pattern of distribution of asymmetries both on the surface of the brain and how this correlates with deeper structures.

Three major brain surface structures were chosen for deep structure analysis, 1) the arcuate sulcus, 2) the central sulcus, and 3) the posterior

portion of the sylvian fissure. Measurements were made on both the left and right hemispheres in a total sample of 17 individuals including eight females and nine males. The sulci were measured by insinuating braided suture cord into the cleft and measuring its extent from its deepest margin to the cortical surface at three separate points, then measuring the length of the cord on a digitizing pad system.

Results from deep structure measures:

Results of arcuate sulcus depth measures (AS-d) showed that values in the left hemisphere were significantly larger in the left hemisphere ($P = 9.5 \times 10^{-4}$). Furthermore, 15 of 17 individuals were larger on the left.

For measures of the depth of the central sulcus (CS-d), there was no significant difference between values for the left and right hemispheres in the total sample (n = 17) where $P = 0.5$, and in males (n = 9) where $P = 0.56$. However, in females (n = 8) values for AS-d were significantly larger on the left hemisphere ($P = 0.05$) with six of eight individuals showing a left hemisphere predominance.

Measures of posterior sylvian fissure depth (SF-d) showed no significant difference between the left and right hemispheres in the total sample (n = 16) where $P = 0.7$ or in the sex-specific sub-sample. In females (n = 7), however, six individuals were larger in the right hemisphere.

There was no apparent pattern of hemispheric co-occurrence in these three measures of cortical/gyral dimensions deep to the surface of the brain.

6.2. SULCAL DEPTH MEASUREMENT METHOD

For this aspect of the quantitative assessment of cerebral asymmetry, freshly perfusion fixed brains of *Macaca fascicularis* that had been prepared as described in Section 3.2.5. were used. The sample comprised a total of 17 brains for measures of arcuate sulcus and central sulcus depth comprising females (n = 8) and males (n = 9). For posterior sylvian fissure depth a total of 16 brains were used, including females (n = 7) and males (n = 9). The depth of the superior temporal sulcus was not included in this analysis since the deeper parts of this sulcus become operculated by the middle and superior temporal gyri. This gives rise to differentiation of the sulcus in an infero-superior dimension. Instead of expanding into the depth of the brain the deep part of the sulcus diverges into an inverted T-shaped structure that could not be quantified with this kind of analysis.

Initially, all of the meningeal coverings were removed from the surface of the brain allowing good exposure of the regions under study. Then, using an operating microscope (Zeiss) at 10x magnification, the sulci were spread open to reveal their deeper margins. The same braided suture material that was used for the 3-D analysis of brain surface structures was manipulated into the depth of the sulcus using fine forceps until the end was touching its deepest margin. The sulcus was then closed, trapping the cord between its walls and preventing displacement. Using straight scissors laid across the surface of the brain, the cord was cleanly cut. This represented the distance

from the deepest point of the sulcus to the surface of the brain as represented by the linear margin defined by the two adjacent gyri on the surface of the brain. This allowed for a standardized measure of the V-shaped area of the sulcus on the surface of the brain as the two adjacent gyri course away.

The sulcus was now spread open and the measuring cord checked for positioning and possible displacement. The cord was then removed from the sulcus, laid flat without stretching on a piece of plastic film, and the two endpoints marked by piercing with a fine-tipped needle probe. In each case, specific specimen details were written alongside the measure. Three separate measures were made of each sulcus and the means used for comparison and statistical analysis. After completion of a series of measures, the plastic sheet was placed on the digitizing pad and the depth value measured with the cursor as an absolute distance in millimeters (Figure 6-1).

Preliminary studies using this method showed the measurement accuracy of repeated individual measures to be < 0.2mm. Data were analyzed using paired sample t-Tests separately for the total sample and for the sex-specific sub-samples. It should be noted that when multiple t-Tests are being used the α - error will be present in proportion to to level of the significance value chosen. For this part of the analysis a P value of $P = <0.01$ was used to assign significance to asymmetry values.

6.3. 3-D MEASURES OF SULCAL AND FISSURAL DEPTHS IN FRONTAL AND TEMPORAL LOBE STRUCTURES

6.3.1. (Depth of Arcuate Sulcus "AS-d" (Figure 6-1)

This measure represented the depth of the middle region of the vertical portion of the arcuate sulcus on the inferior frontal lobe, bordered posteriorly by the walls of the post-arcuate premotor cortex (Brodmann's Area 44) and anteriorly by the walls of the inferior prefrontal cortex (Brodmann's Area 45).

6.3.2. (Depth of Central Sulcus "CS-d" (Figure 6-1)

The depth of the central sulcus in its more inferior portion immediately posterior to the supero-inferior extent of the arcuate sulcus. The sulcus was confined posteriorly by the deep walls of the parietal lobe post-central sensory cortex and anteriorly by the inferior frontal lobe pre-central motor cortex.

6.3.3. Depth of posterior Sylvian Fissure "CS-d" (Figure 6-1)

This measure represents the depth of the sylvian fissure in its more posterior portion defined anteriorly by a line extended inferiorly from the central sulcus and posteriorly by the initiation of full fissural depth several millimeters anterior to the sylvian point.

Note: For all three sulcal / fissural depth measures, three separate measures were made at different points along its middle region and the resultant mean values used for subsequent comparison and data analysis using the paired sample t-Test. A statistical analysis of combined individual measures was also conducted as a more global test of inter-hemispheric asymmetry in which each individual was represented by these three sets of non-paired measures in an expanded sample.

Figure 6-1 **a)** Diagram of the site of 3-D linear measures of the depth, in millimeters, of the arcuate sulcus (AS-d), central sulcus (CS-d) and sylvian fissure (SF-d) on the left and right hemispheres. **b)** Three distinct measures were made in the middle part of the arcuate and central sulci (arrows) away from the sloping end points. **c)** The surface margins of the adjoining gyri (dotted line) were used to define the superficial margin of the sulcal measure (Section 6-2).

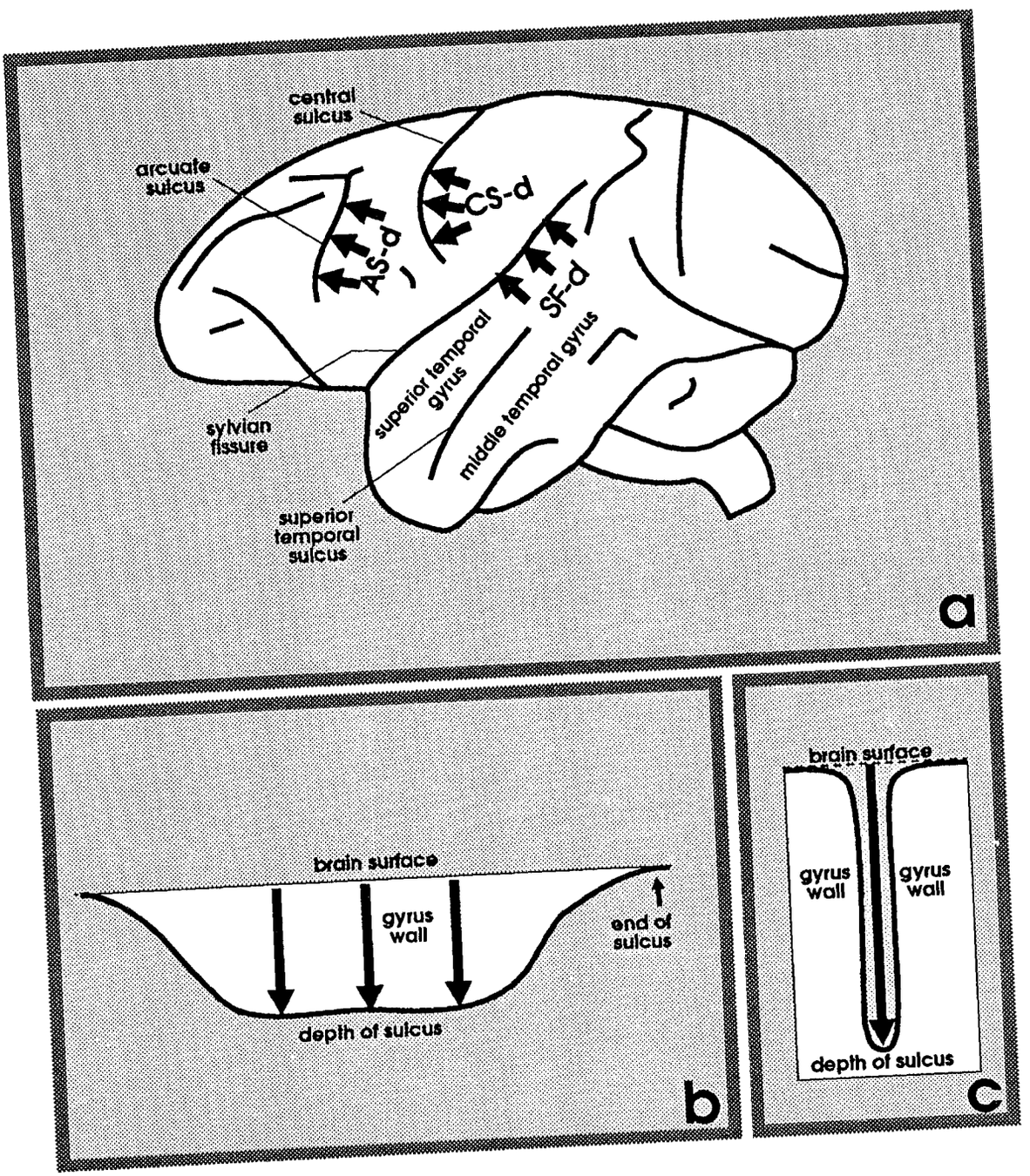
central sulcus
arcuate sulcus
AS-d
CS-d
SF-d
superior temporal gyrus
middle temporal gyrus
sylvian fissure
superior temporal sulcus
a
brain surface
gyrus wall
end of sulcus
depth of sulcus
b
brain surface
gyrus wall
gyrus wall
depth of sulcus
c

6.4. RESULTS OF 3-D MEASURES OF SULCAL AND FISSURAL DEPTH

6.4.1. Depth of Arcuate Sulcus "AS-d" on the left and right hemispheres

The depth of the vertical portion of the arcuate sulcus measured at three independent points along its midsection. Data-points for individuals and sample means represent values based on the mean of these three points.

6.4.1. Inter-hemispheric dimensions of depth measure AS-d:

In the total sample (n = 17) the mean value for the depth of the arcuate sulcus on the left hemisphere was 5.4 ±0.5mm (max = 6.1mm, min = 4.7mm) and on the right hemisphere 5.0 ±0.6mm (max = 6.2mm, min = 3.7mm), (Figure 6-2).

In females (n = 8), the mean of values for arcuate sulcus depth on the left hemisphere was smaller than the total sample value at 5.1 ±0.4mm. On the right hemisphere the mean value was 4.6 ±0.5mm (Figure 6-2). In males (n = 9), the mean value for arcuate sulcus depth on the left hemisphere was larger than the total sample mean at 5.7 ±0.4mm. The mean value for the right hemisphere was also larger at 5.4 ±0.6mm (Figure 6-2). As can be seen in the bar graphs and largest side distribution graphs for the total sample and the sex-specific sub-samples in Figures 6-2 and 6-3, the values for arcuate

Figure 6-2 **a)** 3-D linear measures of the depth (mm) of the arcuate sulcus (AS-d), on the left and right hemispheres. **b)** Comparison of means and standard deviations for total sample (n=17), females (n=8) and males (n=9) **c)** Paired sample t-Tests of hemispheric asymmetry in the three separate samples (Section 6.41.).

Arcuate Sulcus Depth (AS-d) on theLeft and Right Hemispheres

n=	AS-d		PG	SEX
	LEFT	RIGHT	M#	
1	5.0	4.3	57	F
2	4.7	4.5	56	F
3	5.1	4.8	55	F
4	4.8	3.7	54	F
5	5.5	4.8	53	F
6	5.9	5.1	52	M
7	5.8	5.3	48	F
8	5.8	6.2	47	M
9	4.9	4.7	46	F
10	4.9	4.5	45	M
11	5.9	5.6	44	M
12	5.1	5.0	43	M
13	5.9	5.2	42	M
14	6.1	5.7	41	M
15	5.3	4.8	40	M
16	5.9	6.1	39	M
17	5.1	5.1	38	F
Mean	*5.4*	*5.0*	total	
Stdev	*0.5*	*0.6*	sample	
Max	*6.1*	*6.2*		
Min	*4.7*	*3.7*		
Mean	*5.1*	*4.6*	females	
Stdev	*0.4*	*0.5*		
Mean	*5.7*	*5.4*	males	
Stdev	*0.4*	*0.6*		

a

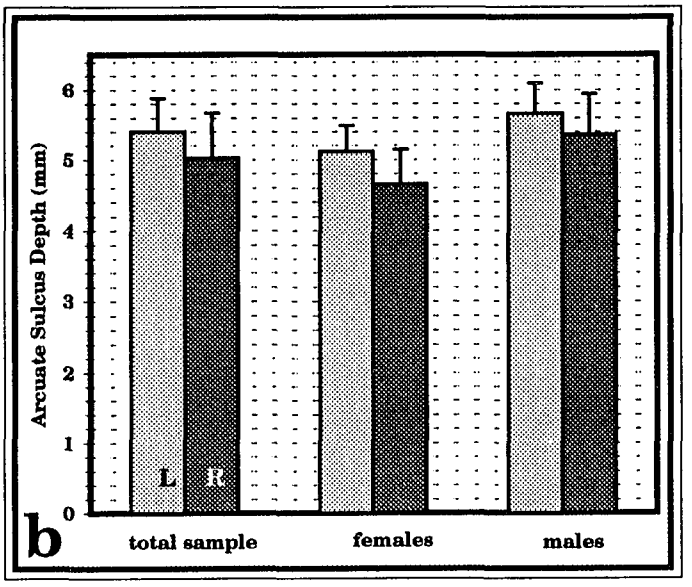

c

Paired t-Test

	Total		Females		Males	
	left	right	left	right	left	right
Mean	5.4	5.0	5.1	4.6	5.7	5.4
Variance	0.2	0.4	0.1	0.3	0.2	0.3
Observations	17	17	8	8	9	9
Pearson Correl'n	0.80		0.65		0.74	
Hypoth Mean Diff	0		0		0	
df	16		7		8	
t Stat	4.04		3.46		2.28	
P(T<=t) one-tail	4.7E-04		0.01		0.03	
t Critical one-tail	1.75		1.89		1.86	
P(T<=t) two-tail	9.5E-04	***	0.01	***	0.05	***
t Critical two-tail	2.12		2.36		2.31	

sulcus depth predominate strikingly in the left hemisphere. In all three samples, average values for the depth of the arcuate sulcus are larger on the left hemisphere than on the right (Figure 6-2b).

In the total sample (n = 17), 15 individuals were larger on the left hemisphere. Only one of these values was less than 0.1mm and as such may have represented hemispheric symmetry of this measure. In females (n = 8) all measures were larger in the left hemisphere (but this included the possibly symmetric measure mentioned above). In males (n = 9) seven measures of arcuate sulcus depth, representing ~78% of the sex-specific sub-sample, were larger in the left hemisphere by a distance greater than 0.2mm (Figure 6-3).

6.4.1.2. Statistical analysis of 3-D measures of arcuate sulcus depth:

Using the type 1 t-Test (paired sample), data were analyzed as the total sample and separately for the sex-specific sub-samples.

In the total sample (n = 17), values for arcuate sulcus depth were highly significantly larger on the left hemisphere than on the right at $P = 9.5 \times 10^{-4}$; see Figure 6-3c). In females (n = 8), values for arcuate sulcus depth were also significantly larger on the left hemisphere than on the right at $P = 0.01$ (Figure 6-3c). In males (n = 9), the values for arcuate sulcus depth were also significantly larger on the left hemisphere, but not as highly significant as the total sample or females, at $P = 0.05$. Although the sample size is

Figure 6-3 a) Plot of inter-hemispheric differences in the depth of the arcuate sulcus (AS-d). Values represent the difference in millimeters of the depth of the arcuate sulcus in the left and right hemispheres, plotted for the largest side in the : total sample (n = 17), female sub-sample (n = 8), and male sub-sample (n = 9). See text, Section 6.4.1. for details.

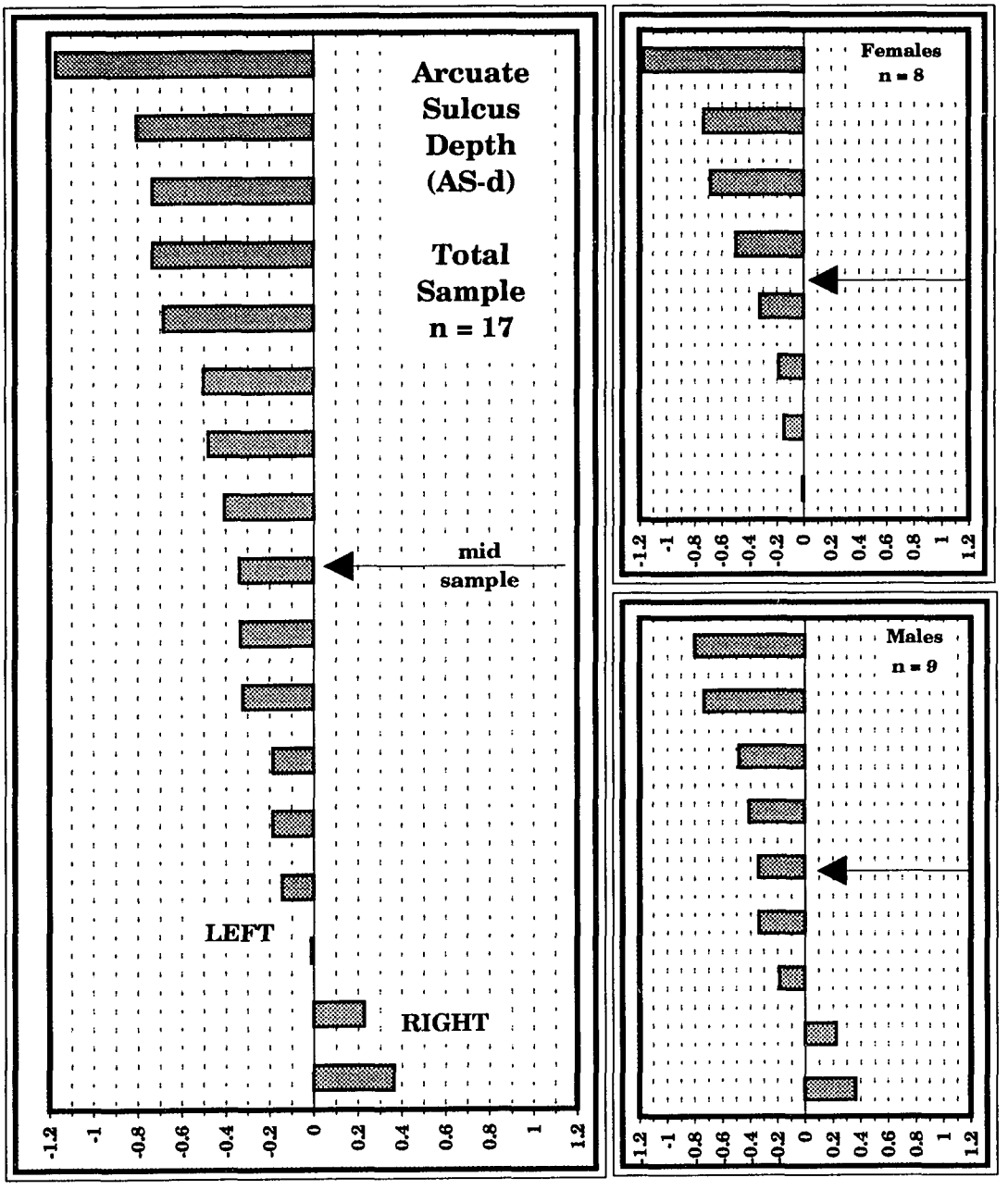
Arcuate
Sulcus
Depth
(AS-d)
Total
Sample
n = 17
mid
sample
LEFT
RIGHT
-1.2
-1
-0.8
-0.6
-0.4
-0.2
0
0.2
0.4
0.6
0.8
1
1.2
Females
n = 8
Males
n = 9

relatively small, especially the sex-specific sub-samples, the difference between males and females may represent a sex difference in this measure of inter-hemispheric asymmetry that may be more evident with larger sample sizes.

Data were also considered as three separate points on each hemisphere for each of the 17 brains in the sample for a total n = 51. Not surprisingly, using the type 1 t-Test for this pooled data, values on the left hemisphere were highly significantly larger than on the right hemisphere at a signifacnce level of $P = 7.8 \times 10^{-6}$.

6.4.2. Depth of Central Sulcus "CS-d" on the left and right hemispheres

These measures represented the depth of the inferior portion of the central sulcus located immediately posterior to the extent of the vertical section of the arcuate sulcus. Data-points for individuals in the total sample (n = 17) were based on mean values obtained from three adjacent independent measures.

6.4.2.1. Inter-hemispheric dimensions of depth measure CS-d:

In the total sample (n = 17), the mean values for CS-d on the left hemisphere was 5.3 ±0.4mm (max = 5.9mm, min = 4.5mm). On the right hemisphere the mean for CS-d was slightly smaller at 5.2 ±0.4mm (max = 6.0, min = 4.5); see Figure 6-4 a & b.

Figure 6-4 **a)** 3-D linear measures of the depth (mm) of the central sulcus (CS-d), on the left and right hemispheres. **b)** Comparison of means and standard deviations for total sample (n=17), females (n=8) and males (n=9) **c)** Paired sample t-Tests of hemispheric asymmetry in the three separate samples (Section 6.4.2.).

Central Sulcus Depth (CS-d) on theLeft and Right Hemispheres

n=	CS-d		PG	SEX
	LEFT	RIGHT	M#	
1	5.4	5.1	57	F
2	5.2	4.9	56	F
3	5.0	4.7	55	F
4	4.6	4.5	54	F
5	5.9	6.0	53	F
6	5.5	5.9	52	M
7	5.2	5.1	48	F
8	5.5	5.2	47	M
9	5.2	4.9	46	F
10	5.7	5.4	45	M
11	5.2	5.6	44	M
12	5.7	5.5	43	M
13	5.0	5.4	42	M
14	5.4	5.3	41	M
15	5.2	5.4	40	M
16	5.8	5.6	39	M
17	4.5	4.6	38	F
Mean	*5.3*	*5.2*	total	
Stdev	*0.4*	*0.4*	sample	
Max	*5.9*	*6.0*		
Min	*4.5*	*4.5*		
Mean	*5.1*	*5.0*	females	
Stdev	*0.4*	*0.5*		
Mean	*5.4*	*5.5*	males	
Stdev	*0.3*	*0.2*		

a

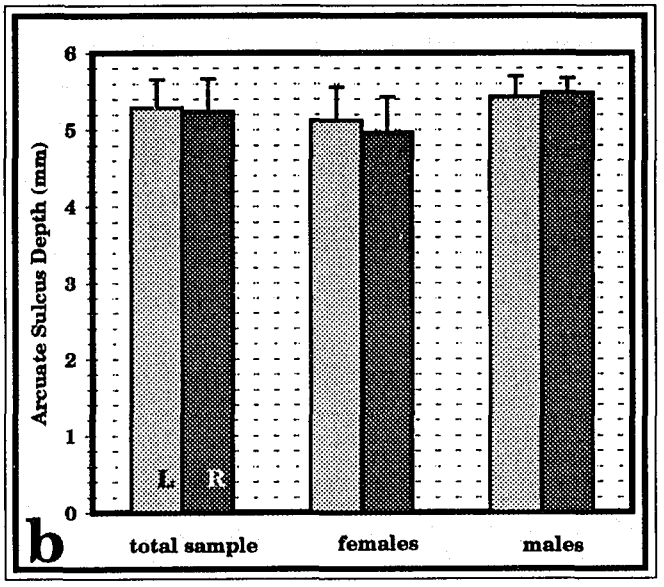

c

Paired t-Test

	Total		Females		Males	
	left	right	left	right	left	right
Mean	5.3	5.2	5.1	5.0	5.4	5.5
Variance	0.1	0.2	0.2	0.2	0.1	0.0
Observations	17	17	8	8	9	9
Pearson Correl'n	0.79		0.91		0.24	
Hypoth Mean Diff	0		0		0	
df	16		7		8	
t Stat	0.69		2.34		-0.60	
P(T<=t) one-tail	0.25		0.03		0.28	
t Critical one-tail	1.75		1.89		1.86	
P(T<=t) two-tail	0.50	N/S	0.05	***	0.56	N/S
t Critical two-tail	2.12		2.36		2.31	

In females (n = 8), the mean value for CS-d was 5.1 ±0.4mm on the left hemisphere, and slightly smaller at 5.0 ±0.5mm on the right hemisphere (Figure 6-4a & b). In males (n = 9), the mean value for CS-d on the left hemisphere was 5.4 ±0.3mm, and on the right hemisphere slightly larger at 5.5 ±0.2mm (Figure 6-4a & b).

In the total sample (n = 17), eleven individuals, representing ~65% of the sample, were larger on the left hemisphere (Figure 6-5). Only one of these values was less than 0.1mm and as such, it may represent hemispheric symmetry of this measure.

In females (n = 8), six individuals, representing 75% of the sex-specific sub-sample, were larger on the left hemisphere. The differences between the two hemispheres were considerably larger in females than they were in males (Figure 6-5). In males (n = 9), five measures were larger in the left hemisphere, one of which was less than 0.05mm. Thus, in males, the inter-hemispheric distribution pattern appeared to be symmetric.

6.4.2.2. Statistical analysis of 3-D measures of central sulcus depth:

The data were considered in three parts, using the type 1 t-Test (paired sample), for the total sample and for the sex-specific sub-samples In the total sample (n = 17), there was no significant difference in the measures of central sulcus depth in the left and right hemispheres (P = 0.5); Figure 6-4.

Figure 6-5 a) Plot of inter-hemispheric differences in the depth of the central sulcus (CS-d). Values represent the difference in millimeters of the depth of the central sulcus in the left and right hemispheres, plotted for the largest side in: the total sample (n = 17), the female sub-sample (n = 8), and the male sub-sample (n = 9). See text, Section 6.4.2. for details.

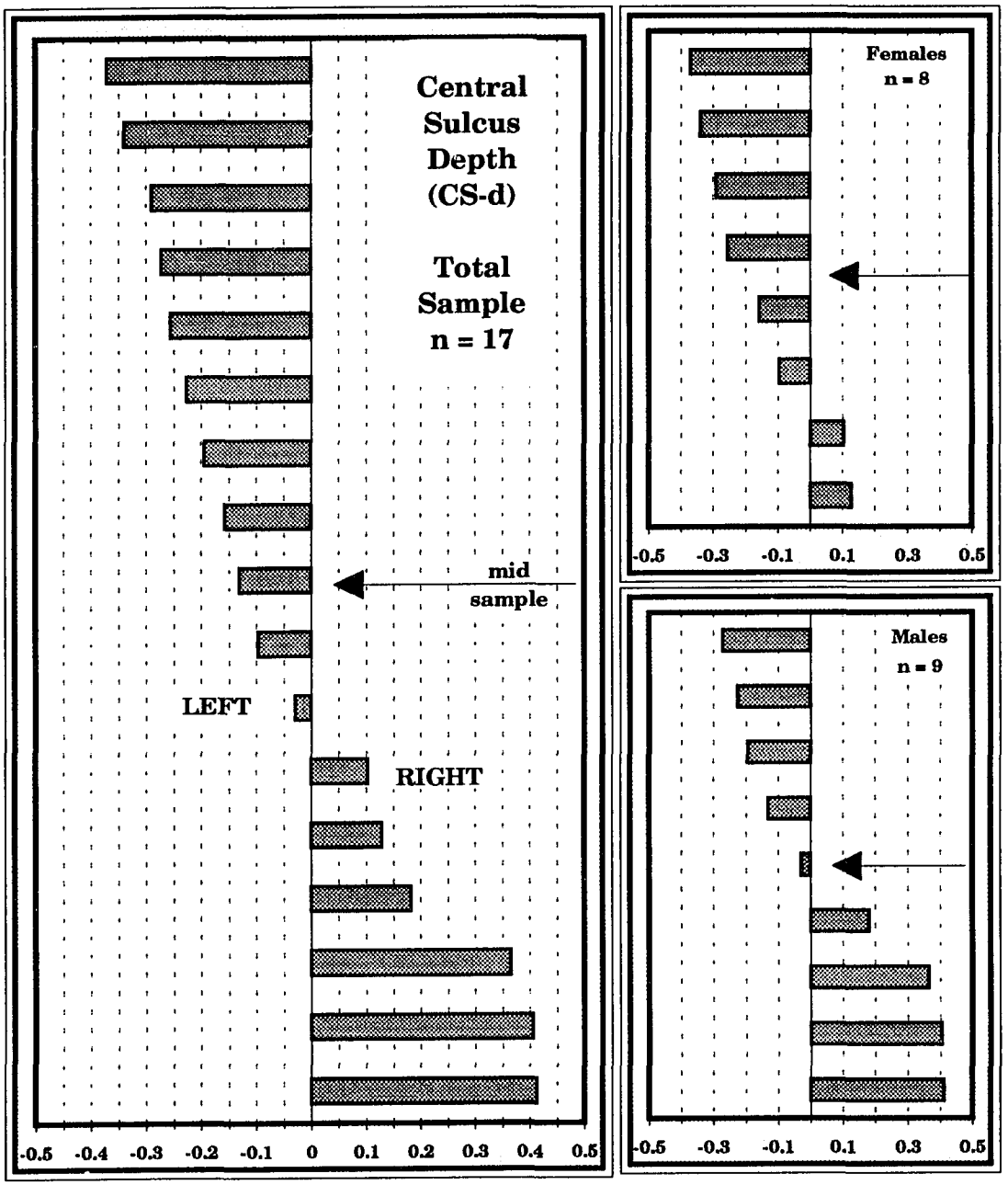
Central
Sulcus
Depth
(CS-d)
Total
Sample
n = 17
mid
sample
LEFT
RIGHT
-0.5 -0.4 -0.3 -0.2 -0.1 0 0.1 0.2 0.3 0.4 0.5
Females
n = 8
-0.5 -0.3 -0.1 0.1 0.3 0.5
Males
n = 9
-0.5 -0.3 -0.1 0.1 0.3 0.5

However, in females (n = 8), the values for CS-d were just significantly larger on the left hemisphere ($P = 0.05$), Figure 6-4). In contrast, males (n = 9), showed no difference between the depth of the central sulcus in the left and right hemispheres at $P = 0.56$ (Figure 6-4).

When data for individual triplicate values, resulting in a total sample of n=51, were used, the mean value for the left hemisphere was 5.4 ±0.62 and on the right hemisphere 5.28 ±0.55mm. Using the paired sample t-Test on this expanded sample, there was no significant difference between the left and right hemispheres at $P = 0.68$.

6.4.3. Depth of posterior Sylvian Fissure "SF-d" on the left and right hemispheres

These depth measures were limited to the posterior portion of the sylvian fissure since this borders the region of the superior temporal gyrus homologous to Wernicke's area. This was demarcated anteriorly by a line extended from the central sulcus, and posteriorly by the sylvian point (the posterior termination of the sylvian fissure). Three equally spaced independent depth measures were taken along the mid-portion of this region and the mean used for comparison and data analysis. One of the brains was damaged in the region so it could not be used for this measure, thus, n = 16.

6.4.3.1 Interhemispheric dimensions of depth measure SF-d

In the total sample (n = 16), the mean value for SF-d on the left hemisphere

Figure 6-6 **a)** 3-D linear measures of the depth (mm) of the sylvian fissure (SF-d), on the left and right hemispheres. **b)** Comparison of means and standard deviations for total sample (n=17), females (n=8) and males (n=9) **c)** Paired sample t-Tests of hemispheric asymmetry in the three separate samples (Section 6.4.3.).

Sylvian Fissure Depth (SF-d) on theLeft and Right Hemispheres

n=	SF-d		PG	SEX
	LEFT	RIGHT	M#	
1	7.8	8.2	57	F
2	7.2	7.3	55	F
3	7.9	8.0	54	F
4	7.9	8.6	53	F
5	8.9	8.4	52	M
6	7.5	7.5	48	F
7	8.1	7.7	47	M
8	8.6	8.6	46	F
9	8.1	8.5	45	M
10	8.7	8.0	44	M
11	7.9	8.7	43	M
12	8.1	8.9	42	M
13	8.3	8.5	41	M
14	8.0	7.4	40	M
15	7.6	7.5	39	M
16	8.0	7.5	38	F
Mean	*8.0*	*8.1*	total	
Stdev	*0.4*	*0.5*	sample	
Max	*8.9*	*8.9*		
Min	*7.2*	*7.3*		
Mean	*7.8*	*7.9*	females	
Stdev	*0.4*	*0.5*		
Mean	*8.2*	*8.2*	males	
Stdev	*0.4*	*0.5*		

a

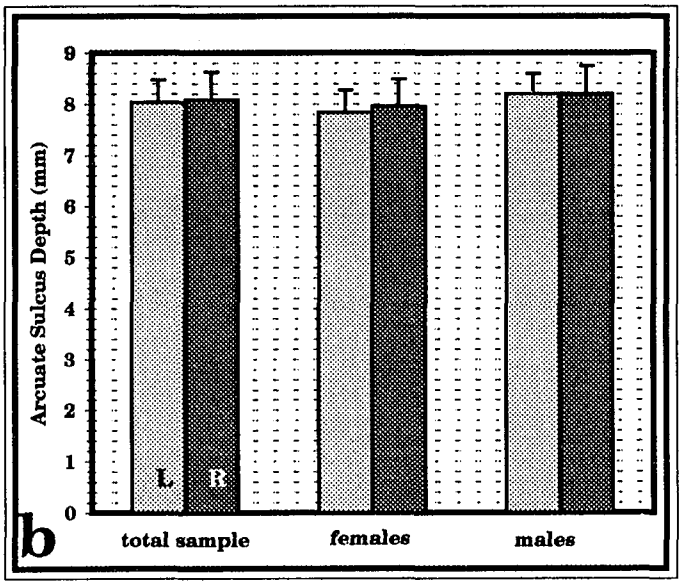

c

Paired t-Test

	Total		Females		Males	
	left	right	left	right	left	right
Mean	8.0	8.1	7.8	7.9	8.2	8.2
Variance	0.2	0.3	0.2	0.3	0.2	0.3
Observations	16	16	7	7	9	9
Pearson Correl'n	0.51		0.73		0.26	
Hypoth Mean Diff	0		0		0	
df	15		6		8	
t Stat	-0.40		-0.83		0.02	
P(T<=t) one-tail	0.35		0.22		0.49	
t Critical one-tail	1.75		1.94		1.86	
P(T<=t) two-tail	0.70	N/S	0.44	N/S	0.99	N/S
t Critical two-tail	2.131		2.45		2.31	

was 8.0 ±0.4mm (max = 8.9mm, min = 7.2mm). The mean for SF-d on the right hemisphere in the total sample was slightly larger at 8.1 ±0.3mm (max = 8.9, min = 7.3); see Figure 6-6a & b.

In females (n = 7), the mean value for SF-d was 7.8 ±0.4mm on the left hemisphere, and once again, slightly larger at 7.9 ±0.5mm on the right hemisphere (Figure 6-6a & b). In males (n = 9), the mean value for SF-d on the left hemisphere was larger than the total sample mean at 8.2 ±0.2mm, and similar on the right hemisphere at 8.2 ±0.5mm (Figure 6-6a & b)

In the total sample (n = 16), six individuals, representing ~38% of the sample, were larger on the left hemisphere (Figure 6-7). All of these values were greater than 0.1. Two of the right hemisphere larger values were less than 0.1mm, thus probably representing hemispheric symmetry.
In females (n = 7), only one individual was larger on the left hemisphere. However, of the six individuals that were larger on the right hemisphere, two were larger by less than 0.1mm, and two by less than 0.2mm (Figure 6-7). The outcome still suggests a right hemisphere predominance in females since only one large size difference was seen in the right hemisphere. However, a substantially larger sample size would be needed to characterize this potential but subtle sex-specific difference.

In males (n = 9), the magnitude of hemispheric differences in the depth of the sylvian fissure were much greater than that seen for females (Figure 6-7). In addition, the male sample appeared to be evenly distributed with

Figure 6-7 **a)** Plot of inter-hemispheric differences in the depth of the sylvian fissure (SF-d). Values represent the difference in millimeters of the depth of the central sulcus in the left and right hemispheres, plotted for the largest side in: the total sample (n = 16), the female sub-sample (n = 7), and the male sub-sample (n = 9). See text, Section 6.4.3. for details.

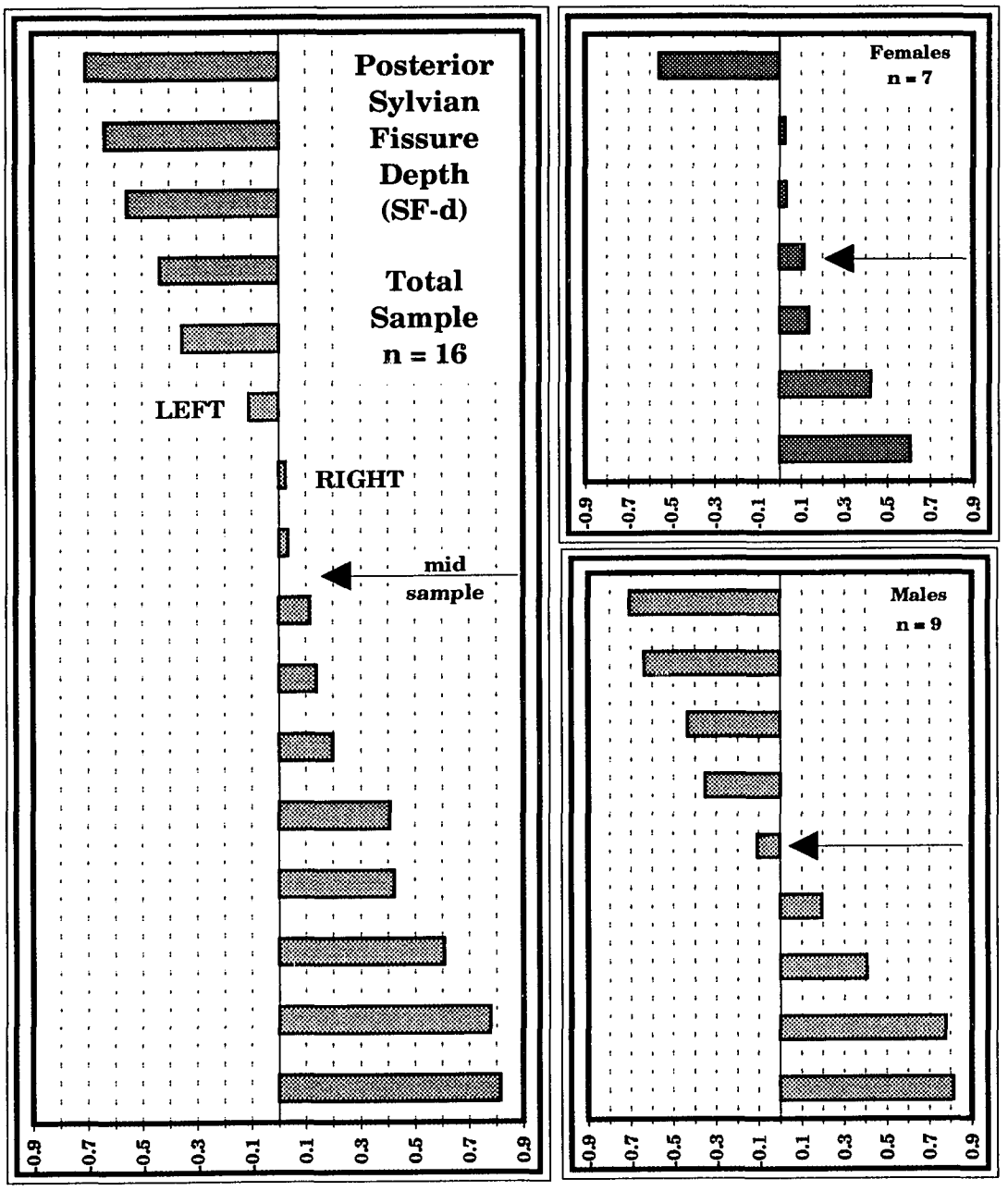
Posterior
Sylvian
Fissure
Depth
(SF-d)
Total
Sample
n = 16
LEFT
RIGHT
mid
sample
-0.9
-0.7
-0.5
-0.3
-0.1
0.1
0.3
0.5
0.7
0.9
Females
n = 7
Males
n = 9

regard to the inter-hemispheric distribution of depth differences, with five individuals being larger in the left hemisphere, only one of which was less than 0.2mm.

6.4.3.2. Statistical analysis of 3-D measures of sylvian fissure depth:

The sample was analyzed, using the paired sample t-Test, first for the total combined sample and then separately for the sex-specific sub-samples. Finally, the three independent values taken from each sylvian fissure in each individual were used separately as an expanded sample (n = 48).

Using the type 1 t-Test (paired sample) for the total sample of values for SF-d on the left and right hemispheres, it was shown that there was no significant size difference between the two hemispheres at $P = 0.7$. Likewise, in the female sub-sample (n = 7), and in the male sub-sample (n = 9), there were no significant hemispheric differences in the depth of the posterior portion of the sylvian fissure in which $P = 0.44$ and $P = 0.99$ respectively.

The three individual data-points for each sylvian fissure were considered separately using the paired sample t-Test. As before, it was shown that there was no significant difference between the left and right hemispheres in the total sample (n = 48) at $P = 0.85$.

6.4.4. Co-occurrence of depth measures of Arcuate Sulcus, Central Sulcus, and posterior Sylvian Fissure on the left and right hemispheres

This final analysis of sulcal/fissural depth measures considers the rate of co-occurrence of values for the largest hemisphere in the three different structures, two on the frontal lobe and one on the temporal lobe (Figure 6-8,).

For the two frontal lobe structures, the arcuate and central sulci, nine individuals were larger on the same left hemisphere. This represented ~53% of the total sample (n = 17). Conversely, of the two arcuate sulci larger on the right side, these same two individuals showed central sulci and sylvian fissures larger on the opposite, left hemisphere (Figure 6-8,).

In the case of the central sulcus and sylvian fissure, only two individuals showed co-occurrence of the largest measure on the left hemisphere. Similarly, only two individuals showed co-occurrence of a larger right hemisphere value for central sulcus and sylvian fissure depth. Surprisingly, the majority of individuals showed the condition in which the central sulcus and sylvian fissure were deeper in the opposite hemisphere. This occurred in 12 of 16 individuals, representing 75% of the sample (Figure 6-8).

Figure 6-8 Plots of co-occurrence of inter-hemispheric differences in depth of the arcuate sulcus, central sulcus, and sylvian fissure. Values represent the difference in millimeters between the left and right hemispheres plotted for the largest side in: the total sample (n = 17), the female sub-sample (n = 8), and the male sub-sample (n = 9). See text, Section 6.4.4. for details.

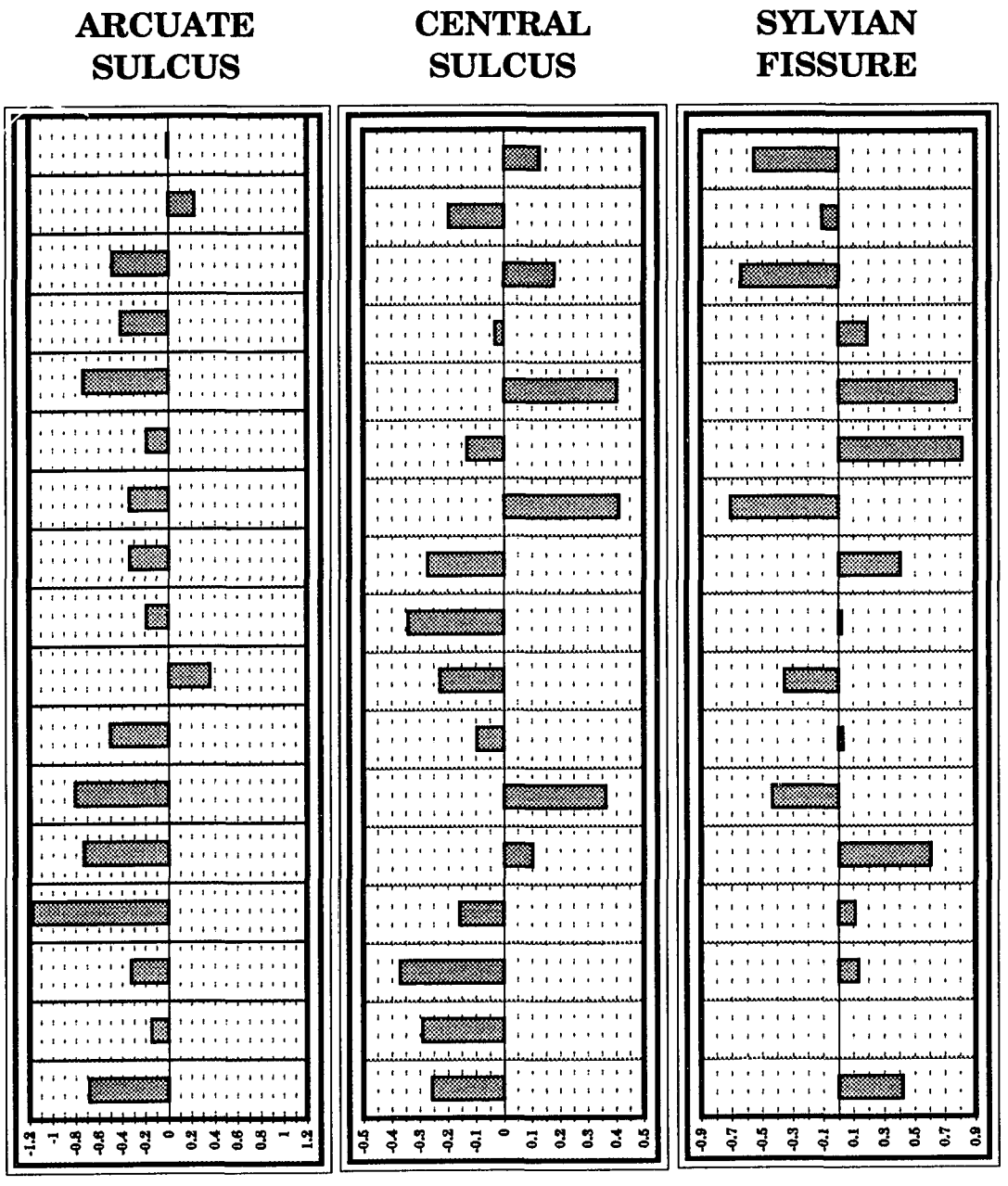
ARCUATE SULCUS
CENTRAL SULCUS
SYLVIAN FISSURE
-1.2 -1 -0.8 -0.6 -0.4 -0.2 0 0.2 0.4 0.6 0.8 1 1.2
-0.5 -0.4 -0.3 -0.2 -0.1 0 0.1 0.2 0.3 0.4 0.5
-0.9 -0.7 -0.5 -0.3 -0.1 0.1 0.3 0.5 0.7 0.9

CHAPTER 7

DISCUSSION AND CONCLUSIONS

7.1. INTRODUCTION

This chapter presents an overview and discussion of the material presented in this dissertation. It is divided into three sections: *1)* Section 7.2 will discuss advances incorporated in this study in methodology and materials used; *2)* Section 7.3 will discuss the results of this study in the context of previous primate brain studies: *3)* Section 7.4 will present the implications from this study for a better understanding of the evolution of the primate brain and primate communication.

7.2 ADVANCES IN METHODS AND SAMPLING IN THIS STUDY OF THE EVOLUTION OF PRIMATE BRAIN ASYMMETRY

7.2.1. Advances in tissue preparation and animal sample

Major confounding variables in the study of primate brains have been the provenance and condition of the tissues being sampled as well as the species under study. Accordingly, it was a major focus of this study to attempt to control these variables with as much precision as possible. These advances will be summarized briefly.

The acquisition of adequate samples of primate brains is a difficult task. As such, most investigations of the subject have relied upon existing collections of brains obtained post mortem, often without specific data

regarding the time or cause of death of the animal (e.g., Yeni-Komshian and Benson, 1976, Heilbroner, 1987). Without these data it is, of course, not possible to chart any *in situ* postmortem changes to brains obtained in this manner. The removal and subsequent fixation of brain tissue from unknown provenance also provides additional complexities. For example, fixation of brains will affect greatly the morphology and anatomy of the tissues. Most brains obtained post mortem have been fixed by gross immersion techniques. This process involves fixation by extremely slow diffusion into brain tissues inwards from the surface. In this technique, the presence of extraneous matter such as accumulated blood may act as a distorting variable. Further, since immersion/diffusion fixation is a slow process, superficial parts of the brain are fixed prior to deeper parts. This differential fixation may produce varying degrees of tissue shrinkage, and thus, give rise to distorted morphology.

A major goal of this project was to control for these brain tissue preparation problems. All of the brains used for this study were obtained from animals that were sacrificed by trans-cardiac perfusion fixation (Sections 3.2.3 - 3.2.8.). In brief, this method involves rapid flushing of all blood followed by global perfusion with fixative. Fixative is able to access the entirety of the brain equally and concurrently. This approach minimizes the potential for *in situ* or post mortem distortions caused by preparation artifact.

For the reasons stated above it is felt that the methods used in this study provide for an advance in the reliability of the tissues used. In particular, these methods may allow for more accurate statements to be made about the pattern and direction of inter-hemispheric asymmetries than has been possible previously.

In order to employ the precise methods described above, it was essential to select an animal model that met the dual criteria of availability and relevance. As detailed in Chapter 3, *Macaca fasicularis* was chosen since it is widely used in the United States for biomedical research and live animals were thus available in large numbers, and it is a member of the most frequently used genus in studies of brain asymmetry (e.g., Yeni-Komshian and Benson, 1976; Falk, 1978b; LeMay et al., 1982; Heilbroner, 1987). In addition, the focus upon one macaque species allowed for detailed examination of sexual dimorphism. As a result of the above, the brains used for this study represent the largest sample of controlled preparation tissues from a primate to date.

7.2.2. Advances in measurement of brain structures

In order to overcome some of the inherent difficulties in using two dimensional measures of brain surface anatomy a number of investigators have attempted three dimensional analysis (e.g., Falk et al, 1986, Heilbroner, 1987). These studies have, however, had inherent difficulties. For example, one of the major problems associated with quantification of brain surface features such as sulci and fissures involves precise and reproducible determination of their points of origin and termination. These points are often difficult to identify due their location on subtle sloping regions of sulci on the brain surface. It is not clear how previous studies determined these specific points. Further, since the assessment of sulcal terminations is extremely difficult even on fresh brains, the placement of these points on endocasts present with even more problems.

In addition, a second potentially compounding problem may involve measurement methods. For example, Heilbroner (1987) used a calibrated

tape attached with pins to the surface of the brain to measure sulcal dimensions. Although this method provided a means of estimating three dimensional sulcal length, the essentially two dimensional nature of the tape may not have allowed for as precise measures as possible. Similarly, the 3-D digitizer method used by Falk (1987) involved summing a succession of straight lines joining a series of points in order to obtain total length. Whether this measure represented the *continuous* three dimensional arc is unclear.

In order to overcome some of these potential measurement problems, new approaches to assessing three dimensionality on the surface of the brain were devised (Chapter 3, Section 4.2). First, this involved improving the identification of sulcal origins and terminations. Briefly, a focused fiber-optic light source was placed at an acute angle to the sulcus in order to create a shadow that clearly demarcated the subtle zone of sulcal origin/termination. Second, braided suture cord which was round and highly flexible was used to measure 3-D sulcal length (Chapter 4, section 4.2). This material offers the advantage of conforming readily, in all planes, to the three-dimensional contours of the structures being measured. The cord was moistened so that it adhered to the surface of the brain without the use of pins. Under view of an operating microscope the cord was placed along the sulcus with particular attention paid to placement at sulcal origins/terminations. The cord was then removed and its length measured using a digitizing pad with a resolution of <0.01mm. Preliminary studies performed to assess the reproducibility of this method showed the margin of error to be consistently <0.2mm.

Although structures such as gyri and fissures were measured as they coursed across the three dimensional surface of the brain, values are not

represented by a three dimensional (3-D) coordinate data matrix (i.e., x, y, and z coordinates). Instead, *curvilinear* measures, which were made directly from the surface of brains, were transposed into two-dimensional (2-D) linear values for subsequent quantitation and statistical analysis. However, since these transposed values reflect directly the length of the complex 3-D contour (and thus contain potentially critical information beyond a 2-D assessment) they will be referred to in this dissertation as "three-dimensional" measures. This also serves to distinguish these measures from my true "two dimensional" linear measures that were taken solely from brain photographs.

While this study has incorporated advances in 3-D applications, 2-D measurements have also been employed. This was due to two reasons: 1) 2-D measures offer valuable information in their own right, and 2) they allow for direct comparison with data from a large number of studies assessing brain asymmetry. Traditionally, 2-D measures have been made directly from photographs (e.g. Falk, 1978, Heilbroner 1987) and thus carry with them all of the inherent limitations of point selection and determination noted above. In order to improve on this, the following new methods were used: 1) the photographic prints from which the measurements were made were magnified 1.5 x to 2.0x in order to increase the field so that point identification could be maximized; 2) operating microscopes were used to view the already enlarged images in order to place as precisely as possible the sulcal termination points; 3) fine needle probes were used to mark points on an sheet of acetate placed over the photograph; 4) a sharp-tipped digitizing pen stylus was used to measure the distance between points; and finally 5) for subtle petelial projections, lines on the acetate overlay were viewed on a light microscope at high magnification (25x) and measures made directly via the microscope eyepiece using an ocular micrometer. These new

methods of 2-D analysis provided improvements for visualization and quantitation of discrete brain surface structures.

7.3 DISCUSSION OF THE RESULTS OF THIS STUDY

7.3.1. Anatomy and variation of structures examined in this study

One of the goals of this study was to assess critically the anatomy and variation present in the structures used for quantitative analysis. The first part of this discussion will review this with regard to the major structures investigated.

7.3.1.1. Arcuate sulcus

Previous studies have described or measured the extent of the vertical and/or horizontal portions of the arcuate sulcus (e.g., Von Bonin,G and Bailey, 1947; Falk, 1978a; Heilbroner, 1987; Heilbroner and Holloway, 1989). Since the "vertical limb" of the arcuate sulcus is adjacent to the region of cortex homologous to Broca's area its quantification may provide more meaningful data on the inter-hemispheric asymmetry of this specific area. For example, in *Macaca fascicularis* and *Macaca mulatta*, the so called "inferior portion of the arcuate sulcus" was reported to be greater in the left hemisphere than in the right, although it is not clear how this portion was distinguished (Heilbroner, 1987). Based on these results Heilbroner stated that, "...it is tempting to suggest that this asymmetry may presage the evolution of Broca's area, and also of the premotor region controlling the forelimbs (and, therefore, is suggestive of right-handedness)." (Heilbroner, 1987: 163). This study presents data on the anatomy and variation of the arcuate sulcus which suggests that separate length measures of the vertical

and/or horizontal "limbs" of the arcuate sulcus are essentially without value due to ambiguous delineation of margins.

In this study, arcuate sulcus variation is described with regard to recognition of major patterns embedded within a continuous spectrum of morphological expression. Three major patterns were distinguished as illustrated in Table 3-1, and Figures 3-6, 3-7 & 3-9. For example, Pattern I of the arcuate sulcus denotes a morphology in which there is a continuous arc-like sweep from the vertical to the horizontal planes. This pattern was present in 48% of the cerebral hemispheres used in this study. Obviously, if this pattern occurs no method can be used to distinguish its vertical and horizontal limbs. In Patterns II and III, a posterior spur of the arcuate sulcus exists to various degrees. Although this spur separates the two limbs of the arcuate sulcus to some extent, it is not present consistently in both hemispheres. This, of course, is necessary for asymmetry measures. In fact, in 32% of individuals that showed Pattern II or III in either the left or right hemisphere, the opposite hemisphere showed Pattern I. As such, for these individuals, only values for the pattern of inter-hemispheric asymmetry in the total length of the arcuate sulcus would have value for a quantitative analysis. Even in individuals with Patterns II or III on both the left and right hemispheres, the accuracy in distinguishing precisely the vertical and horizontal limbs is largely arbitrary due to the lack of reliable landmarks. As a result, the method used for this study was designed to establish a more rigorous vertical-horizontal distinction in order to measure the 2-D length of the vertical portion of the arcuate sulcus.

7.3.1.2. Sub-central dimple

The subcentral dimple (SCD) is located posterior to the inferior portion of the arcuate sulcus in the inferior frontal lobe ("scd" on Figure 3-7 in Chapter 3). Since SCD separates the macaque homolog of Broca's area from a different cytoarchitectonic area located immediately posterior (Area FBA; of Von Bonin and Bailey, 1947), it may represent an important landmark which can delineate inter-hemispheric asymmetry of this region. Although the subcentral dimple was present in all hemispheres examined, it showed a good deal of variation ranging from being barely evident (Figure 3-7a) to being deeply excavated (Figure 3-7b). However, for the purposes of quantitation of its position relative to the arcuate and central sulci, this size variation did not appear to affect the data to any degree. There was no apparent co-occurrence between the magnitude of the sub-central dimple and the patterns of variation present within the arcuate sulcus.

7.3.1.3. Sylvian point

The pattern of appearance of the sylvian point (i.e., the point of posterior termination of the sylvian fissure, Witelson and Kigar, 1992) on the external surface of the brain was determined in a sample of 43 mixed sex individuals. The sylvian point represents an important landmark since a region of the adjacent superior temporal gyrus is homologous to the human Wernicke's area (see Section 2.6.4.2.). Expansion of this cortical region in the left hemisphere gives rise to a left hemisphere predominance of sylvian fissure length, at least in humans and great apes (Yeni-Komshian and Benson, 1976). As such, the ability to distinguish this important brain surface landmark is necessary for establishment of patterns of inter-hemispheric asymmetries in sylvian fissure length. For example, in order to make use of endocasts of fossil or extant species, it is critical that the pattern of sylvian

point anatomy on the surface of the brain is well characterized in fresh brains.

In order to establish a framework which encompasses variation present in the region where the sylvian point is located three patterns were defined (see Section 3.3.2., Figures 3-8 & 3-9, and Table 3-1). In brief, in both Patterns I and Pattern II, the sylvian point was located deep to the surface of the brain due to operculation by the superior temporal and inferior parietal gyri, but to different degrees. These conditions were evident in 77% of the hemispheres used for this study. As a result, in these hemispheres, the exact position of the sylvian point could not be determined absolutely without spreading apart the walls of the overlapping temporal and parietal structures. Conversely, Pattern III (in which the sylvian point was evident on the external surface of the brain) was present in 33% of hemispheres.

This analysis does not support the hypothesis suggested by Falk (1978a) that the inferior parietal cortex of the left hemisphere predominantly opercularizes the sylvian fissure in cercopithecoids in a manner similar to that in humans and great apes. In this study, Patterns I and II, in which the sylvian point was operculated, were present equally on 67% of left and right hemispheres. Similarly, my results do not support data from previous studies in macaques that reported a more frequent "linking" of the superior temporal sulcus and sylvian fissure in the right hemisphere (e.g., Ingalls, 1914; LeMay et al., 1982). Based on these studies, LeMay and colleagues (1982) suggested that the posterior part of the superior temporal gyrus was more developed in the left hemisphere of macaques, i.e., in a manner similar to humans. This suggests that the distinct separation of the superior temporal gyrus and sylvian fissure on either the left or right hemisphere represents the more differentiated or derived state.

The presence of Patterns I or II (sylvian point operculated), would obviously not allow for either endocasts or photographs of brains to be used for measurement of sylvian fissure length since the exact position of the sylvian point could not be determined. For this reason, previous studies of sylvian fissure asymmetry that have used endocasts or lateral photographs, have estimated the approximate location of this point (e.g., Falk, 1978). Such studies have used the confluence of the superior temporal sulcus and sylvian fissure as the posterior termination of the sylvian fissure, the sylvian point.

For this study, 3-D measures of sylvian fissure length (Chapter 4, Section 4.4.2), in which cord was laid along the sylvian fissure, permitted precise quantitation of absolute dimensions since the overlying tissues were easily spread apart allowing full access to the sylvian point. However, for my 2-D measures of sylvian fissure length (Chapter 3, Section 5.3.3.), in which lateral photographs were used, the posterior confluence of the sylvian fissure and the superior temporal sulcus were used as the posterior margin of the sylvian fissure similar to previous studies.

7.3.1.4. Suprasylvian gyrus and supra-sylvian dimple

The suprasylvian gyrus and associated supra-sylvian dimple of macaques may be homologous to one of the discrete sub-areas included within the functional concept called Wernicke's Area in humans. In the majority of *Macaca fascicularis* brains used for this dissertation there was a small dimple located on the inferior parietal lobe immediately posterior and superior to the sylvian point (Chapter 3, Figure 3-10). This dimple has been referred to previously as "BRTS" (Falk, 1978b) and here as the "suprasylvian dimple" (SSD). Falk reported that this dimple was present more often on the left hemisphere in cercopithecoids, supposedly indicating asymmetric inferior

parietal lobe expansion. Neither left or right hemispheric predominance of SSD was seen in the sample of *M. fascicularis* brains used here.

Associated with SSD was a small area of grossly distinct cortex that bulged laterally in comparison with the surrounding area. This bulging area was bounded inferiorly and posteriorly by the superior temporal sulcus, which in some cases appeared to bifurcate, with a small anterior spur being oriented towards the suprasylvian dimple in at least ten of the 44 brains studied. This bulging cortical structure is referred to here as the "supra-sylvian gyrus" (SSG) although whether it warrants gyral distinction is not fully clear. Although the anterior portion of SSG is partly involved in operculation of the sylvian point this does not appear to be the result of an expansion of this cortical area. In fact, SSG does not appear to bulge or to be more expanded in these cases than it does in a non-operculated sylvian point. Whether SSG operculates the sylvian point or not, there in no apparent predominance of either SSD or SSG in the left or right hemisphere .

The degree of lateral bulging of the SSG beyond that of the surrounding cortex was not quantified in this study. However, this could well prove to be an important quantitative measure that would show hemispheric asymmetry, and is one that could be readily measured from either perfusion-fixed brains or endocasts. However, due to the superior location of this bulging area of cortex, the measures used for parietal width which used a dorsal perspective could not be used. Accordingly, a more oblique perspective would be necessary to measure the SSD.

This expanded cortical region in macaques may well represent a functional specialization of the inferior parietal lobe association cortex for polymodal integration of communicative input from the immediately adjacent auditory and visual cortices as is the case in humans. Whether this

strategically located cortical region shows intrinsic hemispheric asymmetry (or left hemisphere functional localization, similar to humans) remains to be established.

7.3.2. Morphometry of frontal lobe structures

This section presents a discussion of the findings obtained from measurements of the dimensions of a series of frontal lobe cerebrocortical structures in both the left and right hemispheres. Refere to Table 7-1 below for a summation of all statistical data in this study.

7.3.2.1 3-D Measures of arcuate sulcus length

These measures of arcuate sulcus length represented its complete length from its antero-superior origin to its inferior termination. Results of this 3-D analysis showed that in the total sample of seventeen individuals there was no significant difference at the $P = < 0.05$ level ($P = 0.3$) in the total length of the arcuate sulcus in the left and right hemispheres (Table 4-1 and Figures 4-1 & 4-2). This was also the case when males and females were considered separately although there was a slight (non-significant) tendency in males at $P = 0.2$, but not in females at $P = 0.74$, for the arcuate sulcus to be larger on the right hemisphere. However, it should be noted that such "trends" are interpreted within the constraints imposed by α - errors within probability levels.

The inferior post-arcuate area in the left hemisphere of macaque brains is homologous to Broca's language area in human as defined by cytoarchitectonic criteria (Galaburda and Pandya, 1982). If this consistent cytoarchitectonic asymmetry is represented by gross anatomic asymmetric features on the surface of the left hemisphere of the brain, this has not been apparent in the 3-D measures used here. A study using endocasts, however,

Table 7-1. Summary table of results showing *P* values from t-Tests from all measures of hemispheric asymmetry presented in Chapters 4, 5 and 6. Shaded areas represent measures that showed statistically significant asymmetry at the $P < 0.05$ level (with predominant side denoted). Bold Italizized values represent *P* values that showed a (non-significant) trend towards hemispheric asymmetry at the $P < 0.01$ level. It should be noted that in each case an α - error will be present in proportion to the significance level chosen.

SUMMARY OF DATA

MEASURES	TOTAL SAMPLE		FEMALES		MALES	
FRONTAL LOBE	**n=**	***p* =**	**n=**	***p* =**	**n=**	***p* =**
3-D AS	17	0.310	8	0.740	9	0.200
3-D CS	17	0.630	8	0.950	9	0.460
AS-v	33	***0.09*** $_{R>L}$	19	0.810	14	**0.04**$_{R>L}$
A-Ci	33	**0.01**$_{R>L}$	19	0.120	14	**0.04**$_{R>L}$
A-Cii	33	**0.04**$_{R>L}$	19	**0.03**$_{R>L}$	14	0.330
A-Ciii	33	0.300	19	0.200	14	0.740
A-Civ	33	**0.005**$_{R>L}$	19	**0.007**$_{R>L}$	14	0.250
A-Cv	33	0.850	19	**0.05**$_{R>L}$	14	0.770
A-Cpool	165	**0.001**$_{R>L}$	95	**0.001**$_{R>L}$	70	**0.05**$_{R>L}$
A-SCD	29	0.240	18	**0.01**$_{R>L}$	11	0.560
C-SCD	29	0.840	18	0.730	11	0.820
A-Ci2	33	0.320	19	0.960	14	0.160
A-Cii2	33	0.410	19	0.980	14	0.200
TEMPORAL LOBE						
3-D SF	18	0.970	8	0.780	9	0.620
3-D STS	18	0.420	8	0.350	9	0.820
SF-ap	34	0.480	16	0.380	18	0.820
STS-ap	34	0.250	16	0.530	18	0.350
STGi	27	0.620	14	0.950	13	0.560
STGii	27	***0.06*** $_{R>L}$	14	0.340	13	0.110
STGiii	27	0.110	14	***0.08*** $_{R>L}$	13	0.590
STGiv	27	0.800	14	0.500	13	0.820
STGv	27	0.240	14	0.800	13	***0.06*** $_{R>L}$
STG pool	135	**0.01**$_{R>L}$	70	***0.08*** $_{R>L}$	65	***0.08*** $_{R>L}$
STG-tot2	33	0.970	15	0.420	18	0.590
STG-Tpt2	26	0.170	13	0.350	13	0.310
PETELIAS & WIDTHS						
FR-pet	10L&9R	0.410	8L&5R	0.500	2L&4R	0.960
OC-pet	13L&6R	0.500	9L&4R	0.260	4L&2R	***0.08*** $_{L>R}$
FRw-a	22	0.510	14	0.580	8	0.750
FRw-p	22	0.800	14	0.730	8	0.930
PAw-a	22	0.750	14	0.710	8	0.980
PAw-p	22	0.700	14	0.830	8	0.750
SULCAL DEPTHS						
AS	17	0.001$_{L>R}$	8	0.01$_{L>R}$	9	0.05$_{L>R}$
CS	17	0.500	8	0.05$_{L>R}$	9	0.560
SF	16	0.700	7	0.440	9	0.990

Shading = Significant at p<0.05 Italic = very low p value

KEY

3-D AS	-	3-D length of arcuate sulcus
3-D CS	-	3-D length of central sulcus
AS-v	-	2-D length of vertical limb of arcuate sulcus
A-Ci	-	Series of 2-D measures on the brain surface of the distance
A-Cii	-	between the arcuate sulcus and the central sulcus
A-Ciii	-	"
A-Civ	-	"
A-Cv	-	"
A-Cpool	-	"
A-SCD	-	2-D distance between the arcuate sulcus and the subcentral dimple
C-SCD	-	2-D distance between the central sulcus and the subcentral dimple
A-Ci2	-	2-D area of the cortex between the arcuate and central sulci
A-Cii2	-	2-D area of the cortex between the inferior arcuate and central sulci
3-D SF	-	3-D length of sylvian fissure
3-D STS	-	3-D length of superior temporal sulcus
SF-ap	-	2-D length of the sylvian fissure
STS-ap	-	2-D length of superior temporal sulcus
STGi	-	Series of 2-D measures on the brain surface of the distance
STGii	-	between the sylvian fissure and superior temporal sulcus
STGiii	-	"
STGiv	-	"
STGv	-	"
STG pool	-	"
STG-tot2	-	2-D area of the total superior temporal gyrus
STG-Tpt2	-	2-D area of the posterior regon of the superior temporal gyrus
FR-pet	-	2-D measure of frontal lobe petelia
OC-pet	-	2-D measure of occipital lobe petelia
FRw-a	-	2-D measure of anterior frontal lobe width
FRw-p	-	2-D measure of posterior frontal lobe width
PAw-a	-	2-D measure of anterior parietal lobe width
PAw-p	-	2-D measure of posterior parietal lobe width
AS	-	3-D depth of arcuate sulcus
CS	-	3-D depth of central sulcus
SF	-	3-D depth of sylvian fissure

did report a trend for the total length of the arcuate sulcus to be longer in the left hemisphere in *Colobus* (Falk, 1978b). However, a more recent study by Falk (1990) showed total arcuate sulcus length to be essentially symmetric in a large sample of latex endocasts of *Macaca mulatta*, which is similar to that found here.

The observations from this study showing symmetry of total arcuate sulcus length may not reflect asymmetries present in specific sub-areas. For example, Heilbroner (1987: 163) reported that the inferior portion (vertical limb) of the macaque arcuate sulcus was asymmetric and predominated in the left hemisphere, while he subsequently noted that the horizontal limb was symmetric (Heilbroner and Holloway, 1989). Should Heilbroner's observations indeed be the case, then one would expect there to be an overall asymmetry due to the contribution provided by left hemisphere predominance of the vertical limb. However, as noted such asymmetry was not found in this study. A possible reason for this discrepancy may relate to the validity of distinctions between the vertical and horizontal limbs of the arcuate sulcus.

7.3.2.2. Two dimensional measures of arcuate sulcus and post arcuate cortex

Two dimensional measures of the arcuate sulcus and post arcuate cortex were made from lateral photographs of the brain. Since the dimensions of associated sulci, however, may not reflect changes in adjacent cortical structures, a series of new measures were devised to quantify different aspects of this cortical region.

A new method was also devised that allowed the vertical and horizontal portions to be divided for measurement (see Section 5.3.1.6.) in cases where a posterior spur of the horizontal limb of the arcuate sulcus was not present.

Results showed that there was a distinct trend for the vertical limb of the arcuate sulcus to be larger in the right hemisphere ($P = 0.09$) in the total sample of 33 individuals. Results showed that this trend was due to the significant asymmetry ($P = 0.04$) present only in the males as opposed to symmetry in females ($P = 0.81$). These results support those of the 3-D analysis of total arcuate sulcus length described above (Section 7.3.2.1.) which showed a slight trend ($P = 0.2$) in males only for the arcuate sulcus to be larger on the right hemisphere. These marked sex differences in arcuate sulcus dimensions may relate to sexual dimorphism in hemispheric size of these brain structures, underlying a sex-specific behavioral outcome.

The area of cortex adjacent to the vertical limb of the arcuate sulcus was similarly assessed in order to determine whether a similar pattern of right hemisphere predominance was present. These dimensions were represented by a series of five separate distance measures, two area measures, and two measures of the relative position of an associated structure, the subcentral dimple (see Section 5.3.1.).

The inter-sulcal linear measures showed a significant right hemisphere size predominance in the majority of cases, similar to that shown for the arcuate sulcus. However, unlike the measures of arcuate sulcus, most of these inter-sulcal measures indicate a significant right hemisphere predominance of asymmetry in females. Although a similar trend was observed in males, it was not significant. However, when the five inter-sulcal measures were pooled, both sexes were shown to be significantly larger in the right hemisphere. This hemispheric asymmetry was considerably more pronounced in females ($P = 0.00002$) than in males ($P = 0.05$).

Inter-sulcal brain surface area was also determined. Unlike the inter-sulcal linear measures, no significant asymmetry was shown for either males

or females in either of the two measures. There was a trend in males only, however, for the inferior inter-sulcal region to predominate on the left hemisphere, whereas the area measure that included the superior portion, tended to be larger on the right hemisphere. The global nature of these area measures, however, may have masked some of the subtle asymmetries that were indicated by the more discrete inter-sulcal linear measures.

The sub-central dimple is located at the most inferior margin of the inter-sulcal region. Linear measures which were made from this dimple to the arcuate and central sulci showed some interesting patterns of asymmetry. The distance between the sub-central dimple and the arcuate sulcus was significantly larger in the right hemisphere of females ($P = 0.01$) but not males ($P = 0.56$), similar to the inter-sulcal linear measures. Interestingly, this area of the inferior post-arcuate cortex represents the region in macaques that is homologous to Broca's area in humans. No hemispheric asymmetry was seen in the measure of distance between the sub-central dimple and the central sulcus, an area of motor cortex that is known to subserve face, tongue, and upper vocal tract motor functions in *Macaca* (Woolsley, 1964)

7.3.2.3. Depth of the arcuate sulcus

Previous studies have focused solely on measures of the external surface of the brain in order to define loci of inter-hemispheric asymmetries. This approach, of course, is absolutely necessary for the analysis of fossil endocasts since only the external surface of the brain is available. However, a good knowledge of the anatomy and asymmetries in these same structures, but deep to the surface of the brain, is critical for a better understanding of the dynamics of inter-hemispheric asymmetries present on the surface. This

study presents the first report of measures of arcuate sulcus dimensions deep to the surface of the brain (Figures 6-2 & 6-3)

Results of arcuate sulcus depth measures showed a highly significant predominance of the left hemisphere in the total sample ($P = 9.5 \times 10^{-4}$). This was the most pronounced example in this study, of a consistent expression of hemispheric asymmetry, since at least 14 of 17 brains measured were larger in the left hemisphere. This effect was more pronounced in females ($P = 0.01$) than in males ($P = 0.05$). However, results of inter-hemispheric measures of the linear dimensions of the post-arcuate cortex on the surface of the brain, showed that females were more right hemisphere dominant. If indeed this is the case, it seems that the expansion of cortical structures in the left hemisphere involved differentiation and expansion of neural loci deep to the surface of the brain, with excavation of the arcuate sulcus. The effect of this expansion into the depth of the arcuate sulcus may have involved a concomitant reduction in the amount of cortical tissue expressed on the surface of the brain and which was more pronounced in females than in males. As such, the impression given by data derived from surface measures is that the cortical area in the right hemisphere is predominant in the expression of asymmetry. On the contrary, asymmetries shown to be present from depth measures are more pronounced and are the opposite of those shown by brain surface measures (i.e., are larger on the left hemisphere). Thus, cortical sites in the left hemisphere of macaques that are homologous to Broca's area in humans are asymmetric and anatomically predominant in the left hemisphere. As is the case in humans (Falzi et al., 1982), these left side predominant asymmetries in macaque brains are evident primarily *deep* to the surface of the brain.

7.3.2.4 Summary

Results of the measures described above may provide new insight into mechanisms underlying the evolution of language substrates. Expanded cortical structures on the surface of the right hemisphere in macaques probably do not reflect the essential shift: expansion in the left hemisphere of the cortical site which potentially subserves communicative functions. Expansion of surface cortex on the right hemisphere may, in turn, represent a right hemisphere predominance and functional localization of a discrete behavior, but within cerebral loci distal to the homotype of the site of interest here (Broca's area homolog). Whether this distal site contributes to communicative behavior remains to be seen.

7.3.3. Measures of the central sulcus

The anterior bank of the central sulcus is the region of the cerebral cortex which subserves motor function. If motor functions are asymmetrically organized, this should be reflected by various measures of its hemispheric dimensions. These motor cortex asymmetries may be related to concomitant asymmetry of associated regions (i.e., homologs to Broca's area in humans). No previous study has reported the dimensions of the central sulcus in perfusion-fixed brains of *Macaca fascicularis*.

7.3.3.1. Central sulcus length

The total 3-D length of the central sulcus from its supero-medial origin to its infero-lateral termination was determined (see Chapter 4, Section 4.3.4., Table 4-2, and Figures 4-7 & 4-8). No significant hemispheric asymmetries were found in the 3-D length of the central sulcus between the left and right hemispheres. There was, however, a non-significant trend towards predominance of central sulcus length in the right hemisphere in males, in

which seven of the total sample of nine individuals were larger. It thus appears that the asymmetries shown to be present within the associated pre-motor regions of the post-arcuate cortex are not expressed in the motor output centers adjacent to the central sulcus.

7.3.3.2. Central sulcus depth

Measures of the depth of the central sulcus were also made. Results from measures of the depth of the central sulcus showed that it was significantly deeper in the left hemisphere of females ($P = 0.05$). In males, the depth of the central sulcus was essentially symmetric ($P = 0.56$) and there was an equal distribution of hemispheric depth measures. These results are interesting since they are similar to those reported for depth of the arcuate sulcus, which predominated in the left hemisphere of females. Although the sex-specific sample sizes are relatively small, these results again point to the importance of considering sex differences in cerebral asymmetry.

7.3.4. Morphometry of temporal lobe structures

7.3.4.1. Sylvian fissure length

The sylvian fissure has long been shown to be an important indicator of cerebral asymmetry in a region of the macaque brain that is homologous to Wernicke's speech-language reception area in humans. For example, in humans and great apes it has been shown that the left sylvian fissure is significantly longer (Yeni-Komshian and Benson, 1976). Studies in both immersion-fixed brains and latex endocasts of macaques, have also shown that the sylvian fissure is significantly longer in the left hemisphere (Falk et al., 1986). In humans, this asymmetry is due to expansion of cortex in the banks of only the posterior region of the sylvian fissure (Witelson and Kigar, 1992). However, in contrast to these data, Heilbroner and Holloway (1988)

have suggested that in macaques, left hemisphere predominance was due to expansion of cortex adjacent to the anterior portion. Asymmetry of the posterior region was explored in detail here.

In marked contrast to the above studies, no significant asymmetry of the sylvian fissure was shown in this analysis. Neither 3-D nor 2-D measures of sylvian fissure length revealed even a trend towards hemispheric asymmetry. However, with 3-D measures, six of the nine males showed a longer sylvian fissure on the left hemisphere, with two on the right and one equal. In contrast, females were equally represented between the two hemispheres. There was no indication of a trend towards hemispheric predominance of this measure in either males or females with 2-D measures .

7.3.4.2. Sylvian fissure depth

An understanding of asymmetries in the depth of the sylvian fissure may be important in interpreting the morphological basis of differences in this region between macaques and humans. The posterior portion of the sylvian fissure is adjacent to the region of cortex that is homologous to Wernicke's area in humans. Expansion of this region, the planum temporale, is thought to be responsible for posterior extension of the sylvian fissure on the left hemisphere in humans. However, most of the bulk of this cortical region is positioned deep to the surface of the brain. Since inter-hemispheric asymmetry in the length of the sylvian fissure was not seen, it could be present deep to the surface, and thus be reflected by the depth of the posterior region of the sylvian fissure. Examination of posterior sylvian fissure depth, however, showed that there were no asymmetries. This is in agreement with the results from both 3-D and 2-D measures of the length of the sylvian fissure. This lack of asymmetry in sylvian fissure depth is in

marked contrast to depth data of the arcuate sulcus in which a highly significant left hemisphere predominance was indicated.

7.3.4.3. Contrasting findings on sylvian fissure dimensions

Results from this study clearly show the absence of gross inter-hemispheric asymmetry in the dimensions of the sylvian fissure. This is particularly interesting in light of previously described cytoarchitectonic asymmetries in this region. The findings of this study contrast sharply with previous work by Falk and co-workers (1986) and Heilbroner and Holloway (1988), who have reported a human-like left hemisphere predominance of hemispheric asymmetry in the brains of macaques and other cercopithecoids.

A number of reasons may underlie the different findings between this and previous studies. First, Falk's study (1986) used latex endocasts in which it is very difficult to determine reliably, and thus to reproduce, the origins and terminations of sulci or fissures. As noted throughout this chapter, precise determination of these landmarks was a major concern of this study. Second, it is neither possible to discriminate clearly in endocasts the location of surface blood vessels, nor to determine how these vessels may have influenced contiguous sulci and fissures. It is quite possible that unidentified vessels may have artificially extended the apparent margins of the sylvian fissure, for example, thus injecting artifact into the data collection. In this study, all vessels were removed along with the meninges, and the impressions left by them on the surface of the brain could not influence determination of fissural dimensions. Third, the study by Heilbroner and Holloway (1988) relied solely upon immersion/diffusion-fixed brains obtained from dead animals. As noted previously, brains such as these are subject to an array of postmortem distortions ranging from

differential shrinkage to morphological distortion. Such distortions may well be represented asymmetrically. All potential variables were controlled for in this study by the use of perfusion-fixed animals, characterization of regional anatomy and variation, development of new and more precise measuring techniques, and finally, the determination of specific fissural origins and terminations through the use of methods designed specifically for this. For these reasons it is proposed that data from this study may provide a more realistic representation of sylvian fissure dimensions.

7.3.4.4. Measures of the superior temporal gyrus and sulcus

In addition to measures of the sylvian fissure, a series of measures were made of the associated superior temporal gyrus and superior temporal sulcus. The brain region in macaques that is considered homologous to Wernicke's receptive language area in humans is located on the postero-superior portion of the superior temporal gyrus in the left hemisphere. As such, this region should be expressed as an expanded area of cortex on the left hemisphere.

The 3-D measures of superior temporal sulcus (STS) length were of its entire antero-posterior length, from its antero-inferior origin close to the temporal pole to its termination on the parietal lobe. Results showed no significant difference between the length of STS in the left and right hemispheres in either the total sample or the sex-specific sub-samples. However, seven of nine females showed a longer STS in the right hemisphere, and accordingly, the probability value was much lower for females ($P = 0.35$) than for males ($P = 0.82$). Similarly, in the total sample, 66% of individuals showed a larger STS on the right hemisphere.

Results of measures of the 2-D length of STS also showed that there was no significant difference between hemispheres in either the total sample or in males and females. These results for STS length are similar to those shown for the sylvian fissure reported above. However, there was some indication of a right hemisphere predominance that may have become more apparent using a larger sample size. For example, 59% of individuals showed a larger STS in the right hemisphere while only 29% were larger in the left hemisphere, and 12% were essentially symmetric. Previous studies in immersion/diffusion-fixed brains of macaques also showed a non-significant tendency for the STS to be longer in the right hemisphere (Heilbroner, 1987). In contrast, other studies using endocasts reported that the STS was longer in the left hemisphere of macaques (Falk, 1978b).

A third measure of superior temporal gyrus (STG) dimensions involved determination of its width at five equidistant points along its posterior extent. The measures commenced anteriorly at the level of the central sulcus and terminated posteriorly at the level of the sylvian point. Results of these measures showed no significant inter-hemispheric asymmetries. Only in two cases was there a trend towards right hemisphere predominance, the most anterior measure (STG-v) in males (P = 0.06), and the middle measure (STG-iii) in females ($P = 0.07$). In addition, in all five measures of STG width, the mean values for the right hemisphere were larger than those for the left. Finally, when all data for the five measures were pooled, it was shown that the STG was significantly wider in the right hemisphere in the total sample ($P = 0.01$).

It is interesting to note that Heilbroner's observation of one width measure of STG in macaques (corresponding to the measure STG-i in this study), showed sex-related differences (1987:114). For example, he found

that the width of STG was larger on the left hemisphere in females, whereas in males it was larger on the right hemisphere, although these results were not statistically significant. In contrast, in this study, both sexes showed a tendency towards predominance in the right hemisphere.

Area measures of STG were also used to determine whether there were any hemispheric asymmetries present in different portions as had been suggested previously (Heilbroner and Holloway, 1988; Witelson and Kigar, 1992). Results showed there were no significant hemispheric differences between the total area of the superior temporal gyrus. Likewise the pattern of hemispheric distribution was symmetric both in distribution and magnitude around the mid-sample point on the distribution graph, both in the total sample and in males and females (see Figure 5-24). Results from area measures of the posterior portion of the superior temporal gyrus showed that there was also no significant inter-hemispheric asymmetry. However, there was a trend in the total sample for the area of the posterior STG to be greater in the right hemisphere ($P = 0.17$), and mean values were larger on the right hemisphere in both sexes. In addition, 73% of individuals in the total sample showed a STG area that was larger in the right hemisphere. This effect was more marked in males in which 85% of individuals were larger in the right hemisphere. This result is similar to that reported by Heilbroner (1987: 114) in which there was a tendency for males to show a wider STG in the right hemisphere. However, this study did not show a reversed pattern of hemispheric asymmetry in females as did Heilbroner.

7.3.4.5. Comparison of these finding with other studies of the superior temporal sulcus and superior temporal gyrus

The long held hypothesis of left side predominance of temporal lobe structures was not supported by data from this study. On the contrary, there

was a marked trend for most of the measures to be larger on the right hemisphere, which was significant in pooled measures. Results of these surface measures are similar to those for the frontal lobe in which dimensions are larger on the right hemisphere. However, unlike data from the frontal lobe sulcal depths, which showed left hemisphere predominance, depth asymmetry was not seen in the temporal lobe.

Findings from this study of predominance of right hemisphere of cortical surface asymmetry may be due to several factors. For example, right predominance may represent a more differentiated region involved with polymodal integration of functions unrelated to communication. Expansion of this discrete cortical region may mask the potential expression of left hemisphere predominance of structures homologous to human speech centers that are involved with communication functions. To the contrary, it may be that in macaques the site involved with communicative receptive functions, unlike humans, is localized to the right hemisphere. This, however, is not supported by most anatomic evidence on regional homology and cytoarchitectonic asymmetry. Further, physiologic studies on hemispheric localization of auditory perception of vocalizations in macaques have shown that there is a right-ear/left-hemisphere advantage (Beecher et al., 1979; Zoloth & Green, 1979; May et al., 1989; Moody et al., 1989). It should be remembered, however, that functional localization does not necessarily have to be associated with a gross anatomical correlate. Finally, it may be that the homotypic region (of Area Tpt or Wernicke's area) on the right hemisphere of macaques is functionally involved in some complementary manner with that in the left hemisphere, different to that of humans. As discussed above in Chapter 2, the roles of right hemisphere structures homotypic to traditional left hemisphere language centers, are becoming better understood with

regard to their contribution to human vocal-auditory communication. Right hemisphere structures in macaques may parallel functionally those in humans. They may, however, be differentially represented corresponding to species-specific communicative demands.

7.3.5. Measures of frontal and occipital lobe petelias

A standard pattern has been described in the brains of right-handed humans (see Section 2.3.7.). This involves an anterior projection of the right frontal pole beyond that of the left in association with a posterior projection of the left occipital pole beyond that of the right. In left handed individuals the pattern is reversed or there is symmetry. As such, these asymmetries are thought to be associated in some general way with speech and handedness functions in humans. It was a goal of this study to determine if similar patterns of petelial projections were present in macaques.

7.3.5.1. Frontal lobe petelias

In the total sample of frontal lobe petelial projections, there appeared to be essentially equal left and right hemispheric representation in which L>R in 45%, R>L in 41% and L=R in 14%. However, when the sexes were considered separately, males showed an indication of right hemisphere predominance and females a left hemisphere predominance. The sample size was too small to make any definitive statement regarding sex differences of frontal lobe petelias at this time. These data do not support results from studies of *Macaca mulatta* endocasts in which significant right hemisphere predominant frontal petelias were shown in 50% of individuals versus 26% on the left (Falk et al., 1990). Likewise, a study of *Papio* brains (Cain and Wada, 1979), which showed predominance of the right frontal lobe in six of seven brains by up to 2mm (mean = 1.2mm) was not shown in this

dissertation using *Macaca fasicularis*. Indeed, in the brains examined in this study, the largest petelial projection of the right frontal pole was less than 0.5mm.

7.3.5.2. Occipital lobe petelias

An asymmetric pattern of occipital lobe petelias was found. In this pattern, the left hemisphere was predominant in 59% of the mixed sex sample compared to 27% on the right and 14% symmetric, which is similar to that shown for humans. In both males and females, the trend towards left hemisphere predominance of occipital lobe petelial projection was evident (see Figure 5-28). Additionally, in males there was a distinct trend (in a one-tailed t-Test), at $P = 0.08$, for the occipital lobe petelial projection to be larger in the left hemisphere. These results contrast with those provided by Falk from a non-metric study of *Macaca mulatta* endocasts, in which she found that the occurrence of occipital petelias was essentially symmetric (Falk, 1990).

7.3.5.3. Co-occurrence of frontal and occipital petelias

Results showed that the patterns of co-occurrence of frontal and occipital petelial projections in macaques were not identical to that of humans (see Section 5.5.3. and Figure 5-29). However, there was a distinct trend towards the human pattern if other factors, such as individual expression of human-like petelias were considered, as discussed below. The pattern of co-occurrence seen in humans, right frontal with left occipital petelias, was present in 27% of macaques; the reverse combination of left frontal with right occipital petelia was present in 23%. These primary patterns of petelial predominance and co-occurrence suggest an essentially equal distribution within this sample.

In addition to patterns of co-occurrence, however, the presence of right frontal only or left occipital only, petelias, may be of particular importance in macaques. When the occurrence of these independent patterns are factored in, this increases the sample distribution of these basic human-like patterns to 50% as opposed to 25% for the opposite situation (left frontal/right occipital co-occurrence, left frontal only and right occipital only). Although the patterns of petelial projection and co-occurrence are not as pronounced in macaques as in humans, there appears to be a distinct trend towards the human pattern. It may well be that the functional substrates that underlie human asymmetries are beginning in macaques, but are expressed less frequently and to a lesser degree.

7.3.6. Measures of frontal and parietal lobe widths

Patterns of hemispheric asymmetry and co-occurrence in the width of the frontal and parietal lobes are similar to those of frontal/occipital petelias in humans (LeMay, 1977). In right-handed individuals, the right frontal, left parietal and left occipital lobes are significantly wider than their contralateral counterparts (Kertesz et al., 1990). It is thought that functions underlying this hemispheric asymmetry, as for petelial patterns, are related to cerebral localization of speech and handedness. It was a goal of this study to determine if patterns of hemispheric width predominance, similar to that of humans, would be present in *Macaca fascicularis*.

The width of both the anterior and posterior portions of the frontal and parietal lobes were measures in both hemispheres. Results of anterior and posterior frontal lobe widths showed that in the total sample this dimension was represented symmetrically (see Chapter 5, Figure 5-29). There were no sex differences evident other than a possible trend in males, in both anterior

and posterior measures, for left hemisphere dominance (5 L>R vs 3 R>L in both cases). For posterior frontal lobe width, there was a similar tendency for females to predominate in the right hemisphere (5 L>R vs 7 R>L vs 2 L=R).

Results of anterior and posterior parietal lobe widths also showed no tendency towards asymmetric inter-hemispheric representation (see Figures 5-32 & 5-33). Some of the values for hemispheric differences were quite large, however, being up to 4mm . For both anterior and posterior measures there appeared to be a tendency in males for the left hemisphere to predominate (5 L>R vs 3 R>L) although the sample size is too small for significance to be inferred.

7.3.7. Conclusions regarding petelial and hemispheric width asymmetries

Understanding how patterns of petelial and hemispheric width asymmetries are distributed in macaques may shed light on how these patterns emerged during human evolution. The petelial pattern most commonly present in right-handed humans, involving co-occurrence of right frontal and left occipital petelias was not present at the same level in this sample of macaque brains. In contrast to previous studies there was an indication for a sample predominance of right frontal and left occipital petelias although the co-occurrence rate of 27% in this study, was considerably less than that seen in humans at approximately 66%. However, the overall distribution pattern of hemispheric predominance for both corresponding and individually expressed, frontal and occipital petelias more closely approximated that reported for humans at 50% (vs 25% for the

opposite pattern). This suggests the presence of a neural substrate in macaques which may represent the precursor to that in humans.

These data demonstrate a relatively even hemispheric distribution pattern of frontal lobe petelias compared to previous studies of *Macaca mulatta* (Falk, 1990). In Falk's study, for example, a distribution pattern was shown in which frontal petelias were represented in the following approximate proportions; R>L in 50%, L>R in 26% and L=R in 24%. My study, although conducted on a smaller sample, showed the following distribution pattern; L>R in 45%, R>L in 41% and L=R in 14% . The study of *Papio* frontal petelias (Cain and Wada, 1979) was remarkable, both in the directionality and magnitude of frontal lobe petelias, in which R>L in 86% of the sample. No such marked effect has been reported before or since and is not supported by data from this analysis.

The highly asymmetric distribution of occipital petelias shown in this study was more similar to the situation present in humans at L>R in 59% versus R>L in 27% and L=R in 14%. These results are in marked contrast to previous studies which have concluded that the distribution of occipital lobe petelias was completely symmetric in macaques (Falk, 1990).

7.4. EVOLUTIONARY IMPLICATIONS

The main purpose of this study was to contribute towards testing the global hypothesis that the neural mechanisms which underlie the modern human communicative and cognitive capacity had a long evolutionary history within primates. This hypothesis embraces the concept of a long-term gradual change in these neural substrates. This view contrasts sharply with the ideas advanced by linguists such as Chomsky, who have suggested that

the neural circuitry underlying human vocal-auditory communication arose quite recently in modern humans in a rapid punctuated event, and essentially had no neural precursor (Chomsky, 1980). However, this latter hypothesis does not include data from studies in non-human primates and focuses only upon the unique nature of the human communicative capacity.

In humans, the localization of specific functions within the cerebral cortex appears to be the result of unilateral regional specialization for more complex behavioral motor tasks. Skilled motor tasks such as elaborate communicative and manipulative regimes, are highly adaptive traits which were probably strongly selected for during the sequence of events that took place during early hominid evolution. Based upon data from this quantitative anatomic study and that of other multidisciplinary studies, it is proposed that the rudiments or basal substrate of the neural circuitry that subserves human language and communication has a long evolutionary history within primates. Data from this study on inter-hemispheric asymmetry in *Macaca fascicularis,* in regions that are homologous to that of language centers in human brains, suggest the presence of a mosaic distribution of these composite neural substrates. In some instances the distribution of asymmetries in macaques show a pattern that is quite similar to that present in humans. In other cases there is no apparent asymmetry or the pattern is reversed. In many cases, the lack of strong polarity in the sample distribution of inter-hemispheric asymmetry in macaques may indicate that the process of hemispheric specialization and lateralization may be in the early stages of expression. However, on the contrary, since functional lateralization does not necessarily have to be expressed anatomically, the presence of associated anatomic asymmetry may represent a strong indicator of a more advanced stage of hemispheric functional

specialization. In this latter case the essential adaptation may have occurred much earlier in primate or mammalian evolution.

Results from many studies that have examined the physiology of neural circuitry underlying non-human primate vocalizations have demonstrated that there is no involvement of the cerebral cortex (see review in Chapter 2,). These findings stand in marked contrast to the condition in humans where regions of the cerebral cortex, such as Broca's and Wernicke's areas, are involved primarily with language functions. This discrepancy is puzzling since it has been demonstrated, using criteria involving cellular and sub-cellular organization of regions in the cerebral cortex, as well as asymmetry data from this dissertation, that there are homologs of these regions present in the brains of cercopithecoids. These contradictory findings raise the following question: If homologous cortical regions in non-human primates are not involved in vocal-auditory communication, what functions do they subserve?

In order to answer this question it is necessary to take a step back and think about what the role of these brain regions really is in humans. Although the main focus in most investigations has been upon their role in the uniquely human capacity for vocal-auditory communication, it seems clear that these regions are involved in a more global framework of inter-individual communication. For example, although the primary neural substrate of speech output functions in humans, Broca's area, is localized to the left cerebral hemisphere, this is by no means the only brain region involved in the delivery of effective and productive vocal output. Recently, many studies have focused on the critical role in human vocal-auditory communication of regions in the right hemisphere that are homotypic to classic left hemisphere speech regions. It is now becoming better understood

(and incorporated into the current paradigm) that these right hemisphere regions provide an important component to the communicative capacity of humans that allows for more efficient conveyance of information between individuals. The archaic notion that only the left hemisphere is essential for language functions has become essentially obsolete.

The idea that brain regions involved with discrete, and potentially equally adaptive, subsets of communication tasks are localized in both cerebral hemispheres in humans, has important implications for our understanding of cerebral localization in non-human primates. For example, the role of these bilaterally homotypic regions in non-human communication may be a matter of degree and one which may be quite different in humans and non-human primates. Since the human communicative capacity has discrete substrates in both hemispheres which provide for the communicative whole, so too may non-human primates distribute their species-specific communicative requirements accordingly. However, the assumption has always been that non-human primates should show a pattern of cerebral localization for communicative functions that essentially mirrors that of the human condition. What if the hemispheric distribution of neural substrates in non-human primates instead reflects an involvement with a communicative repertoire that is quite different from that of humans? This could mean that although the same basic neural circuits are involved in communication in both, the species-specific task is so different that there is a differential contribution of the neural substrates in both hemispheres. This may mean that the right hemisphere counterpart of the homolog of Broca's area in macaques may be primarily involved in processing communicative information. Unfortunately, no studies have tested whether the right hemisphere of non-human primates is involved in these functions. This may

be due to the fact that the important role of the right hemisphere in human communication is only recently becoming understood.

Another line of evidence regarding the nature of cerebral localization of non-human primate communication has been concerned with non vocal-auditory, or more specifically, visual-gestural communication. There is considerable evidence from humans deaf from birth, who use sign language as their only mode of communication, that the neural substrate for language is not limited to the vocal-auditory modality. In fact, physiologic studies of these deaf individuals have shown that the same brain regions that are involved with vocal-auditory language in speaking individuals, are also involved with the visual-gestural based sign language (Bellugi et al., 1983, 1988). Currently, sign language is considered to represent a natural language. Although this may be an artificial situation in a population of individuals with a pathologic disorder, it is an illuminating example which suggests that the neural substrate underlying language functions in humans is not limited to the vocal-auditory modality and can subserve the visual-gestural modality efficiently.

A further example of the responsiveness of brain centers to visual-gestural communication involves physiologic studies in non-human primates which have identified neurons in the temporal cortex responsive to facial imagery. Brain regions in the right hemisphere are involved with facial recognition (Desimone, 1991). In contrast, it has been suggested that the homotypic region in the left hemisphere of macaques, homologous to polymodal language cortex in humans, are involved in processing facial expressions used in a communicative context (Desimone, 1991).

This idea that the primary form of communication in non-human primates may involve primary use of the visual-gestural modality is

supported by two additional lines of evidence. First, there has been extensive work on the vocal apparatus of non-human primates and humans which shows that in this regard, non-human primates exhibit little modification when compared to adult humans (Laitman et al., 1992; Lieberman et al., 1992). Thus, intuitively, one would not expect modification of a brain region to subserve a little modified vocal apparatus. Second, experimental work in free-ranging macaques in which the homolog of Broca's area was lesioned, showed severe deficits in non-vocal communicative behaviors when re-introduced into their social group (Myers and Swett, 1970; Myers, 1973).

In light of the above lines of evidence it would seem that future research into the neural basis of non-human primate communication should incorporate an understanding of communicative modalities other than the vocal-auditory channel. Further, the use of behavioral studies of non-human primates in a natural setting, with an emphasis on the role played by visual-gestural channels, may advance our understanding of the potentially complex mosaic underlying efficient communication.

In addition to the physiologic studies described above, investigations of handedness in non-human primates may shed light on the hemispheric specialization for brain communication substrates. Similarities between patterns of handedness in humans and non-human primates demonstrate that more complex manipulative tasks show a distinct tendency towards functional localization and specialization of the left hemisphere (see Section 2.5.4.). The identification of a human-like pattern of handedness in non-human primates has implications for the evolution of inter-individual communication in cercopithecoids. For example, although the relationship between right handedness and speech in humans is unknown, they are essentially "linked" in their functional localization to the left hemisphere.

This link serves as a strong indicator that "associated" neural circuitry underlying communicative functions may also be present in some form. It has been suggested that the adaptive benefits offered by selection for the neural substrate subserving complex manipulation and tool use in early hominids may have started the evolutionary cascade that gave rise to the unique form of left-hemisphere dominant vocal-auditory communication present in modern humans (Steklis and Harnad, 1976; Corballis, 1983)

Most studies of non-human primate handedness have involved the experimental imposition of non-familiar tasks with varying degrees of complexity. Since many complex manipulative tasks are used on a daily basis in species such as macaques, for behaviors such as food preparation and grooming, it may be illustrative to focus more on this type of common behavior in a natural setting. Similarly, although some studies have reported a lack of asymmetry and handedness for tool use and other manipulative tasks in great apes, observation of spontaneous complex manipulative tasks in a natural setting may offer a more realistic and meaningful view of this specialization.

In sum, the data on non-human primates, especially for cercopithecoids, suggests that a form of handedness, in many ways similar to that in humans, may be present. It is suggested here that the link between the cerebral localization of handedness for complex manipulative tasks and that for equally complex visual-gestural communication was present early in primate evolution and evolved into the functional mosaic that is present in humans. The precise template upon which these functional associations are built is currently unknown. However, the presence of left hemisphere dominance in macaques for execution of the complex motor sequences underlying some of the more demanding manipulative tasks, further supports the global

hypothesis that human-like patterns of cerebral localization in non-human primates suggest a long evolutionary history for the neural circuitry underlying speech and language in humans.

Evidence has been provided in this dissertation for the presence of human-like patterns of asymmetry and hemispheric predominance in specific regions of the cerebral cortex in macaques that are homologous to human language areas. Although the magnitude of these asymmetries in macaques are in most cases less than that seen in humans, the implication is that such asymmetries were present in the common ancestor of cercopithecoids and hominoids.

A large body of physiologic evidence has demonstrated that non-human primate vocalizations are not mediated by these regions of the cerebral cortex. It is proposed here, however, that these asymmetric cortical regions are in fact involved in communication functions in non-human primates, but that the primary communicative modality is visual-gestural and not vocal-auditory as in humans. As discussed above, there is good evidence in humans that these brain language mechanisms process the same communicative information regardless of the modality used. As in humans, the specific cortical region in either the left or right hemisphere that subserves a species specific communicative role, is embedded within a framework of a mosaic of neural subsets. Different elements of this neural mosaic are expressed differential in different species in order to represent the species specific communicative repertoire. During the evolution of hominids this already complex communication circuitry was further modified and enhanced to keep pace with an expanding intellectual capacity. At this time, the gestural-visual modality was probably still the primary means used for inter-individual communication. For selective adaptive reasons that remain

unknown, probably some time during the evolution of early *Homo* or *Australopithecus,* the shift occurred from gestural-visual primacy to that of vocal-auditory primacy that is in place today.

The unifying concept which has emerged from this study is that the same basic neural substrate was utilized during a long evolutionary sequence, but that it was gradually modified and became increasingly more complex with regard to its intrinsic architecture and connections with other brain centers. This was necessary in order to accommodate the ever more demanding requirements for the processing of rapid, complex, interactive information transfer in the increasingly more elaborate cognitive environment during hominid evolution. The enhancement of communicative abilities would have been highly selected for in such a demanding environment.

APPENDIX FOR CHAPTER 5

Appendix 5-1 Series of 2-D distances (A-Ci, A-Cii, A-Ciii, A-Civ, & A-Cv) representing the extent of the antero-posterior distance between the vertical part of the arcuate sulcus anteriorly and the central sulcus posteriorly on both the left and right cerebral hemispheres in the total sample (n = 33). See text, Section 5.3.3.2.

2-D Linear Distance Measures of Arcuate Sulcus to Central Sulcus

n=	*A-Ci*		*A-Cii*		*A-Ciii*		*A-Civ*		*A-Cv*		*PG*	*SEX*
	left	*right*	*left*	*right*	*left*	*right*	*left*	*right*	*left*	*right*	*m#*	
1	9.9	9.8	7.9	7.8	7.8	8.4	10.6	10.8	11.4	12.1	14	F
2	9.9	10.3	8.3	8.2	8.9	8.0	11.6	10.9	12.9	12.7	15	F
3	7.5	7.4	5.6	5.3	6.1	5.3	8.3	8.4	10.1	10.3	16	F
4	9.2	9.4	6.7	6.9	6.9	7.2	9.8	10.6	11.8	13.3	17	F
5	8.6	8.3	6.2	7.2	6.0	7.8	8.4	10.9	9.7	11.7	18	F
6	8.6	11.0	7.5	8.4	7.6	7.4	10.8	11.4	12.4	13.8	19	F
7	8.9	9.2	5.8	5.8	5.5	5.6	8.2	9.4	11.8	12.3	23	M
8	6.8	7.6	5.6	6.2	5.9	6.0	8.2	8.7	10.2	11.0	24	M
9	10.1	9.1	9.8	7.7	10.0	7.0	13.0	10.8	16.8	14.7	25	M
10	8.9	10.8	8.8	8.8	8.3	8.3	11.7	12.4	14.1	12.6	26	F
11	9.2	9.4	6.4	7.0	7.2	7.3	9.3	10.9	11.9	11.4	27	F
12	7.2	8.7	5.9	6.6	5.6	6.0	7.2	8.5	9.8	10.4	29	F
13	8.0	6.6	5.9	5.2	6.1	5.4	9.4	8.2	12.4	11.4	30	F
14	10.1	8.4	6.8	6.8	6.2	6.6	10.6	10.4	13.3	12.7	31	M
15	8.2	9.4	6.1	6.3	6.2	6.4	9.6	10.0	13.8	12.2	32	M
16	10.2	10.6	7.9	8.3	6.4	7.5	9.1	11.5	14.0	15.4	37	M
17	10.2	8.4	6.2	6.7	6.6	6.7	8.2	9.8	10.6	11.7	38	F
18	9.7	12.4	7.1	7.8	7.9	7.3	9.7	9.9	12.3	9.7	39	M
19	11.1	13.1	8.2	7.7	7.5	6.7	9.5	9.1	11.6	12.0	40	M
20	12.8	12.5	10.3	10.2	8.8	11.9	12.7	14.0	15.5	15.7	41	M
21	8.3	9.1	6.2	7.2	6.8	6.7	10.2	10.2	12.6	14.7	42	M
22	8.7	10.6	6.3	8.4	6.3	7.7	9.0	10.6	11.0	11.2	43	M
23	9.0	12.7	7.9	8.7	10.2	9.2	12.5	11.8	13.0	13.3	44	M
24	8.0	8.0	7.4	7.1	8.2	8.6	11.5	11.4	14.8	14.9	45	M
25	10.8	11.4	7.2	7.6	6.2	7.2	9.3	10.5	14.0	15.8	46	F
26	9.4	10.1	7.4	7.7	8.2	8.0	10.1	10.0	12.5	11.9	48	F
27	12.3	11.8	8.3	7.8	8.7	8.0	11.8	11.7	12.1	12.8	49	F
28	11.7	12.9	6.7	7.3	7.6	8.0	11.0	11.8	13.7	13.2	52	M
29	11.3	11.4	8.1	7.8	8.4	8.1	11.1	10.8	12.2	12.3	53	F
30	8.6	10.4	8.0	9.1	8.8	10.0	11.7	13.4	14.2	14.9	54	F
31	9.6	10.6	7.2	8.3	7.9	8.8	9.9	10.0	11.4	10.6	55	F
32	9.2	10.2	6.7	7.3	6.3	6.9	8.6	9.7	11.2	12.4	56	F
33	11.0	10.8	8.2	8.4	6.7	7.9	9.2	10.5	10.3	12.2	57	F
Mean	*9.5*	*10.1*	*7.2*	*7.5*	*7.3*	*7.5*	*10.1*	*10.6*	*12.4*	*12.6*	total	
Stdev	*1.4*	*1.7*	*1.2*	*1.1*	*1.3*	*1.3*	*1.5*	*1.3*	*1.7*	*1.6*	sample	
Max	*12.8*	*13.1*	*10.3*	*10.2*	*10.2*	*11.9*	*13.0*	*14.0*	*16.8*	*15.8*		
Min	*6.8*	*6.6*	*5.6*	*5.2*	*5.5*	*5.3*	*7.2*	*8.2*	*9.7*	*9.7*		
Med	*9.2*	*10.2*	*7.2*	*7.7*	*7.2*	*7.4*	*9.8*	*10.6*	*12.3*	*12.3*		
Mean	*9.4*	*9.8*	*7.2*	*7.5*	*7.3*	*7.5*	*9.9*	*10.5*	*11.8*	*12.3*	females	
Stdev	*1.3*	*1.4*	*1.0*	*1.0*	*1.1*	*1.1*	*1.4*	*1.3*	*1.4*	*1.4*		
Mean	*9.6*	*10.4*	*7.3*	*7.5*	*7.4*	*7.5*	*10.3*	*10.7*	*13.2*	*13.1*	males	
Stdev	*1.6*	*2.0*	*1.4*	*1.1*	*1.5*	*1.6*	*1.6*	*1.4*	*1.8*	*1.8*		

Appendix 5-2 Type 1, t-Tests (paired sample) of values for 2-D distances on the brain surface from the arcuate sulcus to the central sulcus (A-Ci, A-Cii & A-Ciii) on the left and right cerebral hemispheres in total sample (n = 33), female sub-sample (n = 19 and male sub-sample (n = 14). See text, Section 5.3.3.2.

Paired t-Tests of Series of 2-D Linear Distance Measures From Arcuate Sulcus to Central Sulcus

t-Test: Paired Two Sample for Means

	Total Sample		Females only		Males only	
	LEFT	*RIGHT*	*LEFT*	*RIGHT*	*LEFT*	*RIGHT*
Mean	9.49	10.08	9.44	9.83	9.55	10.41
Variance	1.99	2.80	1.67	1.99	2.59	3.92
Observations	33	33	19	19	14	14
Pearson Correl'n	0.69		0.70		0.70	
Hypoth Mean Diff	0		0		0	
df	32		18		13	
t Stat	-2.74		-1.62		-2.23	
P(T<=t) one-tail	0.005		0.062		0.022	
t Critical one-tail	1.69		1.73		1.77	
P(T<=t) two-tail	0.010	***	0.123	N/S	0.044	***
t Critical two-tail	2.04		2.10		2.16	

A-Ci

LEFT vs RIGHT

	Total Sample		Females only		Males only	
	LEFT	*RIGHT*	*LEFT*	*RIGHT*	*LEFT*	*RIGHT*
Mean	7.22	7.49	7.18	7.46	7.29	7.54
Variance	1.36	1.15	0.96	1.09	2.00	1.31
Observations	33	33	19	19	14	14
Pearson Correl'n	0.80		0.86		0.76	
Hypoth Mean Diff	0		0		0	
df	32		18		13	
t Stat	-2.17		-2.31		-1.01	
P(T<=t) one-tail	0.019		0.017		0.164	
t Critical one-tail	1.69		1.73		1.77	
P(T<=t) two-tail	0.038	***	0.033	***	0.329	N/S
t Critical two-tail	2.04		2.10		2.16	

A-Cii

LEFT vs RIGHT

	Total Sample		Females only		Males only	
	LEFT	*RIGHT*	*LEFT*	*RIGHT*	*LEFT*	*RIGHT*
Mean	7.33	7.51	7.28	7.51	7.40	7.52
Variance	1.58	1.76	1.20	1.29	2.22	2.56
Observations	33	33	19	19	14	14
Pearson Correl'n	0.68		0.78		0.61	
Hypoth Mean Diff	0		0		0	
df	32		18		13	
t Stat	-1.03		-1.34		-0.34	
P(T<=t) one-tail	0.156		0.098		0.369	
t Critical one-tail	1.69		1.73		1.77	
P(T<=t) two-tail	0.313	N/S	0.196	N/S	0.738	N/S
t Critical two-tail	2.04		2.10		2.16	

A-Ciii

LEFT vs RIGHT

Appendix 5-3 Type 1, t-Tests (paired sample) of values for 2-D distances on the brain surface from the arcuate sulcus to the central sulcus (A-Civ & A-Cv) on the left and right cerebral hemispheres, in the total sample (n = 33), the female sub-sample (n = 19 and the male sub-sample (n = 14). See text, Section 5.3.3.2.

	Total Sample		Females only		Males only	
	LEFT	*RIGHT*	*LEFT*	*RIGHT*	*LEFT*	*RIGHT*
Mean	10.06	10.58	9.85	10.49	10.34	10.70
Variance	2.14	1.69	1.87	1.67	2.55	1.83
Observations	33	33	19	19	14	14
Pearson Correl'n	0.74		0.76		0.72	
Hypoth Mean Diff	0		0		0	
df	32		18		13	
t Stat	-2.99		-3.03		-1.21	
P(T<=t) one-tail	0.003		0.004		0.125	
t Critical one-tail	1.69		1.73		1.77	
P(T<=t) two-tail	0.005	***	0.007	***	0.249	N/S
t Critical two-tail	2.04		2.10		2.16	

A-Civ

LEFT vs RIGHT

	Total Sample		Females only		Males only	
	LEFT	*RIGHT*	*LEFT*	*RIGHT*	*LEFT*	*RIGHT*
Mean	12.40	12.64	11.84	12.34	13.17	13.06
Variance	2.81	2.58	1.91	1.97	3.20	3.30
Observations	33	33	19	19	14	14
Pearson Correl'n	0.74		0.72		0.74	
Hypoth Mean Diff	0		0		0	
df	32		18		13	
t Stat	-1.16		-2.05		0.30	
P(T<=t) one-tail	0.127		0.028		0.385	
t Critical one-tail	1.69		1.73		1.77	
P(T<=t) two-tail	0.254	N/S	0.055	A/S	0.770	N/S
t Critical two-tail	2.04		2.10		2.16	

A-Cv

LEFT vs RIGHT

Appendix 5-4 **a)** Histogram of means and standard deviation of pooled values for independent measures of the distance betweenthe arcuate sulcus and the central sulcus in the left and right hemispheres (A-Ci, A-Cii, A-Ciii, A-Civ & A-Cv). **b)** T-Tests of differences between the left and right hemisphere in the total sample of pooled values of A-C i-v, in the total sample (n = 165), females (n = 95) and males (n = 70). see text, Section 5.3.3.2.

Pooled Data for 5 Independent Measures of the 2-D Linear Distance from the Arcuate Sulcus to the Central Sulcus

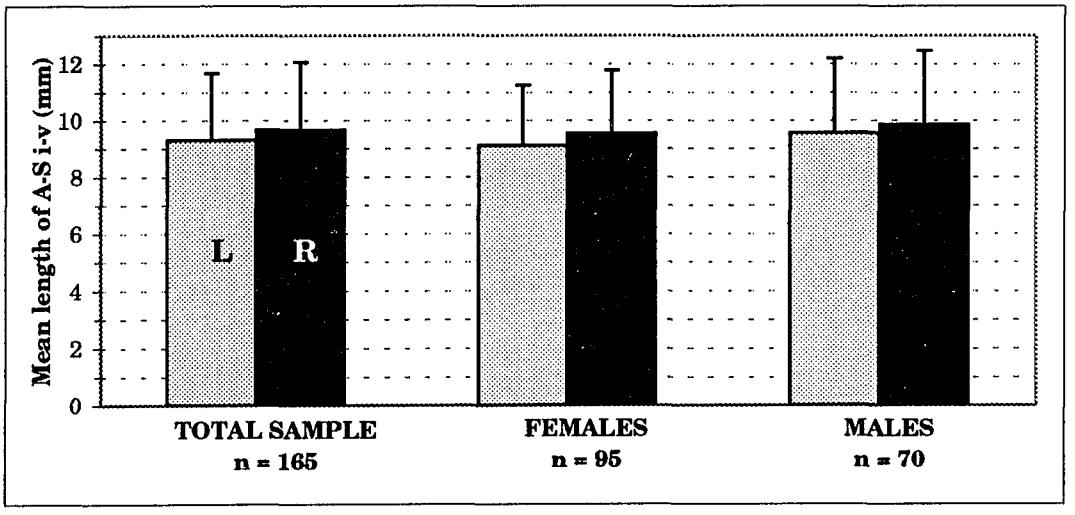

t-Test: Paired Two Sample for Means

	Total Sample		Females only		Males only	
	LEFT	*RIGHT*	*LEFT*	*RIGHT*	*LEFT*	*RIGHT*
Mean	9.30	9.66	9.12	9.53	9.55	9.85
Variance	5.64	5.81	4.53	5.02	7.12	6.92
Observations	165	165	95	95	70	70
Pearson Correl'n	0.90		0.92		0.89	
Hypoth Mean Diff	0		0		0	
df	164		94		69	
t Stat	-4.42		-4.53		-1.99	
P(T<=t) one-tail	0.00001	****	0.00001	****	0.025	****
t Critical one-tail	1.65		1.66		1.67	
P(T<=t) two-tail	0.00002	****	0.00002	****	0.050	****
t Critical two-tail	1.97		1.99		1.99	

Appendix 5-5 Table of 2-D linear measures of the distance between the arcuate sulcus and the sub-central dimple in the left and right hemispheres of the total sample (n = 29) including females (n = 18) and males (n = 11). See text, Section 5.3.3.3.

"A-SCD" Linear Distance from Arcuate Sulcus to Sub-Central Dimple

n=	***A-SCD***		*PG*	
	left	*right*	*M#*	*SEX*
1	7.35	7.96	14	F
2	8.94	9.10	15	F
3	6.38	7.20	16	F
4	8.35	9.37	17	F
5	6.52	7.97	18	F
6	8.77	8.75	19	F
7	8.33	8.24	23	M
8	6.61	7.35	24	M
9	11.77	9.08	25	M
10	8.16	8.03	27	F
11	6.98	6.20	29	F
12	7.55	6.54	30	F
13	9.07	8.52	31	M
14	6.13	6.84	38	F
15	7.67	5.34	39	M
16	6.68	7.23	40	M
17	10.28	10.39	41	M
18	8.25	9.96	42	M
19	6.17	7.64	43	M
20	8.04	7.28	45	M
21	8.61	10.10	46	F
22	8.35	7.41	48	F
23	6.98	8.11	49	F
24	9.60	8.65	52	M
25	7.57	8.14	53	F
26	8.41	9.86	54	F
27	6.43	7.70	55	F
28	6.89	8.11	56	F
29	6.82	8.02	57	F
Mean	*7.85*	*8.11*	total	
Stdev	*1.31*	*1.18*	sample	
Max	*11.77*	*10.39*	n=29	
Min	*6.13*	*8.07*		
Med	*7.67*	*8.03*		
Mean	*7.51*	*8.08*	females, n=18	
Stdev	*0.93*	*1.10*		
Mean	*8.41*	*8.15*	males, n=11	
Stdev	*1.69*	*1.41*		

Appendix 5-6 **a)** Histogram of means and standard deviations of 2-D linear measures of the distance between the arcuate sulcus and the sub-central dimple in the left and right hemispheres of the total sample (n = 29), females (n = 18), and males (n = 11); **b)** Type 1 t-Tests of interhemispheric differences of the measure A-SCD. See text, Section 5.3.3.3.

2-D Linear Distance from the Arcuate Sulcus to the Sub-Central Dimple on the Left an Right Hemispheres

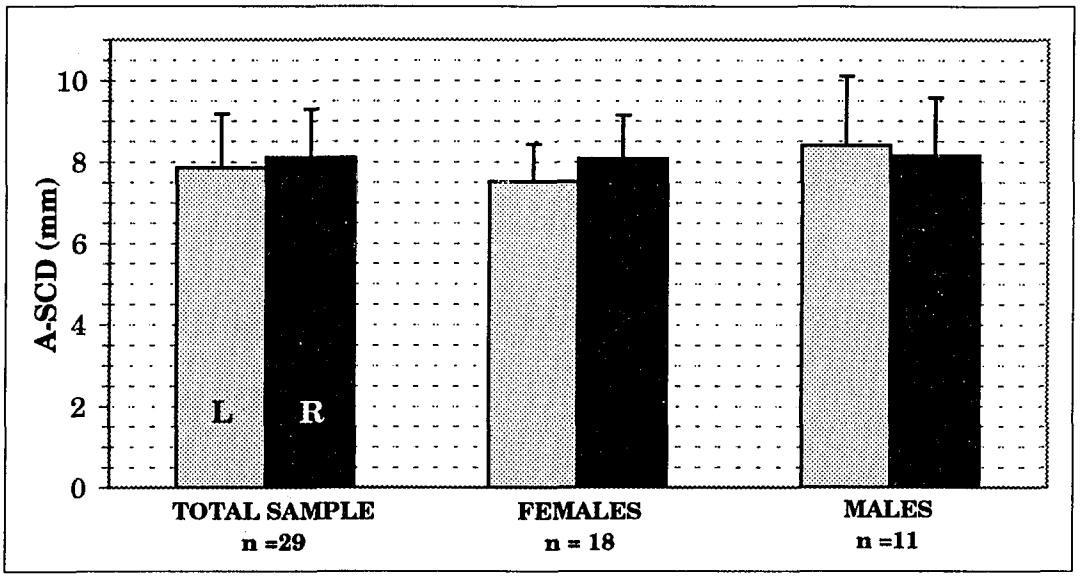

t-Test: Paired Two Sample for Means

	Total Sample		Females only		Males only	
	LEFT	*RIGHT*	*LEFT*	*RIGHT*	*LEFT*	*RIGHT*
Mean	7.8	8.1	7.5	8.1	8.4	8.2
Variance	1.7	1.4	0.8	1.1	2.9	2.0
Observations	29	29	18	18	11	11
Pearson Correl'n	0.6		0.7		0.6	
Hypoth Mean Diff	0		0		0	
df	28		17		10	
t Stat	-1.2		-2.9		0.6	
P(T<=t) one-tail	0.118		0.005	xxxx	0.281	
t Critical one-tail	1.7		1.7		1.8	
P(T<=t) two-tail	0.236	N/S	0.011	xxxx	0.563	N/S
t Critical two-tail	2.0		2.1		2.2	

A-SCD LEFT VS RIGHT

Appendix 5-7 Table of 2-D linear measures of the distance between the central sulcus and the sub-central dimple in the left and right hemispheres of the total sample (n = 29) including females (n = 18) and males (n = 11). See text, Section 5.3.3.3.

"C-SCD" Linear Distance from Central Sulcus to Sub-Central Dimple

n=	***C-SCD***		*PG*	
	left	*right*	*M#*	*SEX*
1	4.46	4.19	14	F
2	4.04	3.60	15	F
3	3.76	3.15	16	F
4	3.70	4.00	17	F
5	3.44	3.74	18	F
6	3.73	5.26	19	F
7	3.71	4.12	23	M
8	3.67	3.78	24	M
9	5.29	5.66	25	M
10	4.07	3.80	27	F
11	3.23	4.42	29	F
12	5.11	4.98	30	F
13	4.30	4.04	31	M
14	4.55	4.92	38	F
15	4.76	4.38	39	M
16	4.90	4.89	40	M
17	5.35	5.40	41	M
18	4.40	4.79	42	M
19	5.13	3.68	43	M
20	6.82	7.59	45	M
21	5.44	5.46	46	F
22	4.49	4.64	48	F
23	5.25	4.83	49	F
24	4.32	4.79	52	M
25	4.77	4.40	53	F
26	5.83	4.40	54	F
27	5.04	2.90	55	F
28	4.46	4.47	56	F
29	3.50	4.41	57	F
Mean	*4.53*	*4.51*	total	
Stdev	*0.81*	*0.89*	sample	
Max	*6.82*	*7.59*	n=29	
Min	*3.23*	*2.90*		
Med	*4.46*	*4.41*		
Mean	*4.38*	*4.31*	females, n=18	
Stdev	*0.74*	*0.71*		
Mean	*4.79*	*4.83*	males, n=11	
Stdev		*1.11*		

Appendix 5-8 **a)** Histogram of means and standard deviations of 2-D linear measures of the distance between the central sulcus and the sub-central dimple (C-SCD) in the left and right hemispheres of the total sample (n = 29), females (n = 18), and males (n = 11); **b)** Type 1 t-Tests of interhemispheric differences of the measure A-SCD. See text, Section 5.3.3.3.

2-D Linear Distance from the Central Sulcus to the Sub-Central Dimple on the Left an Right Hemispheres

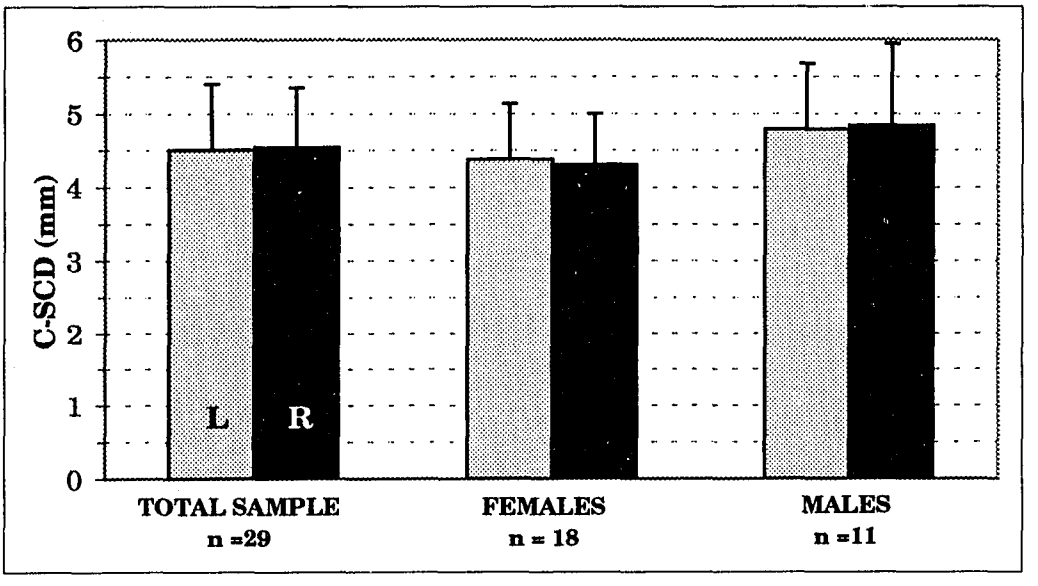

t-Test: Paired Two Sample for Means

	Total Sample		Females only		Males only	
	LEFT	*RIGHT*	*LEFT*	*RIGHT*	*LEFT*	*RIGHT*
Mean	4.5	4.5	4.4	4.3	4.8	4.8
Variance	0.7	0.8	0.6	0.5	0.8	1.2
Observations	29	29	18	18	11	11
Pearson Correl'n	0.6		0.3		0.8	
Hypoth Mean Diff	0		0		0	
df	28		17		10	
t Stat	0.2		0.4		-0.2	
P(T<=t) one-tail	0.422		0.364		0.408	
t Critical one-tail	1.7		1.7		1.8	
P(T<=t) two-tail	0.844	N/S	0.728	N/S	0.816	N/S
t Critical two-tail	2.0		2.1		2.2	

C-SCD LEFT VS RIGHT

Appendix 5-9 Table of 2-D area measures (mm^2), made from lateral brain photographs, of the area between the arcuate sulcus and the central sulcus in the left and right hemispheres of the total sample (n = 33), including females (n = 19) and males (n = 14). See text, Section 5.3.3.4

n=	AREA A-Ci'		AREA A-Cii'		PG	
	left	right	left	right	M#	SEX
1	108.0	105.9	81.6	82.9	14	F
2	137.3	108.8	82.5	107.1	15	F
3	89.8	75.3	59.3	69.6	16	F
4	103.6	80.7	87.5	115.6	17	F
5	92.9	111.9	88.7	70.9	18	F
6	100.2	118.3	90.2	78.2	19	F
7	108.2	115.5	90.0	83.8	23	M
8	72.0	75.4	60.0	57.6	24	M
9	156.8	129.9	97.8	122.3	25	M
10	119.8	134.1	101.6	93.8	26	F
11	112.7	111.0	89.1	86.5	27	F
12	79.3	92.3	67.7	59.5	29	F
13	92.0	74.8	60.0	70.2	30	F
14	117.8	106.8	84.5	89.2	31	M
15	108.2	118.7	90.6	84.5	32	M
16	124.5	130.9	98.8	93.0	37	M
17	111.3	105.2	84.4	86.1	38	F
18	115.9	131.6	94.6	89.9	39	M
19	144.9	128.8	95.6	106.1	40	M
20	168.6	196.1	150.8	123.3	41	M
21	109.4	118.7	94.9	86.9	42	M
22	102.3	133.5	102.0	77.6	43	M
23	133.5	154.4	115.8	105.8	44	M
24	117.6	118.0	94.3	91.9	45	M
25	126.1	145.2	109.0	93.0	46	F
26	136.8	114.6	86.3	104.8	48	F
27	131.1	124.3	93.8	100.0	49	F
28	125.9	136.4	103.6	96.7	52	M
29	137.5	140.7	106.6	104.6	53	F
30	115.9	134.3	105.7	92.1	54	F
31	113.7	123.0	91.7	86.9	55	F
32	108.4	122.1	91.4	79.3	56	F
33	109.3	106.8	81.1	78.3	57	F
Mean	*116.1*	*118.9*	*91.9*	*89.9*	total	
Stdev	*20.5*	*24.2*	*17.1*	*15.9*	sample	
Max	*168.6*	*196.1*	*150.8*	*123.3*		
Min	*72.0*	*74.8*	*59.3*	*57.6*		
Med	*113.7*	*118.7*	*91.4*	*89.2*		
Mean	*111.9*	*112.1*	*87.3*	*87.3*	females	
Stdev	*16.9*	*20.5*	*13.9*	*14.8*		
Mean	*121.8*	*128.2*	*98.1*	*93.5*	males	
Stdev	*24.1*	*26.5*	*19.5*	*17.2*		

Appendix 5-10 Type 1, t-Tests (paired sample) of values for two 2-D areas from the arcuate sulcus to the central sulcus ($A\text{-}Ci^2$ & $A\text{-}Cii^2$) on the left and right cerebral hemispheres in the total sample (n = 33), including females (n = 19) and males (n = 14). See text, Section 5.3.3.4.

t-Test: Paired Two Sample for Means

	Total Sample		Females only		Males only	
	LEFT	*RIGHT*	*LEFT*	*RIGHT*	*LEFT*	*RIGHT*
Mean	116.1	118.9	111.9	112.1	121.8	128.2
Variance	421.4	586.0	284.5	419.7	582.0	700.2
Observations	33	33	19	19	14	14
Pearson Correl'n	0.8		0.7		0.8	
Hypoth Mean Diff	0		0		0	
df	32		18		13	
t Stat	-1.0		-0.1		-1.5	
P(T<=t) one-tail	0.160		0.480		0.081	
t Critical one-tail	1.7		1.7		1.8	
P(T<=t) two-tail	0.321	N/S	0.960	N/S	0.163	N/S
t Critical two-tail	2.0		2.1		2.2	

$A\text{-}Ci^2$ LEFT VS RIGHT

	Total Sample		Females only		Males only	
	LEFT	*RIGHT*	*LEFT*	*RIGHT*	*LEFT*	*RIGHT*
Mean	91.9	89.9	87.3	87.3	98.1	93.5
Variance	292.5	253.0	193.9	219.9	379.3	295.0
Observations	33	33	19	19	14	14
Pearson Correl'n	0.7		0.6		0.8	
Hypoth Mean Diff	0		0		0	
df	32		18		13	
t Stat	0.8		0.0		1.3	
P(T<=t) one-tail	0.204		0.492		0.101	
t Critical one-tail	1.7		1.7		1.8	
P(T<=t) two-tail	0.408	N/S	0.984	N/S	0.203	N/S
t Critical two-tail	2.0		2.1		2.2	

$A\text{-}Cii^2$ LEFT VS RIGHT

Appendix 5-11 Table of 2-D linear measures of the anteroposterior length of the sylvian fissure in the left and right hemispheres of the total sample (n = 34) including females (n = 16) and males (n = 18). See text, Section 5.4.3.1.

2-D Length of the Sylvian Fissure

(SF-ap)

n=	**SF-ap**		*PG*	
	left	*right*	*M#*	*SEX*
1	35.71	36.92	7	M
2	27.92	27.11	8	M
3	34.93	34.62	9	M
4	36.12	38.30	10	M
5	33.18	35.02	11	M
6	27.79	26.20	15	F
7	26.22	26.44	17	F
8	25.88	26.93	18	F
9	32.65	28.23	24	M
10	21.16	22.00	26	F
11	25.77	23.38	28	F
12	23.86	22.96	29	F
13	24.32	23.34	30	F
14	26.62	26.69	32	M
15	25.87	26.88	37	M
16	22.73	25.89	38	F
17	26.71	25.00	39	M
18	28.75	30.32	40	M
19	35.87	35.57	41	M
20	30.70	29.19	42	M
21	26.40	27.70	43	M
22	31.71	29.52	44	M
23	29.46	31.12	45	M
24	26.78	26.40	46	F
25	28.02	27.46	47	M
26	23.99	25.02	48	F
27	26.46	26.85	49	F
28	31.20	33.87	50	M
29	27.46	27.48	52	M
30	28.41	29.09	53	F
31	29.13	30.58	54	F
32	25.29	27.17	55	F
33	26.90	27.04	56	F
34	28.83	29.18	57	F
Mean	*28.32*	*28.51*	total	
Stdev	*3.79*	*4.02*	sample	
Max	*36.12*	*38.30*	n=34	
Min	*21.16*	*22.00*		
Med	*27.63*	*27.32*		
Mean	*25.85*	*26.15*	females, n=16	
Stdev	*2.22*	*2.38*		
Mean	*30.51*	*30.61*	males, n=18	
Stdev	*3.55*	*4.06*		

Appendix 5-12 Type 1 t-Tests of values for the anteroposterior length of the sylvian fissure and superior temporal sulcus in the left and right hemispheres of the total sample (n = 34) including females (n = 16) and males (n = 18). See text, Section 5.4.3.1.

	Total Sample		Females only		Males only	
	LEFT	*RIGHT*	*LEFT*	*RIGHT*	*LEFT*	*RIGHT*
Mean	28.3	28.5	25.8	26.2	30.5	30.6
Variance	14.4	16.2	4.9	5.7	12.6	16.5
Observations	34	34	16	16	18	18
Pearson Correl'n	0.9		0.8		0.9	
Hypoth Mean Diff	0		0		0	
df	33		15		17	
t Stat	-0.7		-0.9		-0.2	
P(T<=t) one-tail	0.238		0.190		0.412	
t Critical one-tail	1.7		1.8		1.7	
P(T<=t) two-tail	0.477	N/S	0.379	N/S	0.823	N/S
t Critical two-tail	2.0		2.1		2.1	

SF-ap LEFT VS RIGHT

	Total Sample		Females only		Males only	
	LEFT	*RIGHT*	*LEFT*	*RIGHT*	*LEFT*	*RIGHT*
Mean	37.5	37.8	35.1	35.3	39.7	40.1
Variance	15.1	17.2	2.9	5.5	16.3	17.3
Observations	34	34	16	16	18	18
Pearson Correl'n	0.9		0.8		0.9	
Hypoth Mean Diff	0		0		0	
df	33		15		17	
t Stat	-1.2		-0.6		-1.0	
P(T<=t) one-tail	0.126		0.263		0.177	
t Critical one-tail	1.7		1.8		1.7	
P(T<=t) two-tail	0.251	N/S	0.527	N/S	0.353	N/S
t Critical two-tail	2.0		2.1		2.1	

STS-ap LEFT VS RIGHT

Appendix 5-13 Table of 2-D linear measures of the anteroposterior length of the superior temporal sulcus in the left and right hemispheres of the total sample (n = 34) including females (n = 16) and males (n = 18). Section text, 5.4.3.2.

2-D Length of the Superior Temporal Sulcus

(STS-ap)

n=	**STS-ap**		*PG*	
	left	*right*	*M#*	*SEX*
1	45.19	45.89	7	M
2	44.20	43.78	8	M
3	44.69	43.47	9	M
4	44.94	45.56	10	M
5	45.00	44.05	11	M
6	37.82	38.12	15	F
7	35.88	35.91	17	F
8	35.70	35.71	18	F
9	36.73	38.01	24	M
10	37.26	37.70	26	F
11	34.37	34.79	28	F
12	33.64	30.62	29	F
13	32.65	30.90	30	F
14	36.91	35.57	32	M
15	32.60	33.99	37	M
16	33.35	35.57	38	F
17	37.61	33.82	39	M
18	34.96	37.15	40	M
19	42.25	43.99	41	M
20	36.84	37.43	42	M
21	39.28	41.86	43	M
22	37.71	37.08	44	M
23	35.73	36.92	45	M
24	34.52	34.58	46	F
25	36.95	36.29	47	M
26	33.99	34.30	48	F
27	33.86	35.10	49	F
28	42.96	44.44	50	M
29	39.97	41.64	52	M
30	36.37	36.31	53	F
31	38.18	39.50	54	F
32	33.88	33.28	55	F
33	34.04	35.91	56	F
34	36.31	36.82	57	F
Mean	*37.54*	*37.83*	total	
Stdev	*3.89*	*4.15*	sample	
Max	*45.19*	*45.89*	n=34	
Min	*32.60*	*30.62*		
Med	*36.78*	*36.87*		
Mean	*35.11*	*35.32*	females, n=16	
Stdev	*1.69*	*2.35*		
Mean	*39.69*	*40.05*	males, n=18	
Stdev	*4.04*	*4.16*		

Appendix 5-14 Table of five independent 2-D linear measures of the width of the superior temporal gyrus in the left and right hemispheres of the total sample (n = 27) including females (n = 14) and males (n = 13). See text Section 5.4.3.3.

2-D Linear Distance Measures of Sylvian Fissure to Superior Temporal Sulcus

n=	*STG-i*		*STG-ii*		*STG-iii*		*STG-iv*		*STG-v*		*PG*	*SEX*
	left	*right*	*left*	*right*	*left*	*right*	*left*	*right*	*left*	*right*	*m#*	
1	2.80	2.05	4.55	3.63	4.62	4.06	4.82	3.81	4.99	4.04	14	F
2	1.62	2.37	2.65	4.54	4.06	5.69	4.68	6.07	4.35	5.86	15	F
3	1.68	1.74	2.95	3.18	3.64	4.16	3.93	4.07	3.69	3.73	16	F
4	1.15	1.25	3.17	3.34	3.85	4.54	3.97	4.59	4.45	5.14	17	F
5	3.03	3.51	3.67	4.56	4.56	5.77	4.97	5.62	5.26	6.12	18	F
6	4.10	2.87	5.41	5.09	7.18	4.90	6.80	4.36	5.15	4.93	23	M
7	1.95	2.25	3.07	3.90	4.10	4.12	4.36	3.72	4.21	3.94	24	M
8	2.67	2.96	3.30	5.12	4.48	5.51	4.71	5.25	5.20	5.99	25	M
9	1.21	1.33	3.33	2.90	4.99	5.52	5.76	5.63	6.31	6.15	29	F
10	1.56	2.35	3.82	3.77	3.97	4.28	4.06	4.32	4.30	4.45	30	F
11	1.43	2.31	2.47	3.31	4.24	4.51	4.61	4.45	4.35	4.56	31	M
12	2.29	2.74	3.28	3.38	4.61	4.99	4.30	4.73	4.44	5.08	37	M
13	1.53	2.06	3.25	3.03	4.02	4.42	4.13	4.49	4.03	4.27	38	F
14	2.87	2.71	3.95	3.94	4.63	5.04	4.93	5.27	5.40	5.38	39	M
15	2.14	2.31	3.80	3.13	4.47	4.54	4.70	5.11	5.19	5.24	40	M
16	2.81	3.38	3.48	4.03	4.01	4.76	4.02	4.45	4.00	4.39	41	M
17	3.91	4.10	3.95	4.98	4.98	5.28	4.32	4.42	4.01	4.50	42	M
18	2.03	3.06	3.48	3.77	4.28	4.10	4.24	4.54	4.85	5.44	43	M
19	3.55	3.40	4.02	4.07	4.43	4.76	4.58	4.56	4.58	4.95	44	M
20	4.19	2.66	3.93	3.27	3.84	3.90	4.48	4.29	4.18	3.85	45	M
21	1.00	1.10	3.05	3.31	4.50	4.06	4.66	4.32	4.78	4.77	48	F
22	1.60	2..28	4.23	4.50	5.53	5.22	5.62	4.87	6.61	5.80	49	F
23	1.06	1.90	2.92	3.51	3.57	3.98	3.69	3.90	4.05	4.09	52	M
24	3.89	3.87	4.58	4.95	5.12	5.18	5.33	5.36	6.20	5.57	53	F
25	4.09	2.75	3.68	3.45	4.28	4.89	4.76	5.08	5.05	4.87	54	F
26	3.95	2.96	4.03	4.70	4.61	4.74	4.78	5.11	4.87	4.99	55	F
27	3.03	2.68	3.75	3.36	4.54	4.25	4.57	4.30	5.35	5.11	57	F
Mean	*2.49*	*2.56*	*3.62*	*3.88*	*4.49*	*4.71*	*4.66*	*4.69*	*4.81*	*4.93*	total	
Stdev	*1.07*	*0.76*	*0.64*	*0.69*	*0.70*	*0.56*	*0.65*	*0.59*	*0.74*	*0.71*	sample	
Max	*4.19*	*4.10*	*5.41*	*5.12*	*7.18*	*5.77*	*6.80*	*6.07*	*6.61*	*6.15*		
Min	*1.00*	*1.10*	*2.47*	*2.90*	*3.57*	*3.90*	*3.69*	*3.72*	*3.69*	*3.73*		
Med	*2.29*	*2.67*	*3.67*	*3.77*	*4.47*	*4.74*	*4.61*	*4.54*	*4.78*	*4.95*		
Mean	*2.30*	*2.31*	*3.62*	*3.80*	*4.45*	*4.77*	*4.72*	*4.83*	*5.02*	*5.06*	females	
Stdev	*1.12*	*0.85*	*0.59*	*0.70*	*0.52*	*0.61*	*0.58*	*0.67*	*0.87*	*0.77*		
Mean	*2.69*	*2.82*	*3.62*	*3.96*	*4.52*	*4.64*	*4.59*	*4.54*	*4.59*	*4.80*	males	
Stdev	*1.01*	*0.58*	*0.71*	*0.70*	*0.88*	*0.51*	*0.74*	*0.47*	*0.51*	*0.64*		

Appendix 5-15 Type 1 t-Tests of three of five independent 2-D linear measures of the width of the superior temporal gyrus in the left and right hemispheres of the total sample (n = 27) including females (n = 14) and males (n = 13). See text, Section 5.4.3.3.

Paired t-Tests of Series of 2-D Linear Distance Measures From Sylvian Fissure to Superior Temporal Sulcus

t-Test: Paired Two Sample for Means

	Total Sample		Females only		Males only	
	LEFT	*RIGHT*	*LEFT*	*RIGHT*	*LEFT*	*RIGHT*
Mean	2.49	2.55	2.30	2.31	2.69	2.82
Variance	1.14	0.56	1.26	0.66	1.02	0.34
Observations	27	27	14	14	13	13
Pearson Correl'n	0.76		0.82		0.65	
Hypoth Mean Diff	0		0		0	
df	26		13		12	
t Stat	-0.50		-0.06		-0.60	
P(T<=t) one-tail	0.312		0.476		0.280	
t Critical one-tail	1.71		1.77		1.78	
P(T<=t) two-tail	0.624	N/S	0.953	N/S	0.560	N/S
t Critical two-tail	2.06		2.16		2.18	

STG-i

LEFT vs RIGHT

	Total Sample		Females only		Males only	
	LEFT	*RIGHT*	*LEFT*	*RIGHT*	*LEFT*	*RIGHT*
Mean	3.62	3.88	3.62	3.80	3.62	3.96
Variance	0.41	0.48	0.35	0.49	0.51	0.49
Observations	27	27	14	14	13	13
Pearson Correl'n	0.47		0.45		0.50	
Hypoth Mean Diff	0		0		0	
df	26		13		12	
t Stat	-1.95		-0.98		-1.74	
P(T<=t) one-tail	0.031	***	0.171		0.053	***
t Critical one-tail	1.71		1.77		1.78	
P(T<=t) two-tail	0.062	A/S	0.343	N/S	0.107	N/S
t Critical two-tail	2.06		2.16		2.18	

STG-ii

LEFT vs RIGHT

	Total Sample		Females only		Males only	
	LEFT	*RIGHT*	*LEFT*	*RIGHT*	*LEFT*	*RIGHT*
Mean	4.49	4.71	4.45	4.77	4.52	4.64
Variance	0.49	0.31	0.28	0.37	0.77	0.26
Observations	27	27	14	14	13	13
Pearson Correl'n	0.40		0.41		0.46	
Hypoth Mean Diff	0		0		0	
df	26		13		12	
t Stat	-1.66		-1.92		-0.55	
P(T<=t) one-tail	0.054		0.039		0.295	
t Critical one-tail	1.71		1.77		1.78	
P(T<=t) two-tail	0.108	N/S	0.077	A/S	0.590	N/S
t Critical two-tail	2.06		2.16		2.18	

STG-iii

LEFT vs RIGHT

Appendix 5-16 Type 1 t-Tests of two of five independent 2-D linear measures of the width of the superior temporal gyrus in the left and right hemispheres of the total sample (n = 27) including females (n = 14) and males (n = 13). See text, Section 5.4.3.3.

Paired t-Tests of Series of 2-D Linear Distance Measures From Sylvian Fissure to Superior Temporal Sulcus (cont'd)

	Total Sample		Females only		Males only		
	LEFT	*RIGHT*	*LEFT*	*RIGHT*	*LEFT*	*RIGHT*	**STG-iv**
Mean	4.66	4.69	4.72	4.83	4.59	4.54	
Variance	0.42	0.35	0.33	0.45	0.54	0.22	
Observations	27	27	14	14	13	13	
Pearson Correl'n	0.38		0.53		0.20		**LEFT**
Hypoth Mean Diff	0		0		0		**vs**
df	26		13		12		**RIGHT**
t Stat	-0.26		-0.71		0.24		
P(T<=t) one-tail	0.398		0.245		0.409		
t Critical one-tail	1.71		1.77		1.78		
P(T<=t) two-tail	0.795	N/S	0.490	N/S	0.818	N/S	
t Critical two-tail	2.06		2.16		2.18		

	Total Sample		Females only		Males only		
	LEFT	*RIGHT*	*LEFT*	*RIGHT*	*LEFT*	*RIGHT*	**STG-v**
Mean	4.81	4.93	5.02	5.06	4.59	4.80	
Variance	0.55	0.51	0.76	0.59	0.26	0.41	
Observations	27	27	14	14	13	13	
Pearson Correl'n	0.73		0.68		0.82		**LEFT**
Hypoth Mean Diff	0		0		0		**vs**
df	26		13		12		**RIGHT**
t Stat	-1.21		-0.25		-2.07		
P(T<=t) one-tail	0.119		0.402		0.030	***	
t Critical one-tail	1.71		1.77		1.78		
P(T<=t) two-tail	0.239	N/S	0.804	N/S	0.060	A/S	
t Critical two-tail	2.06		2.16		2.18		

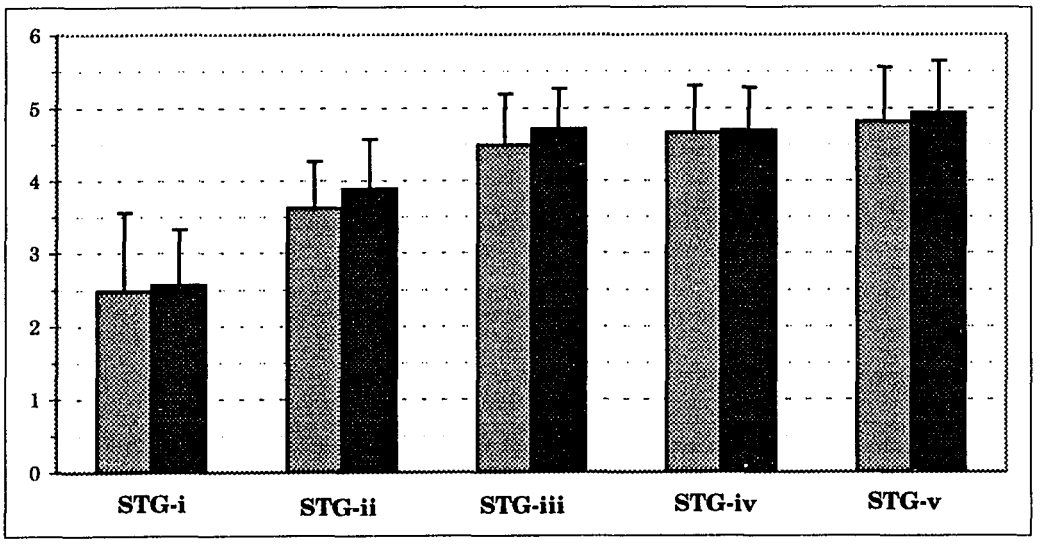

Appendix 5-17 Table of 2-D measures of the total area of the superior temporal gyrus in the left and right hemispheres of the total sample (n = 33), including females (n = 15) and males (n = 18). See text, Section 5.4.3.4.

n=	STG-tot²		PG	
	left	*right*	*M#*	*SEX*
1	305.31	297.34	7	M
2	191.69	195.32	8	M
3	257.88	247.53	9	M
4	262.60	229.76	10	M
5	216.30	252.04	11	M
6	175.21	181.00	15	F
7	131.24	143.49	17	F
8	190.57	184.84	18	F
9	177.99	160.15	24	M
10	115.94	121.14	26	F
11	159.51	140.24	28	F
12	162.45	141.93	29	F
13	150.35	128.99	30	F
14	155.37	165.06	32	M
15	143.00	176.77	37	M
16	153.06	172.82	38	F
17	203.77	199.72	39	M
18	175.22	198.82	40	M
19	243.18	244.95	41	M
20	199.94	198.91	42	M
21	169.99	205.25	43	M
22	203.74	174.79	44	M
23	188.70	204.32	45	M
24	211.39	220.38	47	M
25	176.93	163.18	48	F
26	193.74	192.64	49	F
27	227.09	200.22	50	M
28	156.09	167.31	52	M
29	228.26	204.13	53	F
30	208.13	220.86	54	F
31	169.28	163.20	55	F
32	184.06	191.35	56	F
33	186.39	190.07	57	F
Mean	*190.13*	*190.26*	total	
Stdev	*39.75*	*37.86*	sample	
Max	*305.31*	*297.34*	n=33	
Min	*115.94*	*121.14*		
Med	*186.39*	*191.35*		
Mean	*172.34*	*169.32*	females, n=15	
Stdev	*28.74*	*29.28*		
Mean	*204.96*	*207.70*	males, n=18	
Stdev	*42.22*	*35.83*		

2-D Area of the Superior Temporal Gyrus

(STG-tot²)

Appendix 5-18 Top: Histogram of means and standard deviations of measures of the total area of the superior temporal gyrus (STG-tot^2). Below: Type 1 t-Tests of these area measures in the left and right hemispheres of the total sample (n = 33) including females (n = 15) and males (n = 18). See text, Section 5.4.3.4.

2-D Area of the Superior Temporal Gyrus (STG-tot²)

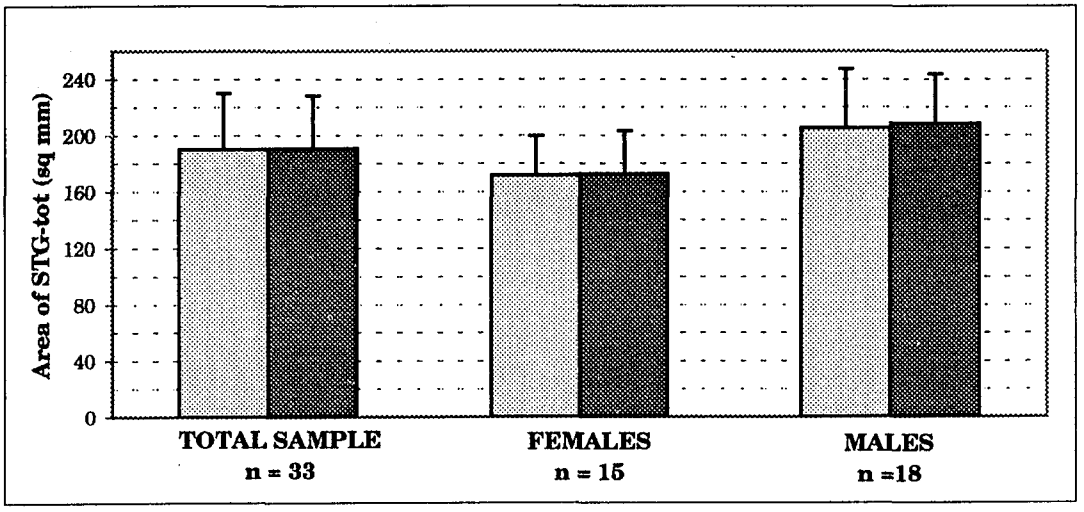

	Total Sample		Females only		Males only	
	LEFT	*RIGHT*	*LEFT*	*RIGHT*	*LEFT*	*RIGHT*
Mean	190.13	190.26	172.34	169.32	204.96	207.70
Variance	1580.22	1433.59	825.70	857.37	1782.52	1283.58
Observations	33	33	15	15	18	18
Pearson Correl'n	0.89		0.88		0.86	
Hypoth Mean Diff	0		0		0	
df	32		14		17	
t Stat	-0.04		0.83		-0.54	
P(T<=t) one-tail	0.484		0.211		0.297	
t Critical one-tail	1.69		1.76		1.74	
P(T<=t) two-tail	0.969	N/S	0.421		0.593	N/S
t Critical two-tail	2.04		2.14		2.11	

STG-tot²

LEFT vs RIGHT

Appendix 5-19 Table of 2-D measures of the total area of the posterior portion of the superior temporal gyrus (STG-Tpt[2]) including Area Tpt, the homolog of Wernicke's area in humans, in the left and right hemispheres of the total sample (n = 26), including females (n = 13) and males (n = 13). See text, Section 5.4.3.5.

n=	**STG-tot²**		*PG*	
	left	*right*	*M#*	*SEX*
1	56.14	43.06	14	F
2	42.75	67.94	15	F
3	40.86	47.54	16	F
4	52.40	55.00	17	F
5	67.27	86.29	18	F
6	48.92	51.04	23	M
7	51.84	63.79	24	M
8	54.90	53.60	25	M
9	40.71	42.76	29	F
10	40.03	48.08	30	F
11	50.28	55.15	31	M
12	46.46	55.68	37	M
13	64.57	65.54	38	F
14	59.78	63.51	39	M
15	66.11	68.08	40	M
16	73.27	76.34	41	M
17	45.12	49.69	42	M
18	76.24	78.22	43	M
19	60.46	44.39	44	M
20	52.66	49.77	45	M
21	69.78	66.37	48	F
22	48.24	52.82	49	F
23	88.70	90.82	52	M
24	74.57	63.26	53	F
25	71.59	66.88	54	F
26	72.26	73.28	55	F
Mean	58.30	60.73	total	
Stdev	13.13	13.06	sample	
Max	88.70	90.82	n=33	
Min	40.03	42.76		
Med	55.52	59.47		
Mean	57.01	59.91	females, n=15	
Stdev	13.53	12.97		
Mean	59.60	61.54	males, n=18	
Stdev	13.13	13.63		

2-D Area of the posterior portion of the Superior Temporal Gyrus

(STG-Tpt²)

Appendix 5-20 Top: Histogram of means and standard deviations of measures of the area of the posterior portion of the superior temporal gyrus (STG-Tpt[2]). Below: Type 1 t-Tests of these area measures in the left and right hemispheres of the total sample (n = 26) including females (n = 13) and males (n = 13). See text, Section 5.4.3.5.

2-D Area of the Posterior Superior Temporal Gyrus (STG-Tpt²)

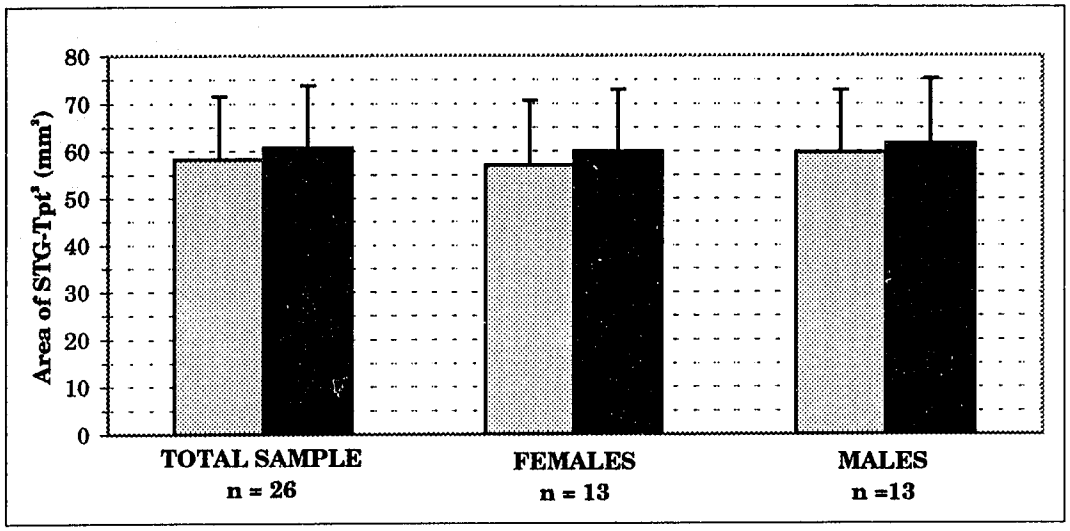

t-Test: Paired Two Sample for Means

	Total Sample		Females only		Males only	
	LEFT	*RIGHT*	*LEFT*	*RIGHT*	*LEFT*	*RIGHT*
Mean	58.30	60.73	57.01	59.91	59.60	61.54
Variance	172.27	170.53	183.00	168.13	172.28	185.69
Observations	26	26	13	13	13	13
Pearson Correl'n	0.78		0.68		0.88	
Hypoth Mean Diff	0		0		0	
df	25		12		12	
t Stat	-1.42		-0.98		-1.06	
P(T<=t) one-tail	0.084	A/S	0.173		0.156	
t Critical one-tail	1.71		1.78		1.78	
P(T<=t) two-tail	0.169	N/S	0.346	N/S	0.312	N/S
t Critical two-tail	2.06		2.18		2.18	

STG-Tpt²

LEFT vs RIGHT

Appendix 5-21 Table of 2-D measures of petelial projections of the frontal and occipital lobes on the left and right hemispheres of the total sample (n = 22), including females (n = 14) and males (n = 8). See text, Section 5.5.3.

FRONTAL AND OCCIPITAL LOBE PETELIAL PROJECTIONS
FR-pet & OC-pet

n=	FR-pet (mm)		OC-pet (mm)		*PG*	
	LEFT	*RIGHT*	*LEFT*	*RIGHT*	*M#*	*SEX*
1		0.44	0.11		7	M
2		0.26	NONE		8	M
3	0.37			0.18	9	M
4	NONE		0.65		10	M
5		0.24		0.09	11	M
6		0.24	0.14		14	F
7	0.26			0.43	15	F
8	0.18			0.16	16	F
9	NONE		0.11		17	F
10	0.23			0.84	18	F
11	0.22			1.51	46	F
12	NONE		0.42		47	M
13		0.11	0.15		48	F
14		0.24	0.51		49	F
15	0.23		0.77		50	M
16	0.20		0.65		51	F
17		0.24	NONE		52	M
18	0.27		0.22		53	F
19	0.23		NONE		54	F
20		0.34	0.16		55	F
21		0.35	0.69		56	F
22	0.28		0.11		57	F
Mean	0.25	0.27	0.36	0.53	total	
Stdev	0.05	0.09	0.26	0.55	sample	
Max	0.37	0.44	0.77	1.51	n=22	
Min	0.18	0.11	0.11	0.09		
Med	0.23	0.24	0.22	0.30		
Mean	0.23	0.26	0.31	0.73	females, n=14	
Stdev	0.03	0.10	0.24	0.59		
Mean	0.30	0.30	0.49	0.13	males, n=8	
Stdev	0.10	0.10	0.29	0.06		

Appendix 5-22 *Top:* Histogram of means and standard deviations of measures of the petelial projection of the frontal lobe, (FR-pet). *Below:* Type 3 t-Tests of these measures in the left and right hemispheres of the total sample (n = 19 of 22; 3 did not have petelias) including females (n = 13 of 14) and males (n = 6 of 8). See text, Section 5.5.3.

FRONTAL LOBE PETELIAL PROJECTION

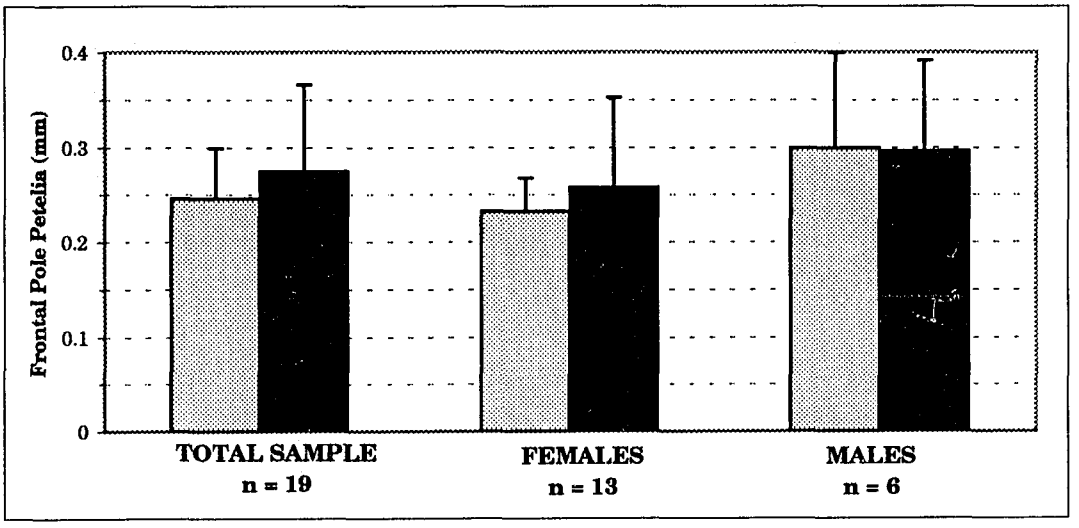

t-Test: Two Sample Assuming Unqual Variance

	Total Sample		Females only		Males only	
	LEFT	*RIGHT*	*LEFT*	*RIGHT*	*LEFT*	*RIGHT*
Mean	0.25	0.27	0.23	0.26	0.30	0.30
Variance	0.003	0.008	0.001	0.009	0.01	0.01
Observations	10	9	8	5	2	4
Pearson Correl'n	0.005		0.004		0.01	
Hypoth Mean Diff	0		0		0	
df	17		11		4	
t Stat	-0.84		-0.68		0.05	
P(T<=t) one-tail	0.205		0.256		0.482	
t Critical one-tail	1.74		1.80		2.13	
P(T<=t) two-tail	0.410	N/S	0.513		0.964	
t Critical two-tail	2.11		2.20		2.78	

FR-pet

LEFT vs RIGHT

Appendix 5-23 *Top:* Histogram of means and standard deviations of measures of the petelial projection of the occipital lobe, (OC-pet). *Below:* Type 3 t-Tests of these measures in the left and right hemispheres of the total sample (n = 19 of 22; 3 did not have petelias) including females (n = 13 of 14) and males (n = 6 of 8). See text, Section 5.5.3.

OCCIPITAL LOBE PETELIAL PROJECTIONS

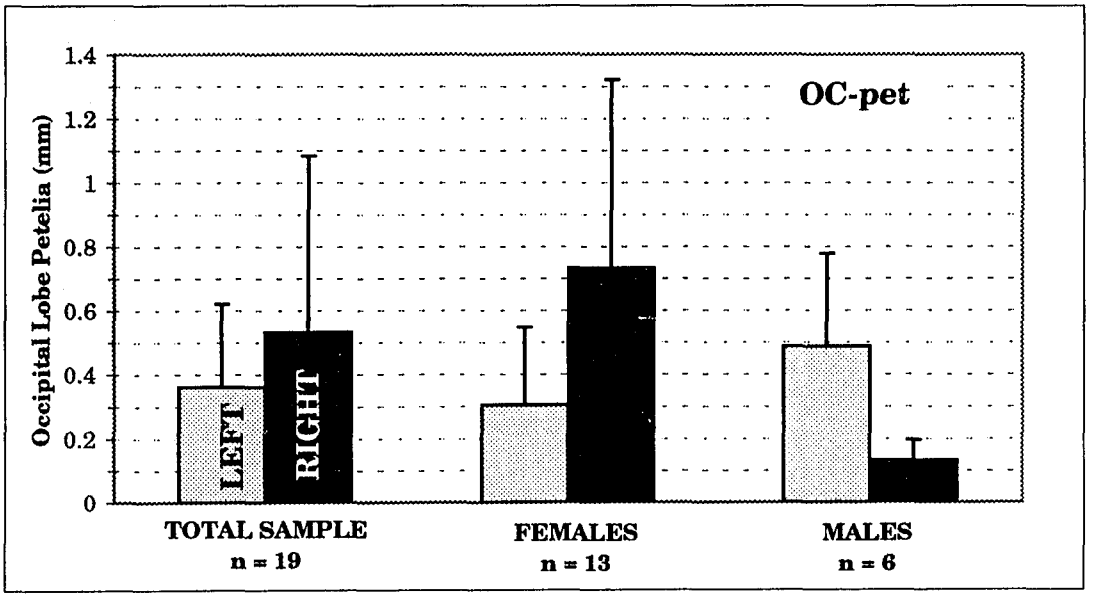

t-Test: Two Sample Assuming Unqual Variance

	Total Sample		Females only		Males only	
	LEFT	*RIGHT*	*LEFT*	*RIGHT*	*LEFT*	*RIGHT*
Mean	0.36	0.53	0.31	0.73	0.49	0.13
Variance	0.068	0.304	0.058	0.345	0.08	0.004
Observations	13	6	9	4	4	2
Hypoth Mean Difference	0		0		0	
df	6		3		4	
t Stat	-0.721		-1.404		2.353	
P(T<=t) one-tail	0.25		0.13		0.04	
t Critical one-tail	1.943		2.353		2.132	
P(T<=t) two-tail	0.50	N/S	0.26	N/S	0.08	
t Critical two-tail	2.447		3.182		2.776	

OC-pet

LEFT vs RIGHT

Appendix 5-24 Table of 2-D measures (mm) of the width of anterior (FR-w-a) and posterior (FR-w-p) regions of the frontal lobe on the left and right hemispheres of the total sample (n = 22), including females (n = 14) and males (n = 8). See text, Section 5.5.4.

WIDTH OF THE ANTERIOR AND POSTERIOR PORTIONS OF THE FRONTAL LOBE (FRw-a & FRw-p)

n=	**FRw-a**		**FRw-p**		*PG*	
	LEFT	*RIGHT*	*LEFT*	*RIGHT*	*M#*	*SEX*
1	20.35	19.37	23.50	22.80	7	M
2	19.08	18.24	24.32	22.55	8	M
3	18.81	20.66	22.58	25.35	9	M
4	19.19	18.19	22.29	21.46	10	M
5	20.50	19.11	24.42	23.44	11	M
6	15.67	16.89	17.86	19.94	14	F
7	13.94	14.06	17.92	18.63	15	F
8	15.75	16.14	17.34	17.59	16	F
9	13.84	16.01	15.51	20.37	17	F
10	15.81	14.93	18.67	17.65	18	F
11	16.60	17.70	21.10	22.92	46	F
12	17.22	18.17	21.08	22.60	47	M
13	16.59	16.89	20.50	20.92	48	F
14	18.15	16.10	20.79	19.73	49	F
15	16.97	17.94	20.36	21.03	50	M
16	17.60	15.21	22.17	18.58	51	F
17	18.92	18.22	22.14	21.03	52	M
18	19.01	17.83	22.86	22.38	53	F
19	18.98	18.14	21.74	21.74	54	F
20	16.80	17.60	19.83	20.29	55	F
21	17.46	17.76	20.85	20.85	56	F
22	18.46	16.50	21.35	19.51	57	F
Mean	17.53	17.35	20.87	20.97	total	
Stdev	1.82	1.54	2.29	1.95	sample	
Max	20.50	20.66	24.42	25.35	n=22	
Min	13.84	14.06	15.51	17.59		
Med	17.53	17.73	21.09	20.97		
Mean	16.76	16.55	19.89	20.08	females, n=14	
Stdev	1.66	1.23	2.12	1.63		
Mean	18.88	18.74	22.59	22.53	males, n=8	
Stdev	1.27	0.93	1.45	1.44		

Appendix 5-25 *Top:* Histogram of means and standard deviations of measures of the width of the anterior portion of the frontal lobe, (FRw-a). *Below:* Type 1 t-Tests of these measures in the left and right hemispheres of the total sample (n = 22) including females (n = 14) and males (n = 8). See text, Section 5.5.4.

WIDTH OF THE ANTERIOR PORTION OF THE FRONTAL LOBE (FRw-a)

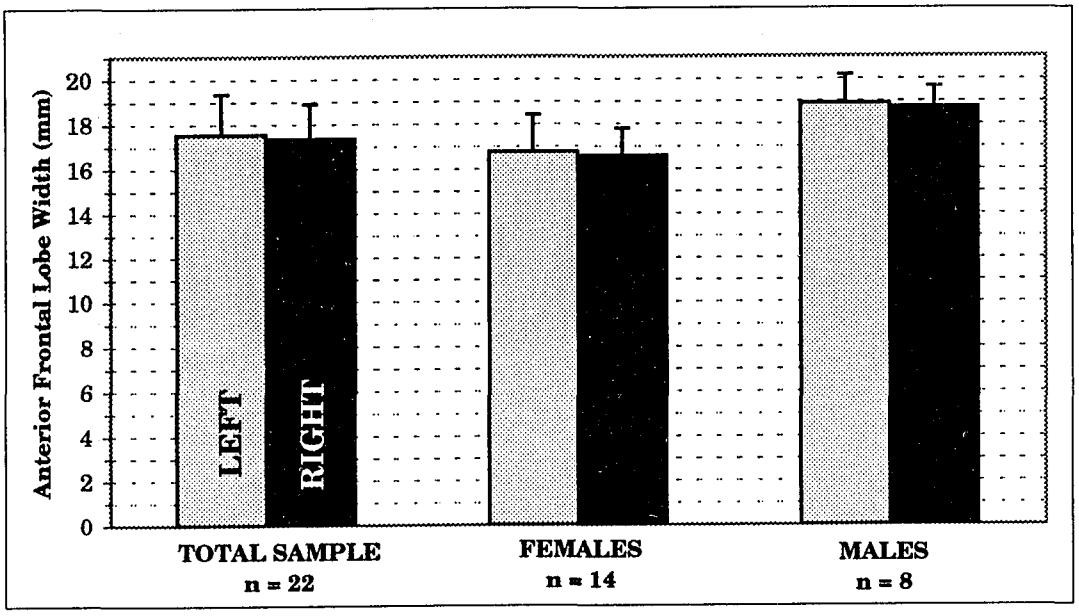

t-Test: Paired Two Sample for Means

	Total Sample		Females only		Males only	
	LEFT	*RIGHT*	*LEFT*	*RIGHT*	*LEFT*	*RIGHT*
Mean	17.53	17.35	16.76	16.55	18.88	18.74
Variance	3.329	2.372	2.745	1.507	1.62	0.856
Observations	22	22	14	14	8	8
Pearson Correl'n	1		1		0	
Hypoth Mean Diff	0		0		0	
df	21		13		7	
t Stat	0.67		0.56		0.34	
P(T<=t) one-tail	0.255		0.291		0.374	
t Critical one-tail	1.72		1.77		1.89	
P(T<=t) two-tail	0.510	N/S	0.583	N/S	0.747	N/S
t Critical two-tail	2.08		2.16		2.365	

FRw-a

LEFT vs RIGHT

Appendix 5-26 *Top:* Histogram of means and standard deviations of measures of the width of the posterior portion of the frontal lobe, (FRw-p). *Below:* Type 1 t-Tests of these measures in the left and right hemispheres of the total sample (n = 22) including females (n = 14) and males (n = 8). See text, Section 5.5.4.

WIDTH OF THE POSTERIOR PORTION OF THE FRONTAL LOBE (FRw-p)

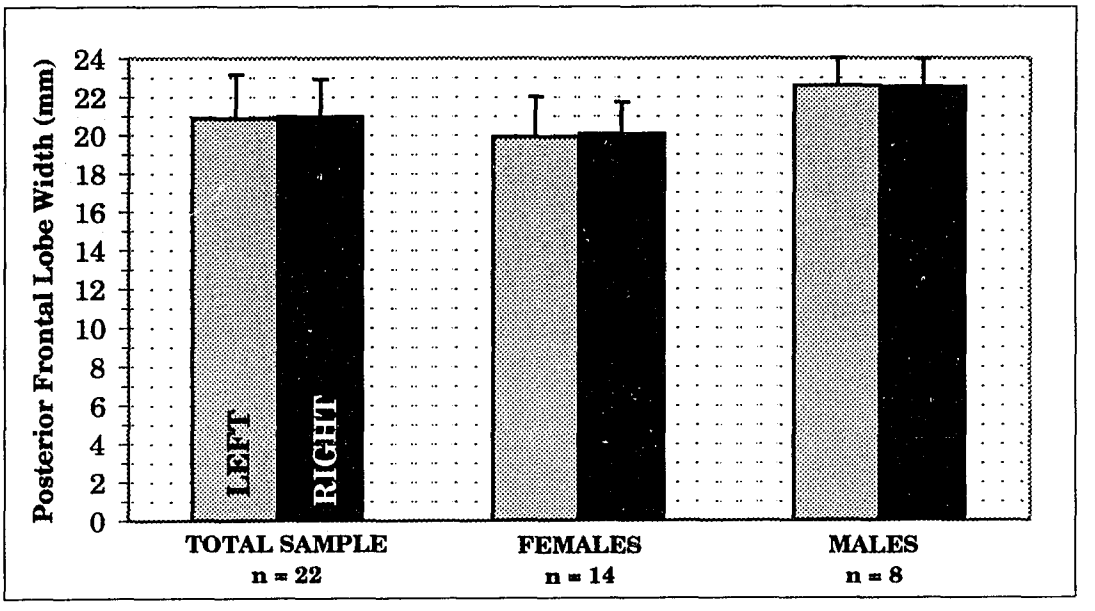

t-Test: Paired Two Sample for Means

	Total Sample		Females only		Males only	
	LEFT	*RIGHT*	*LEFT*	*RIGHT*	*LEFT*	*RIGHT*
Mean	20.87	20.97	19.89	20.08	22.59	22.53
Variance	5.239	3.792	4.489	2.648	2.10	2.070
Observations	22	22	14	14	8	8
Pearson Correl'n	1		0		0	
Hypoth Mean Diff	0		0		0	
df	21		13		7	
t Stat	-0.26		-0.35		0.10	
P(T<=t) one-tail	0.399		0.365		0.463	
t Critical one-tail	1.72		1.77		1.89	
P(T<=t) two-tail	0.798	N/S	0.729	N/S	0.926	N/S
t Critical two-tail	2.08		2.16		2.365	

FRw-p

LEFT vs RIGHT

Appendix 5-27 Table of 2-D measures (mm) of the width of anterior (PAw-a) and posterior (PA-w-p) regions of the parietal lobe on the left and right hemispheres of the total sample (n = 22), including females (n = 14) and males (n = 8). See text, Section 5.5.4.

WIDTH OF THE ANTERIOR AND POSTERIOR PORTIONS OF THE PARIETAL LOBE
(PAw-a & PAw-p)

n=	PAw-a		PAw-p		*PG*	
	LEFT	*RIGHT*	*LEFT*	*RIGHT*	*M#*	*SEX*
1	24.62	24.07	25.68	25.04	7	M
2	26.66	24.74	28.14	25.67	8	M
3	24.14	27.47	24.06	26.33	9	M
4	25.21	24.33	25.73	24.63	10	M
5	26.78	25.89	26.08	24.96	11	M
6	20.30	22.32	21.10	22.56	14	F
7	19.92	20.57	21.26	21.19	15	F
8	19.35	19.15	19.70	20.00	16	F
9	18.50	22.55	19.00	23.11	17	F
10	20.65	20.17	19.25	19.45	18	F
11	22.92	24.08	23.23	23.59	46	F
12	23.78	25.07	22.96	24.48	47	M
13	22.61	23.45	22.55	23.27	48	F
14	22.90	21.90	22.25	20.68	49	F
15	23.03	23.82	23.28	24.36	50	M
16	24.09	21.45	23.40	21.18	51	F
17	25.01	23.96	23.85	22.79	52	M
18	24.66	24.85	24.67	24.05	53	F
19	23.89	23.23	23.47	23.29	54	F
20	21.78	21.31	21.43	20.74	55	F
21	22.06	22.30	22.54	20.73	56	F
22	22.93	21.55	22.40	21.10	57	F
Mean	22.99	23.10	23.00	22.87	total sample n=22	
Stdev	2.23	1.99	2.26	1.98		
Max	26.78	27.47	28.14	26.33		
Min	18.50	19.15	19.00	19.45		
Med	22.98	23.34	23.09	23.19		
Mean	21.90	22.06	21.87	21.78	females, n = 14	
Stdev	1.88	1.54	1.68	1.48		
Mean	24.90	24.92	24.97	24.78	males, n = 8	
Stdev	1.32	1.24	1.75	1.04		

Appendix 5-28 *Top:* Histogram of means and standard deviations of measures of the width of the anterior portion of the parietal lobe, (PAw-a). *Below:* Type 1 t-Tests of these measures in the left and right hemispheres of the total sample (n = 22) including females (n = 14) and males (n = 8). See text, Section 5.5.4.

WIDTH OF THE ANTERIOR PORTION OF THE PARIETAL LOBE (PAw-a)

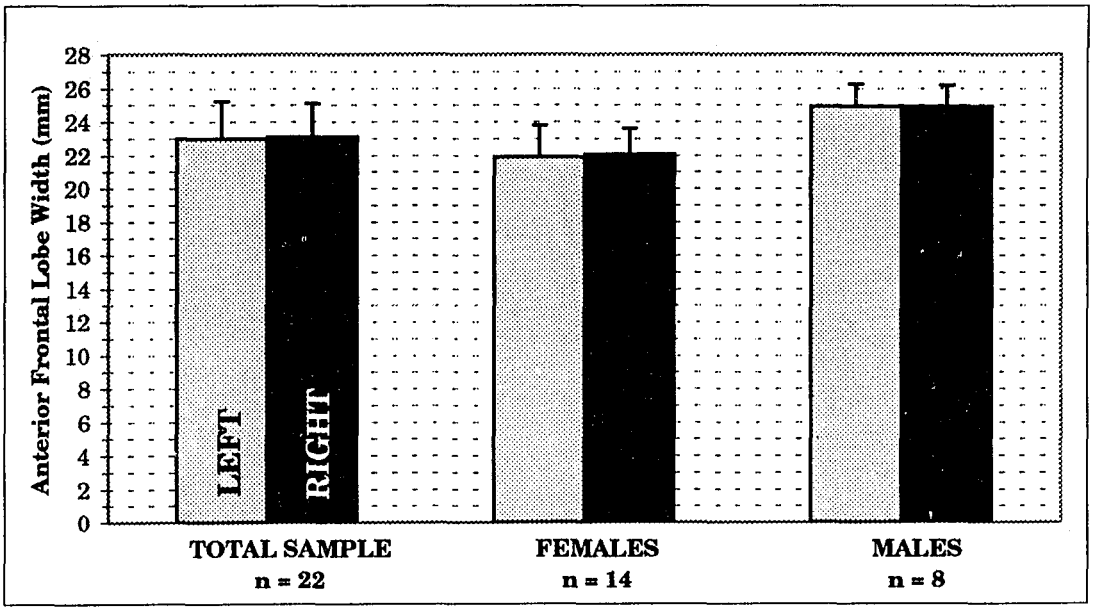

t-Test: Paired Two Sample for Means

	Total Sample		Females only		Males only	
	LEFT	*RIGHT*	*LEFT*	*RIGHT*	*LEFT*	*RIGHT*
Mean	22.99	23.10	21.90	22.06	24.90	24.92
Variance	4.965	3.962	3.547	2.383	1.73	1.532
Observations	22	22	14	14	8	8
Pearson Correl'n	1		1		0	
Hypoth Mean Diff	0		0		0	
df	21		13		7	
t Stat	-0.33		-0.39		-0.02	
P(T<=t) one-tail	0.374		0.353		0.491	
t Critical one-tail	1.72		1.77		1.89	
P(T<=t) two-tail	0.748	N/S	0.705	N/S	0.981	N/S
t Critical two-tail	2.08		2.16		2.365	

PAw-a

LEFT vs RIGHT

Appendix 5-29 *Top:* Histogram of means and standard deviations of measures of the width of the posterior portion of the parietal lobe, (PAw-p). *Below:* Type 1 t-Tests of these measures in the left and right hemispheres of the total sample (n = 22) including females (n = 14) and males (n = 8). See text, Section 5.5.4.

WIDTH OF THE POSTERIOR PORTION OF THE PARIETAL LOBE (PAw-p)

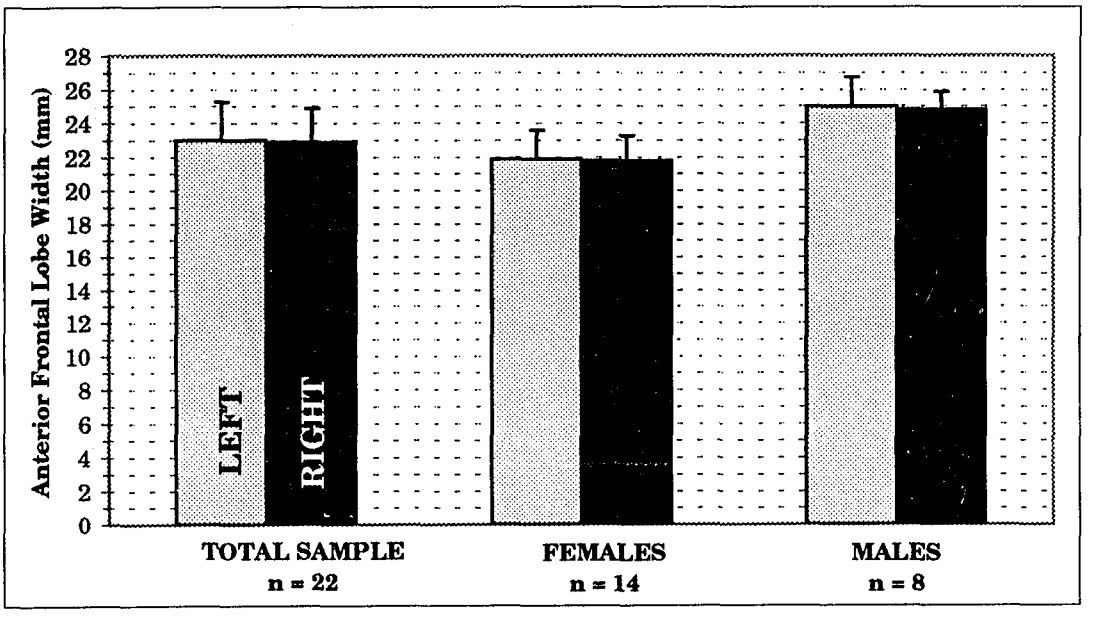

t-Test: Paired Two Sample for Means

	Total Sample		Females only		Males only	
	LEFT	*RIGHT*	*LEFT*	*RIGHT*	*LEFT*	*RIGHT*
Mean	23.00	22.87	21.87	21.78	24.97	24.78
Variance	5.098	3.902	2.839	2.192	3.05	1.079
Observations	22	22	14	14	8	8
Pearson Correl'n	1		1		0	
Hypoth Mean Diff	0		0		0	
df	21		13		7	
t Stat	0.39		0.22		0.33	
P(T<=t) one-tail	0.352		0.414		0.376	
t Critical one-tail	1.72		1.77		1.89	
P(T<=t) two-tail	0.704	N/S	0.829	N/S	0.751	N/S
t Critical two-tail	2.08		2.16		2.365	

PAw-p

LEFT vs RIGHT

BIBLIOGRAPHY

Ackermann H, Hertrich I and Ziegler W (1993) Prosodic disorders in neurologic disease: A review of the literature. Fortschr. Neurol. Psychiatr. *61:*241-253.

Ahern GL, Schomer DL, Kleefield J, Blume H, Cosgrove GR, Weintraub S and Mesulam MM (1991) Right hemisphere advantage for evaluating emotional facial expressions. Cortex *27:*193-202.

Aitken PG (1981) Cortical control of conditioned and spontaneous vocal behavior in rhesus monkeys. Brain Lang. *13:*171-184.

Akshoomoff NA, Courchesne E (1992) A new role for the cerebellum in cognitive operations. Behav. Neurosci. *106:*731-738.

Alekoumbides A (1978) Hemispheric dominance for language: Quantitative aspects. Acta Neurol. Scand. *57:*97-140.

Angst W (1975) Basic data and concepts on the social organization of *Macaca fascicularis*. Primate Behav. *4:*325-388.

Annett M (1992) 5 tests of hand skill. Cortex *28:*583-600.

Apfelbach R (1972) Electrically elicited vocalizations in the gibbon *Hylobates lar* (Hylobatidae), and their behavioral significance. Z. Tierpsychol. *30:*420-430.

Arbas EA, Meinertzhagen IA and Shaw SR (1991) Evolution in nervous systems. Ann. Rev. Neurosci. *14:*9-38.

Babcock LE (1993) The right and the sinister. Nat. Hist. :32-38.

Bachman DL, Albert ML (1991) The cerebral organization of language. In EG Jones and A Peters (eds): Cerebral Cortex. New York: Plenum, pp. 213-262.

Bauer RH (1993) Lateralization of neural control for vocalization by the frog (*Rana pipiens*). Psychobiol. *21:*243-248.

Baynes K (1990) Language and reading in the right hemisphere: Highways or byways of the brain. J. Cogn. Neurosci 2:159-179.

Baynes K, Gazzaniga MS (1988) Right hemisphere language: Insights into normal language mechanisms. In F Plum (ed): Language, Communication and the Brain. New York: Raven Press, pp. 117-126.

Bear D, Schiff D, Saver J, Greenberg M and Freeman R (1986) Quantitative analysis of cerebral asymmetries: Fronto-occipital correlation sexual dimorphism and association with handedness. Arch. Neurol. *43:*598-603.

Beecher MD, Petersen MR, Zoloth SR, Moody DB and Stebbins WC (1979) Perception of conspecific vocalizations by Japanese macaques; Evidence for selective attention and neural lateralization. Brain Behav. Evol. *16:*443-460.

Bellugi U, Poizner H and Klima ES (1983) Brain organization for language: clues from sign aphasia. Human Neurobiol. *2:*155-170.

Bellugi U, Klima ES and Poizner H (1988) Sign language and the brain. Res. Publ. Assoc. Res. Nerv. Ment. Dis. *66:*39-56.

Bever T, Chiarello R (1974) Cerebral dominance in musicians. Science *185:*537-539.

Blamire AM, Ogawa S, Ugurbil K, Rothman D, McCarthy G, Ellermann JM, Hyder F, Rattner Z and Shulman RG (1992) Dynamic mapping of the human visual cortex by high-speed magnetic resonance imaging. Proc. Nat. Acad. Sci. *89:*11069-11073.

Blonder LX, Bowers D and Heilman KM (1991) The role of the right hemisphere in emotional communication. Brain. *114:*1115-1127.

Bloom RL, Borod JC, Obler LK and Koff E (1990) A preliminary characterization of lexical emotional expression in right and left brain-damaged patients. Int. J. Neurosci. *55:*71-80.

Blumstein JL, Goodglass H and Tartter V (1975) The reliability of ear advantage in dichotic listening. Brain Lang. *2:*226-236.

Blumstein S, Cooper WE (1974) Hemisphere processing on intonation contours. Cortex *10:*146-158.

Bock WJ (1969) Discussion: The concept of homology. In Petras and Noback (eds): Comparative and Evolutionary Aspects of the Vertebrate Nervous System. New York: Ann. N.Y. Acad. Sci., pp. 71-73.

Bock WJ (1977) Foundations and methods of evolutionary classification. In MK Hecht, PC Goody and BM Hecht (eds): Major Patterns in Vertebrate Evolution. New York: Plenum Press, pp. 851-895.

Bock WJ (1981) Functional-adaptive analysis in evolutionary classification. Amer. Zool. *21:*5-20.

Bogen J, Bogen G (1975) Wernicke's region - where is it? Ann. N.Y. Acad. Sci. *280:*834-843.

Borod JC, Andelman F, Obler LK, Tweedy JR and Welkowitz J (1992) Right hemisphere specialization for the identification of emotional words and sentences - evidence from stroke patients. Neuropsychol. *30:*827-844.

Box HO (1977) Observations on spontaneous hand use in the common marmoset (*Callithrix jacchus*). Primates *18:*395-400.

Bradshaw JL (1988) The evolution of human lateral asymmetries: New evidence and second thoughts. J. Hum. Evol. *17:*615-637.

Bradvik B, Dravins C, Holtas S, Rosen I, Ryding E and Ingvar DH (1991) Disturbances of speech prosody following right hemisphere infarcts. Acta Neurol. Scand. *84:*114-126.

Bramwell B (1899) On 'crossed aphasia' and the factors which go to determine whether the 'leading' or 'driving' speech-centers shall be placed in the left or the right hemisphere of the brain, with notes of a case of 'crossed' aphasia (aphasia with right side hemiplegia) in a left-handed man. Lancet *1:*1473-1479.

Brickner RM (1940) A human cortical area producing repetitive phenomena when stimulated. J. Neurophysiol. *3:*44-52.

Broadbent DE (1954) The role of auditory localization in attention and memory span. J. Exp. Psychol. *47:*191-196.

Broca P (1861) Remarques sur la siège de la faculté du langage articulé, suivés d'une observation d'aphèmie (perte da la parole). Bull. Soc. Anat. Paris *6:*330-357.

Broca P (1865a) Nouvelle observation d'aphemie produite par une lesion de la moitie posterieure des deuxieme circonvolutions frontales gauches. Bull. Soc. Anat. Paris *6:*398-407.

Broca P (1865b) Perte de la parole, ramollissement chronique et destruction partielle du lobe anterior gauche du cerveau. Bull. Soc. Anat. Paris *2:*235-238.

Brodmann K (1909) Vergleichende Lokalsationslehere der Grosshirnrinde. Leipzig: Barth.

Brookshire KH, Warren JM (1962) The generality and consistency of handedness in monkeys. Anim. Behav. *10:*222-227.

Bryden MP (1967) An evaluation of some models of laterality effects in dichotic listening. Acta. Otolaryngol. *63:*395-435.

Bryden MP (1988) An overview of the dichotic listening procedure and its relation to cerebral organization. In K Hugdahl (ed): Handbook of Dichotic Listening: Theory, Methods and Research. Chichester, UK: Wiley & Sons, pp. 1-44.

Bryden MP, Hécaen H and DeAgostini M (1983) Patterns of cerebral organization. Brain Lang. *18:*249-262.

Bryden MP, Ardila A and Ardila O (1993) Handedness in native Amazonians. Neuropsychol. *31:*301-308.

Burling R (1993) Primate calls, human language, and non-verbal communication. Curr. Anthropol. *34:*25-53.

Cain DP, Wada JA (1979) An anatomical asymmetry in the baboon brain. Brain Behav. Evol. *16:*222-226.

Calvin WH (1982) Did throwing stones shape hominid brain evolution? Ethology and Sociobiology *3:*115-124.

Campbell CB, Hodos W (1970) The concept of homology and the evolution of the nervous system. Brain Behav. Evol. *3:*353-367.

Cancelliere AEB, Kertesz A (1990) Lesion localization in acquired deficits of emotional expression and comprehension. Brain Cogn. *13:*133-147.

Caplan D (1981) On the cerbral localization of linguistic functions: Logical and empirical issues surrounding deficit analysis and functional localization. Brain Lang. *14:*120-137.

Cheney DL, Seyfarth RM (1990) How Monkeys See the World. Chicago: University of Chicago Press.

Chi JG, Dooling EC and Gilles FH (1977) Gyral development of the human brain. Ann. Neurol. *1:*86-93.

Chomsky N (1980) Rules and representations. Behav. Brain Sci. *3:*1-61.

Chueca JAI, Gimeno ML and Marco JAR (1992) Morphometric study on the interhemispheric asymmetries in the Wistar rat and the effects of early experience. Hist. Histop. *7:*489-492.

Chui HC, Damasio AR (1980) Human cerebral asymmetries evaluated by computed tomography. J. Neurol. Neurosurg. Psychiat. *43:*873-878.

Connolly CJ (1950) External Morphology of the Primate Brain. Springfield Illinois: Charles C. Thomas.

Connolly KJ, Bishop DVM (1992) The measurement of handedness: A cross cultural comparison of samples from England and Papua New Guinea. Neuropsychol. *30:*13-26.

Conrad K (1949) Über aphasische SprachstÖrungen bei hirnverletzen Linkshänder. Der Nervenartz *20:*148-154.

Corballis MC (1983) Human Laterality. New York: Academic Press.

Coren S, Porac C (1977) Fifty centuries of right handedness: The historical record. Science *198:*631-632.

Cowell PE, Kertesz A and Denenberg VH (1993) Multiple dimensions of handedness and the corpus callosum. Neurology *43:*2353-2357.

Cracraft J (1981) The use of functional and adaptive criteria in phylogenetic systematics. Amer. Zool. *21:*21-36.

Crelin E (1987) The Human Vocal Tract: Anatomy, Function, Development and Evolution. New York, Vantage Press.

Creutzfeldt O, Ojemann G and Lettich E (1989) Neuronal activity in the human lateral temporal lobe .1. Responses to Speech. Exp. Brain Res. *77:*451-475.

Cunningham DJ (1892) Contribution to the Surface Anatomy of the Cerbral Hemispheres. Dublin: Royal Irish Academy.

Daffner KR, Schomer DL, Cosgrove GR, Rubin N and Mesulam MM (1991) Broca's aphasia following damage to Wernicke's area - For or against traditional aphasiology. Arch. Neurol. *48:*766-768.

Damasio AR, Geschwind N (1984) The neural basis of language. Ann. Rev. Neurosci. *7:*127-147.

Damasio H (1989) Neuroimaging Contributions to the Understanding of Aphasia. Amsterdam: Elsevier.

Damasio H, Damasio AR (1980) The anatomical basis of conduction aphasia. Brain. *103:*337-350.

Damasio H, Damasio AR (1983) Localization of lesions in conduction aphasia. In A Kertesz (ed): Localization in Neuropsychology. New York: Academic Press, .

Damasio H, Damasio A, Hamsher K and Varney N (1979) CT scan correlates of aphasia and allied disorders. Neurology *29:*572.

Darby DG (1993) Sensory Aprosodia - A clinical clue to lesions of the inferior division of the right middle cerebral artery. Neurology *43:*567-572.

Darwin C (1859) The Origin of Species. London: John Murray.

Darwin C (1887) The Descent of Man, and Selection in Relation to Sex. London: John Murray.

Dax G (1865a) Aphasie. Gazette Hebdomadaires de Médecine et de Chirurgie (Paris) *2:*250.

Dax G (1865b) Sur le même sujet. Gazette Hebdomadaires de Médecine et de Chirurgie (Paris) *2:*260-262.

Dax M (1865) Lésions de la moitiué gauche de l'encephale coincidant avec l'oubli des singes de la pensée (lu à Montpellier en 1836). Gazette Hebdomadaires de Médecine et de Chirurgie (Paris) *2:*259-260.

Deacon TW (1984): Connections of the inferior periarcuate area in the brain of *Macaca fascicularis*: An experimental and comparative neuroanatomical

investigation of language circuitry and its evolution. PhD Thesis, Harvard University. 355 p.

Deacon TW (1988) Human brain evolution: I. Evolution of language circuits. In HJ Jerison and I Jerison (eds): Intelligence and Evolutionary Biology. Berlin: Springer-Verlag, pp. 363-381.

Deacon T (1989) The neural circuitry underlying primate calls and human language. Hum. Evol. *4:*367-401.

Deacon TW (1992a) Brain-language coevolution. In JA Hawkins and Gell-Mann (eds): The Evolution of Human Languages. Reading, MA: Addison-Wesley, pp. 49-83.

Deacon TW (1992b) Cortical connections of the inferior arcuate sulcus cortex in the macaque brain. Brain Res. *573:*8-26.

de Lanerolle NC, Lang FF (1988) Functional neural pathways for vocalization in the domestic cat. In JD Newman (ed): The Physiological Control of Mammalian Vocalization. New York: Plenum Press, pp. 21-41.

Denny-Brown D (1958) The nature of apraxia. J. Nerv. Ment. Dis. *126:*9-32.

Desimone R (1991) Face-selective cells in the temporal cortex of monkeys. Journal of Cognitive Neuroscience *3:*1-8.

Doyle FH, Pennock JM, Orr JS, Gore JC, Bydder GM and Steiner RE (1981) Imaging of the brain by nuclear magnetic imaging. Lancet *1:*53-58.

Duara R, Kushch A, Grossglenn K, Barker WW, Jallad B, Pascal S, Loewenstein DA, Sheldon J, Rabin M, Levin B and Lubs H (1991) Neuroanatomic Differences Between Dyslexic and Normal Readers on Magnetic Resonance Imaging Scans. Arch. Neurol. *48:*410-416.

Dusser de Barenne JGF, Carol HW and McCulloch WS (1941) The 'motor' cortex of the chimpanzee. J. Neurophysiol. *4:*287-303.

Ebbesson SOE (1984) Evolution and ontogeny of neural circuits. Behav. Brain Sci. *7:*321-366.

Eberstaller O (1884) Zur oberflächenanatomie der grosshirnhemsiphären. Wien Med. Blätter *7:*642-644.

Eidelberg D, Galaburda AM (1984) Inferior parietal lobule: Divergent architectonic asymmetries in the human brain. Arch. Neurol. *41:*843-852.

Eldredge N, Cracraft J (1980) Homology. In (): Phylogenetic Patterns and the Evolutionary Process. New York: Columbia University Press, pp. 35-40.

Erickson TC, Woolsey CN (1951) Observations on the supplementary motor area of man. Trans. Amer. Neurol. Assoc. *76:*50-56.

Fagot J, Vauclair J (1988) Handedness and bimanual coordination in the lowland gorilla. Brain Behav. Evol. *32:*89-95.

Fagot J, Vauclair J (1991) Manual laterality in nonhuman primates - A distinction between handedness and manual specialization. Psychol. Bull. *109:*76-89.

Fagot J, Drea CM and Wallen K (1991) Asymmetrical hand use in rhesus monkeys (*Macaca-mulatta*) in tactually and visually regulated tasks. J. Comp. Psychol. *105:*260-268.

Falk D (1978a) Cerebral asymmetry in Old World monkeys. Acta. Anat. *101:*334-339.

Falk D (1978b) External neuroanatomy of old world monkeys (Cercopithecoidea). In FS Szalay (ed): Contributions to Primatology. New York: Karger, pp. 1-95.

Falk D, Cheverud J, Vannier MW and Conroy GC (1986) Advanced computer graphics technology reveals cortical asymmetry in endocasts of rhesus monkeys. Folia Primatol. *46:*98-103.

Falk D, Hildebolt C, Cheverud J, Vannier M, Helmkamp RC and Konigsberg L (1990) Cortical asymmetries in frontal lobes of rhesus monkeys (Macaca mulatta). Brain Res. *512:*40-45.

Falk D, Hildebolt C, Cheverud J, Kohn LAP, Figiel G and Vannier M (1991) Human Cortical Asymmetries Determined with 3D-MR Technology. J. Neurosci. Methods *39:*185-191.

Falzi G, Perrone P and Vignolo LA (1982) Right-left asymmetry in anterior speech region. Arch. Neurol. *39:*239-240.

Fitch RH, Brown CP, O'Connor K and Tallal P (1993) Functional lateralization for auditory temporal processing in male and female rats. Behav. Neurosci. *107*:844-850.

Ferreira F (1993) Creation of Prosody During Sentence Production. Psychol. Rev. *100*:233-253.

Fooden, J (1976) Provisional classification and key to living species of macaques (Primates: *Macaca*). Folia Primatol. *25*:225-236.

Forbes BF, Moskowitz N (1977) Cortico-cortical connections of the superior temporal gyrus in the squirrel monkey. Brain Res. *136*:547-552.

Frackowiak RSJ (1994) Functional mapping of verbal memory and language. Trends Neurosci. *17*:109-115.

Frackowiak RSJ, Friston KJ (1994) Functional neuroanatomy of the human brain: positron emission tomography - a new neuroanatomical technique. J. Anat. *184*:211-225.

Fragaszy DM, Mitchell SR (1990) Hand Preference and Performance on Unimanual and Bimanual Tasks in Capuchin Monkeys *(Cebus-Apella)*. J. Comp. Psychol. *104*:275-282.

Frotscher M (1992) Specificity of interneuronal connections. Ann. Anat. *174*:377-382.

Galaburda AM (1980) La région de Broca: Observations anatomiques faites un siécle aprés la mort de son découvrer. Rev. Neurol. (Paris). *136*:609-616.

Galaburda AM (1984) Anatomical asymmetries. In N Geschwind and AM Galaburda (eds): Cerebral Dominance; the Biological Foundations. Cambridge, Massachusetts: Harvard University Press, pp. 11-25.

Galaburda AM, Pandya DN (1982) Role of architectonics and connections in the study of primate brain evolution. In E Armstrong and D Falk (eds): Primate Brain Evolution: Methods and Concepts. New York: Plenum, pp. 203-216.

Galaburda AM, Sanides F (1980) Cytoarchitectonic organization of the human auditory cortex. J. Comp. Neurol. *190*:597-610.

Galaburda AM, LeMay M, Kemper T and Geschwind N (1978a) Right-left asymmetries in the brain: Structural differences between the hemispheres may underlie cerebral dominance. Science *199:*852-856.

Galaburda AM, Sanides F and Geschwind N (1978b) Human Brain: cytoarchitectonic left-right asymmetries in the temporal speech region. Arch. Neurol. *35:*812-817.

Galaburda AM, Corsiglia J, Rosen GD and Sherman GF (1987) Planum temporale asymmetry: reappraisal since Geschwind and Levitsky. Neuropsychol. *25:*853-868.

Gall FJ (1810) Anatomie et physiologie du système nerveux en géneral, et du cerveau en particulier: Premier volume. Anatomie et physiologie du système nerveux en général, et cerveau en particulier. Paris: F. Schoell.

Gall FJ (1819) Anatomie et physiologie du système nerveux en général, et du cerveau en particulier. Paris: Chez N. Maze, Libraire.

Gazzaniga MS, Smylie CS (1984) Dissociation of language and cognition: A psychological profile of two disconnected right hemispheres. Brain. *107:*145-153.

Gazzaniga MS, Sperry RW (1967) Language after section of the cerebral commisures. Brain. *90:*131-138.

Gazzaniga MS, Volpe BT, Smylie CS, Wilson DH and LeDoux JE (1979) Plasticity in speech organization following commissurotomy. Brain. *102:*805-815.

Geschwind N (1970) The organization of language in the brain. Science *170:*940-944.

Geschwind N, Galaburda AM (1984) Cerebral Dominance: The Biological Foundations. Cambridge: Harvard University Press.

Geschwind N, Levitsky W (1968) Human brain: left right asymmetries in temporal speech region. Science *161:*186-187.

Geschwind N, Quadfasel FA and Segarra JM (1968) Isolation of the speech area. Neuropsychol. *6:*327-340.

Ghiselin MT (1966a) An application of the theory of definitions to systematic principles. Syst. Zool. *15:*127-130.

Ghiselin MT (1966b) On psychologism in the logic of taxonomic controversies. Syst. Zool. *15:*207-215.

Gilbert AN, Wysocki CJ (1992) Hand preference and age in the united-states. Neuropsychol. *30:*601-608.

Goldstein K (1927) Die Lokalisation in der Grosshirnrinde. In (): Handbuch der Normalen und Pathologischen Physiologie. Berlin: Springer, pp. 600-795.

Gorelick PB, Ross ED (1987) The aprosodias: Further functional-anatomical evidence for the organization of affective language in the right hemisphere. J. Neurol. Neurosurg. Psychiat. *50:*553-560.

Gowers WR (1885) Diagnosis of the diseases of the brain and spinal cord. New York: William Wood & Co.

Grasby PM, Frith CD, Friston KJ, Bench C, Frackowiak RSJ and Dolan RJ (1993) Functional mapping of brain areas implicated in auditory - verbal memory function. Brain. *116:*1-20.

Groves CP, Humphrey NK (1973) Asymmetry in gorilla skulls: Evidence of lateralized brain function? Nature *244:*53-54.

Grüsser OJ, Kirchhoff N and Naumann A (1990) Brain mechanisms for recognition of faces, facial expression, and gestures: Neuropsychological and electroencephalographic studies in normals, brain-lesioned patients, and schizophrenics. New York: Raven Press.

Haglund MM, Ojemann GA, Lettich E, Bellugi U and Corina D (1993) Dissociation of cortical and single unit activity in spoken and signed languages. Brain Lang. *44:*19-27.

Hahn WK (1987) Cerebral lateralization of function: From infancy through childhood. Psych. Bull. *101:*376-392.

Hamilton CR, Vermiere BA (1985) Complementary hemispheric superiority in monkeys. Soc. Neur. Abstr. *11:*869.

Harris LJ (1991) Cerebral control for speech in right-handers and left-handers: An analysis of the views of Paul Broca, his contemporaries, and his successors. Brain Lang. *40:*1-50.

Hast MH, Milojevic B (1966) The response of the vocal fold to electrical stimulation of the inferior frontal cortex of the squirrel monkey. Acta. Otolaryngol. *61:*196-204.

Hauser MD, Evans CS and Marler P (1993) The role of articulation in the production of rhesus monkey, *Macaca mulatta*, vocalizations. Animal. Behav. *45:*423-433.

Hécaen H, De Agostini M and Monzon-Montes A (1981) Cerebral organization in left handers. Brain Lang. *12:*261-284.

Heilbroner PL (1987): A Study of Cerebral Asymmetry and Sexual Dimorphism in Five Nonhuman Primate Species. Ph.D. Dissertation, Columbia University, New York. 288 p.

Heilbroner PL, Holloway RL (1988) Anatomical brain asymmetries in New World and Old World monkeys: stages of temporal lobe development in primate evolution [published erratum appears in Am. J. Phys. Anthropol. 1988;77(1):141]. Am. J. Phys. Anthropol. *76:*39-48.

Heilbroner PL, Holloway RL (1989) Anatomical brain asymmetry in monkeys: frontal, temporoparietal, and limbic cortex in *Macaca*. Am. J. Phys. Anthropol. *80:*203-211.

Heilman KM, Scholes R and Watson RT (1975) Auditory affective agnosia: Disturbed comprehension of affective speech. J. Neurol. Neurosurg. Psychiat. *38:*69-72.

Heilman KM, Bowers D, Valenstein E, et al (1986) The right hemisphere: Neuropsychological functions. J. Neurosurg. *64:*693-704.

Hennenberg M, Symons J (1992) Petelial asymmetries of cerebral hemispheres and the asymmetry in the drainage of the superior sagittal sinus. ASSA *25:*17.

Hepper PG, Shahidullah S and White R (1990) Origins of fetal handedness. Nature *347:*431.

Hepper PG, Shahidullah S and White R (1991) Handedness in the human fetus. Neuropsychol. *28:*1107-1111.

Hicks R (1975) Intrahemispheric response condition between vocal and unimanual tapping rate. J. Comp. Physiol. Psychol. *89:*50-60.

Hinke RM, Hu XP, Stillman AE, Kim SG, Merkle H, Salmi R and Ugurbil K (1993) Functional magnetic resonance imaging of Broca's area during internal speech. NeuroReport *4*:675-678.

Hochberg FH, LeMay M (1975) Arteriographic correlates of handedness. Neurology *25*:218-222.

Holloway RL (1980) Indonesian "Solo" (Ngandong) endocranial reconstructions: some preliminary observations and comparisons with Neandertal and *Homo erectus* groups. Am. J. Phys. Anthropol. *53*:285-295.

Holloway RL (1981) Volumetric and asymmetry determinations on recent hominid endocasts: Spy I and II, Djebel Ihroud I, and the Sale *Homo erectus* specimens, with some notes on Neanderthal brain size. Am. J. Phys. Anthropol. *55*:385-393.

Holloway RL, De La Coste-Lareymondie MC (1982) Brain endocast asymmetry in pongids and hominids: some preliminary findings on the paleontology of cerebral dominance. Am. J. Phys. Anthropol. *58*:101-110.

Hopkins WD, Washburn DA and Rumbaugh DM (1989) Note on hand use in the manipulation of joysticks by rhesus monkeys *Macaca mulatta* and chimpanzees *Pan troglodytes*. J. Comp. Psychol. *103*:91-94.

Hutner N, Liederman J (1991) Right hemisphere participation in reading. Brain Lang. *41*:475-495.

Hynd GW (1989) Developmental dyslexia. Psych. Bull. *106]*:447-482.

Hynd GW, Semrud-Clikeman M (1989) Dyslexia and brain morphology. Psych. Bull. *106*:447-482.

Hynd GW, Semrud-Clikeman M, Lorys AR, Novey ES and Eliopulos D (1990) Brain morphology in developmental dyslexia and attention deficit disorder/hyperactivity. Arch. Neurol. *47*:919-926.

Ingalls NW (1914) The parietal region in the primate brain. J. Comp. Neurol. *24*:291-339.

Ishii T, Horiguchi S, Kato T, Waturi N, Hirose M and Hirota K (1991) If the fetus can vocalize, how can we detect it? Biol. Neonate *60*:52-61.

Itani J (1957) Personality of Japanese monkeys. Iden *11*:29-33.

Itani J, Tokuda K, Furaya Y, Kano K and Shin Y (1963) The social construction of natural groups of Japanese monkeys in Takasakiyama. Primates *4:*1-42.

Jackson JH (1874) On the nature of the duality of the brain. Medical Press and Circular *1:*19-43.

Jackson JH (1880) On aphasia with left hemiplegia. Lancet *1:*637-638.

Jäncke L (1992) Stimulus-dependent ear asymmetry in a dichotic monitoring test. Percept. Mot. Skills. *75:*691-695.

Jäncke L, Steinmetz H and Volkmann J (1992) Dichotic listening - what does it measure. Neuropsychol. *30:*941-950.

Jaynes J (1976) The Origin of Consciousness in the Breakdown of the Bicameral Mind. Boston: Houghton Mifflin Co.

Jernigan TL (1990) Techniques for imaging brain structure - neuropsychological applications. Neuropsychol. *17:*81-105.

Joanette Y (1989) Aphasia in left-handers and crossed aphasia. In F Boller and J Grafman (eds): Handbook of Neuropsychology. New York: Elsevier, pp. 173-183.

Joanette Y, Goulet P and Hannequin D (1990) Right Hemisphere and Verbal Communication. New York: Springer-Verlag.

Jürgens U (1976) Projections from the cortical larynx area in the squirrel monkey. Exp. Brain Res. *25:*401-411.

Jürgens U (1979) Neural control of vocalization in nonhuman primates. In HD Steklis and MJ Raliegh (eds): Neurobiology of Social Communication in Primates: An evolutionary perspective. New York: Academic Press, pp. 11-44.

Jurgens U, Ploog D (1970) Cerebral representation of vocalization in the squirrel monkey. Exp. Brain Res. *10:*246-434.

Kaas JH (1989) The evolution of complex sensory systems in mammals. J. Exp. Biol. *146:*165-176.

Kappers ACU, Huber GC and Crosby EC (1967) The Comparative Anatomy of the Nervous System of Vertebrates Including Man. New York: Hafner.

Kawai M (1967) Catching behavior in the Koshima troop: A case of newly acquired behavior. Primates *8:*181-186.

Kent RD, Rosenbeck JC (1982) Prosodic disturbance and neurologic lesion. Brain Lang. *15:*259-291.

Kertesz A, Polk M, Black SE and Howell J (1990) Sex, handedness, and the morphometry of cerebral asymmetries on magnetic resonance imaging. Brain Res. *530:*40-48.

Kertesz A, Polk M, Black SE and Howell J (1992) Anatomical asymmetries and functional laterality. Brain. *115:*589-605.

Kim SG, Ashe J, Hendrich K, Ellerman JM, Merkle H, Ugurbil K and Georgopoulos AP (1993) Functional magnetic imaging of motor cortex: Hemispheric asymmetry and handedness. Science *261:*615-617.

Kimura D (1961) Cerebral dominance and the perception of verbal stimuli. Can. J. Psychol. *15:*166-171.

Kimura, D (1992) Sex differences in the brain. Sci. Am. *267:*119-125.

King BJ (1991) Social information transfer in monkeys, apes and hominids. Yrbk. Phys. Anth. *34:*97-115.

King JE, Landau VI, Scott A and Berning AL (1987) Hand preference during capture of live fish by squirrel monkeys. Int. J. Primatol. *8:*540.

Kirzinger A, Jürgens U (1982) Cortical lesion effects and vocalization in the squirrel monkey. Brain Research *233:*299-315.

Kuhl PK (1979) Models and mechanisms in speech perception: Species comparisons provide further contributions. Brain Behav. Evol. *16:*374-408.

Kulynych JJ, Vladar K, Jones DW and Weinberger DR (1993) 3-Dimensional surface rendering in MRI morphometry - A study of the planum-temporale. J. Comput. Assist. Tomogr. *17:*529-535.

Kurland JA (1973) A natural history of Kra macaques *(Macaca fascicularis* Raffles 1821) at the Kutai Reserve, Kalimantan, Timur, Indonesia. Primates *14:*245-262.

Kuypers HGJM (1958a) Corticobulbar connections to the pons and lower brainstem in man. Brain. *81:*364-388.

Kuypers HGJM (1958b) Some projections from the peri-central cortex to the pons and lower brainstem in monkey and chimpanzee. J. Comp. Neurol. *110:*221-255.

Laitman JT (1983) The evolution of the hominid upper respiratory system and implications for the origins of speech. In E deGrolier (ed.): Glossogenetics. Paris: Harwood Academic Publishers, pp. 63-90.

Laitman JT, Reidenberg JS (1988) Advances in understanding the relationship between the skull base and larynx with comments on the origins of speech. Human Evol. 3:99-109.

Laitman JT, Reidenberg JS and Gannon PJ (1992) Fossil skulls and hominid vocal tracts: New approaches to charting the evolution of human speech. In J Wind, B Bichakjian, A Nocentini and A Jonker (eds): Language Origins: A Multidisciplinary Approach. Dordrecht, Netherlands: Kluwer Academic Publishers, pp. 385-397.

Laitman JT, Reidenberg JS (1993) Specialization of the human upper respiratory and upper aerodigestive systems as seen through comparative and developmental anatomy. Dysphagia *8:*318-325.

Larsen JP, Odegaard H, Grude TH and Hoien T (1989) Magnetic resonance imaging - a method of studying the size and asymmetry of the planum temporale. Acta Neurol. Scand. *80:*438-443.

Le Brun Kemper T, Galaburda AM (1984) Principles of cytoarchitectonics. In A Peters and EG Jones (eds): Cerebral Cortex: Cellular Components of the Cerebral Cortex. New York: Plenum Press, pp. 35-57.

Leiner HC, Leiner AL and Dow RS (1991) The Human Cerebro-Cerebellar System - Its Computing, Cognitive, and Language Skills. Behav. Brain. Res. *44:*113-128.

LeMay M (1976) Morphological cerebral asymmetries of modern man, fossil man, and nonhuman primates. Ann. N.Y. Acad. Sci. *280:*349-366.

LeMay M (1977) Asymmetries of the skull and handedness: Phrenology revisited. J. Neurol. Sci. *32:*243-253.

LeMay M (1984) Radiological, developmental, and fossil asymmetries. In N Geschwind and AM Galaburda (eds): Cerebral Dominance - The Biological Foundations. Cambridge, Massachusetts: Harvard Univ. Press, pp. 26-42.

LeMay M, Culebras A (1972) Human brain - morphologic differences in the hemispheres demonstrable by carotid arteriography. New England J. Med. *287:*168-170.

LeMay M, Geschwind N (1975) Hemispheric differences in the brains of great apes. Brain Behav. Evol. *11:*48-52.

LeMay M, Geschwind N (1981) Morphological cerebral asymmetries in primates. In B Preilowski and C Engele (eds): Is There Cerebral Hemispheric Asymmetry in Non-Human Primates? Tübingen: University of Tübingen, .

LeMay M, Kido DK (1978) Asymmetries of the cerbral hemispheres on computed tomograms. J. Comput. Assist. Tomogr. *2:*471-476.

LeMay M, Billig MS and Geschwind N (1982) Asymmetries of the brains and skulls of nonhuman primates. In E Armstrong and D Falk (eds): Primate Brain Evolution: Methods and Concepts. New York: Plenum Press, pp. 263-277.

Leonard CM, Voeller KKS, Lombardino LJ, Morris MK, Hynd GW, Alexander AW, Andersen HG, Garofalakis M, Honeyman JC, Mao JT, Agee OF and Staab EV (1993) Anomalous cerebral structure in dyslexia revealed with magnetic resonance imaging. Arch. Neurol. *50:*461-469.

Lieberman P (1984) The Biology and Evolution of Language. Cambridge MA, Harvard University Press.

Lieberman P, Laitman JT, Reidenberg JS and Gannon PJ (1992) The anatomy, physiology, acoustics and perception of speech: Essential elements in analysis of the evolution of human speech. J. Hum. Evol. *23:*447-467.

Lieberman PH, Klatt DH and Wilson WH (1969) Vocal tract limitations on the vowel repertoires of rhesus monkey and other nonhuman primates. Science *164:*1185-1187.

Leyton ASF, Sherrington CS (1917) Observations on the excitable cortex of the chimpanzee, orangutan and gorilla. J. Exp. Physiol. *11:*135-222.

Lüders H, Lesser RP, Hahn J, Dinner DS, Morris HH, Wyllie E and Godoy J (1991) Basal Temporal Language Area. Brain. *114:*743-754.

MacNeilage PF, Studdert-Kennedy MG and Lindblom B (1987) Primate handedness reconsidered. Behav. Brain Sci. *10:*247-303.

Majnemer A, Rosenblatt B (1992) Functional interhemispheric asymmetries at birth as demonstrated by somatosensory evoked potentials. J. Child Neurol. *7:*408-412.

Mandal MK, Tandon SC and Asthana HS (1991) Right brain damage impairs recognition of negative emotions. Cortex *27:*247-253.

May B, Moody DB and Stebbins WC (1989) Categorical perception of conspecific communication sounds by Japanese macaques, *Macaca fuscata*. J. Acoust. Soc. Am. *85:*837-847.

Mayr E (1982) The Growth of Biological Thought. Boston, Mass: Belknap Press of Harvard University Press.

Mazzocchi F, Vignolo L (1979) Localization of lesions in aphasia: Clinical-CT scan correlations in stroke patients. Cortex *15:*627-654.

McCarthy G, Blamire AM, Rothman DL, Gruetter R and Shulman RG (1993) Echo-planar magnetic resonance imaging studies of frontal cortex activation during word generation in humans. Proc. Nat. Acad. Sci. *90:*4952-4956.

McGlone J (1980) Sex differences in human brain asymmetry: A critical survey. Behav. Brain Sci. *3:*215-263.

McGuire PK, Shah GMS and Murray RM (1993) Increased blood flow in Broca's area during auditory hallucinations in schizophrenia. Lancet *342:*703-706.

McLean PD (1985) Brain evolution relating to family, play, and the separation call. Arch. Gen. Psychiatry *42:*405-417.

McLean PD, Newman JD (1988) Role of midline frontolimbic cortex in production of the isolation call of squirrel monkeys. Brain Res. *450:*111-123.

McManus IC (1991) The Inheritance of Left-Handedness. Ciba Foundation Symposium - Biological Asymmetry and Handedness *162:*251-281.

Mesulam MM (1982) Principles of horseradish peroxidase neurohistochemistry and their applications for tracing neural pathways - axonal transport, enzyme histochemistry and light microscopic analysis. In MM Mesulam (ed): Tracing Neural Connections With Horseradish Peroxidase. New York: John Wiley & Sons, pp. 1-151.

Meynert T (1865) Anatomie der hirnrinde und ihre verbindungsbahnen mit den empfindenden oberflächen und den bewegenden massen. In (): Leidesdorf's Lehrbuch der Psychiatrie. Erlangen: Krankheiten, .

Moen I (1993) Functional lateralization of the perception of Norwegian word tones - Evidence from a dichotic listening experiment. Brain Lang. *44:*400-413.

Moody DB, Stebbins WC and May BJ (1989) Auditory perception of communication signals by Japanese monkeys. In WC Stebbins and M Berkley (eds): Comparative Perception. New York: John Wiley & Sons, pp. 311-343.

Myers RE (1972) Role of prefrontal and anterior temporal cortex in social behavior and affect in monkeys. Act. Neurobiol. Exp. *32:*567-579.

Myers RE, Swett C (1970) Social behavior deficits of free-ranging monkeys after anterior temporal cortex removal: A preliminary report. Brain Res. *64:*551-556.

Myers RE, Swett C (1973) Loss of social group affinity following prefrontal lesions in free-ranging macaques. Brain Research *64:*257-269.

Naeser MA, Hayward RW (1978) Lesion localization in aphasia with cranial compound tomography and the Boston Diagnostic Aphasia Exam. Neurology *28:*545-551.

Newman JD (1988) The physiological control of mammalian vocalization. New York: Plenum Press.

Newman JD, Winslow JT and Murphy DL (1991) Modulation of vocal and nonvocal behavior in adult squirrel monkeys by selective MAO-A and MAO-B inhibition. Brain Res. *538:*24-28.

Nishikawa KC, Anderson CW, Deban SM and O'Reilly JC (1992) The evolution of neural circuits controlling feeding behavior in frogs. Brain Behav. Evol. *40:*125-140.

Northcutt RG (1984) Evolution of the vertebrate nervous system: patterns and processes. Amer. Zool. *24:*701-716.

Nowak RM, Paradiso JL (1983) Walker's Mammals of the World. Baltimore: The Johns Hopkins University Press.

O'Boyle MW, Alexander JE and Benbow CP (1991) Enhanced right hemisphere activation in the mathematically precocious: A preliminary EEG investigation. Brain Cogn. *17:*138-153.

O'Brien JH, Pimpaneau A and Albe-Fessard D (1971) Evoked cortical responses to vagal, laryngeal and facial efferents in monkeys under chloralose anesthesia. Electroencephalogr. Clin. Neurophysiol. *31:*7-20.

Ojemann GA (1978) Organization of short-term verbal memory in language areas of human cortex: evidence from electrical stimulation. Brain Lang. *5:*331-348.

Ojemann GA (1983) Brain organization for language from the perspective of electrical stimulation mapping. Behav. Brain Sci. *2:*189-230.

Ojemann GA (1991) Cortical Organization of Language. J. Neurosci. *11:*2281-2287.

Ojemann G (1992) Localization of language in frontal cortex. In P Chauvel, AV Delgado-Escueta, et al (eds): Advances in Neurology. New York: Raven Press, pp. 361-368.

Ojemann G, Whitaker H (1978) The bilingual brain. Arch. Neurol. *35:*409-412.

O'Kusky J, Strauss E, Kosaka B, Wada J, Li D, Druhan M and Petrie J (1988) The corpus callosum is larger with right-hemisphere cerebral speech dominance. Ann. Neurol. *24:*379-383.

Olson DA, Ellis JE and Nadler RD (1990) Hand preferences in captive gorillas, orang-utans and gibbons. Am. J. Primatol *20:*83-94.

Orsini DL, Satz P, Soper HV and Light R (1985) The role of familial sinistrality in cerebral organization. Neuropsychol. *23:*223-232.

Owen R (1843) Lectures on the Comparative Anatomy and Physiology of the Invertebrate Animals. London: Longman, Brown, Green and Longmans.

Paget GE (1887) Notes on an exceptional case of aphasia. Br. Med. J. *2:*1258-1259.

Pandya DN, Sanides F (1973) Architectonic parcellation of the temporal operculum in rhesus monkey and its projection pattern. Z. Anat. Entwickl.-Gesch. *139:*127-161.

Pandya DN, Seltzer B (1982) Intrinsic connections and architectonics of the posterior parietal cortex in the rhesus monkey. J. Comp. Neurol. *204:*196-210.

Penfield W, Rasmussen T (1950) The Cerebral Cortex of Man. New York: The Macmillan Company.

Penfield W, Roberts L (1959) Speech and Brain Mechanisms. Princeton: Princeton University Press.

Penfield W, Welch K (1951) The supplementary motor area of the cerebral cortex: A clinical and experimental study. Arch. Neurol. Psychiat. *66:*289-317.

Perrett DI, Mistlin AJ, Chitty A, Smith PAJ, Potter DD, Broennimann R and Harris M (1988) Specialized face processing and hemispheric asymmetry in man and monkey: Evidence from single unit and reaction time studies. Behav. Brain. Res. *29:*245-258.

Perrett DI, Hietanen JK, Oram MW and Benson PJ (1992) Organization and functions of cells responsive to faces in the temporal cortex. Philos. Trans. R. Soc. Lond. (Biol.) *335:*23-30.

Petersen SE, Fiez JA (1993) The processing of single words studied with positron emission tomography. Ann. Rev. Neurosci. *16:*509-530.

Petersen SE, Fox PT, Posner MI, Mintun M and Raichle ME (1988) Positron emission tomographic studies of the cortical anatomy of single word processing. Nature *331:*585-589.

Petersen SE, Fox PT, Posner MI, Mintun M and Raichle ME (1990) Positron emission tomographic studies of the processing of single words. J. Cogn. Neurosci. *1:*153-170.

Pfeifer RA (1936) Pathologie der hörstrahlung und der corticalen hörsphäre. In O Bumke and O Foerster (eds): Handbuch der Neurologie. Berlin: Springer Verlag, pp. 523-626.

Pieniadz JM, Naeser MA (1984) Computed tomographic scan cerebral asymmetries and morphological brain asymmetries. Arch. Neurol. *41:*403-409.

Ploog D (1981) Neurobiology of primate audio-vocal behavior. Brain Res. Rev. *3:*35-61.

Posner MI, Sandson J, Dhawan M and Shulman G (1989) Is word recognition automatic? A cognitive anatomical approach. J. Cogn. Neurosci. *1:*50-60.

Price C, Wise R, Ramsay S, Friston K, Howard D, Patterson K and Frackowiak R (1992) Regional response differences within the human auditory cortex when listening to words. Neurosci. Lett. *146:*179-182.

Rademacher J, Galaburda AM, Kennedy DN, Filipek PA and Caviness VS (1992) Human cerebral cortex: localization, parcellation, and morphometry with magnetic resonance imaging. J. Cogn. Neurosci. *4:*352-374.

Rademacher J, Caviness VS, Steinmetz H and Galaburda AM (1993) Topographical Variation of the Human Primary Cortices - Implications for Neuroimaging, Brain Mapping, and Neurobiology. Cereb. Cortex *3:*313-329.

Raichle ME (1987) Circulatory and metabolic correlates of brain function in normal humans. In F Plum (ed): Handbook of Physiology: The Nervous System. New York: Oxford University Press, pp. 643-674.

Ranck JJ (1975) Which elements are excited in electrical stimulation of mammalian central nervous system: A review. Brain Res. *98:*417-440.

Rausch R, Risinger M (1990) Intracarotid sodium amobarbital procedure. Neuropsychol. *17:*127-146.

Ristau CA, Robbins D (1982) Language in the great apes: A critical review. C. R. Acad. Sci. Paris *12:*141-255.

Robinson BW (1967) Vocalization evoked from forebrain in *Macaca mulatta.* J. Neurophysiol. *2:*345-354.

Romani GL, Williamson SJ, Kaufman L and Brenner D (1982) Characterization of the human auditory cortex by the neuromagnetic method. Exp. Brain Res. *47:*381-393.

Roonwal ML, Mohnot SM (1977) Primates of South Asia. Cambridge: Harvard University Press.

Ross ED, Mesulam M-M (1979) Dominant language functions of the right hemisphere: Prosody and emotional gesturing. Arch. Neurol. *36:*144-148.

Ross EE (1981) The aprosodias: Functional-anatomic organization of the affective components of language in the right hemisphere. Arch. Neurol. *38:*561-570.

Sade DS (1967) Determinants of dominance in a group of free ranging rhesus monkeys. In SA Altmann (ed): Social Communication Among Primates. Chicago: Univ. Chicago Press, pp. 99-114.

Sakurai Y, Momose T, Iwata M, Watanabe T, Ishikawa T and Kanazawa I (1993) Semantic process in Kana word reading - Activation studies with positron emission tomography. NeuroReport *4:*327-330.

Sams M, Aulanko R, Hämäläinen M, Hari R, Lounasmaa OV, Lu ST and Simola J (1991) Seeing speech - Visual information from lip movements modifies activity in the human auditory cortex. Neurosci. Lett. *127:*141-145.

Sanides F (1970) Functional architecture of motor and sensory cortices in primates in the light of a new concept of neocortex evolution. In CR Nobak and W Montagna (eds): The Primate Brain: Advances in Primatology. New York: Appleton-Century-Crofts, pp. 137-208.

Sanides F (1972) Representation in the cerebral cortex and its area lamination patterns. In GA Bourne (ed): Structure and Function of Nervous Tissue. New York: Academic Press, pp. 329-453.

Sarnat HB, Netsky MG (1981) Evolution of the Nervous System. New York: Oxford University Press.

Schmahmann JD (1991) An Emerging Concept - The cerebellar contribution to higher function. Arch. Neurol. *48:*1178-1187.

Segalowitz SJ, Bryden MP (1983) Individual differences in hemispheric representation of language. In SJ Segalowitz (ed): Language Functions and Brain Organization. New York: Academic Press, pp. 341-372.

Seldon HL (1985) The anatomy of speech perception: Human auditory cortex. In A Peters and EG Jones (eds): Cerebral Cortex: Association and Auditory Cortices. New York: Plenum Press, pp. 273-327.

Serafetinides EA, Hoare RD and Driver MV (1965) Intracarotid sodium amylobarbitone and cerebral dominance for speech and consciousness. Brain *88:*107-130.

Shankweiler D, Studdert-Kennedy M (1967) Identification of consonants and vowels presented to left and right ears. Q. J. Exp. Physiol. *19:*59-63.

Sherman GF, Galaburda AM and Geschwind N (1982) Neuroanatomical asymmetries in non-human species. Trends Neurosci. *5:*429-431.

Simon TJ, Sussman HM (1987) The dual task paradigm: Speech dominance or manual dominance. Neuropsychol. *25:*559-569.

Sjöberg J, Kanje M (1990) The initial period of peripheral nerve regeneration and the importance of the local environment for the conditioning lesion effect. Brain Res. *529:*79-84.

Snowdon CT (1979) Response of nonhuman animals to speech and to species-specific sounds. Brain Behav. Evol. *16:*409-429.

Snowdon GF (1990) Language capacities of non-human animals. Yrbk. Phys. Anth. *33:*215-243.

Sokoloff AJ (1989): The organization of the hypoglossal nucleus. An experimental neuroanatomical investigation of hypoglossal-lingual and cortico-hypoglossal projections in *Macaca fascicularis* and other vertebrates. PhD Thesis, Harvard University.

Sokoloff A, Deacon T (1990) Direct projections from the face area of primary motor cortex to the facial nucleus in the cynomolgus monkey but not in the cat or rat. Am. J. Phys. Anthropol. *81:*298.

Spiegler BJ, Yeni-Komshian GH (1983) Incidence of left-handed writing in a college population with reference to family patterns of hand preference. Neuropsychol. *1:*651-659.

Staab EV (1993) Anomalous Cerebral structure in dyslexia revealed with magnetic resonance imaging. Arch. Neurol. *50:*461-469.

Steinmetz H, Rademacher J, Huang Y, Hefter H, Zilles K, Thron A and Freund HJ (1989) Cerebral asymmetry: MR planimetry of the human planum temporale. Journal of Computer Assisted Tomography *13:*996-1005.

Steklis HD, Harnad SR (1976) From hand to mouth: some critical stages in the evolution of language. Ann. N.Y. Acad. Sci. *280:*445-455.

Steklis HD, Marchant LF (1987) Primate handedness: Reaching and grasping for straws? Behav. Brain Sci. *10:*284-286.

Steklis HD, Raleigh MJ (1979) Neurobiology of Social Communication in Primates. An Evolutionary Perspective. New York: Academic.

Strauss E, Gaddes WH and Wada J (1987) Performance on a free-recall dichotic listening test and cerebral dominance determined by the carotid amytal test. Neuropsychol. *25:*747-753.

Striedter GF, Northcutt RG (1991) Biological hierarchies and the concept of homology. Brain Behav. Evol. *38:*177-189.

Studdert-Kennedy M, Shankweiler D (1970) Hemispheric specialization for speech perception. J. Acoust. Soc. Am. *48:*579-594.

Sugar O, Chusid JG and French JD (1948) A second motor cortex in the monkey. J. Neurophysiol. *7:*182-189.

Susman RL (1988) Hand of *Paranthropus robustus* from Member 1, Swartkrans: Fossil evidence for tool behavior. Science *240:*781-784.

Sutton D (1979) Mechanisms underlying vocal control in nonhuman primates. In HD Steklis and MJ Raliegh (eds): Neurobiology of Social Communication in Primates: An evolutionary perspective. New York: Academic Press, pp. 45-67.

Sutton D, Jürgens U (1988) Neural control of vocalization. In HD Steklis and J Erwin (eds): Comparative Primate Biology. Neurosciences. New York: Alan R. Liss, pp. 625-647.

Sutton D, Larson C and Lindeman RC (1974) Neocortical and limbic lesion effects on primate phonation. Brain Res. *71:*61-75.

Tallal P, Miller S and Fitch RH (1993) Neurobiological basis of speech: A case for the preeminence of temporal processing. Ann. NY Acad. Sci. *682:*27-47.

Tamas LB, Shibasaki T, Horikoshi S and Ohye C (1993) General activation of cerebral metabolism with speech - A PET study. Int. J. Psychophysiol. *14:*199-208.

Tan U (1992) Similarities between sylvian fissure asymmetries in cat brain and planum-temporale asymmetries in human brain. Int. J. Neurosci. *66:*163-175.

Tan U, Ors R, Kurkcuoglu M and Kutlu N (1992) The lateralization of the grasp reflex in human newborns. Int. J. Neurosci. *62:*1-8.

Tison F, Geffard M and Henry P (1990) Tryptamine Is found closely associated to the serotoninergic pathways when using an immunohistochemical method of detection in the rat central nervous system. Biogenic. Amines. *7:*235.

Tobias PV (1965) *Australopithecus, Homo habilis*, tool-using and tool-making. S. Afr. J. Sci. *20:*167-192.

Tokuda K (1969) On the handedness of Japanese monkeys. Primates *10:*41-46.

Tooze ZJ, Harrington FH and Fentress JC (1990) Individually distinct vocalizations in timber wolves, *Canis lupus*. Anim. Behav. *40:*723-730.

Toth n (1990) The prehistoric roots of a human concept of symmetry. Symmetry: Culture and Science *1:*257-281.

Tranel D, Brady DR, Van Hosen GW and Damasio AR (1988) Parahippocampal projections to the posterior auditory association cortex (area Tpt) in Old World monkeys. Exp. Brain Res. *70:*406-416.

Trauner DA, Ballantyne A, Chase C, and Tallal P (1993) Comprehension and expression of affect in language-impaired children. J. Psycholinguist. Res. *22:*445-452.

Van Valen LM (1982) Homology and causes. J. Morphol. *173:*305-312.

Vauclair J, Fagot J (1993) Manual and hemispheric specialization in the manipulation of a joystick by baboons (*Papio papio*). Behav. Neurosci. *107:*210-214.

Vogt C, Vogt O (1919) Allgemeinere ergebnisse unserer hirforschung. J. Psychol. Neurol. *25:*279-461.

Von Bonin G, Bailey P (1947) The neocortex of *Macaca mulatta*. Urbana, Illinois: University of Illinois Press.

Von Bonin J (1962) Interhemispheric Relations and Cerebral Dominance. Baltimore: Johns Hopkins Press, pp. 1-6.

von Cramon D, Jürgens U (1983) The anterior cingulate cortex and the pnonatory control in monkey and man. Neurosci. Biobehav. Rev. *7:*423-425.

von Monakow C (1914) Die Lokalisation im Grosshirn. Weisbaden: Bergmann.

Wada J (1949) A new method for the determination of the side of cerebral speech dominance. A preliminary report on the intracarotid injection of sodium amytal in man. Med. Biol. *14:*221-222.

Wada J, Rasmussen T (1960) Intracarotid injection of sodium amytal for the lateralization of cerebral speech dominance. J. Neurosurg. *17:*266-282.

Wada J, Clarke R and Hamm A (1975) Cerebral asymmetry in humans. Arch. Neurol. *32:*239-246.

Walker SF (1980) Lateralization of functions in the vertebrate brain: a review. Br. J. Psychol. *71:*329-367.

Wallesch CW, Henriksen L, Kornhuber HH and Paulson OB (1985) Observations on regional cerebral blood flow in cortical and subcortical structures during language production in normal man. Brain Lang. *25:*224-233.

Ward JP, Milliken GW, Dodson DL, Stafford DK and Wallace M (1990) Handedness as a function of sex and age in a large population of *Lemur*. J. Comp. Psychol. *104:*167-173.

Warren JM, Nonneman AJ (1976) The search for cerebral dominance in monkeys. In SR Harnad, HD Steklis and J Lancaster (eds): Origins and Evolution of Language and Speech. New York: New York Academy of Sciences, pp. 732-744.

Waxman SG, Geschwind N (1974) Hypergraphia in temporal lobe epilepsy. Neurology *24:*629-636.

Weintraub S, Mesulam M-M and Kramer L (1981) Disturbances in prosody. A right hemisphere contribution to language. Arch. Neurol. *38:*742-744.

Wernicke C (1874) Der Aphasische Symptomemkomplex. Eine Psychologische Studie auf Anatomischer Basis. Breslau: Cohn und Weigart.

Wheatley BP (1980) Feeding and ranging of East Bornean *Macaca fascicularis*. In DG Lindburg (ed): The Macaques: Studies in Ecology, Behaviour and Evolution. New York: Van Nostrand Reinhold, pp. 215-246.

Wiley EO (1981) Phylogenetics. New York: Wiley & Sons.

Williams H, Crane LA, Hale TK, Esposito MA and Nottebohm F (1992) Right-side dominance for song control in the zebra finch. J. Neurobiol. *23:*1006-1020.

Wise R, Chollet F, Hadar U, Friston K, Hoffner E and Frackowiak R (1991a) Distribution of cortical neural networks involved in word comprehension and word retrieval. Brain. *114:*1803-1817.

Wise R, Hadar U, Howard D and Patterson K (1991b) Language activation studies with positron emission tomography. Ciba Found. Symp. *163:*218-228.

Witelson SF (1985) The brain connection: The corpus callosum is larger in left-handers. Science *229:*665-668.

Witelson SF (1989) Hand and sex differences in the isthmus of the human corpus callosum: A postmortem morphological study. Brain. *112:*799-835.

Witelson SF, Kigar DL (1992) Sylvian fissure morphology and asymmetry in men and women - bilateral differences in relation to handedness in men. J. Comp. Neurol. *323:*326-340.

Wittleson S, Pallie R (1973) Left-hemisphere specialization for language in the newborn. Neuroanatomical evidence for asymmetry. Brain. *96:*641-646.

Woolsley CN (1964) Cerebral localization as defined by evoked potential and electrical stimulation studies. In Schaltenbrand and CN Woolsey (eds): Cerebral Localization and Organization. Madison: University of Wisconsin Press, pp. 17-26.

Yamadori A (1992) Role of the right hemisphere in linguistic function. Biomed. Res. *13:*73-76.

Yamadori A, Osumi Y, Tabuchi Y, Mori E, Yoshida T, Ohkawa S and Yoneda Y (1990) Hyperlalia: A right cerebral hemisphere syndrome. Behav. Neurol. *3:*143-151.

Yeni-Komshian G, Benson D (1976) Anatomical study of cerebral asymmetry in the temporal lobe of humans, chimpanzees and rhesus monkeys. Science *192*:387-389.

Yuanye M, Yunfen T and Ziyun D (1986) Handedness of golden and leaf monkeys in picking up food. Prim. Rep. *14*:248.

Zatorre RJ, Evans AC, Meyer E and Gjedde A (1992) Lateralization of phonetic and pitch discrimination in speech processing. Science *256*:846-849.

Zealear DL (1991) The brainstem connections with the laryngeal region of the motor cortex in the monkey. In T Baer, C Sasaki and KS Harris (eds): Laryngeal Function in Phonation and Respiration. San Diego: Singular, pp. 168-177.

Zeller AC (1986) Communication by sight and smell. In BB Smuts, DL Cheney, RM Seyfarth, RW Wrangham and TT Struhsaker (eds): Primate Societies. Chicago: University of Chicago Press, pp. 433-439.

Zilles K (1992) Neuronal plasticity as an adaptive property of the central nervous system. Annals of Anatomy - Anatomischer Anzeiger *174*:383-391.

Zimmer EZ, Fifer WP, Kim YI, Rey HR, Chao CR and Myers MM (1993) Response of the premature fetus to stimulation by speech sounds. Early Hum. Dev. *33*:207-215.

Zoloth S, Green S (1979) Monkey vocalizations and human speech: parallels in perception? Brain Behav. Evol. *16*:430-442.